# Platelet-Surface Interactions Using a Cone and Plate Device

# Investigation of Platelet-Surface Interactions Using a Novel Cone and Plate Device

By

Gary Alan Skarja, B.Eng.

A Thesis
Submitted to the School of Graduate Studies
in Partial Fulfilment of the Requirements
for the Degree
Master of Engineering

McMaster University
August 1994

MASTER OF ENGINEERING (1994)
(Chemical Engineering)

MCMASTER UNIVERSITY
Hamilton, Ontario

TITLE: Investigation of Platelet-Surface Interactions Using a Novel Cone and Plate Device

AUTHOR: Gary Alan Skarja, B. Eng. (McMaster University)

SUPERVISOR: Professor J.L. Brash

NUMBER OF PAGES: xvii, 191

## ABSTRACT

Polymers are frequently utilized in blood-contacting biomaterials. Although, these materials exhibit generally favourable mechanical properties, the presence of these artificial surfaces in contact with blood initiates the mechanisms of thrombosis. This occurrence may, in turn, lead to a variety of serious clinical complications.

A great deal of work has been done in this laboratory in the past to investigate the interactions of a variety of proteins (particularly coagulation proteins) with artificial surfaces. This interaction is believed to be the initial step in the physiological response to artificial surfaces in contact with blood. A secondary but equally important process is the adhesion and activation of blood platelets to artificial surfaces which may then lead to the formation of thrombi.

The work performed here involves the investigation of platelet-surface interactions with a variety of surfaces, primarily a series of sulphonate ion-containing polyurethanes. Similar polymers have been shown by other researchers to exhibit favourable blood-contacting responses while retaining the attractive mechanical properties of polyurethanes in general.

To perform the work outlined above, a novel cone and plate device was designed and built which enables the experimenter to investigate platelet-surface interactions under varying shear flow conditions. Collagen and albumin-coated test surfaces were utilized to investigate the platelet adhesion results generated in the device with varying fluid shear rate and time. A typical adhesion time response curve was generated with increasing levels of adhesion noted for increasing shear rate, as expected due to increased platelet transport to the surface. As well, effective platelet diffusion coefficients were calculated from the adhesion data collected using the collagen surface and was found to agree broadly with those found by other researchers.

A series of sulphonated polyurethanes were synthesized and both the bulk and surface properties were characterized. A variety of polymer sulphonate concentrations were achieved by use of different constituent molecules (specifically chain extenders and polyols). The polymers, in general, showed high levels of water absorption and increased hydrophilicity in comparison to non-sulphonated analogs.

The cone and plate device was used to investigate the platelet adhesion response in a shear flow environment to these surfaces. In general, sulphonate incorporation resulted in a dramatic increase in the level of adhesion to the polyurethane surfaces, indicating that platelets are able to form adhesive interactions with sulphonate functional groups. Platelet adhesion levels to the sulphonated polyurethanes exhibited both time and shear rate dependence. However, differences in adhesion levels between the sulphonated polyurethanes did not appear to be a simple function of the sulphonate concentration. This may indicate that the local environment of the incorporated sulphonate groups in the polyurethane can affect the ability of these groups to interact with the platelet membrane.

## ACKNOWLEDGEMENTS

The author would like to thank a number of people who have contributed to the completion of this thesis. To Dr. John Brash who provided guidance and encouraged independent thought as well as the resources required to complete the project. To Dr. Raelene Rathbone who provided the equipment necessary for the platelet preparations. Thanks to Dennis Perry and Amar Chahil who instructed me on the preparation and handling of platelets. Thanks to all of my blood donors who donated to my cause. I would like to thank a variety of students and technicians from the lab who contributed in a multitude of ways to my experiences here over the last three years: Dr. Kim Woodhouse, Bryan Wickson, Jacques Archambault, Peter Lee, Rena Cornelius, Glenn McClung, Lindsay Smith and Yuan Tian. I would like to especially thank my wife, Julie, for her support over the last three years. Finally, I would like to acknowledge the financial support of McMaster University and the Department of Chemical Engineering.

## TABLE OF CONTENTS

## LIST OF FIGURES

## LIST OF TABLES

## 1.0 INTRODUCTION

The use of synthetic materials in biomedical applications has grown significantly in the relatively recent past [Kambic et al, 1986]. However, while advances in materials development have occurred over this time period, several serious problems persist. A definition of the requirements of a biomaterial given by Hench and Etheridge [1982] highlights the challenges of producing a satisfactory biomaterial: "The purpose of a biomaterial is to replace a part or a function of the body in a safe, reliable, economic and physiologically acceptable manner".

A wide range of biomaterials are employed in a variety of applications. These include hip replacement, dental materials, contact lenses, and heart valves as well as many others. As might be expected from such varied applications, each must deal with a unique set of both materials and biological criteria. The work reported here is concerned specifically with the subset of biomaterials used in blood-contacting applications.

### 1.1 Blood-Contacting Biomaterials

In the case of blood-contacting biomaterials, such as heart valves, vascular grafts and hemodialysis membranes, an array of interactions of the elements of blood and the material surface must be confronted. Blood is a complex fluid, primarily made up of proteins and cells [Guyton, 1987]. Therefore, any material placed in contact with blood must not only meet a set of mechanical and processing criteria, but must also avoid any blood-based pathologic responses such as coagulation, thrombosis and infection. The most immediate problem concerning blood-contacting materials is surface induced thrombosis. The exposure of a foreign surface to blood invariably leads to thrombus formation and possibly subsequent detachment (embolization) which in turn can lead to strokes, infarcts and other serious complications. The many clinical complications

observed for blood-contacting biomaterials shown in Figure 1.1 highlights the persistence and scope of the problem. Although the phenomenon of material-induced thrombosis has been an area of intensive research for several years, limited success has been achieved and the use of anticoagulants is still required which may lead to bleeding complications with long term use [Hirsh, 1991]. The work reported here, then, deals with the investigation of blood-material interactions from the standpoint of one of the key agents of thrombus formation, namely the blood platelets. The materials of interest here are segmented polyurethanes.

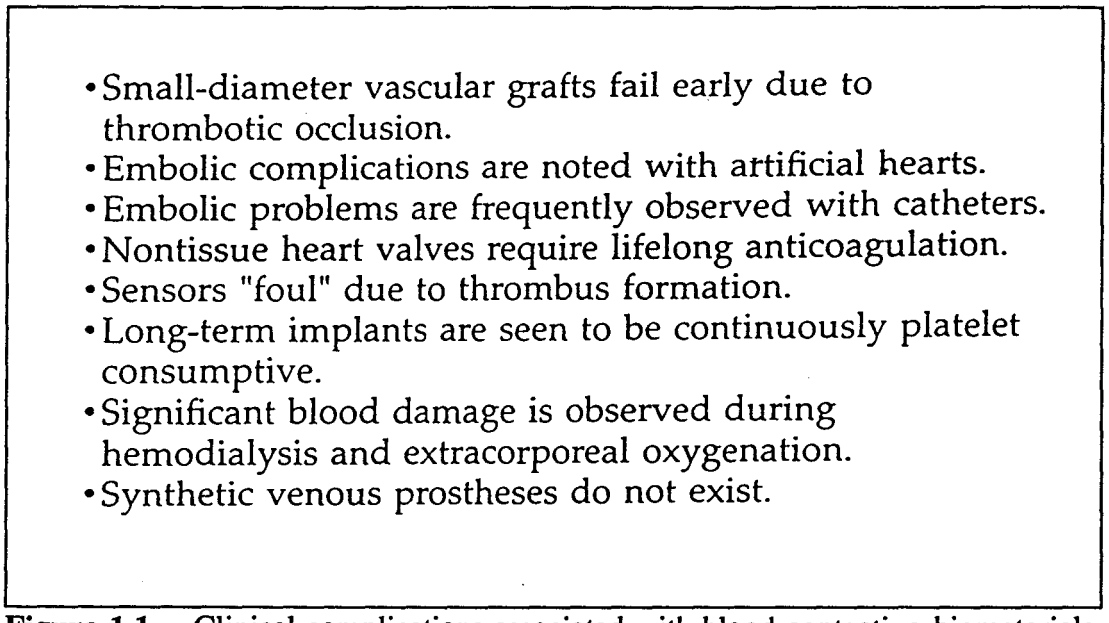


**Figure 1.1** - Clinical complications associated with blood-contacting biomaterials, from [Ratner, 1993].

## 1.2 Polymeric Biomaterials

Polymeric materials are often employed as blood-contacting biomaterials due to their excellent elastomeric mechanical properties, and the ability to tailor these materials chemically with relative ease to create a broad range of products [Lelah and Cooper, 1986]. A number of polymeric materials are used in direct contact with blood in a variety

of applications such as blood storage containers, catheters, drainage tubes, oxygenators, and various implants. Such materials include polyvinyl chloride, silicone rubber, polyethylene and polyurethanes. However, since clotting mechanisms are activated when blood contacts polymeric biomaterials, anticoagulation therapy is necessary.

Polyurethanes are block copolymers which have been found to exhibit relatively good blood compatibility [Lelah and Cooper, 1986]. This unique class of polymers may be synthesized to form a wide variety of products which can display a range of both mechanical and chemical properties [Saunders and Fritsch, 1967]. It is the combination of versatility and biocompatibility demonstrated by these polymers that has led to their wide use as blood-contacting biomaterials.

## 1.3 In vitro Investigation of Blood-Material Interactions

The study of blood-material interactions is complicated both by the array of biological reactions involved in the blood response to foreign materials and the inherent difficulty in modelling the biological system experimentally. To investigate a particular facet of the blood-material response, some degree of simplification must be made. However, since the hemostatic reactions are interdependent and often synergistic in nature [Guyton, 1987], the validity of any simplified in vitro system is always in question. Nonetheless, the impossibility of human in vivo examination requires that in vitro experimental procedures be developed which attempt to reflect as far as possible the in vivo situation. To this end, a variety of in vitro experimental systems have been developed to simulate the in vivo situation both biologically and rheologically [Baumgartner, 1973 ; Feuerstein et al, 1975 ; Sakariassen et al, 1983 ; Fukuyama et al, 1989].

In addition there is no single in vitro test for material blood compatibility. A variety of tests exists such as clotting time, protein adsorption, and platelet adhesion response. A great deal of work has been performed in this laboratory previously to determine the protein adsorption characteristics of various biomaterial surfaces. The

present work focusses on the other key agent of thrombosis, namely platelets. The work reported here involves the development and testing of a novel experimental flow system to investigate platelet-surface interactions with both biological and synthetic surfaces. It is hoped that this investigation may contribute to a more thorough understanding of blood-material interactions.

# 2.0 LITERATURE REVIEW

## 2.1 Mechanisms of Hemostasis and Thrombosis

The term hemostasis literally means the stoppage of blood flow. This occurrence is necessary in instances of vascular injury to prevent excessive blood loss and involves a surprisingly complex series of interactions between blood proteins, cells and the vessel wall.

The normal, undamaged vascular surface is lined with endothelial cells and does not facilitate the process of hemostasis. However, when the endothelial lining is disrupted, as in the case of a cut, the exposure of the subendothelial region of the vessel wall results in the rapid activation of hemostatic mechanisms. A hemostatic plug is formed preventing blood loss.

The same blood elements that react quickly to prevent blood loss can be triggered inappropriately or excessively to cause the stoppage of blood flow through an intact vessel resulting in tissue death. This occurrence is termed thrombosis and involves the same physiologic mechanisms as hemostasis. The distinction lies in the definition of hemostasis as a physiologic response and thrombosis as a pathologic response.

### 2.1.1 Blood Coagulation

The protein-based mechanism of hemostasis is called coagulation. This response consists of a cascading series of enzymatic reactions involving several proteins resulting in the formation of a blood clot (Figure 2.1). The clot develops within 15 to 20 seconds if the trauma to the vessel wall is severe and in 1 to 2 minutes if minor [A.C. Guyton, 1987].

The mechanism of blood coagulation illustrated in Figure 2.1 is described as the classical coagulation cascade. This process can be activated either by the expression of

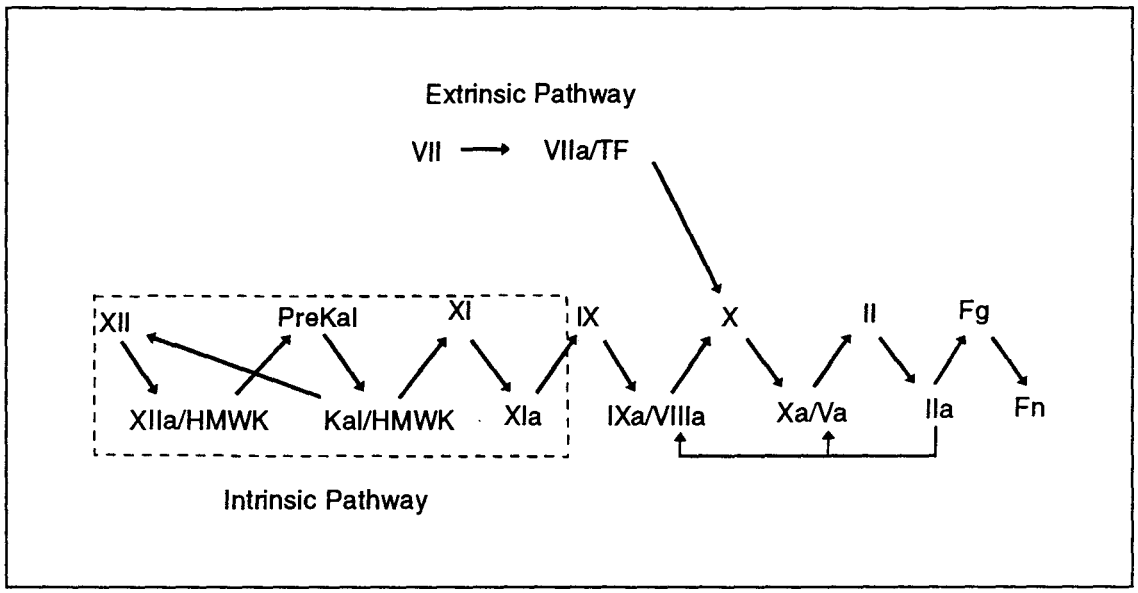


**Figure 2.1** - Classical blood coagulation cascade

tissue factor (TF), in which case the extrinsic pathway is said to be activated, or the activation of factor XII usually by a foreign surface resulting in the activation of the intrinsic pathway. In this model, we see the activation of blood zymogens (clotting factors) to proteolytic enzymes which then specifically attack the next zymogen in the cascade, converting it into an active enzyme in turn [Guyton, 1987]. A common feature among these proteolytic reactions is that most of them require free calcium ions. As well, at each step along the pathway there is an amplification of the response caused by downstream enzymes feeding back to augment the response. Therefore, a small initial stimulus can result in an "explosive" response as is necessary to prevent substantial blood loss.

While Figure 2.1 depicts the intrinsic and extrinsic pathways as distinct and separate until coinciding at the activation of factor X, it is likely that the two paths are interrelated to a greater degree and act synergistically to facilitate coagulation [Lawson and Mann, 1991].

The key reaction in the coagulation cascade involves the conversion of prothrombin to thrombin (factor II to IIa). This enzyme can then act to convert

fibrinogen to fibrin resulting in solid clot formation, feed back in the cascade to activate factors V, VIII, and XIII, the latter resulting in the crosslinking of the fibrin clot, as well as strongly stimulating platelets [Hirsh, 1987].

### 2.1.2 Platelet Response in Hemostasis

Platelets are non-nucleated, granular cells which circulate in the cardiovascular system in a discoid shape. Platelets do not adhere to the normal, undisturbed endothelial lining of the vasculature. However, once the circulating platelet contacts an abnormal surface (i.e. damaged vessel wall, artificial surface, atherosclerotic plaque) it rapidly responds by adhering to the surface and spreading. As platelets in the initial layer attached to the surface spread, they release their granular contents. The released material contains compounds which are capable of activating platelets in the vicinity of the initial site of adhesion, most notably adenosine diphosphate (ADP) [Kinlough-Rathbone and Mustard, 1987]. As well, coagulation factors are released (factor V, factor VIII and fibrinogen) which facilitate the concomitant process of coagulation [Niewiarowski and Varma, 1987].

Therefore, a platelet plug is created by the successive piling of activated platelets upon each other and the platelet membrane provides a surface for formation of coagulation complexes, thus increasing the rate of the coagulation reactions [Mann et al, 1990]. The initiation of the coagulation cascade results in the production of thrombin which in concert with platelet-produced ADP and thromboxane $A_2$ ($TxA_2$) induces platelet contraction creating a fused mass of platelets or "secondary hemostatic plug" [Guyton, 1987]. The concurrent initiation of the coagulation cascade results in the deposition of fibrin throughout the platelet mass stabilizing the plug and entrapping circulating red cells (Figure 2.2).

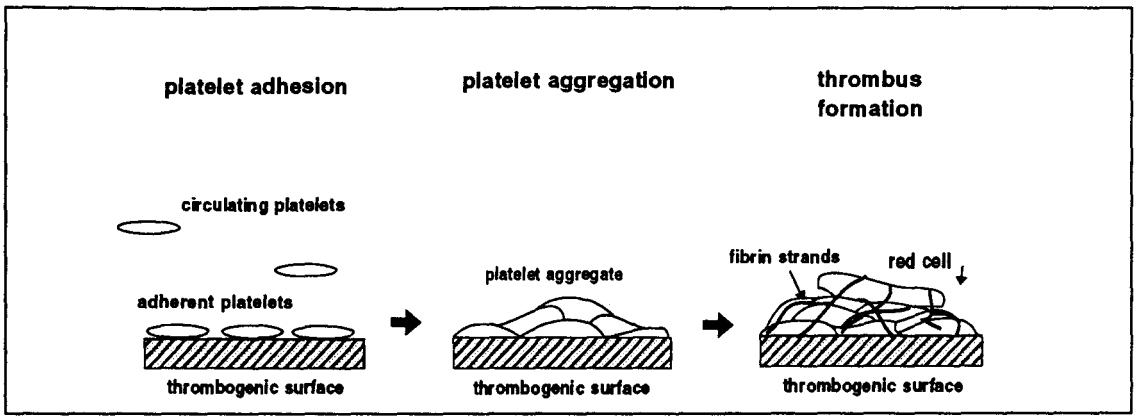


**Figure 2.2** - Illustration of thrombus evolution

### 2.1.3 Vessel Wall Interactions

The site for activation of the hemostatic system is provided by the vascular surface. Although blood vessels vary in nature throughout the cardiovascular system, there are many common features. Indeed, the role of the vessel wall in supporting hemostasis and thrombosis is a unifying feature.

The endothelial lining of the vessel lumen provides a barrier between the subendothelial matrix and the flowing blood. As the normal, undisturbed vessel wall does not stimulate the hemostatic system, it is apparent that the endothelial surface is inherently non-thrombogenic. The endothelial layer is composed of many closely adjoining endothelial cells. These cells are large, flat structures with the long axis aligned on the vessel wall parallel to the direction of blood flow [Stemerman, 1987]. While it was initially believed that the endothelium functioned simply as a passive barrier between the flowing blood and the thrombogenic subendothelium, it has now become apparent that the endothelial cell plays an active role in the processes of coagulation and fibrinolysis (the process of breaking down formed clots). Endothelial cells are capable of synthesizing subendothelial matrix proteins such as laminin and fibronectin which are ligands for platelet adhesion receptors [Foidhart et al, 1980 ; Jaffe and Mosher, 1978]. Coagulation factor V and tissue factor as well as thromboxane $A_2$ are synthesized by

endothelial cells, promoting both coagulation and platelet activation [Maynard et al, 1977 ; Ingerman-Wojenski et al, 1981]. Conversely, the same cells may exhibit anticoagulant and antiplatelet properties by expressing heparin-like molecules on the membrane surface to inactivate thrombin, as well as producing prostacyclin, a platelet inhibitor [Marcum et al, 1984 ; Moncada et al, 1976]. Thus, the endothelial cell is a surprisingly versatile and active cell that can act both to stimulate and inhibit the processes of thrombosis.

The region of the vessel wall immediately below the endothelium is the subendothelial matrix. This region is highly platelet-reactive and can also serve as a site for activation of the coagulation cascade. The region consists of many adhesive and connective molecules such as collagen, fibronectin, von Willebrand factor, laminin, and elastin [Kefalides, 1987]. Collagen is a potent initiator of platelet activation as well as a substrate for activation of the extrinsic coagulation pathway [Stemerman, 1987]. Fibronectin is a ubiquitous adhesive protein while von Willebrand factor is considered to be a key ligand for platelet adhesion under conditions of high shear flow [Roth, 1992].

As well, the muscular layer of the vessel wall in arteries reduces blood loss after rupture by transient vasoconstriction and this response can be mediated by platelet release products (serotonin and epinephrin) [Guyton, 1987].

Thus, a complex interaction between the vessel wall and the blood constituents regulates the mechanisms of hemostasis and thrombosis in the vascular system. These components serve to maintain blood fluidity under normal physiologic conditions while also responding rapidly to vessel wall trauma by creating a stoppage of blood flow by creation of a solid "plug". It is the complexity of the hemostatic process with its various checks and balances which makes the development of materials which mimic the endothelium for use as nonthrombogenic vascular prostheses very difficult.

## 2.2 Platelet Physiology and Response

Circulating, quiescent platelets have a characteristic discoid shape and are produced by budding from megakaryocyte cells. The platelet surface in the quiescent

state is smooth and convex, with no significant protuberances (Figure 2.3). Undisturbed platelets are approximately 2 μm in diameter and number 200,000 to 400,000 /μL in normal blood. Platelets circulate for an average of 10 days before being removed in the spleen and liver [Shulman and Jordan, 1987].

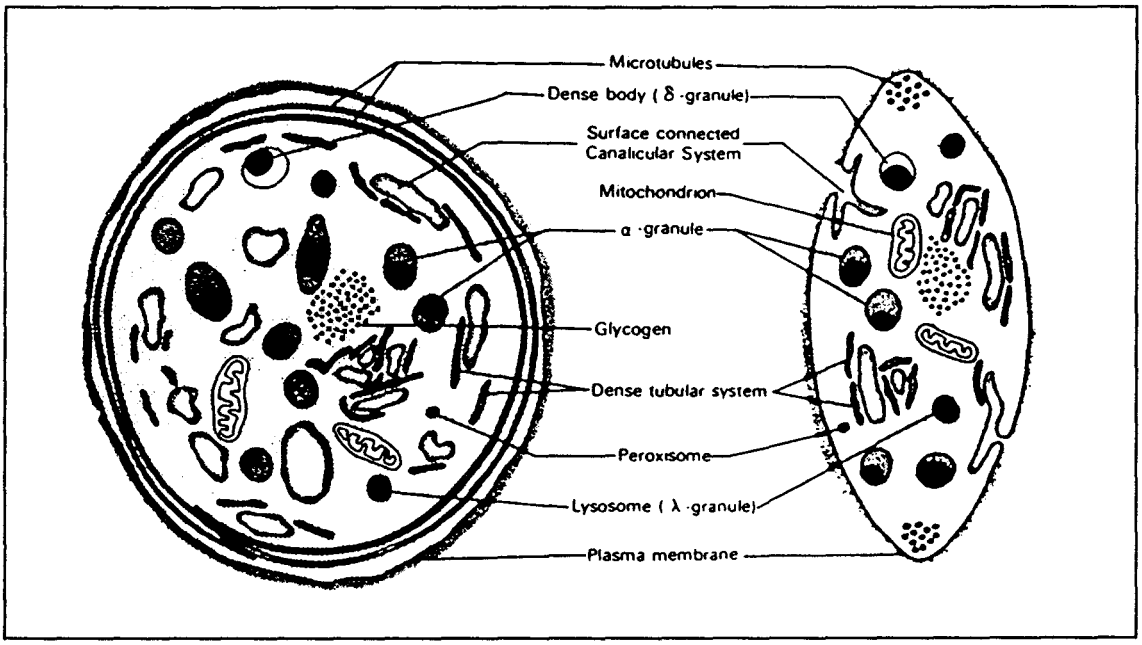


**Figure 2.3** - Platelet structural features [Bentfield-Barker and Bainton, 1982]

### 2.2.1 Platelet Structure and Physiology

Platelets contain three basic regions: the peripheral zone containing the cell membrane; the sol-gel zone or cytoplasmic region; and the organelle zone consisting of various types of cell granules.

The platelet's peripheral zone consists of the outer membrane and closely associated structures which provide the surface of the platelet including the walls of the surface-connected open canalicular system (OCS) (Figure 2.3). This system of channels greatly increases the surface area of the platelet membrane and serves as a transport route for the uptake of plasma-borne substances and the secretion of granular products during the release reaction [White, 1987]. As well, the open canalicular system interacts with

the dense tubular system (DTS) which is the site of calcium sequestration and enzymes utilized in prostaglandin synthesis.

The platelet membrane is a typical unit membrane consisting of a phospholipid bilayer similar to those of other cells. The stimulated platelet membrane provides a surface for interaction with coagulation proteins. It has been demonstrated that factors VIIIa, IXa, X and Va form complexes on the platelet membrane, thus enhancing prothrombin conversion [Hemker and Kahn, 1967 ; Kane et al, 1980]. In fact assembly of the prothrombinase complex on the membranes of activated platelets results in a significant increase in the rate of thrombin generation [Nesheim et al, 1992].

Imbedded in the platelet membrane are various adhesive molecules known as glycoproteins. These molecules are capable of recognizing and adhering to specific physiological ligands present in both the circulating blood and the vessel wall. This adhesion response is closely related to cell activation whereby the activity of the membrane receptors triggers chemical messengers which act to cause physical and chemical alterations in platelet functions [Nishizuka, 1989].

Therefore, the peripheral zone of the platelet serves both as a barrier between the cellular constituents and the flowing blood and as a communication pathway and selective transporter both into and out of the cell.

The sol-gel zone is so named because the cytoplasmic matrix of the cell resembles a gel. Various fiber systems are located in this region which support the discoid shape of the undisturbed platelet and provide a contractile system necessary for shape change, pseudopod formation, external contraction and secretion [White, 1987].

Platelets contain a circumferential band of microtubules found in a variety of cells (Figure 2.3). The primary role of these tubules appears to be the maintenance of the discoid shape of the quiescent platelet. During platelet activation and spreading, the organelles centralize to form a granulomere. In this configuration the central lump of organelles is encircled by a band of microtubules which are either constricted or disassembled and moved by a contractile wave to the cell center [White and Gerrard,

1987]. Thus, the microtubules appear to participate in both the maintenance of normal cell shape and the activation response.

Microfilaments represent the second system of fibers in the sol-gel zone. In the undisturbed platelet, it appears that the microfilaments are uniformly distributed, as actin filament precursors or extremely short filaments, in an unordered arrangement [Loftus and Albrecht, 1984]. After platelet activation, an increased number of filaments appear in the cytoplasm. These filaments become more highly organized during the course of activation. Filament arrays in the early stages of activation are randomly organized while those in the latter stages are more structured as shown by electron microscopic evaluation of Triton-extracted mounts [Loftus and Albrecht, 1984].

The organelles of the platelet are embedded in the cytoplasm. Platelets contain α-granules, dense granules, lysosomes, peroxisomes and mitochondria which are dispersed randomly throughout the cytoplasm of the quiescent platelet [Hawiger, 1989]. α-granules form the majority of the platelet granules and are a storage location for many biologically active molecules [White, 1993]. The dense granules (so called due to their electron opacity) also store a variety of substances which are active in hemostasis some of which are listed in Table 2.1. Since these granular contents are destined to be released during platelet activation, they will play an important role in hemostasis and thrombosis. The method of secretion appears to involve the fusion of the granule with OCS and release into the canalicular system [Harrison and Cramer, 1993]. As well, internal contraction of the platelet is necessary to drive the products extruded into the OCS into the surrounding media.

| Granule type | Contents |
|---|---|
| Dense body | adenine nucleotides (ADP & AMP)<br>guanine nucleotides (GTP & GDP)<br>serotonin<br>calcium & magnesium ions<br>inorganic phosphate |
| Alpha Granule | fibrinogen<br>von Willebrand factor<br>fibronectin<br>thrombospondin<br>high molecular weight kininogen<br>albumin<br>platelet factor 4<br>coagulation factor V<br>platelet-derived growth factor<br>transforming growth factor beta<br>alpha 2 antiplasmin<br>plasminogen activator inhibitor<br>IgG IgA |
| Lysosome | heparitinase<br>cathepsin<br>acid phosphatase<br>aryl sulphatase<br>beta glucuronidase |
| Peroxisome | catalase |

**Table 2.1** - Platelet granules and granule contents, from [White, 1993].

### 2.2.2 Platelet Receptors

Platelets are designed to recognize and seal any breaches in the endothelial lining of the vascular wall. Therefore, a recognition mechanism must exist alerting the platelet to the exposed subendothelial matrix resulting from injury. This role of "molecular sensor" is performed by the various platelet receptors for the adhesion molecules present in the extracellular matrix.

Platelet receptors are membrane proteins which can interact with a specific agonist

causing, in turn, a distinctive intracellular response which may be reversible. The importance of adhesive interactions in normal platelet function is reflected in the battery of receptors present on the cell membrane. However, the receptors utilized by platelets are very similar to those present on a variety of cells and are therefore representatives of larger adhesive gene families such as integrins, selectins and leucine-rich glycoproteins [Kieffer and Phillips, 1990].

A degree of conformational similarity is necessary between ligands and platelet membrane receptors. Since the molecules affecting platelet function are diverse in structure, it can be expected that a different receptor must exist for most stimulating agents. This supposition is borne out by the remarkable variety of receptors present on the platelet membrane (Table 2.2).

| Receptor | Ligand | Platelet Function |
|---|---|---|
| GP IIb-IIIa | fibrinogen<br>von Willebrand factor<br>fibronectin<br>thrombospondin<br>vitronectin | aggregation<br>adhesion at low shear rates |
| GP Ib-IX | von Willebrand factor | adhesion at high shear rates |
| GP Ia-IIa | collagen | adhesion |
| GP Ic-IIa | fibronectin | adhesion |
| GMP 140 | unknown | platelet-leucocyte interaction |
| GP Ic'-IIa | laminin | adhesion |
| Thrombin receptor | thrombin | activation |
| PECAM-1 | unknown | unknown |

**Table 2.2** - Platelet membrane receptors, ligands and the platelet function mediated by interaction [Kieffer and Phillips, 1990 ; Coughlin, 1993].

However, many receptors contain common subunits and therefore recognize similar amino acid sequences present in adhesive proteins. Thus it is possible to classify groups of receptors into gene families as described above. Most of the platelet surface

glycoproteins have been cloned and sequenced permitting classification into known gene families. A review of the literature on platelet receptors is somewhat confusing due to the inconsistent usage of nomenclature in this area of study. This confusion arises from the use of several different receptor designations. This review will circumvent the problem by use of the most commonly used terminology for platelet receptors based on the molecular weight of the glycoproteins comprising the receptors (eg. GP IIb-IIIa).

The two main adhesion receptors expressed by platelets are the GPIb-IX and GP IIb-IIIa complexes, their respective ligands being vWf and fibrinogen [Ruggeri, 1993]. On activated platelets, GPIIb-IIIa (member of integrin family) is a "promiscuous" receptor capable of interacting with several ligands (vWf, fibrinogen, vitronectin and fibronectin). However, on unactivated platelets the receptor has been shown to interact only with immobilized fibrinogen [Savage and Ruggeri, 1991]. The receptor complex requires free calcium ions in solution to achieve the correct conformation for adhesive interactions. Along with the fact that GPIIb-IIIa is the most abundant adhesive receptor on platelets (50,000 copies per platelet) it is not surprising that GPIIb-IIIa is required for platelet spreading over the subendothelium with its variety of adhesive ligands [deGroot, 1990]. GPIIb-IIIa is also considered to be the principal receptor involved in venous platelet adhesion (low shear flow environment) [Roth, 1992].

The GPIb-IX receptor (25,000 copies per platelet) is a member of the leucine-rich glycoprotein family of receptors and is considered to be the principal receptor mediating arterial platelet adhesion [Roth, 1992]. The interaction of GPIb-IX and vWf is unique in that it has been shown to be "shear-dependent". Under static conditions the two molecules have no affinity for each other. However, when shear forces are applied to the molecules, they develop a specific affinity for one another. Although the GPIb-IX complex does not require platelet activation to interact with vWf, it appears to require the presence of wall shear rates in excess of 650 $s^{-1}$ to facilitate vWf binding [Baumgartner, 1973]. It is uncertain whether the presence of shear alters the vWf molecule or the receptor or both, thus enabling interaction [Roth, 1991].

The principal collagen receptor on platelets is GPIa-IIa, a member of the integrin family. This receptor is present at 2000 copies per platelet [Hemler et al, 1988]. Although GPIa-IIa is a relatively minor component of the platelet membrane, its role in platelet adhesion is demonstrated by the inhibition of platelet adhesion to collagen resulting from the administration of a monoclonal antibody to GPIa-IIa [Kunicki et al, 1988]. Magnesium cations are required to enable the receptor complex to attain its reactive conformation [Morton et al, 1989]. While being the most commonly implicated collagen receptor, GPIa-IIa may not be the only receptor for collagen on platelets as GPIIb-IIIa and GPIV have also been implicated in this role [deGroot, 1990 ; Colman, 1991].

### 2.2.3 Response to Stimuli

When circulating platelets are exposed to any thrombogenic surface, such as the subendothelium or an artificial surface, a series of mechanisms constituting platelet activation are triggered. The stimulus results in an increase in cytosolic calcium levels leading in turn to several activation responses such as receptor upregulation, shape change, cytoskeletal organization, and centralization and release of granules. This response can be subdivided into three general phases: adhesion, aggregation and secretion.

#### 2.2.3.1 Platelet Adhesion

The adhesion of platelets to the vessel wall or any other surface is one of the first and most critical steps in the process of hemostasis or thrombosis. Morphological observations by Baumgartner and colleagues showed that platelets adhere to the arterial subendothelium through sequential stages: platelet-surface "contact", followed by activation and spreading of the individual contact platelets on the surface [Baumgartner, 1973]. Contact platelets remain discoid in shape but are rigidly attached to the surface. This "contact" represents the first phase of the adhesion process where an unactivated

platelet stops and "sticks" at a reactive surface [Sakariassen et al, 1989].

Once contact has occurred, the platelet becomes activated and begins to spread over the surrounding surface. This phenomenon is termed shape change and involves the extension of pseudopods, upregulation and redistribution of membrane receptors (notably GPIIb-IIIa), and the organization of the platelet cytoskeleton microfilaments including granule centralization [Kieffer et al, 1992]. The characteristic "fried egg" appearance of spread platelets results when viewed by electron microscope [Barnhart et al, 1972].

Much study in the area of biomaterials has been focused on the phenomenon of platelet adhesion in an attempt to evaluate material blood compatibility (discussed in section 2.3.2). As well, platelet adhesion to components of the extracellular matrix has received much attention in an attempt to elucidate the mechanisms at work in response to vascular damage [I.A. Feuerstein et al, 1975 ; Nievelstein et al, 1988 ; Sakariassen et al, 1989].

#### 2.2.3.2 Platelet Aggregation

At the conclusion of the initial adhesion event, a monolayer of spread platelets adhere to the surface. Additional platelets then adhere to the monolayer of spread cells, attaching to each other and forming aggregates. Platelet aggregation requires the normal functioning of the GPIIb-IIIa receptor complex [Phillips et al, 1988]. As well, platelet aggregation requires the presence of bifunctional adhesive proteins which are able to bind to the GPIIb-IIIa complexes of adjacent platelets, thus inter-connecting them [Hawiger, 1987]. The first and most common protein shown to bind to activated platelets is fibrinogen, both from plasma and from platelet granules [Mustard et al, 1978 ; Peerschke et al, 1990].

Platelets suspended in media containing no fibrinogen have been shown to aggregate poorly in response to stimulants which do not facilitate the release reaction, pointing to the importance of fibrinogen in aggregation [Harfenist et al, 1987 ; Suzuki et al, 1988]. However, release-promoting stimulants such as collagen and thrombin do

promote aggregation in the absence of exogenous fibrinogen. This may be due to the release of fibrinogen from the α-granules of the activated platelets [Legrand, 1989].

#### 2.2.3.3 Platelet Granule Secretion

The platelet release reaction entails the specific extrusion of the granule contents. This reaction can be induced by several agonists including thrombin and collagen as well as synthetic surfaces. Granule clustering in the centre of the activated platelet is an immediate precursor to granule release. The primary route for secretion of granular contents appears to be the open canalicular system (OCS) as the granules have been observed to fuse with the OCS immediately prior to secretion [White and Krumwiede, 1987].

The process of secretion is rapid, occurring within 20 to 120 seconds of stimulation depending on the strength of the stimulant. Many of the secreted substances have either direct action on cells or are converted to active substances in plasma or on cell surfaces (Table 2.1). The contents of the different types of platelet granules are secreted at different rates and to different degrees by various agonists [Harrison and Cramer, 1993]. For example, α-granule secretion may occur exclusively upon platelet stimulation by weak agonists whereas lysosomal secretion requires stronger stimulation [Kaplan et al, 1979 ; Holmsen et al, 1982].

Once secretion has occurred, the life-cycle of the platelet is complete. The platelet then serves as a substrate for coagulation reactions and a physical impediment to flow until either embolization or thrombus dissolution occurs.

### 2.2.4 Platelet Suspensions and Handling

The study of platelet response has been frequently performed in both plasma and buffer systems. While plasma systems offer the advantage of a more physiological environment, they are limited by the need for an anticoagulant which can often affect platelet function [Cazenave et al, 1979]. Kinlough-Rathbone et al summarized the

advantages of suspending platelets in an artificial medium as follows: physiological concentrations of divalent cations may be present; plasma enzymes are excluded, thus isolating platelet interactions; it is possible to manipulate the constituents of the medium easily [Kinlough-Rathbone et al, 1977]. As well, from a clinical perspective, storage of platelets for transfusion in an artificial medium saves donated plasma and avoids reactions caused by incompatible plasma proteins [Holme, 1992]. However, the principal limitation of the use of artificial suspensions is that they are artificial and therefore experimental results obtained using these suspensions may not apply to the physiological environment.

The concept of storing platelets in a plasma-free artificial medium began in the 1950's. Several attempts at preservation were made utilizing different suspension recipes but were not generally successful [Holme, 1992]. Eventually, by the 1970's some agreement was reached as to the characteristics of a successful suspension medium [Day et al, 1975]. Although suspension media vary from lab to lab, there are some essential elements common to most suspension formulas: divalent cations, glucose, a buffer solution, inhibitors of activation, and albumin or other plasma proteins.

The presence of divalent cations, namely calcium and magnesium, is essential for several platelet-ligand adhesive interactions. Most notably, the GPIIb-IIIa receptor complex requires free calcium ions to achieve a conformation capable of interacting with fibrinogen. As citrated plasma contains reduced free calcium ion concentration, studies of platelet adhesion in these environments have been shown to result in significantly reduced levels of platelet adhesion as compared to divalent ion-containing suspensions [Cazenave et al, 1979]. As well, it has been shown that calcium ions are required to facilitate platelet adherence to the subendothelium of human arteries (via factor VIII-vWf) [Sakariassen et al, 1984], and magnesium ion dependent platelet adhesion to collagen via GPIa-IIa has been reported [Zijenah et al, 1990].

Glucose is utilized in platelet suspensions as a nutrient, and is metabolized to lactic acid [Holme, 1992]. This reaction will cause a decrease in suspension pH unless

a buffer system is used. (Another approach to avoid this drop in pH involves the use of a glucose-free medium [Murphy et al, 1991]. However, it is seems likely that glucose is required for maintenance of normal platelet function). A fall in pH to a value less than 6.2 during storage has been associated with loss of platelet viability [Murphy, 1985]. Buffering is generally achieved through the addition of $NaHCO_3$ and $NaH_2PO_4$ (Tyrodes buffer solution) to the suspension fluid [Mustard et al, 1972 ; Holme, 1992].

It is also necessary that the suspension medium contain some inhibitor of platelet activation at least during the isolation and handling of the platelet concentrates. This need arises from the carry over of red cells from the separation of the red cell concentrate and the platelet-rich plasma. These red cells may lyse or otherwise release ADP, a known platelet activating compound. Thus, either an ADP scavenger such as apyrase [Mustard et al, 1972] or a blocker of platelet activation such as prostacyclin [Rhodes, 1993] must be present in the suspension in sufficient quantity to prevent shape change and aggregation during handling.

The addition of albumin to the suspension medium reduces the metabolic activity of the platelets and results in an improved maintenance of function and cellular integrity [Holme, 1992]. Albumin is also known to inhibit the adhesion of platelets to surfaces [Mulvihill et al, 1990 ; Amiji et al, 1992]. As well, the presence of albumin in the suspension medium reduces the loss of platelet constituent materials during handling and resuspension procedures [Doery et al, 1973]. The mechanism by which albumin exerts a protective effect on suspended platelets is unknown, but is probably related to the maintenance of cell membrane integrity. Since albumin does inhibit platelet adherence to surfaces, it is necessary to use as little as possible in the final suspension when studying platelet adhesion.

## 2.3 Blood-Material Interactions

The exposure of blood in devices which contain artificial surfaces can lead to several harmful events, the most immediately important being thrombosis and subsequent

embolization. The development of a thrombus may impede flow through the device conduits thereby compromising the performance of the device. The thrombus may then be dislodged by the shearing action of circulatory flow and subsequently lodge downstream with dire consequences (stroke, myocardial infarct). While the development of thrombi and emboli are generally the most immediate and life-threatening consequences resulting from blood-material interactions, there are other less drastic consequences such as increased platelet consumption, remote systemic effects resulting from the local production of thrombosis byproducts, and abnormalities in platelet function resulting from platelet interactions with the artificial surface.

### 2.3.1 Protein Deposition

It is widely believed that the initial composition of the deposited protein layer influences subsequent blood-surface events, namely platelet adhesion and activation. Additionally, the conformation of the adsorbed proteins is critically important since maintenance of structure is often required for the facilitation of biological reactions.

Fibrinogen is one of the most extensively studied plasma proteins related to blood-material interactions. It appears to be deposited on a number of surfaces in excess of its relative concentration in plasma [Brash, 1977 ; Vroman et al, 1977]. The adsorption of fibrinogen to material surfaces is known to accelerate platelet adhesion and activation [Brash, 1987]. Conversely, the adsorption of albumin to artificial surfaces tends to render the surface platelet-resistant [Packham et al, 1969 ; Park et al, 1986].

The adsorption of other plasma proteins has been less thoroughly studied, although several platelet adhesion promoting proteins have been investigated. These include fibronectin [Nievelstein et al, 1988], vitronectin [Bale et al, 1989], thrombospondin [Young et al, 1982], von Willebrand factor [Ruggeri, 1993], and thrombin [McManama et al, 1986]. While these proteins promote adhesion, they do not provoke the complete platelet reaction. The adsorption of coagulation factor XII to an artificial surface is felt to alter its conformation in such a way as to activate the protein thus initiating the

intrinsic coagulation pathway [Furie and Furie, 1988].

Upon adsorption, a protein may undergo structural alteration which can lead to an alteration in biological activity. The physical characteristics of the artificial surface will affect the protein's affinity for the surface and its subsequent adsorption conformation [Vroman and Leonard, 1977]. Material surface characteristics implicated in modulating adsorption are surface charge, structural mobility, interfacial free energy and hydrophobicity. However, no consensus has been reached regarding the most favourable material surface characteristics due to both the difficulty in accurately characterizing surfaces and the inherent complexity of the blood environment.

### 2.3.2 Platelet Interactions

Platelet deposition onto the artificial surface follows the initial adsorption of plasma proteins and occurs on virtually all artificial surfaces to varying degrees. Under normal blood flow conditions, platelets continually collide with the vessel surface. Once the platelet has reached the surface it may either "stick" or "bounce off" depending on the degree of activation of the platelet and its surface binding affinity [Adams, 1985].

To withstand the shear forces exerted on adherent platelets by flowing blood, strong bonds form between the platelet and the surface. These bonds likely involve GPIIb-IIIa since this receptor is able to bind to a variety of adhesive ligands and is abundant in the platelet membrane [Ruggeri, 1993]. Presumably the nature of the adsorbed protein layer dictates the strength of platelet adhesion.

The number of adherent platelets is the parameter most often used to characterize the platelet-contacting response of a material [Okkema and Cooper, 1991 ; Takahara et al, 1991]. This type of data may be obtained either by radiolabelling platelets with $^{51}Cr$ [Dosne et al, 1976] or $^{111}In$ [Thakur et al, 1976] isotopes or by microscopic evaluation. Other platelet parameters have been studied, including amount of granular contents released and degree of spreading of adherent platelets [Ito et al, 1991 ; Silver et al, 1993]. While the above measures of surface platelet reactivity can be obtained from in vitro, in

vivo or ex vivo experiments, platelet consumption tests are necessarily performed ex vivo or in vivo. Consumption can indicate a type of platelet-surface interaction that is not apparent in experiments which measure adhesion at discrete time intervals [Ip and Sefton, 1991].

While simple studies of platelet adhesion are instructive in examining material thrombogenicity, the results obtained by in vitro and ex vivo methods are often dissimilar [Silver et al, 1993]. As well, there is no general agreement on what type of platelet response is most desirable. For example, a quickly formed spread monolayer of platelets may act to form a neointima which is relatively unreactive but will yield high values of platelet adhesion by experimental observation. Conversely, a surface which stimulates platelet adhesion and subsequent release may appear to be unreactive towards platelets by standard measures such as adhesion number, but may result in high levels of platelet consumption and altered platelet function.

### 2.3.3 Thrombus Formation and Embolization

Thrombi formed on artificial surfaces are similar to those formed on the injured vessel wall. The growth of the thrombus begins with the initial attachment of a platelet to the artificial surface. This adherent platelet then acts as a nucleation site for the further attachment of platelets resulting in thrombus growth [Adams, 1985]. The coagulation system is also activated, producing fibrin strands which intertwine throughout the thrombus, thereby stabilizing it.

Once the thrombus has grown to a "threshold" size, it may become dislodged from the surface by the shearing action of the flowing blood (embolization). The surface site previously occupied by the thrombus is then temporarily passivated by unknown mechanisms [Lelah and Cooper, 1986]. The entire process may then be repeated. This mechanism will lead to increased platelet consumption as the aggregated emboli will be removed from the circulation, or tissue death resulting from downstream blockage of lesser diameter vessels will occur (Figure 2.4).

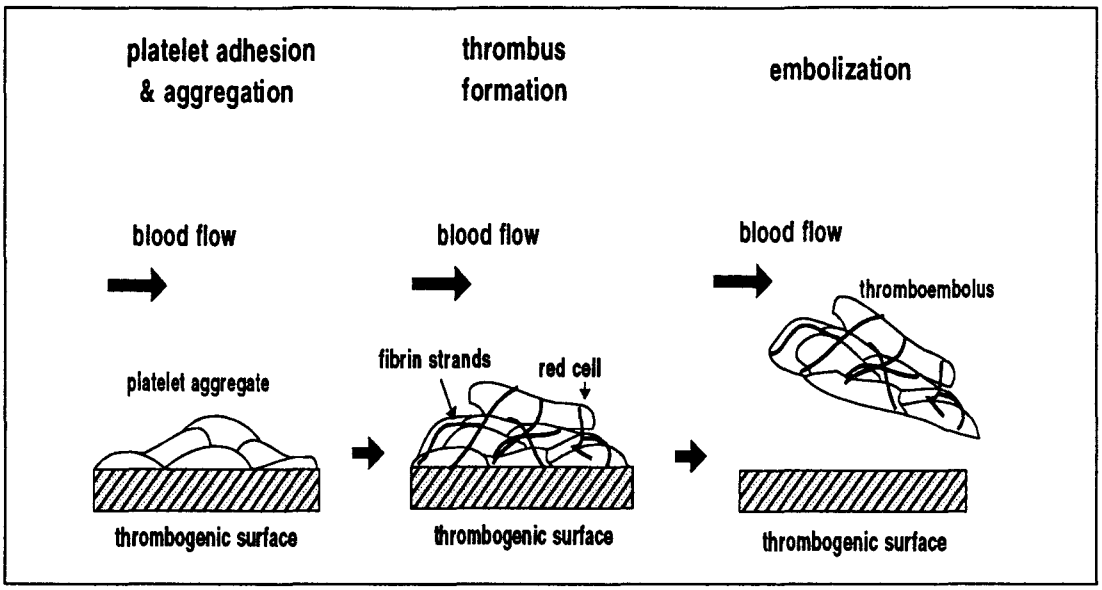


**Figure 2.4** - Illustration of the process of thromboembolism resulting from surface-induced thrombosis

If the thrombus does not become dislodged and continues to grow, it may occlude the entire vessel causing stoppage of blood flow.

It is evident that many of the same mechanisms active in the physiological processes of hemostasis are at work when blood contacts artificial surfaces. The lack of a nonthrombogenic endothelial lining predisposes any artificial surface to thrombus formation to some degree depending on the nature of the adsorbed protein layer and the rheological properties of the system.

## 2.4 Techniques for Studying Platelet-Surface Interactions

The processes of hemostasis and thrombosis are intimately interrelated with the dynamics of blood flow. Therefore, it is essential to consider the rheological behaviour of blood and the impact this will have on the transport of reactive components (notably platelets) to and from material surfaces. A number of flow chambers utilizing various flow geometries have been developed over the past several decades in order to examine the interactions of blood components, particularly platelets, with various surfaces. The

central consideration in designing these devices is the development of defined fluid shear flow similar to that which is present in the vasculature.

### 2.4.1 Fluid Dynamics of Blood

Thrombosis can be viewed as a process whereby flowing blood components interact with the vessel wall and which, therefore, will be influenced by hemodynamics. Plasma viscosity, red cell concentration (hematocrit), and red cell deformability are parameters which greatly influence and dictate blood flow characteristics. These parameters have been found to be abnormal in several thromboembolic disease states [Chien, 1977 ; Letcher and S. Chien, 1981].

#### 2.4.1.1 Poiseuille Flow

Perhaps the simplest way to begin a discussion of the mechanics of blood flow is to consider the most commonly applied model of steady, pressure-driven flow in a rigid, circular tube. The pressure-flowrate relation is described by the well-known Poiseuille equation (Equation 2.1): indicating a parabolic velocity profile, with shear rate and shear stress distributions as shown in Figure 2.5.

$$Q = \frac{\pi(\Delta P)}{8\mu L}R^4 \qquad (2.1)$$

$Q$ = *volumetric flow rate*
$\Delta P$ = *pressure difference*
$\mu$ = *fluid viscosity*
$L$ = *tube length*
$R$ = *tube radius*

It is observed that the shear rate and shear stress reach their maximal values at the tube wall. However, blood in the vasculature does not flow steadily through circular, rigid

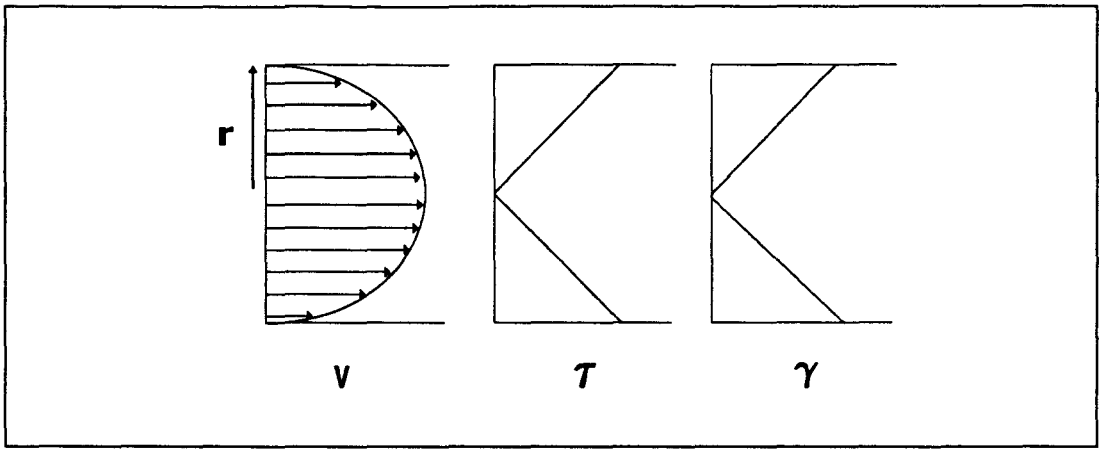


**Figure 2.5** - Velocity (v), shear stress ($\tau$) and shear rate ($\gamma$) profiles across the radius (r) of a tube derived from Poiseuille equation.

tubes. The blood vessel walls are elastic in nature and blood flow is pulsatile, particularly in the arteries. As well, blood vessels frequently branch and bend causing significant deviations from simple Poiseuille flow.

### 2.4.1.2 Characteristics of Blood Flow

There are several reasons for the deviation of actual blood flow dynamics from those described by the Poiseuille equation. These include the presence of entrance effects, pulsatile flow, vessel wall elasticity, and turbulence as well as the geometry of the vessels and the non-Newtonian behaviour of blood.

Blood flow in the vasculature is generally not fully developed. The entrance length in the aorta required for fully developed flow is calculated to be greater than 0.26 m [Goldsmith and Turitto, 1986]. This length is greater than the distance travelled by blood in the aorta before branching occurs, and branching leads to flow disturbances. Therefore, it appears that blood circulates in the vasculature in a flow field which is never fully developed leading to a blunting of the velocity profile predicted by the Poiseuille equation and thus to higher wall shear stresses as well.

Pulsatile flow prevails throughout the arterial tree, with decreasing pressure pulse amplitude as distance from the heart increases. This in turn leads to a transient, time-

dependent velocity profile not accounted for by the Poiseuille equation and not often modeled by in vitro experiments [van Breugel et al, 1988]. Vessel wall elasticity results in the radial dilatation of the vessel due to the pressure pulse, thus imparting a radial component to the flow. This effect, however, appears to be appreciable only in the aorta and pulmonary arteries. The internal surface area of the ascending aorta at peak systolic pressure may increase by more than 10% compared to the diastolic value [Turitto, 1982].

The continuous branching of the vasculature creates sudden changes in fluid direction and velocity which may in turn lead to the formation of secondary flows and vortices [Goldsmith and Turitto, 1986]. The geometric complexity of the vascular route makes the precise modeling of blood flow behaviour in vivo extremely challenging. However, some research has investigated the flow patterns present at vessel bifurcations and junctions [Goldsmith and Turitto, 1986] as well as at vessel stenoses (pathologic narrowing of lumen) [Turitto, 1982 ; Back et al, 1977].

Strictly speaking, blood is not a Newtonian fluid, since it exhibits shear-thinning behaviour (Figure 2.6).

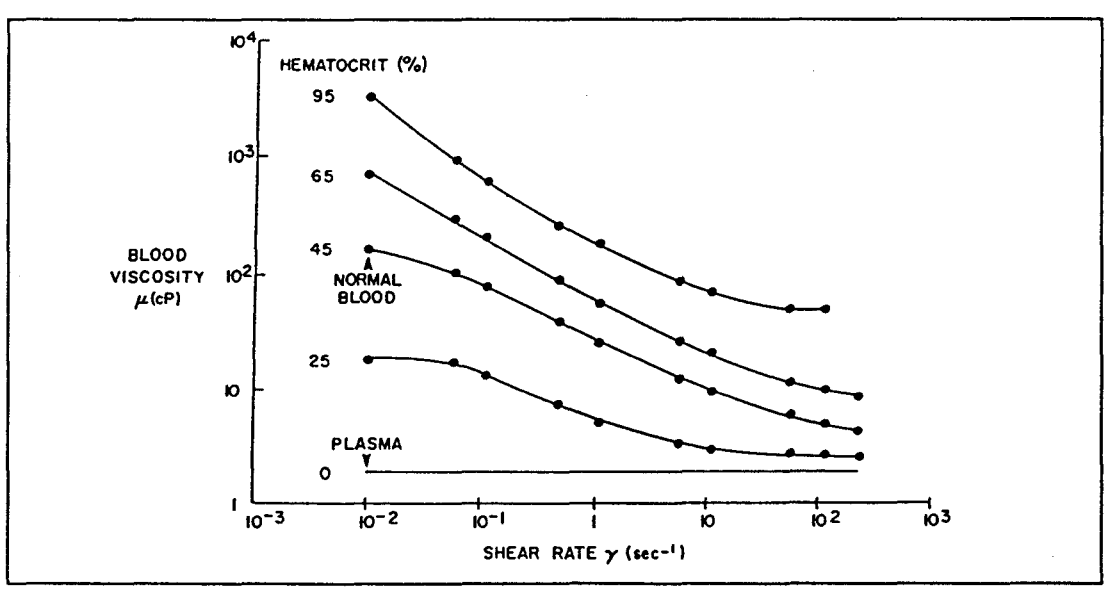


**Figure 2.6** - Shear-dependent viscosity characteristics of whole blood [Chien, 1975].

The Newtonian behaviour of plasma [Harkness, 1971] indicates that the non-ideal

properties of blood flow can be attributed essentially to the presence of red cells which comprise a large portion of the blood volume (40 to 45%). As is evident from Figure 2.6, blood viscosity is a strong function of red cell concentration. In addition, the viscosity is shear rate-dependent at shear rates less than approximately 50 $sec^{-1}$. The unique physical nature of the red cell, however, results in a lower fluid viscosity than would be achieved by the use of equivalent rigid particles in suspension [Goldsmith and Turitto, 1986]. This is due to the deformability of red cells. It is this property which allows red cells to flow through capillaries of lesser diameter than the red cell itself. In addition, as fluid shear rates are increased, red cells have been demonstrated to align their major axis along the direction of flow and display a "tank-tread" motion where the membrane rotates around the cell interior. This motion is believed to transmit the shear stress of the flow across the interface thereby reducing the cell's resistance to flow much as in the case of fluid drops [Keller and Skalak, 1982].

At low fluid shear rates, the non-Newtonian behaviour of blood has been attributed to the formation of red cell aggregates or rouleaux [Chien, 1975]. These aggregates are believed to be held together by fibrinogen bridges and are dispersed by the shearing forces of flow when the fluid shear rate exceeds approximately 50 $s^{-1}$ [Goldsmith and Turitto, 1986]. However, when the red cells are washed and placed in a protein-free suspension medium, the non-Newtonian behaviour at low shear rates is much less pronounced.

Therefore, while blood flow is commonly modeled as well-defined and laminar in the circulation, there are several complicating factors introduced both by the unique nature of blood and of the vasculature.

### 2.4.2 Platelet Transport in Flow

The local motions of red cells in flowing blood play an essential role in the process of thrombosis. In order for platelets to interact with a surface, they must first travel through the blood in a direction normal to that of the flow. Assuming the flow to

be essentially laminar in nature, there are no convective forces which may transport platelets to the tube wall. Therefore, Brownian motion considerations should yield appropriate platelet diffusion coefficients, assuming the blood medium may be considered to be a continuum. Use of the Stokes-Einstein equation (Equation 2.2) to estimate

$$D=\frac{k_B T_A}{6\pi \mu_f R_P} \tag{2.2}$$

$k_B$=*Boltzmann's constant*
$T_A$=*absolute temperature(K)*
$R_P$=*mean effective platelet radius*
$\mu_f$=*plasma viscosity*

platelet diffusion coefficients yields values which are orders of magnitude lower than those experimentally observed in whole blood [Turitto et al, 1972]. The diffusion coefficients for platelets have been determined experimentally to be of the order of $10^{-7}$ $cm^2/s$, similar to many plasma proteins [Slack et al 1993]. As well, the rate of platelet diffusion in flowing blood is dependent on the fluid shear rate [Grabowski et al, 1972]. In systems devoid of red cells, a marked decrease in platelet transport and adhesion have been observed [Goldsmith and Turitto, 1986]. While the effect of red cells was originally attributed to ADP released from the cells under flow conditions, it has been subsequently shown to be a physical rather than chemical affect.

These seemingly curious observations are a result of the motions of red cells in shear flow which serve to augment platelet transport in the radial direction [Goldsmith and Turitto, 1986]. The rotation and radial motions of red cells in flow act to increase the effective platelet diffusivity. As well, a concentration gradient whereby red cells are more abundant in the central core of the tube results in an increased concentration of platelets close to the vessel wall [Eckstein et al, 1988]. The physical role of red cells in augmented platelet diffusion has been established repeatedly; however, the precise origin

of the forces involved is still somewhat obscure [Slack et al, 1993].

Feuerstein et al calculated platelet diffusion coefficients by measuring platelet adhesion to reconstituted collagen and artificial surfaces in a rotating probe device [Feuerstein et al, 1975].

The following solution to the diffusion equation was used:

$$M=C_o[-\frac{D}{k}+\frac{2}{\sqrt{\pi}}\sqrt{Dt}] \tag{2.3}$$

$M$ = *surface platelet concentration*
$C_o$ = *bulk platelet concentration*
$D$ = *diffusivity*
$k$ = *reaction rate constant*
$t$ = *exposure time*

The separation of platelet-surface reaction and platelet diffusion terms in the above equation enables one to ascertain the relative contributions of these processes to adhesion.

Obviously, any study of platelet-surface interactions should be performed in a flow environment as similar to that of the vasculature as possible, and certainly in the presence of red cells. To this end, several devices have been developed over the past several years.

### 2.4.3 Glass Bead Columns

In 1960, Hellem [Hellem, 1960] utilized a column packed with small-diameter beads to measure platelet-surface interactions. The technique involved pumping whole blood through the packed column and measuring the reduction in platelet count in the outlet stream. In the column, platelets adhered to the bead surfaces and to each other as well as releasing granule contents. This test is now referred to as a platelet retention test since no differentiation can be made between retention by adhesion or aggregation within the column. This procedure was used to diagnose patients with von Willebrand's disease [Salzman, 1963], a disorder involving a lack of the adhesive protein vWf. In subsequent

studies, the packed beads were coated with various plasma proteins to elucidate protein-platelet interactions, most notably albumin and fibrinogen [Packham et al, 1969 ; Zucker and Vroman, 1969].

The most serious drawback of this apparatus is the lack of defined flow in the packed column. This deficiency makes the quantitative study of platelet transport and adhesion with respect to fluid flow parameters impossible. Therefore, this device is of limited use for research aimed at a mechanistic understanding of platelet adhesion.

### 2.4.4 Baumgartner Flow Chamber

One of the first platelet perfusion devices which considered the effects of fluid flow was the Baumgartner chamber [Baumgartner, 1973]. This apparatus was originally employed to study platelet interactions with the subendothelium of an everted vessel segment using anticoagulated blood. The device employs a central rod, which supports the test material in the form of a tube, inside a cylindrical chamber (Figure 2.7).

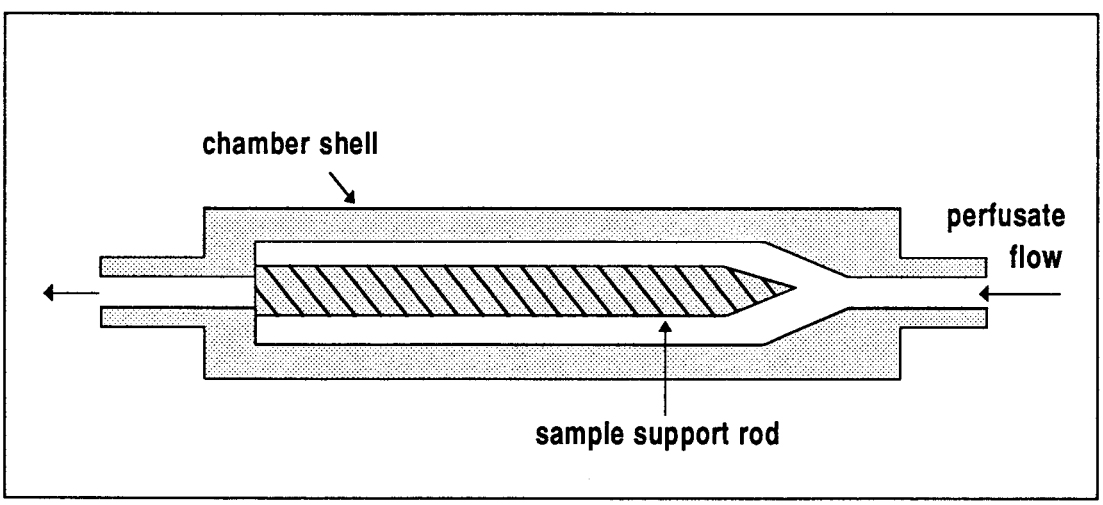


**Figure 2.7** - Diagram of Baumgartner flow chamber. Adapted from [Baumgartner, 1973]

Following the perfusion period, the test material is removed and prepared for microscopic evaluation. This technique allows the experimenter to examine separately the adhesive and cohesive interactions of platelets as well as the morphological features

of shape change and spreading [Turitto and Baumgartner, 1979]. As well, a range of fluid shear rates can be achieved by varying the flow rate through the chamber and varying the chamber geometry [Sakariassen et al, 1989].

Limitations of this device include the need for anticoagulation, common to all in vitro procedures, and the relatively large volume of blood that is necessary for perfusion, necessitating a recirculation system and pump. Pumps have been found to cause significant damage to the formed elements of blood, notably red cells. Red cell lysis results in ADP release into the test fluid causing platelet activation and confusing adhesion measurements.

### 2.4.5 Rectangular Slit Perfusion Chamber

Sakariassen et al developed a parallel plate chamber to study platelet-surface interactions using a rectangular flow geometry [Sakariassen et al, 1983]. This chamber permits the use of flat test specimens which are much easier to prepare than cylindrical configurations when studying artificial surfaces or coated surfaces [Sakariassen et al, 1988 ; Sakariassen et al, 1990].

The flow slit is rectangular in cross-section (Figure 2.8). Various fluid shear rates can be produced by varying the slit height and fluid flow rate; however, slit heights smaller than 0.6 mm may produce flow disturbances [Sakariassen et al, 1989]. The test surface is positioned on a knob which is placed into the perfusion chamber forming a portion of the upper surface of the rectangular chamber.

A drawback of this apparatus is again the need for blood recirculation using a pump as described above. However, this chamber requires less blood than the Baumgartner chamber because of the small size of the rectangular slit.

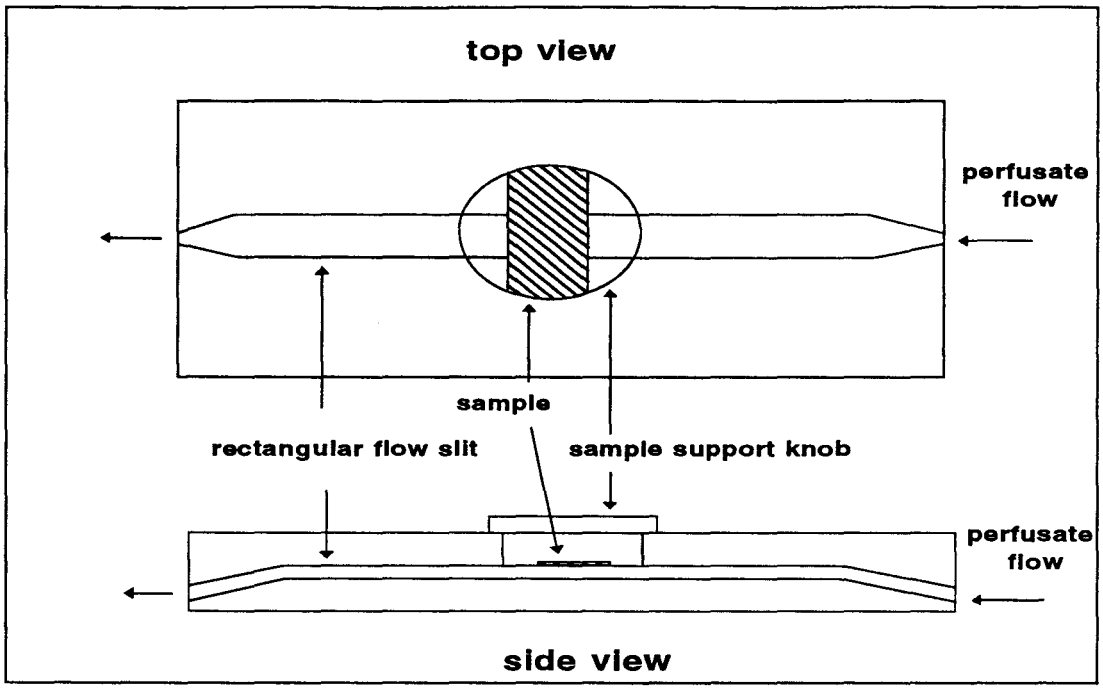


**Figure 2.8** - Rectangular slit perfusion chamber described by Sakariassen et al [1983].

### 2.4.6 Cone and Plate Apparatus

The cone and plate geometry commonly employed in commercial viscometers has been adapted for the study of platelet aggregation [Yung and Frojmovic, 1982 ; Fukuyama et al, 1989 ; Belval et al, 1984]. This geometry has also been employed in blood viscometry [Schmid-Schoenbein et al, 1973]

The cone and plate apparatus consists of a cone, the tip of which touches a flat base plate. A fluid is placed in the gap between the cone and plate and the cone is rotated at a set speed (Figure 2.9). The cone and plate geometry leads to a uniform rate of shear in the fluid present in the gap between the cone and plate, across the entire radius of the rotating cone. However, the cone angle $\Theta$ must be small (less than 10°) to satisfy the uniform shear condition.

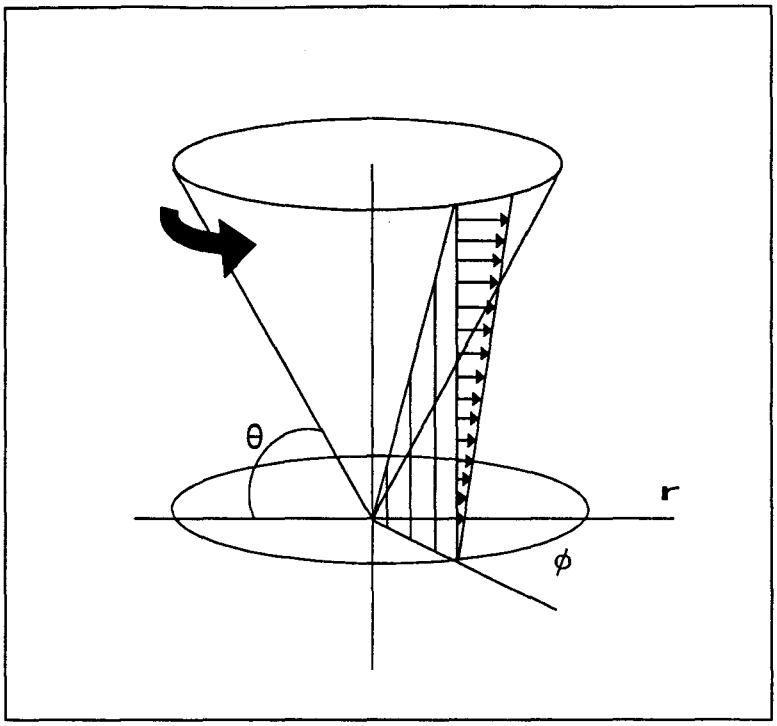


**Figure 2.9** - Fluid flow profile for cone-and-plate flow geometry.

For small angles, the fluid shear rate is given by

$$\gamma = \frac{\Omega}{\theta} \tag{2.4}$$

$\gamma$ = *shear rate* ($sec^{-1}$)
$\Omega$ = *cone rotation rate* (*rad/s*)
$\theta$ = *cone pitch* (*rad*)

The apparatus permits the use of flat test surfaces serving as the plate in the system, and the fluid shear rate can be easily varied by adjusting the rotational speed of the cone or the cone angle. A small volume of blood is sufficient to fill the gap between the cone and plate, eliminating the need for a recirculation pump. A cone-and-plate apparatus was developed for use in the present work. The details of this device are discussed in Section 3.3.

The principal drawbacks of this apparatus are the closed nature of the system which allows activation factors to accumulate, and the relatively large area presented by the cone surface. It is possible that platelets may be activated on contact with this surface, and the activation products may influence events at the test surface (plate).

### 2.4.7 Cone-and-Plate Flow Characteristics

The established theory of cone-and-plate fluid mechanics assumes that the streamlines of the fluid present in the gap between the cone and plate are circles and the shearing stress of the fluid is constant across the entire radius of the rotating cone [Walters, 1975]. The central equation for cone-and-plate flow (Equation 2.4) relies on the existence of a simple type of flow throughout the liquid (Figure 2.9) and numerous assumptions are made to ensure such flow. Therefore, it is instructive to consider the extent to which these assumptions are valid in practical situations.

First, a constant shear rate throughout the liquid is assumed. This assumption is largely dependent on the gap angle of the cone [Walters, 1975]. The cone angle must be sufficiently small to validate this assumption. The flow equations may be solved exactly for a Newtonian fluid assuming negligible fluid inertia and compared to Equation 2.4 [Adams and Lodge, 1964]. Table 2.3 shows the effect of cone angle on the validity of Equation 2.4. It is noted from this analysis that an acceptably small amount of error is introduced even for cone angles as great as 10°. Therefore, the constant shear rate assumption appears to be a reasonable one.

Second, for theoretical purposes it is assumed that the cone and plate are infinite in diameter. Obviously, all practical devices are finite in size and, therefore, edge effects will arise. Analyses of this phenomenon generally focus on the effect of the finite dimensions of the device assuming a "free" liquid surface, i.e. a liquid surface at the outermost portion of the gap in contact with air [Slattery, 1964 ; Tanner, 1970]. The flow distortion caused by edge effects can be visualized and has been shown to result in vortices at the cone periphery (Figure 2.10).

| *Gap angle (degrees)* | *Variation of shear rate across gap (%)* | *Error in using formula* $q = \Omega_1 / \theta_0$ *(%)* |
|---|---|---|
| 1 | 0.03 | 0.02 |
| 2 | 0.21 | 0.08 |
| 3 | 0.28 | 0.18 |
| 4 | 0.49 | 0.32 |
| 5 | 0.77 | 0.50 |
| 7 | 1.5 | 0.98 |
| 10 | 3.1 | 2.0 |

**Table 2.3** - Shear rate deviation from that predicted using Equation 2.4 as a function of cone angle [Adams and Lodge, 1964].

vortices at the cone periphery (Figure 2.10).

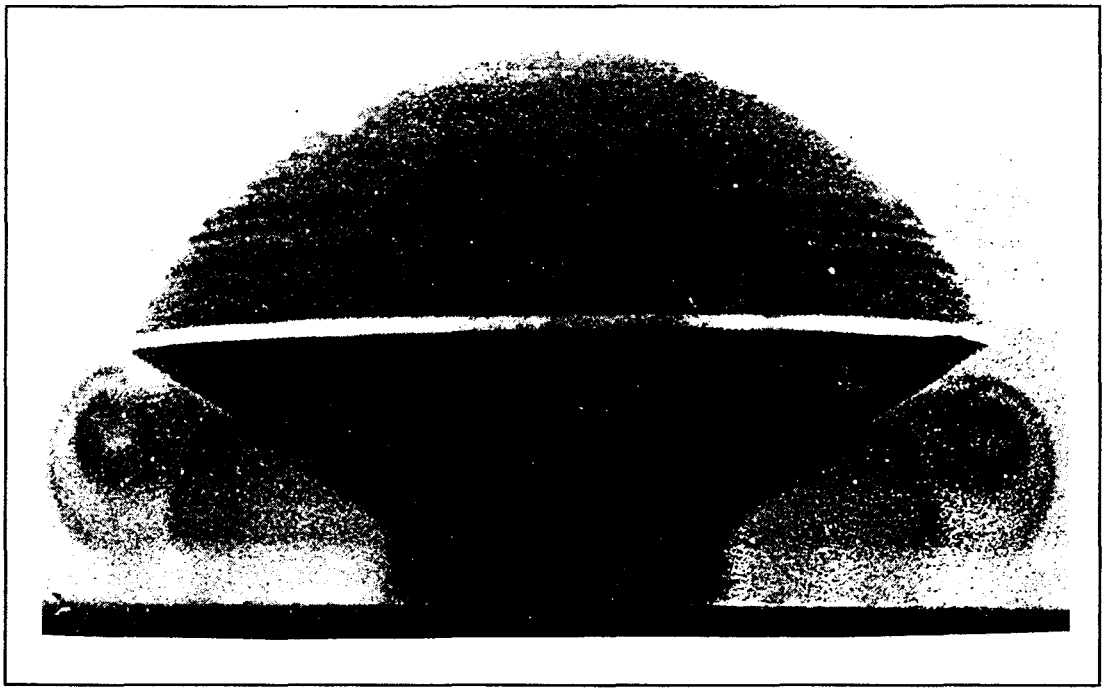

**Figure 2.10** - Flow distortions created by edge effects of cone-and-plate device [Griffiths and Walters, 1970].

Finally, Equation 2.4 is obtained in part by the assumption of steady shearing flow

for the infinite cone-and-plate geometry are shown in Figure 2.11.

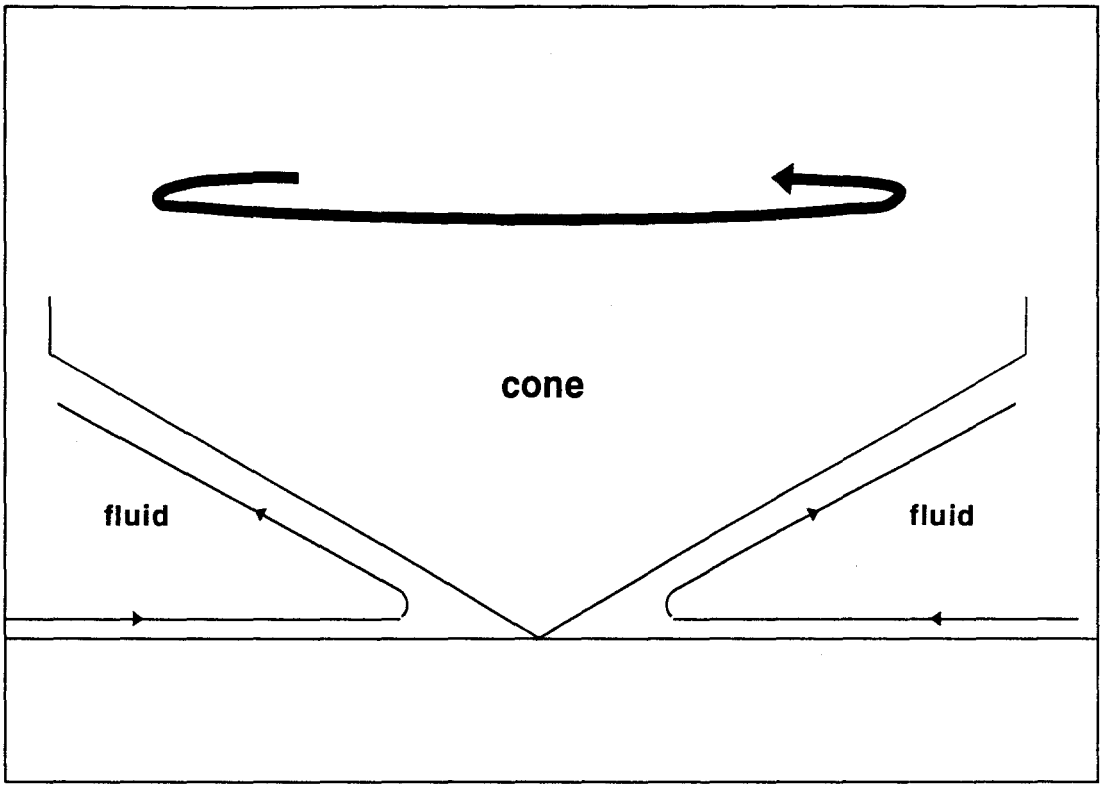


**Figure 2.11** - Secondary flows in cone-and-plate flow, from [Walters, 1975].

These secondary flows give rise to "secondary stresses" which may become significant when fluid inertia is important as in the case of relatively low viscosity liquids in high speed rotation [Walters, 1975].

Due to the complexity of the problem of cone-and-plate flow with appreciable fluid inertial effects, theoretical considerations have met with limited success [Walters, 1975]. Analytical solutions to the problem have been attempted for Newtonian liquids [King and Waters, 1970], and Turian developed an equation relating the Reynolds number of the system to the effect of secondary flows on the measured torque (T) on the cone, in comparison to the torque generated by purely tangential flow ($T_o$), where the Reynolds

number and the torque equation are stated as

$$Re = \frac{\rho \Omega R^2}{\mu} \tag{2.5}$$

$$\frac{T}{T_o} = 1 + \frac{3}{4900} Re^2 \tag{2.6}$$

$\rho$ = *fluid density*
$\Omega$ = *cone rotation rate*
$R$ = *cone radius*
$\mu$ = *fluid viscosity*

However, agreement with experimental observation was found to be limited to low Re number flows ($Re^2 \leq 1000$) [Turian, 1972]. Additionally, this treatment leads to the prediction of decreasing torque on the plate with increasing Re, while an increase is observed experimentally [Turian, 1972]. Heuser and Krause have remarked that good agreement between prediction and experiment is achieved up to a Reynolds number of 4 [Heuser and Krause, 1979].

A numerical solution to the problem was presented by [Hou, 1981] using a finite difference technique to model the flow in a truncated cone-and-plate system. Hou investigated the effect of cone angle and Re on the deviation of the calculated fluid shear rate ($\gamma$) across the cone radius from that predicted by Equation 2.4 ($\gamma_o$). Figures 2.13 and 2.14 show the effect of cone angle and Re, respectively.

Figures 2.12 and 2.13 clearly demonstrate that both increasing cone angle and increasing Re serve to exaggerate shear flow deviations from that predicted by Equation 2.4. However, gross deviations appear to require extremely large Re numbers and cone angles. Additionally, maximum deviations in shear rate were seen to occur at the cone periphery [Hou, 1981]. This effect may be limited by sampling the inner region of the gap.

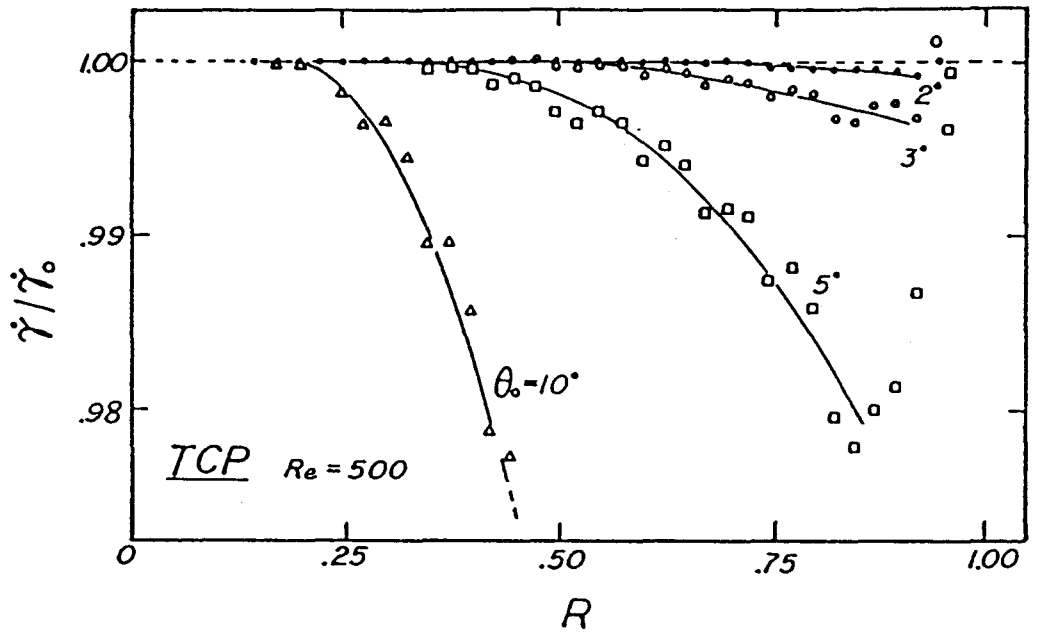


**Figure 2.12** - Shear rate deviation across cone radius from ideal as a function of cone angle, R=cone radius [Hou, 1981].

An alternate method of investigating the fluid flow behaviour in cone-and-plate devices is flow visualization studies. Flow visualization studies performed by Hoppmann and Miller [1963] indicate that the assumption of purely circular streamlines is at least to some degree false. By injecting dye into the flow they demonstrated that the "particles" of the fluid do not follow simple in concentric circular paths about the axis of rotation of the cone, but rather spiral around the central curve of a vortex as they also move around the cone axis (Figure 2.14). Viewed from the bottom of the well, the particles were noted to move from the periphery to the centre and also from the centre to the periphery [Hoppmann and Miller, 1963]. However, these authors did not comment on the effect of such a flow deviation on the validity of the simple rheological equation (Equation 2.4) which is commonly employed to describe cone-and-plate flow.

From the above discussion, it appears that Equation 2.4 describes cone-and-plate flow adequately provided cone angles and Reynolds numbers are within prescribed limits. While it appears that the nature of the fluid flow is somewhat more complicated is

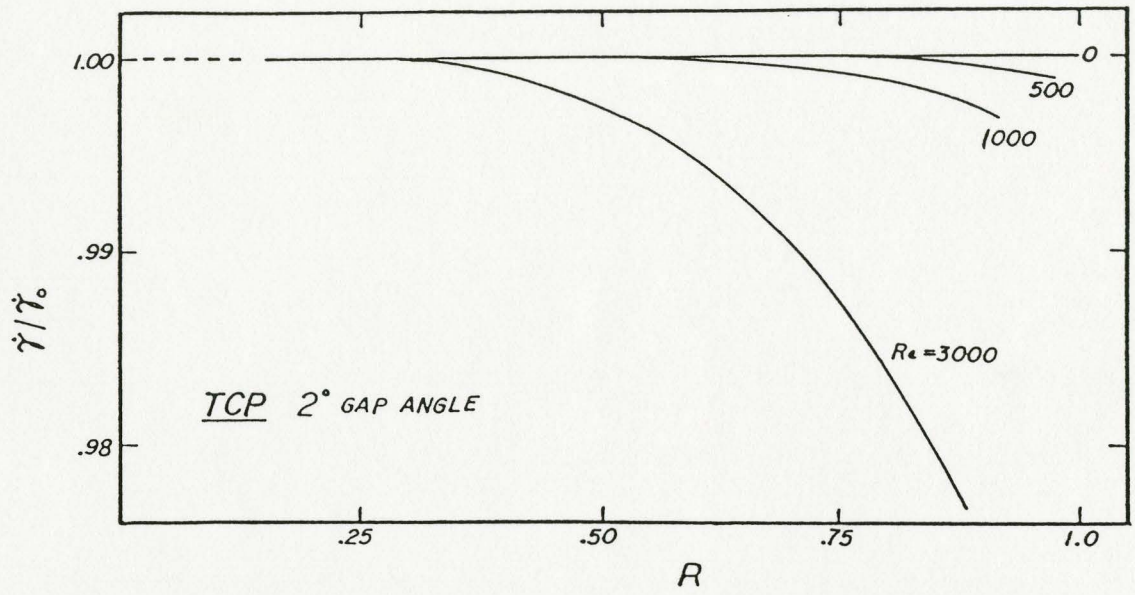


**Figure 2.13** - Shear rate deviation across cone radius as a function of Re for cone angle of 2°, R=cone radius [Hou, 1981].

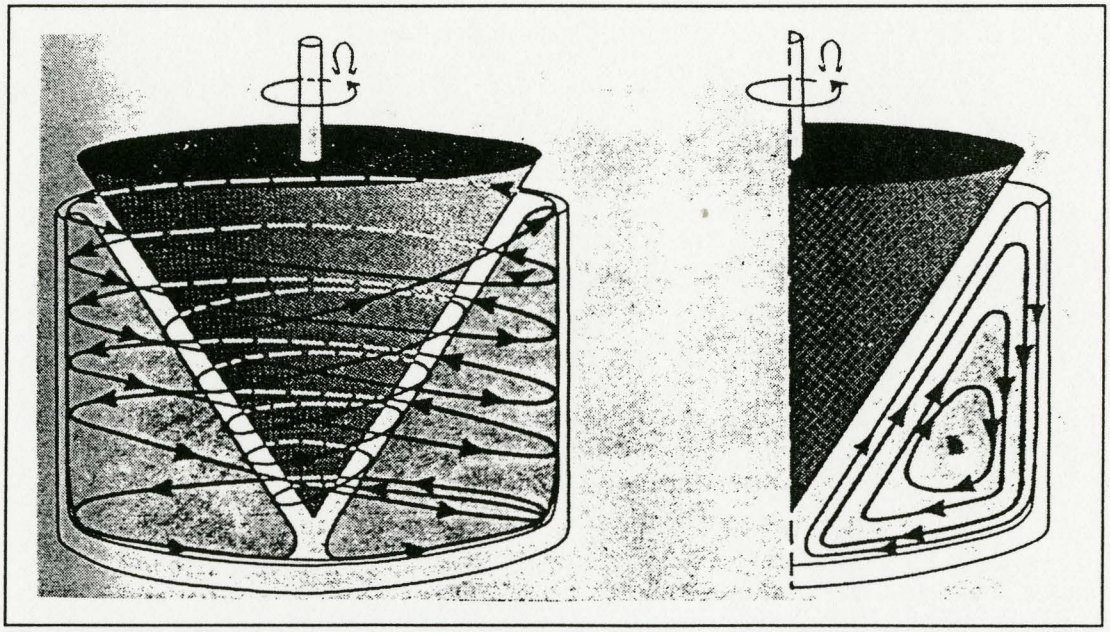


**Figure 2.14** - Fluid flow pattern of cone-and-plate geometry [Hoppmann and Miller, 1963].

implied, it does not appear that this creates a significant deviation in fluid shear rate from that estimated by Equation 2.4. Of course, other factors may influence device

performance such as geometric imperfections in the system due to machining tolerances; however, these are generally assumed to of negligible importance [Walters, 1975].

## 2.5 Polyurethane Chemistry and Structure

Polyurethanes have been employed as biomaterials for several decades as a result of their excellent mechanical properties and relatively good biocompatibility. These block copolymers are unique in structure and may be tailored for a wide range of applications.

### 2.5.1 Polyurethane Elastomer Synthesis

Polyurethane elastomers are usually prepared from a long chain diol such as a linear polyester or polyether of relatively high molecular weight (1000 to 2000), a diisocyanate and a low molecular weight "chain extender" (usually a glycol or diamine) [Saunders and Frisch, 1965].

The synthesis of polyurethanes is generally performed by a two-step reaction procedure in which a low molecular weight prepolymer is first formed by the reaction of a diisocyanate with the hydroxyl-terminated polyether or polyester.

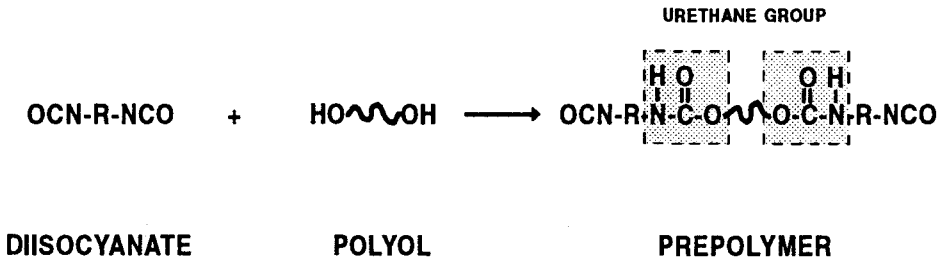


The reaction of diisocyanate with diol shown above produces the characteristic urethane linkage. The prepolymer thus formed is a liquid or solid of intermediate molecular

weight containing terminal isocyanate groups.

The second step is the reaction of the prepolymer with the chain extender. This reaction may be require several hours depending on the reactivity of the chain extender toward the terminal isocyanate groups of the prepolymer. During this reaction, the low molecular weight prepolymer units are linked together via urethane or urea linkages depending on the nature of the chain extender molecule. With equimolar amounts of the reactants, the product of this reaction is a high molecular weight polymer.

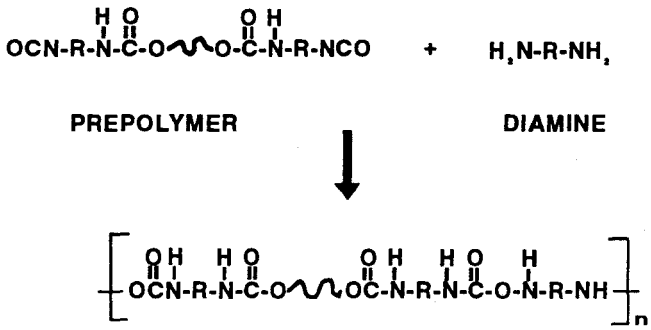


Several side reactions may occur during the synthesis procedure. The reaction apparatus must be kept dry as water will react with the isocyanate groups to form amines with the liberation of $CO_2$ gas. A diisocyanate can thus form a diamine.

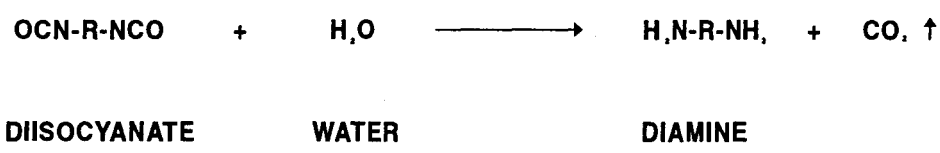


The diamine thus formed can react quickly with unreacted diisocyanate to form

urea linkages, thus upsetting the stoichiometric balance of the polymer forming reactions [Lelah and Cooper, 1986]. In addition, both the urethane and urea groups are capable of nucleophilic attack on isocyanate to give allophanates and biurets respectively.

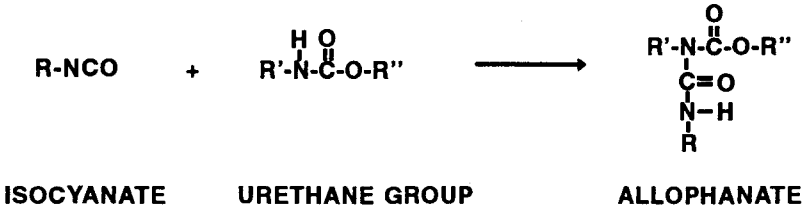


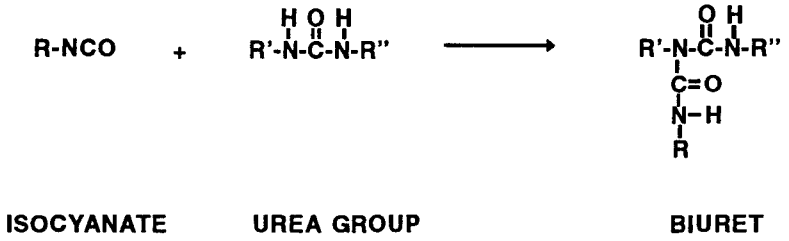


These reactions are particularly troublesome at elevated reaction temperatures. The biuret reaction generally requires temperatures in excess of 100°C while the allophanate reaction occurs readily at temperatures greater than 120°C [Saunders and Frisch, 1965]. The reactions shown above will obviously lead to branching and crosslinking with bifunctional components. These reactions are generally undesirable in the synthesis of polyurethane elastomers as they tend to impair the mechanical properties of the product [Lelah and Cooper, 1986].

### 2.5.2 Microphase Separation

Polyurethanes are considered to be block copolymers with an $(AB)_n$ structure in which A may be considered the hard block or segment and B the soft block or segment. The hard segment consists of the diisocyanate and chain extender while the soft segment is formed by the polyether or polyester sequence. In solid polyurethane materials, the hard segments separate into glassy or semicrystalline microdomains. The polyether or polyester soft segments form an amorphous matrix in which the hard segment domains are dispersed. It must also be noted that the exact morphology also depends on the relative contents of hard and soft segment (Figure 2.10).

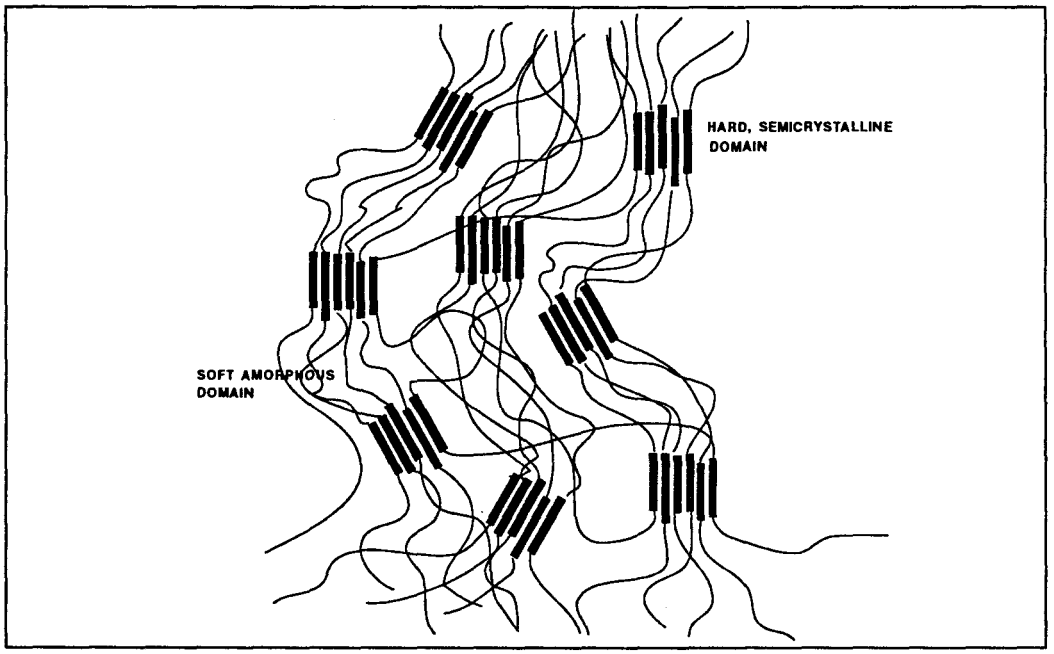


**Figure 2.15** - Illustrative model of the microphase structure exhibited by polyurethanes. Adapted from [R. Bonart, 1968]

The formation of these microdomains is believed to be the result of a positive free energy associated with the interface between the segments providing a driving force for the phase separation in order to reduce the interfacial surface area. The possible degree of separation is limited by the chemical bonds holding the disparate groups in proximity and the magnitude of the interfacial free energy between the domains with a typical

domain size of the order of 50 Å [Lelah and Cooper, 1986].

Microphase separation is the basis of the excellent mechanical properties of these polymers since the hard domains act as multifunctional interchain cross-links while the soft segment matrix imparts a high degree of flexibility and elasticity to the solid materials. Thus the polymer possesses both a relatively high modulus and good elasticity.

The degree of phase separation is affected by several parameters including segment length, segment polarity and crystallisability, overall composition, mechanical and thermal history, and the possibility of hydrogen bonding between the urethane linkages and the carbonyl or ether functional groups [Lelah and Cooper, 1986]. In general, increased phase separation leads to improved mechanical properties as hard segment interaction is uninterrupted allowing for semicrystalline domain formation.

As well, polyurethane domain structure has been implicated in the blood contacting response of polyurethanes as a possible cause of the relatively good hemocompatibility of these polymers, although the reason for this is not clear presently [Goodman et al, 1990 ; Cho et al, 1993].

### 2.5.3 Hydrogen Bonding

Polyurethanes are generally subject to interchain hydrogen bonding, involving the N-H group as the donor and the urethane carbonyl, the ester carbonyl (polyesterurethanes) or the ether oxygen (polyetherurethanes) as the acceptor.

At room temperature, approximately 90% of the N-H groups in the hard segment of a typical polyurethane are hydrogen bonded [Seymour and Cooper, 1973]. Hydrogen bonding is expected to enhance the mechanical properties of polyurethanes as a result of interchain interactions.

### 2.5.4 Thermal Properties

The thermal properties of polyurethanes are a direct result of their morphology. The microphase separated structure of these materials leads to the observation of thermal

transitions based on the separate domains. For example, the glass transition temperature ($T_g$) exhibited by a given polyurethane is dependent on the $T_g$ of the soft segment macroglycol. As the $T_g$s of commonly used macroglycols are far below room temperature, the soft domain will consist of a region of randomly oriented chains, leading to an amorphous structure.

Changes in $T_g$ of the soft domain compared to that of the pure macroglycol have been interpreted as an indication of phase mixing [Buist, 1978]. An increase in polymer $T_g$ is observed with penetration of hard segment material into the soft segment. Also, since polyethers are generally less polar than polyesters, polyurethanes synthesized using polyether soft segment exhibit less phase mixing, and relatively constant glass transition temperatures are observed over a range of isocyanate content whereas polyester-based polyurethanes show increasing glass transition temperatures with increasing isocyanate incorporation [Lelah and Cooper, 1986].

In addition, the hard, semi-crystalline domains of the polyurethane display a melt endotherm which is related to the disordering of these regions at elevated temperatures [Spathis et al, 1990]. The sharpness and temperature range of this transition may be used to infer the cohesiveness of the hard segment domains. Side chain groups present on the hard segment molecules may act to reduce segment packing efficiency [Okkema et al, 1991] resulting in the apparent absence of the crystal melt endotherm. In contrast, a small linear chain molecule such as ethylene diamine employed as a chain extender serves to enhance hard segment packing and thus the mechanical strength of the polymer [Lelah and Cooper, 1986].

Several thermal transitions also occur corresponding to the loss of long range order of the hard segment domains at temperatures in the range of 60 to 80°C [Noshay and McGrath, 1977]. Therefore, the thermal analysis of polyurethanes can be used as a valuable indicator of microdomain structure.

### 2.5.5 Polyurethane Ionomers

The introduction of ionic groups into polyurethanes has profound effects on the physical properties of the polymers. The hypothesis that ionic groups impart improved biocompatibility to polyurethanes has been extensively examined in recent years [Ito et al, 1991 ; Okkema and S.L. Cooper, 1991 ; Santerre et al, 1992 ; Silver et al, 1993 ; Han et al,1993]. Ion incorporation is generally in the hard segment; although there are some reports of incorporation in the soft segment, for example via the grafting of ion-containing side chains [Takahara et al, 1991].

Ionic groups incorporated into polymers are believed to form clusters and multiplets [Eisenberg and King, 1977]. A multiplet is a "domain" containing tightly bound ion pairs with dimensions on the order of 0.6 nm. A cluster is a domain containing several multiplets and some backbone chain, with dimensions of 2 to 10 nm (similar to 5 to 10 nm for hard domains). As indicated, the ionic groups are usually present in the hard segment, and they may either disrupt or enhance phase separation. An enhanced polarity difference between the ion-containing hard segment and the soft segment would be expected to increase phase separation, as has been observed in a number of studies [Hwang et al, 1984 ; Okkema et al, 1991]. However, the method of ion incorporation into the hard segment is important: the introduction of pendant side chains may disrupt hard segment packing thereby serving to decrease phase separation [Okkema and Cooper, 1991].

Other characteristics of ion-containing polyurethanes are their tendency to swell significantly when place in an aqueous environment, and their ability to form stable emulsions [Dieterick et al, 1970]. The ability to form stable emulsions stems from the fact that ionic polyurethanes are able to orient the hydrophobic soft segments toward the interior of the emulsion particle while the hydrophilic hard segment orients toward the water. As well, the ionic groups present in the surface-oriented hard segments tend to stabilize the emulsion by ionic repulsion due to electrostatic double layer interactions [Woods, 1992].

The degree of water absorption of ionic polymers has been found to be directly related to the ionic content, with a sufficient concentration resulting in water solubility [Santerre, 1990 ; Okkema and Cooper, 1991]. It was also reported by Santerre that, for a class of sulphonate containing polyurethanes, a sulphonate content in excess of 3.4% was impractical as a loss of elastomeric behaviour was apparent [Santerre, 1990].

The effect of sulphonate incorporation on the surface properties of polyurethanes, which is the main interest for the present work, is not a simple function of the ion concentration. The ability of the ionic groups to be expressed at the surface of the polymer, the polyol type, the nature of the contacting environment, and the method of incorporation are all parameters which influence the ionomer's surface properties [Takahara et al, 1991 ; Silver et al, 1993a].

## 2.6 Polyurethanes as Blood Contacting Biomaterials

While it is widely believed that segmented polyurethane elastomers are "good" blood-contacting biomaterials, both from a mechanical and biological viewpoint, the long-term hemocompatibility leaves much to be desired. The mechanisms of coagulation and thrombosis are triggered upon exposure of blood to conventional polyurethane surfaces, leading to the biological consequences outlined in Section 2.3. Therefore, much research has been focused on modification of these materials to improve blood-contacting behaviour. A few examples of this approach are presented in this section.

### 2.6.1 Heparinized Polyurethanes

Heparin-derivatized polymers have been extensively studied as possible blood compatible materials. Heparin is a sulphated mucopolysaccharide (Figure 2.11) which is used clinically to inhibit coagulation. Heparin acts by forming a complex with antithrombin III, which neutralizes several of the coagulation factors, most notably, the key coagulation enzyme thrombin. Therefore, it has been suggested that the incorporation of heparin into polyurethanes would impart them with these same anticoagulant properties.

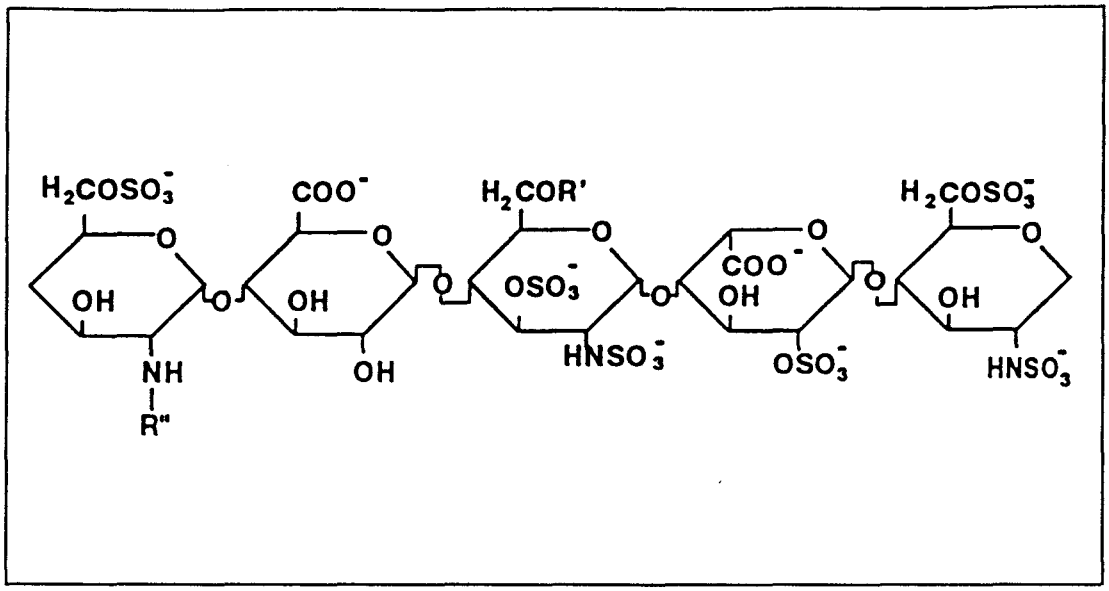


**Figure 2.16** - The essential pentasaccharide sequence of heparin [Casu, 1989].

The incorporation of active heparin molecules into polyurethanes has been achieved by ionic binding [Shibuta et al, 1986 ; Ito et al, 1990]. This method, however, has shown limited effectiveness due to the release of the bound heparin from the surface. Thus, while short-term antithrombogenicity was achieved, this feature was lost over time.

Work by Nojiri et al employed polyethylene oxide (PEO) spacer groups to covalently bind heparin to the surface of Biomer™ (a commercial biomedical polyurethane) [Nojiri et al, 1988]. Spacer groups have been shown to increase the anticoagulant activity of bound heparin, most likely due to increased availability and conformational mobility [Ebert and Kim, 1982]. These heparinized polyurethanes were found to prolong occlusion times in a rabbit arterio-arterial shunt model and to reduce platelet activation. This improved blood-contacting behaviour was attributed to the ability of the material to prevent fibrin formation resulting in decreased platelet aggregation and thrombus formation. This approach was also taken by Park et al who observed an increase in occlusion time of a canine ex vivo shunt and decreased in vitro protein adsorption and platelet deposition [Park et al, 1992].

While covalently bound heparin is not lost as rapidly due to desorption, it is

recognized and eventually degraded by blood heparinases [Jozefowicz and Jozefonvicz, 1984]. As well, platelets have been demonstrated to bind selectively to free heparin resulting in their activation and removal from the circulation [Sobel and Adelman, 1988 ; Greinacher et al, 1993].

The inherent long-term effectiveness of heparinized polyurethanes is thus questionable, although for short term applications this approach may be of value.

### 2.6.2 Functional Group Incorporation

The incorporation of functional groups similar to those present in biological molecules (eg. ions) may be seen as an attempt to mimic the biological activity of these molecules. Incorporation of such groups is less difficult than incorporation of the active biological substance itself. Additionally, the resulting material is generally more stable.

Most of the work in this area has been concerned with the incorporation of sulphonate functional groups into polyurethanes (and other polymers). This approach is a result of the recognition that heparin is a highly sulphated molecule and these as well as carboxylate groups are believed to be of great importance in the activity of heparin [Hovingh et al, 1986].

Early work by Grasel and Cooper involving the grafting of propyl sulphonate groups onto the urethane nitrogens of polyurethanes resulted in materials which exhibited low levels of platelet deposition and spreading in a canine ex vivo shunt experiment [Grasel and Cooper, 1989]. However, significant levels of fibrinogen adsorption were observed.

Ito et al grafted poly(sodium vinyl sulphonate) onto the surface of a segmented polyurethane by gas plasma methods. This material showed reduced protein adsorption and platelet adhesion and release in both in vitro and ex vivo experiments [Ito et al, 1991]. To investigate the respective roles of sulphonate and carboxylate functionalities, carboxylate and sulphonate groups were introduced into the surface of the polymer using sodium acrylate and vinyl sulphonate. In contrast to the effect of sulphonate group

incorporation, carboxylate groups appeared to have no effect on the blood-contacting behaviour of the material [Ito et al, 1991].

The effect of sulphonate and carboxylate incorporation on blood compatibility was also studied by Okkema and Cooper. Propyl sulphonate and ethyl carboxylate groups were grafted onto the urethane nitrogens of polytetramethylene oxide (PTMO)-based polyurethanes. No statistically significant effect was observed in the canine ex vivo blood response due to carboxylate incorporation, while sulphonate incorporation reduced platelet deposition for very short times. As well, enhanced fibrinogen adsorption was reported for the sulphonate-containing polyurethanes [Okkema and Cooper, 1991]. Thus, the carboxyl group appeared to have little effect on the behaviour of the material.

Santerre synthesized sulphonated, polypropylene oxide (PPO)-based polyurethanes using a sulphonated diamine chain extender. These polymers demonstrated increasing levels of fibrinogen adsorption with increasing sulphonate content. The polymers also displayed prolonged thrombin times compared to control polystyrene resins [Santerre, 1990].

Several polyurethanes were synthesized by Okkema et al using a sulphonic acid-containing diol and both PTMO and polyethylene oxide (PEO) soft segments. The PTMO-based polymers showed significant reductions in the number of adherent platelets and the degree of platelet activation in canine ex vivo shunt experiments. However, once again, fibrinogen adsorption levels increased with increasing sulphonate content. The PEO-based sulphonated polyurethanes showed enhanced platelet and fibrinogen deposition suggesting that the surface composition of the polymer resulting from the soft segment polarity affects the ability of the sulphonate groups to interact with plasma proteins [Okkema et al, 1991].

Similar results were obtained by Silver et al. Both PTMO and PEO-based sulphonated polyurethanes were examined for blood-contacting response. The PTMO-based polyurethanes showed enhanced thromboresistance in a canine ex vivo shunt experiment compared to the PEO-based materials. Interestingly, the in vitro evaluation

of platelet spreading yielded the lowest degree of platelet spreading on the unsulphonated PEO-based polyurethane. These results highlight the lack of correlation between in vitro and ex vivo studies particularly when different species are involved [Silver et al, 1993b].

The nature of the anticoagulant effects imparted by sulphonation was examined by Silver et al using a series of water-soluble sulphonated polyurethanes. The polymers were shown to delay clot formation by the following mechanisms: direct complex formation between the polymer and thrombin; interference with fibrin polymerization; and complex interactions between the polymer, thrombin, antiproteases and fibrinogen in plasma [Silver et al, 1992]. However, these mechanisms may not be applicable in the case of solid surface-plasma interactions where conformational mobility is restricted.

Polyurethanes incorporating sulphonated soft segment side chains were synthesized and evaluated by Takahara et al. A canine ex vivo shunt experiment showed an increasing thrombogenic response with increasing sulphonate side chain content [Takahara et al, 1991]. This result is in contrast to the improved blood contacting behaviour of polyurethanes which contain sulphonate groups in the hard segment, thus indicating that the location and structural mobility of the sulphonate group may dictate blood response.

Ionizable functional groups have also been demonstrated to enhance leucocyte adhesion to polyurethanes in vitro [Bruil et al, 1992]. As well, sulphonated, PEO-based polyurethanes were reported to display enhanced calcification resistance and a decreased degree of surface cracking following implantation into rats [Han et al, 1993].

It is apparent that the incorporation of ionic functional groups into polyurethanes has significant effects on both the physical properties and the blood-contacting response of these materials. However, the mechanisms responsible for the biological effects are unknown.

### 2.6.3 Endothelialization of Polyurethanes

Perhaps the most promising approach to creating truly blood compatible polyurethanes lies in creating an endothelial cell layer on the surface of the polymer. For

example, attempts are being made to culture stable, viable layers of endothelial cells on polyurethanes. This process has the advantage of both mimicking the normal vessel wall surface and providing a barrier to the processes of foreign body reaction and degradation while retaining the excellent mechanical properties of the polyurethane substrate.

Zhu et al have cultured lamb jugular vein endothelial cells on the surface of two commercial polyurethanes (Biomer™ and Mitrathane™). They were able to achieve high levels of endothelialization (88 to 95% coverage) in 3 to 4 weeks of culturing. These endothelialized surfaces remained intact under conditions of shear flow for 48 h and showed decreased in vitro platelet adhesion [Zhu et al, 1990].

In a rat model, a porous, 1.5 mm diameter graft, consisting of a polyurethane-polydimethylsiloxane blend, was completely endothelialized when implanted into the infrarenal aorta [Okoshi et al, 1993]. A 76% patency rate was reported for porous prostheses after 3 months of implantation while a low porosity graft showed only 8% patency, indicating that the surface texture of the graft may play an important role in endothelial cell attachment. However, extension of these results to humans is difficult.

Bordenave et al also studied the endothelial cell compatibility of several commercial polyurethanes (Pellethanes™) using human umbilical vein endothelial cells (HUVECs). A functional monolayer was observed on one of the three polymers studied while one displayed a cytotoxic effect attributed to leachable low molecular weight materials, and the other showed an absence of cell proliferation. However, all of the polyurethanes showed significantly higher levels of endothelial cell attachment when coated with fibronectin prior to cell attachment, indicating the importance of preconditioning the substrates with adhesive proteins [Bordenave et al, 1993].

Another approach taken by Lin et al involves the modification of polyurethanes by attaching RGD peptides. These peptides are present in a variety of adhesive proteins (notably fibrinogen, fibronectin and vitronectin) and are recognized by the integrin family of cell surface receptors. The RGD peptide derivatized polyurethanes were found to support endothelial cell (HUVEC) attachment and spreading even in the absence of serum

in the culture medium [Lin et al, 1992]. This method of polymer modification provides a simplified approach to the process of cell adhesion as no preconditioning of the surface is necessary.

The inability of human endothelial cells to proliferate spontaneously and cover an implanted material is an important restriction. The need for the high level of non-thrombogenicity afforded by endothelialized surfaces is great, particularly for small diameter vessels. However, the extensive incubation period required to obtain a monolayer of cells and the limited viability of the attached cells are important limitations of this procedure.

### 2.6.4 Other Approaches

A variety of other strategies have been employed in an attempt to improve the blood-contacting characteristics of polyurethanes. These include the introduction of hydrophilic additives in an attempt to decrease the blood-solid interfacial free energy, resulting in a decreased driving force for protein adsorption [Coleman et al, 1982]. This notion has been extended to include surface mobility of the polymer which may potentially allow proteins to adsorb without denaturation resulting in a less thrombogenic surface [Brunstedt et al, 1993].

Other approaches focus on developing potentially "bioactive" polyurethanes by the incorporation of specific amino acids [Ito et al, 1989 ; Santerre et al, 1992]. The introduction of specific amino acids which may attract "desirable" proteins preferentially to the surface of the polymer has shown limited success probably because high degrees of protein selectivity using short amino residues is not achievable. Another attempt to promote preferential adsorption of a particular protein to the polymer surface involves grafting octadecyl (C18) chains [Munro et al, 1983 ; Chinn et al, 1991]. Albumin appears to bind selectively to C18 groups resulting in very low levels of platelet adhesion and activation on C18-derivatized surfaces. Improvement of hemocompatibility involving the use of PEO modified polyurethanes has also been attempted since PEO has been

found to inhibit protein adsorption [Merrill and Salzman, 1983]. The synthesis of a modified polyurethane to promote plasminogen adsorption was described by Woodhouse [Woodhouse, 1992]. It was hypothesized that such a surface might have fibrinolytic properties.

Despite all of the intensive research devoted to this problem, it can safely be said that no polyurethane, or any other synthetic material, has been developed which can provide long-term hemocompatibility in all applications presently desired [Ratner, 1993].

## 2.7 Objectives of the Present Research

The difficulty in attaining acceptable biocompatibility in blood-contacting polymers points to the need for investigation of the interaction of polymer surfaces with blood and blood constituents, particularly the agents of thrombosis present in the blood (coagulation proteins and platelets). These fundamental investigations are required to facilitate the development of any potential blood-contacting material.

A substantial amount of work has been performed in this laboratory in the past to study the nature of blood protein interactions with various artificial surfaces. This interaction is believed to be the first step in a series of events which take place upon exposure of artificial surfaces to the blood environment and therefore mediates the subsequent responses. Many researchers have judged the hemocompatibility of surfaces under examination based upon the protein adsorption characteristics (particularly fibrinogen). However, the impact of nature of the adsorbed layer of proteins on the onset of thrombosis is unclear.

The limited success of sulphonated polyurethanes described in Section 2.6.2 suggests that the incorporation of sulphonate ions into the polyurethane directly affects the blood-contacting response of these materials. However, little evidence has been provided on the mechanism by which sulphonate ions improve blood response. Previous work performed in this laboratory [Santerre et al, 1992] has demonstrated that sulphonate-containing polyurethanes display promising anticoagulant behaviour. The present work

extends the investigation of sulphonated polyurethanes to the study of platelet-surface interactions. To facilitate this investigation, a novel cone-and-plate device was developed to study platelet-surface interactions under conditions of controlled shear flow. The effect of plasma proteins on platelet adhesion can be studied since the protein content of the platelet suspension fluid is controlled and constant. The aim of this research is to contribute to the fundamental understanding of platelet-polymer surface interactions under varying conditions of both shear flow and polymer structural parameters.

Specifically, the work has involved:

1) The development and testing of a novel experimental apparatus which permits the study of platelet interactions with test surfaces under varying conditions of controlled shear flow.
2) The synthesis and characterization of several novel sulphonated polyurethanes.
3) The study of platelet interactions with several test surfaces, including the above sulphonated polyurethanes, collagen-coated polymers, and albumin-coated polymers.

# 3. EXPERIMENTAL METHODS

## 3.1 Polyurethane Synthesis

Several novel polyurethanes were synthesized incorporating sulphonate functional groups, as well as a number of conventional non-sulphonated polyurethanes.

### 3.1.1 Materials

Tables 3.1a, b and c list the chemicals, solvents and materials used in the experimental work of this project along with the source and location of the supplier.

### 3.1.2 Polyols

The polyol chosen for the synthesis of the polyurethanes was polytetramethylene oxide (PTMO). The use of this polyol was a departure from the work done previously in this lab which utilized polypropylene oxide (PPO) [Santerre, 1990]. The reasons for choosing PTMO are its widespread use in synthesizing polyurethane elastomers [Lelah et al, 1986 ; Ito et al, 1991 ; Okkema et al, 1991], and the generally superior mechanical properties of PTMO-based polyurethanes [Lelah and Cooper, 1986]. The commercially available biomedical polyurethanes such as Biomer™ and Pellethane™ are based on PTMO. As well, a limited number of polyurethanes were synthesized using polyethylene oxide (PEO) as the polyol. These were initially included due to the previously reported protein-resistant nature of PEO [Merrill and Salzman, 1983]. The chemical structures of polyether polyols commonly used in polyurethane synthesis are shown in Figure 3.1.

While conventional non-sulphonated polyurethanes based on PEO were relatively easy to synthesize, the sulphonated polyurethanes incorporating PEO were either water soluble or extremely weak mechanically, apparently decomposing on contact with water. Since the polyurethanes are being studied in relation to their blood contacting properties,

| Material | Supplier | Location |
|---|---|---|
| Solvents | | |
| Acetone | BDH Chemicals | Toronto, ON |
| Dimethyl formamide (DMF) | BDH Chemicals | Toronto, ON |
| Dimethyl sulphoxide (DMSO) | Aldrich | Milwaukee, WI |
| Dimethyl d6 sulphoxide | Aldrich | Milwaukee, WI |
| Methanol | BDH Chemicals | Toronto, ON |
| Polyurethane Reagents | | |
| Bis(hydroxyethyl)amino-ethanesulphonic acid (BES) | Aldrich | Milwaukee, WI |
| Diamino biphenyl disulphonic acid (BDDS) | Eastman-Kodak | Rochester, NY |
| Methylene dianiline (MDA) | Aldrich | Milwaukee, WI |
| Methylene di-p-phenyl diisocyanate (MDI) | Eastman-Kodak | Rochester, NY |
| Polyethylene oxide (PEO) | Aldrich | Milwaukee, WI |
| Polytetramethylene oxide (PTMO) | QO Chemicals | West Lafayette, IN |
| Stannous octoate | Sigma | St. Louis, MO |
| Biological Materials | | |
| Albumin (bovine) | Boehringer-Mannheim | Dorval, PQ |
| Collagen (bovine, type I) | Sigma | St. Louis, MO |
| Heparin | Sigma | St. Louis, MO |

**Table 3.1a** - Experimental materials and suppliers

| Material | Supplier | Location |
|---|---|---|
| Buffer and Platelet Suspension Materials | | |
| Acetic acid | BDH Chemicals | Toronto, ON |
| Apyrase | Prepared from potatoes | McMaster University |
| Calcium chloride hexahydrate | BDH Chemicals | Toronto, ON |
| Citric acid monohydrate | " | " |
| Dextrose | " | " |
| Eagles minimum essential medium | Grand Island Biologic | Grand Island, NY |
| Ethylenediamine tetraacetic acid (EDTA) | BDH Chemicals | Toronto, ON |
| Glucose | " | " |
| Magnesium chloride hexahydrate | " | " |
| Sodium bicarbonate | " | " |
| Sodium dihydrogen orthophosphate | " | " |
| Trisodium citrate | " | " |
| Miscellaneous | | |
| Isoton II (saline sol'n) | Coulter Electronics Canada | Burlington, ON |
| Liquinox (detergent) | Alconox | New York, NY |
| Lithium bromide | Aldrich | Milwaukee, WI |
| Potassium chloride | BDH Chemicals | Toronto, ON |
| Rhodamine-phalloidin dye | Molecular Probes | Eugene, OR |
| Sodium chloride | BDH Chemicals | Toronto, ON |

**Table 3.1b** - Experimental materials and suppliers

| Material | Supplier | Location |
|---|---|---|
| Miscellaneous (cont'd) | | |
| Sodium chromate-51 isotope | Dupont-NEN Research Products | Boston, MA |
| Sodium hydroxide | BDH Chemicals | Toronto, ON |

**Table 3.1c** - Experimental materials and suppliers

it is obviously necessary that they be mechanically stable in an aqueous environment. Therefore, the PEO-based polyurethanes were not characterized further or tested for platelet response.

The PTMO polyols were received in three molecular weight forms: 650, 980, and 2000. Polyurethane synthesis was attempted using all three molecular weight forms since varying the polyol chain length enables one to vary hard segment content and sulphonate content of the final polymer. However, polyurethane synthesis involving the 2000 molecular weight PTMO was unsuccessful due to the low solubility of this high molecular weight form in the reaction solvent, dimethyl sulphoxide (DMSO). Therefore, all polyurethanes synthesized and characterized utilized the 650 and 980 molecular weight forms of PTMO to form the soft segment of the polymer. These lower molecular weight PTMOs were soluble at about 20% wt/vol. in DMSO when heated to 60°C.

Prior to use, PTMO was placed in a vacuum oven at 60°C for 48 hours to drive off any residual water. Water removal required at least 48 hours under these conditions, since shorter times resulted in significant water contamination which was evident during the prepolymer reaction.

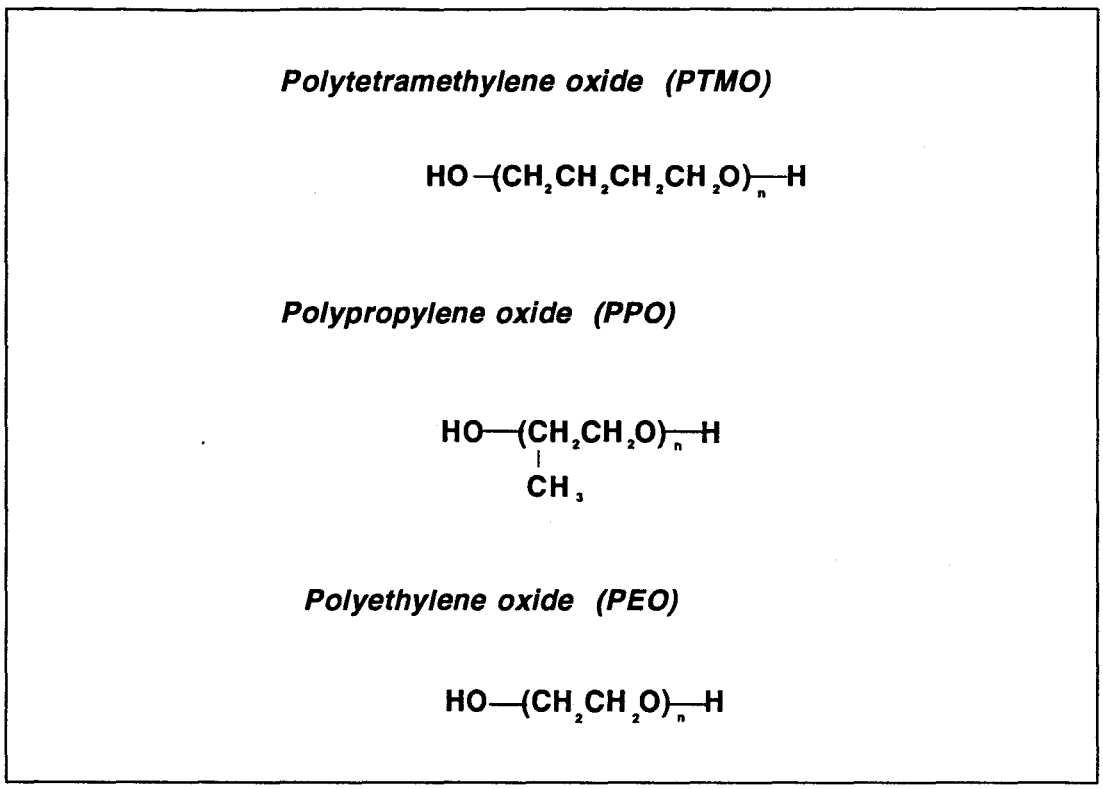


**Figure 3.1** - Polyols commonly used for polyurethane elastomer synthesis (molecular weights of 1000 to 2000 commonly used).

### 3.1.3 Diisocyanate Distillation

The diisocyanate utilized in the polyurethane synthesis was methylene di-p-phenyl diisocyanate (MDI). It was necessary to vacuum distill the MDI, since the received material contains some dimers and trimers of MDI.

The MDI was placed in a 500 mL round bottom flask connected to a vacuum distillation apparatus and melted slowly at 60 to 70°C until all of the MDI was liquefied. Vacuum was then applied and the temperature was increased until the distillation temperature stabilized around 170°C. The condenser was wrapped with heating tape to avoid blockage by solidifying MDI.

The first 25-50 mL of distillate collected was discarded and the remaining MDI distilled was collected and immediately placed in a bottle for storage at -25°C until use.

### 3.1.4 Chain Extender Selection and Purification

The chain extenders employed in the various polyurethane syntheses are shown in Figure 3.2. The two sulphonated chain extenders were selected in order to incorporate sulphonate functional groups into the polymer chain, while the methylene dianiline (MDA) chain extender was employed to create non-sulphonated polyurethanes of similar structure. In this way, it was hoped to be able to evaluate the effect of sulphonate incorporation on the polyurethane properties. Chain extension using all three of the listed compounds yielded polymers of satisfactory molecular weight, ranging from 40,000 to 60,000.

The use of N,N-bis(2-hydroxyethyl)-2-amino-ethane sulphonic acid (BES) as a chain extender was based on work reported by Okkema et al [1991]. This sulphonated diol was used as received and was found to be highly soluble in the reaction solvent (DMSO), readily dissolving completely at 15% wt/vol. However, due to the relatively low reactivity of diols employed as chain extenders, it was necessary to catalyze the chain extension reaction using stannous octoate [Saunders and Frisch, 1965]. The catalyst was added during the chain extension step at 0.15 wt% (based on total feed reactant weight) via syringe.

4,4' Diamino-2,2'-biphenyl disulphonic acid (BDDS) has been used previously in this laboratory [Santerre, 1990 ; Santerre et al, 1992]. The diamine was received in the sulphonic acid form shown in Figure 3.2 but was converted to the sodium salt form for use in the syntheses. The sodium salt form of BDDS is soluble in DMSO at low concentrations (up to 3% wt/vol) while the sulphonic acid form is essentially insoluble. First, however, the as-received material required purification involving rinsing the BDDS powder with double distilled water until the deep purple colour of the material essentially disappeared. This step removes water soluble impurities leaving a purified product in the form of a white powder.

To convert the sulphonic acid to the sodium salt, 1000 mL of a 1 M NaOH solution was added to 250 g of the purified BDDS powder until a homogeneous solution

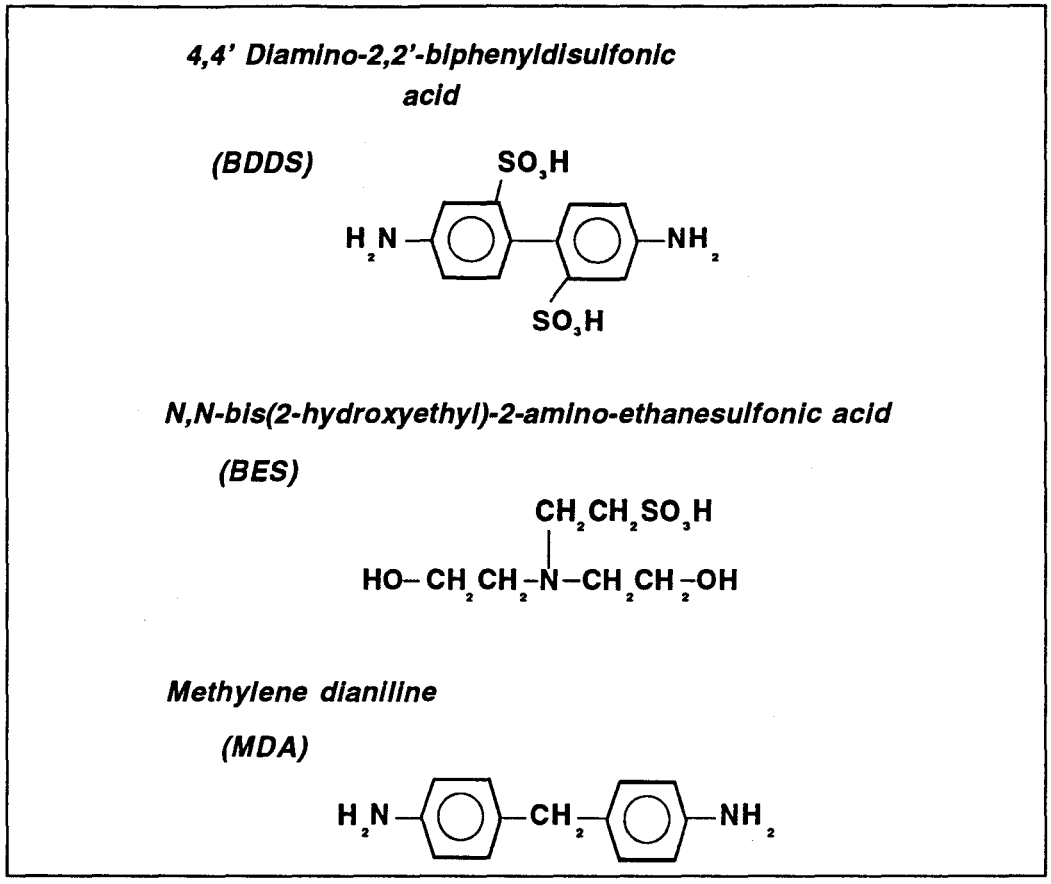


**Figure 3.2** - Chain extenders employed in polyurethane syntheses

deep pink in colour was formed. This is achieved by adding increasing amounts of NaOH to the BDDS suspension while stirring until the powder completely dissolves. At this point, gentle heating (50 to 60°C) was applied for several hours to concentrate the solution (500 mL) to a deep red colour. To precipitate the BDDS salt, 1 L of chilled acetone was added to the solution. The solid was collected by filtration, rinsed with several litres of distilled water and allowed to dry for 72 hours in a vacuum oven at 60°C to yield a light pink powder which was soluble in DMSO at 3% wt/vol.

### 3.1.5 Reaction Solvent

The reaction solvent chosen was dimethyl sulphoxide based on its ability to

dissolve most of the polyols of interest as well as the various chain extenders. An anhydrous form of this solvent (99.995% water free) was purchased as water contamination must be avoided during all stages of the polymer synthesis.

To avoid water contamination of the solvent by contact with air during withdrawal and transfer, the DMSO contained in an Aldrich sureseal™ bottle with septum was placed in a dry $N_2$ gas environment as shown in Figure 3.3. The solvent could then be withdrawn using a syringe with a 12" stainless steel needle. After use, the bottle was removed from the $N_2$ gas environment, capped tightly and stored in a solvent cabinet until further use.

### 3.1.6 Prepolymer Reaction

The polymerization reaction was carried out using the standard two-step process, with molar ratios of polyol : diisocyanate : chain extender of 1:2:1 in all cases.

All glassware used during the reaction was cleaned with Liquinox detergent and rinsed with acetone immediately before use to remove any residual water present on the glass surfaces.

The prepolymer reaction was performed by adding a heated PTMO/DMSO solution (20% wt/vol) dropwise into an MDI/DMSO solution (15% wt/vol) maintained at 90°C in a 500 mL reaction kettle. The solution was blanketed with dry $N_2$ gas to prevent water contamination, and the reaction was allowed to proceed with stirring at 90°C for 90 minutes.

### 3.1.7 Chain Extension Reaction

At the conclusion of the prepolymer reaction step, the temperature was lowered to 80°C and a solution of chain extender in DMSO (3 to 15% wt/vol) was added dropwise to the reaction kettle. Chain extension was then allowed to proceed for a variable length of time, ranging from 30 min. to several hours depending on the chain extender employed. As mentioned previously, for the BES chain extension, a stannous octoate

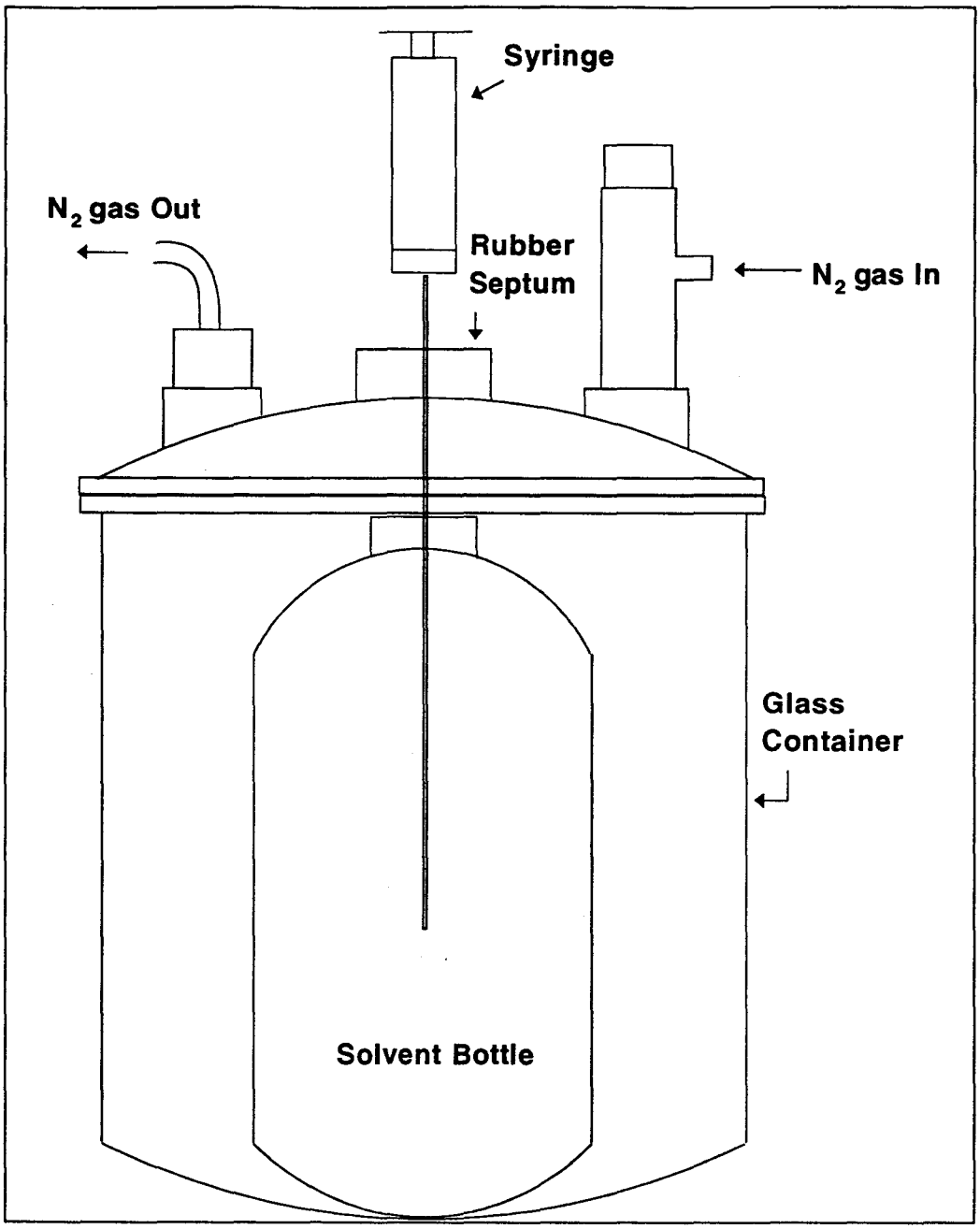


**Figure 3.3** - Apparatus used for solvent withdrawal in a nitrogen environment

catalyst (0.15 wt%) was also added along with the chain extender. The chain extension reaction is illustrated in Figure 3.5 and essentially involves joining the prepolymer segments previously formed to create long chain linear polymers.

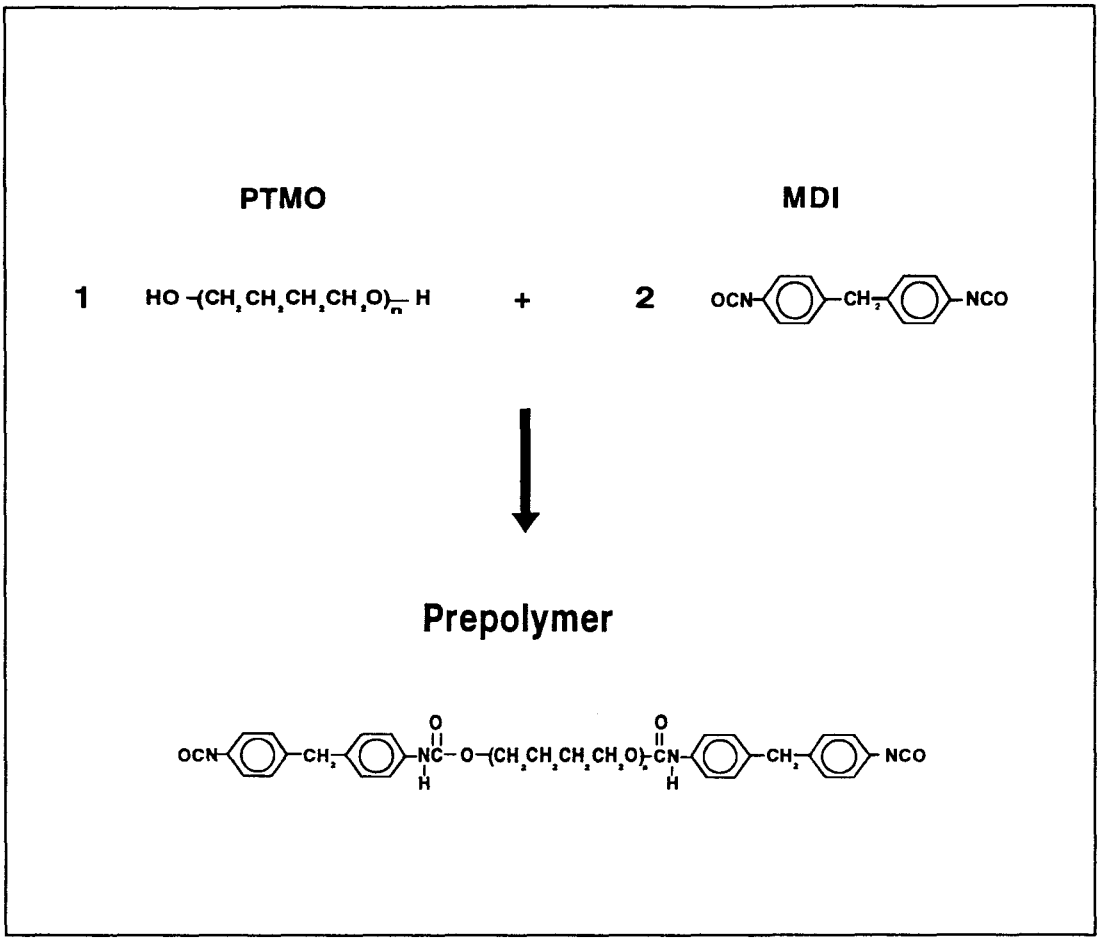


**Figure 3.4** - Polyurethane prepolymer reaction

### 3.1.8 Polymer Precipitation and Purification

After the chain extension reaction had proceeded for the desired length of time, the reaction vessel was allowed to cool to 50°C. The contents were then poured into a solution of double distilled water saturated with KCl. The polymer precipitate was then vacuum filtered and washed several times with double distilled water. The precipitate was dried for several days in a conventional forced air drying oven at 50°C. The solid polyurethane was then dissolved in dimethyl formamide at approximately 5% wt/vol. Any material that did not dissolve (usually only traces) was removed and discarded. This solution was then precipitated and washed as before, and the solid immersed in double

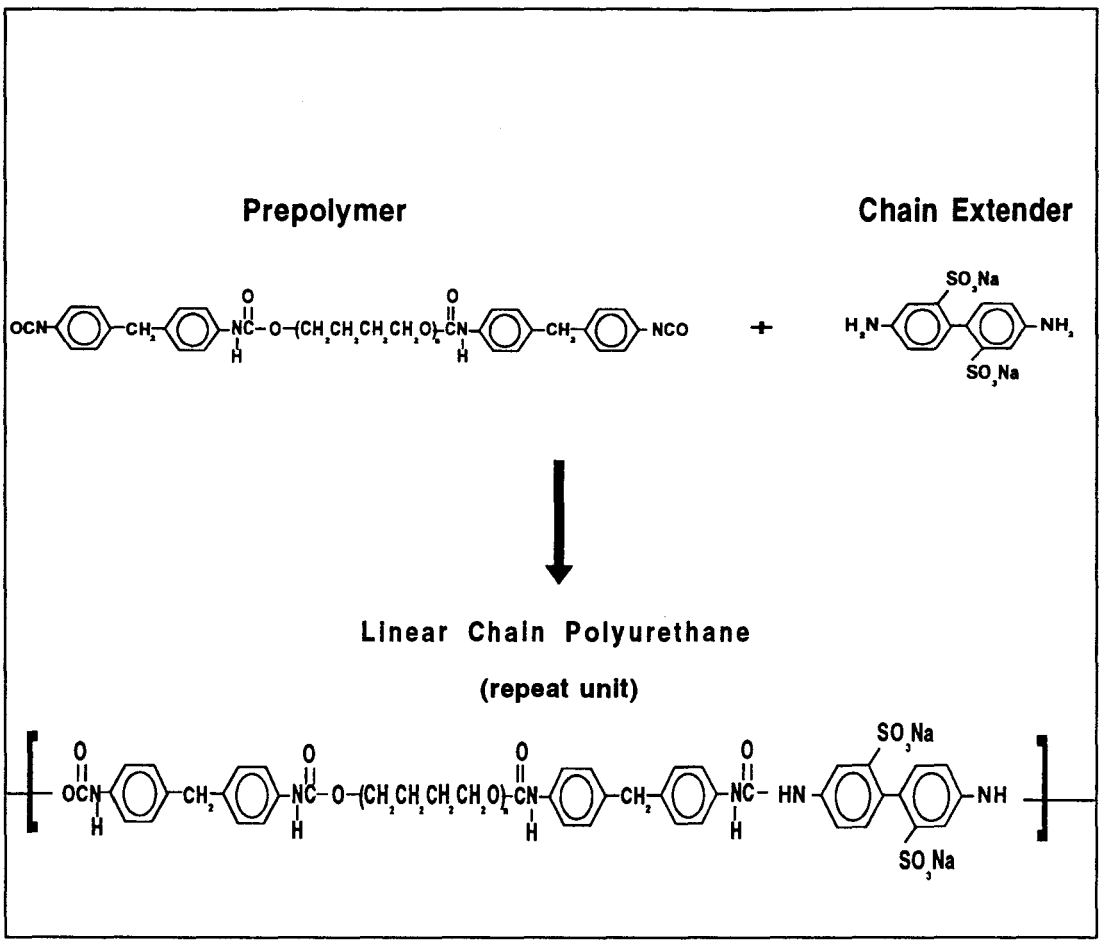


**Figure 3.5** - Polyurethane chain extension reaction employing BDDS

distilled water for 48 h to allow residual solvent to diffuse out of the polymer.

The polymer was then dried for at least 48 h at 60°C in a vacuum oven followed by 72 h in a conventional forced air oven at 50°C. After the drying steps, the solvent odour had completely disappeared from the polymer precipitate indicating only small traces, at most, of residual DMF. The polymer thus prepared was then weighed for calculation of reaction yield and stored in a brown bottle in the dark to prevent UV degradation until use.

In the case of the MDA chain extended polyurethanes, precipitation was carried out in double distilled water since no electrolyte was necessary to facilitate precipitation in this case. Clearly this is related to the lack of negative charge present in these

polymers, probably preventing the formation of stable emulsions.

### 3.1.9 Film Casting

Polymer specimens in film form were required for several characterization tests and for platelet adhesion studies. The polyurethanes were dissolved in DMSO at a concentration of 6% wt/vol. Fifty milliliters of this solution was then poured into a 10 cm glass crystallizing dish (Pyrex) which had been previously placed in a small drying oven and levelled. The dishes were covered with cardboard sheets to keep out dust and to prevent excessively fast drying, resulting in surface irregularities. The oven temperature was set to 60°C. The time required to cast the films in this manner was 2 to 3 days. After casting was complete, the films were placed in a vacuum oven at 60°C for at least 48 h prior to use to remove the last traces of solvent.

## 3.2 Polyurethane Characterization

Due to the inherent complexity of polyurethane structure and chemistry, it is necessary to perform a range of tests to characterize these polymers adequately. The methods used in this work address chemical, physical, bulk phase and surface properties.

### 3.2.1 Water Uptake Studies

To characterize the bulk hydrophilicity and swelling properties of the polymers developed, the amount of water absorbed by each polyurethane was measured. This test entailed cutting out three small rectangular pieces of cast polymer film (10 x 20 x 1 mm), rinsing them in methanol to remove any organic surface contamination, drying them in a vacuum oven overnight, and weighing the three clean, dry polymer samples. The samples were then placed in a 15 mL glass scintillation vial which was filled with double distilled water and then capped. The samples remained in the water at room temperature for 20 days. After 3, 10 and 20 days, the films were removed, blotted to remove surface moisture and weighed. The percentage increase in sample weight was then calculated and

recorded over the experimental time period.

### 3.2.2 Gel Permeation Chromatography (GPC)

Gel permeation chromatography (GPC) was employed to determine polyurethane molecular weight. GPC is a size-sorting technique whereby the polymer molecules dissolved in the solvent carrier phase are retained in the pores of the solid column packing. Therefore, the pore size of the column packing material determines the molecular weight range where separation takes place [Yau et al, 1979]. The polymer molecules elute from the columns in order of decreasing size.

The GPC system used in this research consists of: 1) a high pressure solvent delivery system (Waters M6000 A pump); 2) four ultrastyragel columns with pore sizes of 1000, 10000 and 100000 Å; 3) a thermostatted column jacket; 4) a temperature controller (Waters); 5) a sample injector (Rheodyne 7125) and precolumn filter (2 μm pore size); a differential refractive index detector (Waters R-401); and a Zenith 158 computer equipped with a data acquisition board for analog to digital conversion and a Epson LX-80 printer. Data analysis was performed with the Zenith computer using ASYST 1,2,3 software package. The GPC data analysis program enables one to calculate sample molecular weights and obtain printed outputs of the chromatograms obtained.

Preparation for analysis by GPC entailed dissolving the dry, clean polymer at 0.4% wt/vol in the GPC carrier solvent (0.1 M LiBr in DMF). Prior to use, DMF was vacuum filtered through a 0.5 μm Millipore filter to remove solid impurities present in the received solvent. The GPC columns were flushed with LiBr/DMF overnight at a flowrate of 0.1 mL/min. to equilibrate the columns. As well, the column temperature was increased to 80°C. Prior to polymer injection the flowrate was increased to 1.0 mL/min. The polymer solution was injected (0.5 mL) and the sample retention time was determined by refractometer output via computer. The sample molecular weight was then calculated based on a calibration curve obtained using polystyrene standards (Varian, Sunnyvale, CA) of known molecular weight (Figure 3.6).

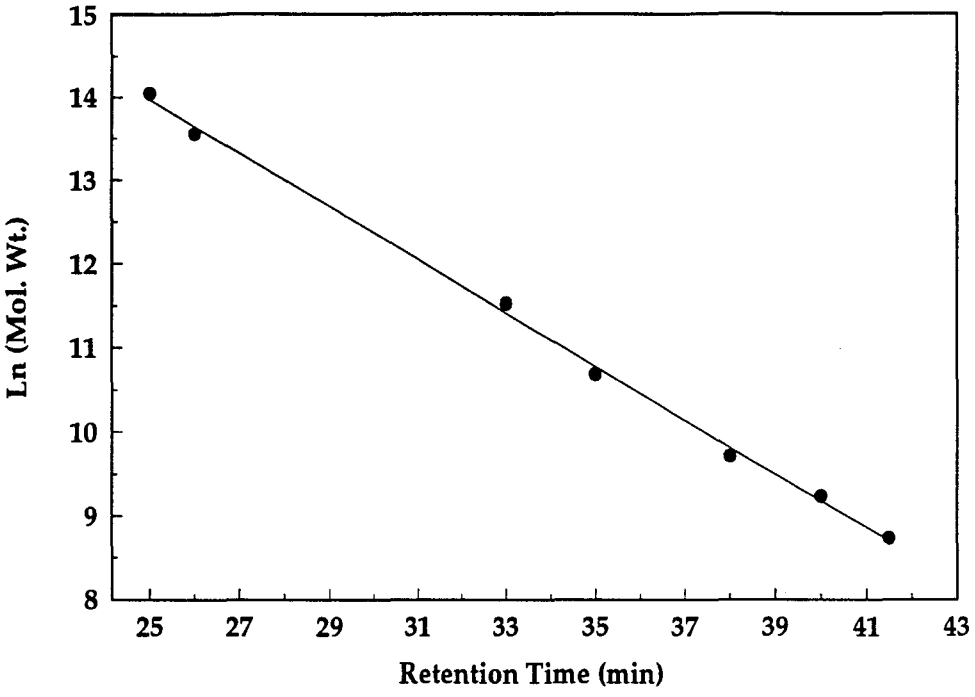


**Figure 3.6** - Calibration curve for GPC based on polystyrene standards.

### 3.2.3 Contact Angle Measurement

Contact angle analysis of the polyurethane surfaces was used to determine the relative hydrophilicity/hydrophobicity of the materials. Samples for the contact angle measurement were obtained from the films cast for the platelet adhesion studies. These films were approximately 1 to 2 mm in thickness and were sufficiently smooth to facilitate accurate determination of contact angles. The samples were placed in a vacuum oven at 60°C overnight to remove any volatile impurities. The samples were then removed and rinsed with methanol immediately prior to contact angle measurement.

The advancing and receding contact angles were measured by goniometer using the sessile drop method (see Figure 3.7) with water as the test fluid. Water was chosen

as the test fluid since physiologic environments are aqueous in nature. A minimum of five drops were measured for each polymer surface, taking both advancing and receding contact angle readings from both sides of each drop. Thus, a minimum of 10 advancing and receding contact angle measurements were made for each surface of interest.

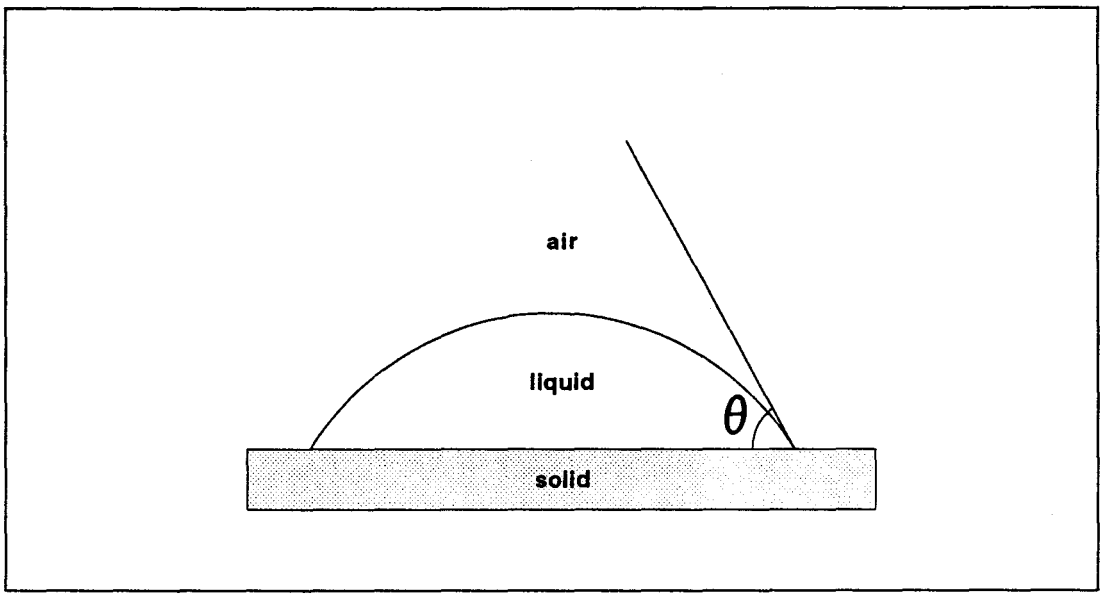


**Figure 3.7** - Sessile drop measurement of contact angle Θ

The advancing contact angle was obtained by introducing a small drop of water onto the test surface via a syringe. The drop was allowed to spread to an equilibrium position (generally requires about 30 sec) and the tangent to the contact line of the drop measured as shown in Figure 3.7. This angle is termed the advancing contact angle since the contact line of the drop is allowed to "advance" across the test surface until an equilibrium position is reached. This equilibrium position is a function of the surface energetics of both the solid and the test liquid. Therefore, the use of a common test liquid for several solids of interest enables one to probe the relative differences in surface energetics of the test solids quickly and relatively easily.

The receding contact angle is observed when a drop of liquid present on the solid surface is withdrawn, causing the contact line to retreat across the surface to a new equilibrium position. The receding contact angle is then measured as above and is almost

always lower than the advancing angle. The difference between the receding and advancing angles is known as contact angle hysteresis. The cause of this phenomenon is not completely understood, but is felt to result from several conditions: surface roughness which may result in several quasi-equilibrium states, surface chemical heterogeneity, the adsorption of a thin film of liquid to the test surface which alters the surface dynamics, and surface reorientation for relatively mobile solids [Wu , 1982 ; Woods, 1990]. In general, the receding angle is believed to be indicative of the surface energetics of the wetted solid. Therefore, this property is of interest in studying biomaterials which will be placed in contact with aqueous physiological solutions.

### 3.2.4 Nuclear Magnetic Resonance Spectroscopy (NMR)

Nuclear magnetic resonance spectroscopy was employed to provide information on polyurethane chemical composition. The analysis was performed using a Bruker AC200 proton NMR spectrometer (McMaster University) with an average number of scans of 64. Polymer samples were dissolved in deuterated DMSO at a concentration of 3% wt/wt in 1 mL NMR glass tubes. To aid in the peak assignment process, NMR spectra were also obtained for the various reagents utilized in the polyurethane syntheses. Based on the peak assignments, the incorporation of the monomers was estimated and compared to theoretical values (based on feed stoichiometry).

### 3.2.5 Elemental Analysis

Conventional elemental analysis was performed on all of the sulphonated polyurethanes to determine weight percent sulphur. This was done to evaluate the extent of sulphonate incorporation via the chain extension reaction. Clean, dry polyurethane samples of 500 mg were sent to Galbraith Laboratories (Knoxville, TN) for these analyses which are based on combustion methods. These data were compared to "theoretical" values of sulphur content based on the 2:1:1 MDI:PTMO:chain extender stoichiometry.

### 3.2.6 Differential Scanning Calorimetry (DSC)

Differential scanning calorimetry was performed on the polyurethanes produced to determine thermal transition temperatures using a TA Instruments DSC 2910 differential scanning calorimeter (McMaster University). Analysis of the thermograms was performed using a Thermal Analyst 2100 thermal analyzer and the thermograms were plotted using a Hewlett-Packard Colorpro plotter. Samples used for DSC were obtained from films cast for platelet adhesion studies. The sample weights were approximately 10 mg (10 mm x 10 mm) and were scanned from -100°C to 250°C at a rate of 15°C per minute. The samples were initially cooled to -100°C using liquid nitrogen. Once the samples reached a temperature of 250°C, they were rapidly cooled again to -100°C and a second scan was performed. A comparison of the first and second scans provides insight into the microstructure of the polymer and helps to differentiate thermal transitions related to the thermal history of the polymer and hard segment crystallization. The sharpness and temperature of the glass transition was used as an indicator of the degree of phase separation of the synthesized polymers. Additionally, the hard segment crystallinity was inferred from the presence and nature of a crystal melt endotherm in the temperature region of 200 to 250°C.

### 3.2.7 X-Ray Photoelectron Spectroscopy (XPS)

XPS was employed to provide quantitative chemical information about the composition of the surface region of the polyurethanes. This technique employs an X-ray beam to induce photoelectron emission from the sample. The energy of the emitted photoelectrons is indicative of the chemical elements of origin and their bonding energy while the intensity of the emission is related to the concentration of the chemical species. This technique enables one to sample the upper 100 Å of the material of interest. The analysis was performed at the University of Toronto Surface Analysis Facility using a Leybold Max 200 X-ray photoelectron spectrometer. This machine utilizes a magnesium anode nonmonochromatic X-ray source and a spot size of 1000 Å.

XPS measurements were obtained using take-off angles ranging from 90 to 20° to obtain a compositional depth profile of the polyurethanes. The take-off angle controls the depth in the sample from which photelectrons may reach the detector (Figure 3.8). As the take-off angle is decreased from 90 to 20°, the sampling depth of the instrument

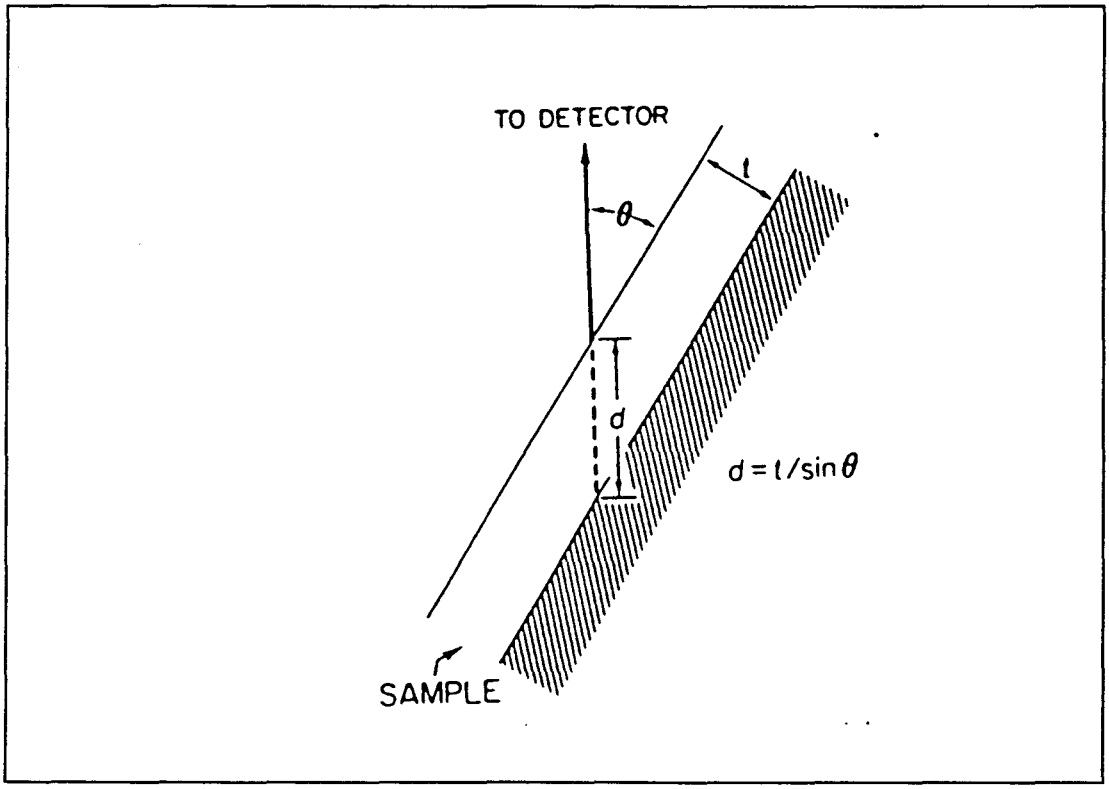


**Figure 3.8** - Variable angle XPS. Decreasing the angle between the detector and the sample (Θ) leads to decreasing sampling depth (t) or increasing surface sensitivity [Andrade, 1985].

is decreased resulting in more surface specific compositional data.

A low resolution, widescan spectrum was performed on each polymer to determine the atomic concentrations of all species present in the polymers at three take-off angles i.e. 90°, 30° and 20°. High resolution spectra were obtained for the carbon 1s signal to evaluate the contributions of urethane and hydroxyl/ether groups.

Samples for XPS analysis were prepared from films cast for platelet adhesion

studies. The samples had dimensions of approximately 10 mm x 10 mm x 1 mm. These samples were rinsed in methanol and placed in a vacuum oven at 60°C for 48 hours prior to measurement.

## 3.3 Cone and Plate Apparatus

In order to evaluate platelet response to the various surfaces of interest, an experimental apparatus was developed which would facilitate the contact of platelet suspensions with test surfaces under conditions of well-defined shear flow. The cone and plate geometry commonly used in commercial viscometers was adapted for this purpose.

### 3.3.1 Apparatus Development

When contacting platelet suspensions or blood with artificial surfaces, it is desirable to do so under flow conditions comparable to those that exist in the normal vasculature. For the most part, flow in the blood vessels is considered to be laminar in nature [Guyton, 1987]. The presence of turbulent flow is undesirable as the attendant flow disturbances have been shown to play a role in the development of intravascular thrombosis through endothelial wall damage and the local pooling of coagulation factors and platelet stimulants in stagnant regions [Slack et al, 1993].

The cone and plate geometry used in the present work is capable of producing well-defined laminar flow in the gap between the cone and plate. In the configuration used, the test surface forms the plate while the cone surface is always the same (Figure 3.9).

The cone and plate system has several unique features which are advantageous for studying the blood contacting characteristics of polymer films. The cone and plate geometry is a closed system; therefore, no pump is necessary to circulate the fluid from a reservoir through the apparatus. This is an advantage because even the more "gentle" pumps such as peristaltic pumps may cause significant blood damage [Haycox and Ratner, 1993]. Most notably, damage may include red cell lysis which results in the release of

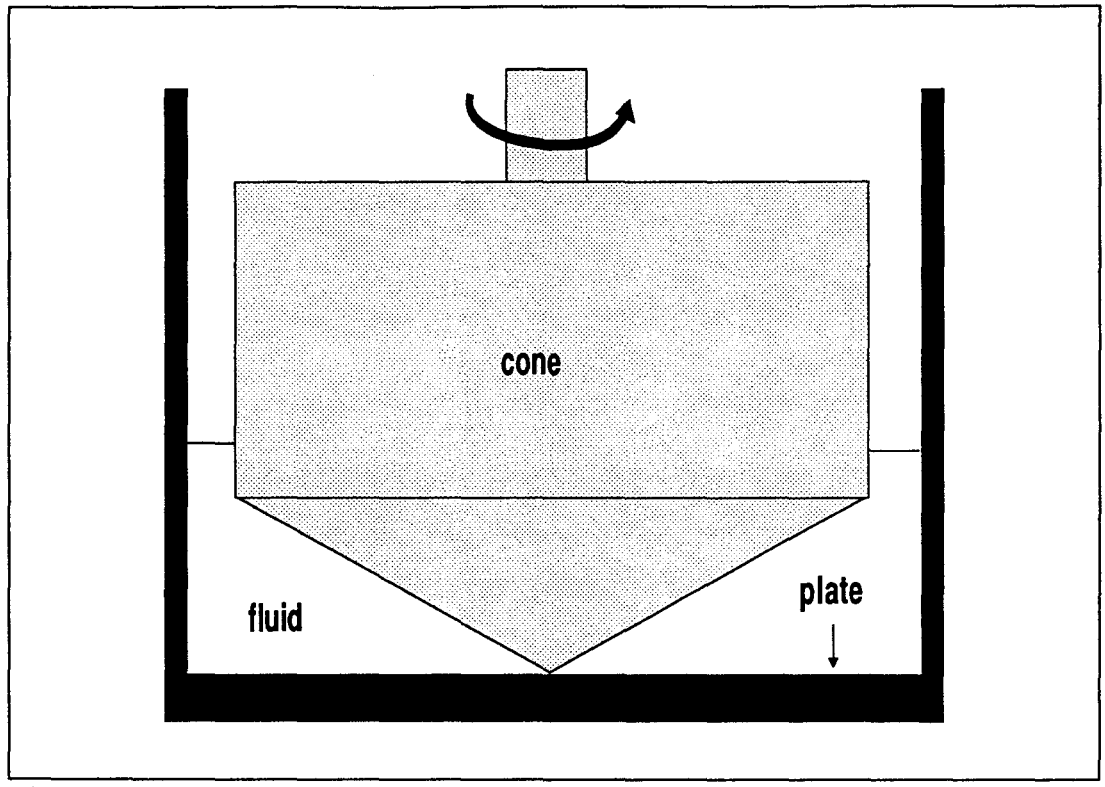


**Figure 3.9** - Simple illustration of cone-and-plate geometry.

ADP, a platelet stimulating agent, into the test fluid. This occurrence can confuse experimental results as the platelets are no longer in a quiescent state. As well, when a recirculation system is employed, it is necessary to use a significant amount of connecting tubing to which the circulating platelets are exposed. Since the tubing is an artificial material itself, the platelets will probably be activated and perhaps even destroyed via contact with this surface. The closed system of the cone and plate geometry results in the continuous contact of the platelet suspension with the test material forming the plate. Contact with the cone material can also potentially activate platelets which may affect test results.

A second advantage of the cone and plate geometry results from the nature of the flow field produced in the gap between the cone and plate. This flow field is unique in that, under certain conditions, constant shear exists across the entire radius of the rotating

cone [Walters, 1975]. This enables the experimenter to investigate the effect of fluid shear rate on the platelet-surface interaction. In addition, the fluid shear rate can be easily varied in this system by varying either the rotational speed of the cone or the cone angle.

As indicated, the test surface contacting the platelet suspension in the apparatus developed is the plate of the cone and plate geometry. The use of a test surface in planar geometry is advantageous from a practical perspective. While casting flat, uniform polymer films is relatively straightforward, it is a fairly difficult task to coat tubes or other formed pieces uniformly as is necessary in other geometries. Further, it is easier to prepare and examine the planar polymer film after the experiment using microscopic methods.

As the cone angle must be small (maximum value of $\approx 10°$) to achieve the constant fluid shear condition, the gap between the cone and plate is also small [Walters, 1975]. Therefore, very little fluid is required to fill this gap for each experiment. (The volume required in the apparatus used here is 1 to 1.5 mL). Thus, a large number of runs can be carried out with the blood obtained from a single human donor. This is an important practical advantage since the use of human platelets for adhesion experiments is more relevant than using experimental animals and the availability of human donors is limited.

Finally, it was decided to design a device which incorporated several cones operated at the same rotational speed by a common drive motor. In this way, it was possible to perform several replicates for any set of experimental conditions chosen, thus facilitating the application of statistical analyses to the data. This is an important consideration due to the high degree of variability in platelet function between donors, and even daily variations for the same donor [Fujimura et al, 1992].

### 3.3.2 Description of Cone and Plate Apparatus

The cone and plate apparatus designed for platelet adhesion studies is shown in Figure 3.10. The device was constructed with four plexiglass cones having cone angles of 7°. In preliminary work, 2° cone angles were employed; however, the very small gap

between the cone and plate in this apparatus was found to be impractical due to geometric imperfections in the system. Reynolds numbers generated by these 7° cones range from 0 to approximately 3000 when the rotational speed is varied from 0 to 350 rpm (Equation 2.5).

The cones (**A**) are connected to stainless steel drive spindles (**B**) by a small set screw which, when loosened, allows vertical adjustment of the cones ensuring that all four cones touch the base simultaneously. As opposed to conventional cone-and-plate viscometers where the cone and plate are fixed in position relative to each other, the cones are lowered into the touch position after filling the "wells" (see Figure 3.10) with the platelet suspension.

The entire cone-motor assembly (**C**) can be raised and lowered on a central screw (**D**) threaded finely for fine control of cone height. Rollers running in guide slots in the front and rear of the brass support frame (**E**) assist in stabilizing the vertical motion of the cone-motor assembly.

The four cones are rotated at a uniform speed by a small DC motor (**F**) through a series of gears and belts. The rotational speed of the cones is controlled by adjustment of a variable speed RPM feedback controller with digital display. The RPM reading of the controller was verified by stroboscopic measurement. A removable plexiglass bracket (**G**) which holds the four-well plate (**H**) in position is attached to the aluminum base plate (**I**) of the apparatus.

### 3.3.3 Four-Well Plates

The layout of the four-well plates was initially based on the dimensions of commercial six-well tissue culture plates. The use of these plates involved removing the bottoms from the four wells at the corners, inverting the plate and fastening it to an aluminum base plate, the test film being "clamped" between the two pieces. In this way, the test film formed the base of each well, and served as the plate in each cone and plate "cell" once the cones were lowered. However, the multiwell plates were found to be

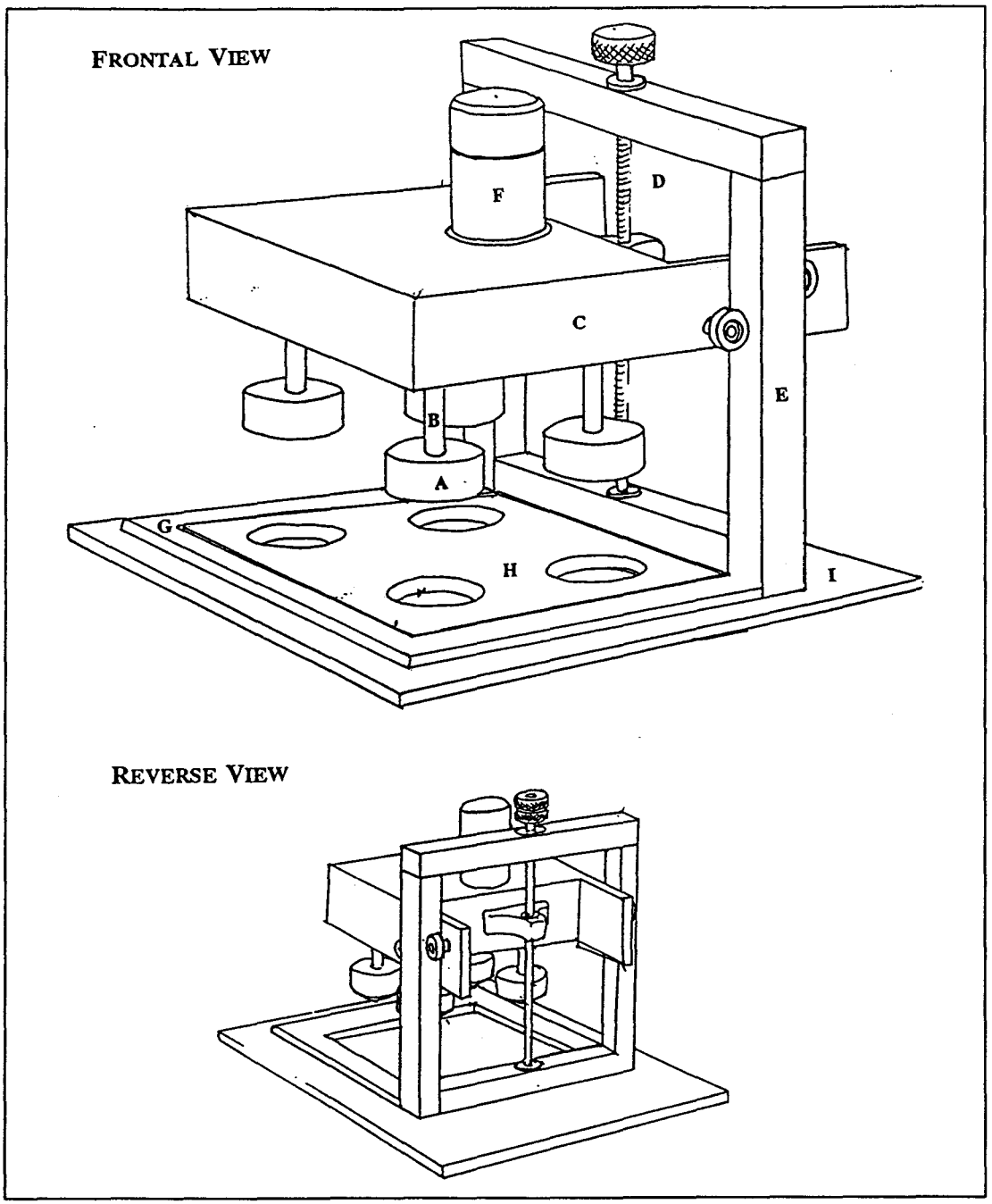


**Figure 3.10** - Illustration of cone-and-plate device. **A**) cone; **B**) drive spindle; **C**) cone-motor assembly; **D**) central screw; **E**) support frame; **F**) DC motor; **G**) bracket for four-well plate; **H**) four-well plate; **I**) base plate.

structurally poor, and they often cracked and buckled.

It was eventually decided to build the plates using aluminum with internal plexiglass sleeves to form wells of internal diameter 35 mm (Figure 3.11). The plexiglass sleeves were machined so that they fitted snugly into the aluminum plate. The sleeves were glued in place to prevent any slippage or breakage during tightening of the assembly. The plates so designed were able to withstand the stresses produced as the four-well plate and the base plate were fastened together. It was necessary to fasten the plates together firmly to avoid any fluid leakage during the experiment.

The base plate was also made of aluminum and was provided with eight threaded holes enabling the two plates to be fastened together with screws. In addition, a thin sheet of latex was placed between the plates under the test surface to provide additional gasketing material to prevent leakage from the wells during the experiment. This was required because it was found that the polyurethane and other test materials could not of themselves provide a water tight seal, due in part to small imperfections in the base of the plexiglass sleeves. The latex gasket layer used was as thin as possible to prevent unnecessary deformation of the test surface upon tightening and on contact of the cone tip.

### 3.3.4 Adjustment of Cone Height

To ensure that all four cones touched the base of the four-well plate simultaneously, a piece of carbon paper was placed between the upper and lower plates. In this way, the carbon paper covered the base of each well. The cone-motor assembly was lowered until contact of the cones with the base was made. The cones were then rotated briefly (approximately 15 sec.), stopped and raised. The carbon paper on the base was examined for small dots in the center of each well caused by rubbing of the cone tip. If all four cones were not touching the base, the cones corresponding to the wells where no dot was observed were adjusted by loosening the set screw and sliding the cone down the drive spindle. This procedure was repeated until it was determined that all cone tips were touching the base simultaneously. This procedure was also employed to verify that

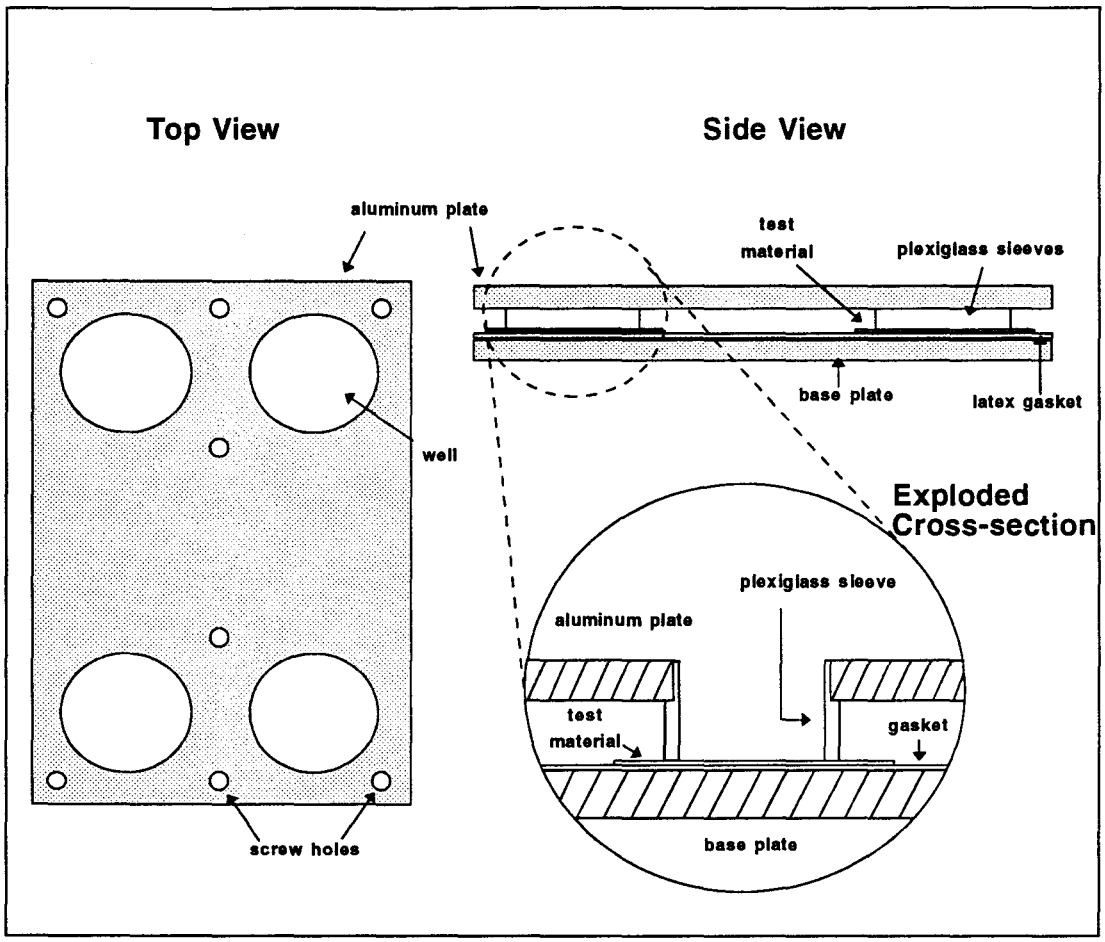


**Figure 3.11** - Final design of four-well plates used for platelet adhesion studies.

there was no excessive rubbing of the cone on the plate due to misalignment (Figure 3.12).

## 3.4 Platelet Suspension Preparation

### 3.4.1 Platelet Preparation

The method of Mustard et al [1972] was used for isolation of platelets from whole human blood. This involves washing in Tyrodes buffer containing albumin and apyrase to inhibit ADP which may be present in the supsension (Platelet buffer solutions and acid citrate dextrose preparations listed in Appendix A). The viability of such preparations has

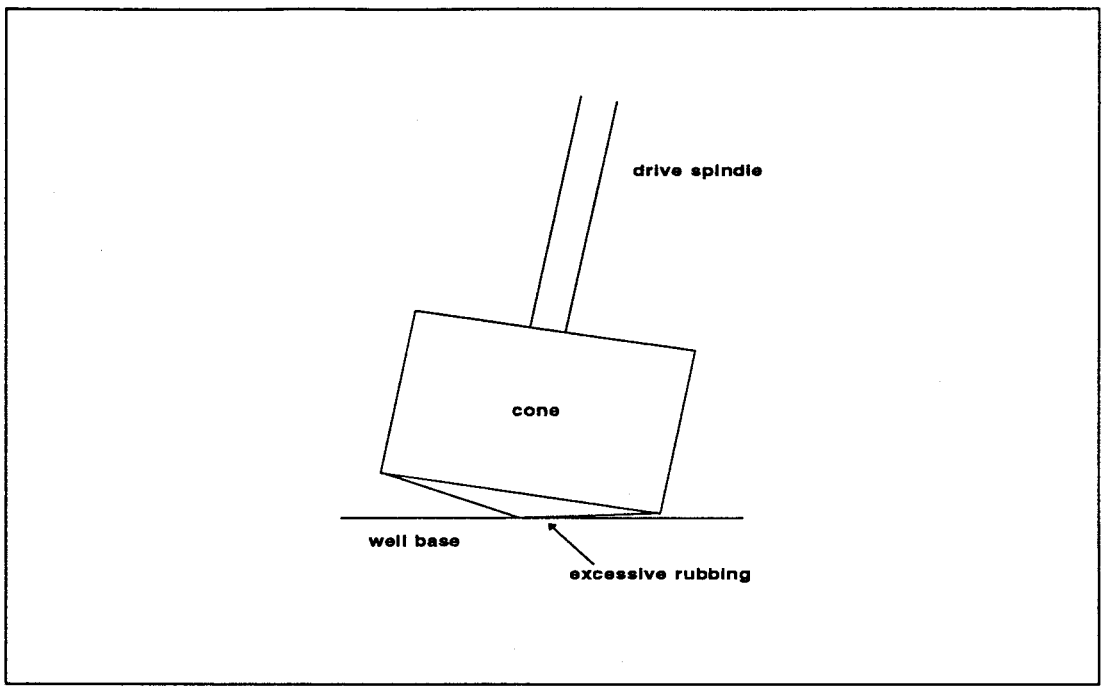


**Figure 3.12** - Excessive rubbing caused by misalignment of drive spindle

been demonstrated in many studies [Rathbone et al, 1977 ; Cazenave et al, 1979].

Blood was collected from healthy human donors via syringe into an acid citrate dextrose (ACD) solution (1 part ACD in 6 parts whole blood) to prevent surface-induced coagulation during handling and preparation. The blood (120 mL from a given donor) was collected into three 50 mL polyethylene centrifuge tubes.

The citrated blood was immediately centrifuged at 2500 x g (3000 rpm) for 90 s twice to separate platelet rich plasma (PRP) from red blood cells. The PRP was then centrifuged at 2500 x g for 15 min. The platelet poor plasma (PPP) thus obtained was carefully aspirated leaving a small platelet button. The platelets were then transferred to the first washing solution (Figure 3.13) using a siliconized glass pipet. The washing solutions were prepared in 15 mL polyethylene centrifuge tubes and placed in a water bath at 37°C.

In addition, 200 to 500 μL of sodium $^{51}$Cr-chromate (1 mCi/mL) was added to the first washing solution (Figure 3.13). The platelets were allowed to incubate in this

suspension at 37°C for 45 to 60 min depending on the level of labelling necessary for the subsequent experiments.

After labelling, the suspension was centrifuged at 1200 x g (2200 rpm) for 10 min. in a temperature-controlled centrifuge at 37°C. The suspension fluid was then discarded and the platelets were transferred into the second washing solution (Figure 3.14) by siliconized pipette. The platelets were incubated for 20 min. to allow for acclimation and recovery from the transferral step. At this point, a 5 µL sample of the suspension was transferred to 15 mL of saline solution (Isoton II, Coulter Electronics Canada) for determination of platelet concentration by Coulter Counter. In this way it was possible to determine the volume of suspension to obtain a final platelet suspension concentration of 500,000 to 600,000 platelets/µL.

The suspension was then centrifuged again at 1200 x g for 10 min. at 37°C. The wash fluid was discarded and the platelets were transferred to the final suspension fluid

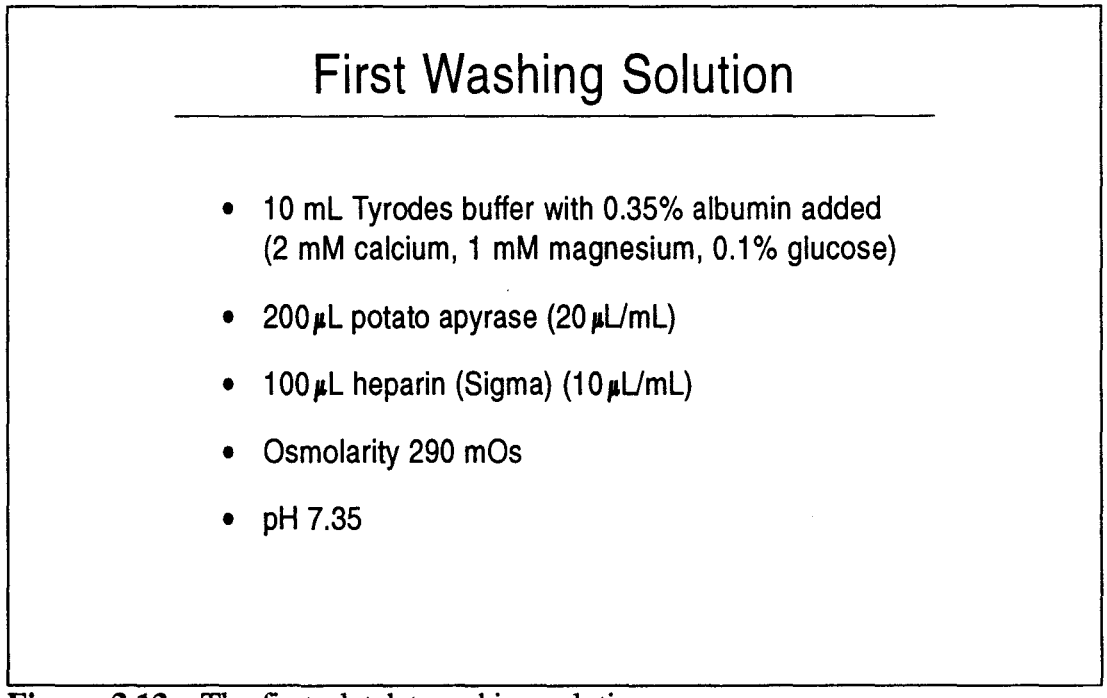


**Figure 3.13** - The first platelet washing solution

by siliconized pipette. The final suspension fluid is identical to the second washing

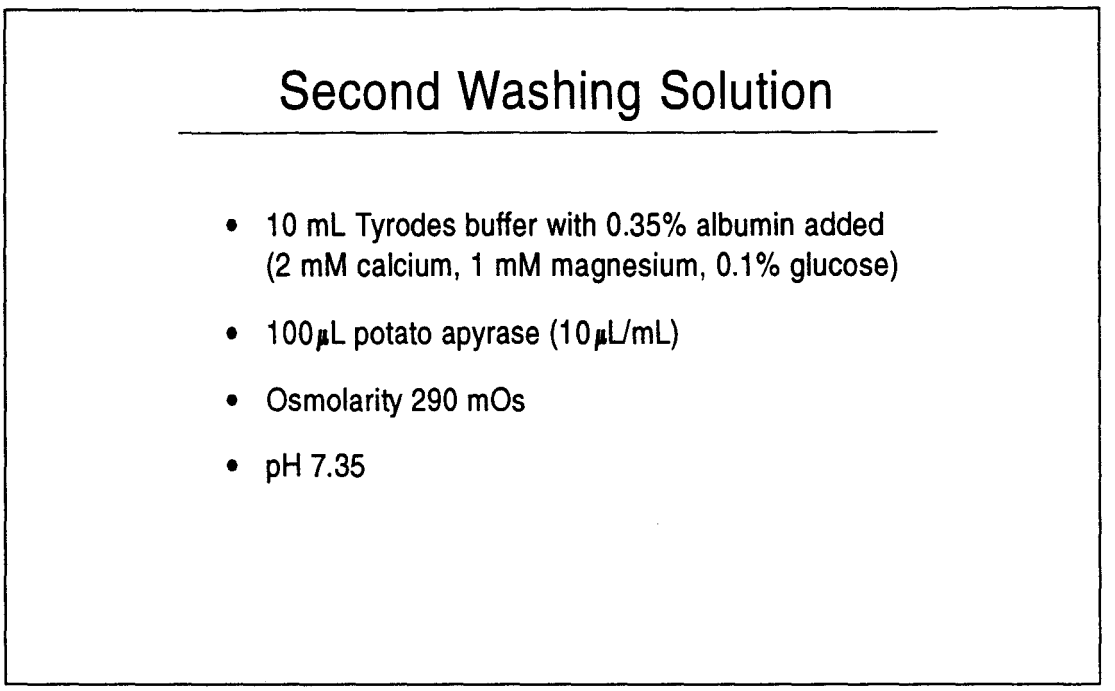


**Figure 3.14** - The second platelet washing solution

solution except that the apyrase concentration is reduced to 1 μL/mL of suspension. The platelet concentration was determined by Coulter Counter as before and the suspension kept at 37°C in a water bath.

Platelets prepared in this manner and stored at 37°C remain responsive to ADP for many hours in the presence of fibrinogen [Kinlough-Rathbone et al, 1977].

### 3.4.2 Red Cell Preparation

The red cells separated during the first two centrifugations were washed and prepared separately from the platelets. The red cell concentrate was washed three times using a washing solution containing plain Tyrodes buffer, and 0.1% wt/vol glucose at pH 8.3. The washing steps consisted of the addition of the washing solution to the red cell concentrate in a 50 mL polyethylene centrifuge tube, mixing the suspension by inverting the tube several times, and centrifuging the suspension at 2500 x g for 10 min. The fluid was then discarded. The procedure was repeated three times to minimize plasma

carryover.

At the conclusion of the three washing steps, the red cell concentrate was suspended in Eagles minimum solution containing glucose (0.1% wt/vol) and bovine albumin (4% wt/vol) at pH 8.3. The red cells were stored at room temperature in this solution until use.

### 3.4.3 Final Platelet/Red Cell Suspension

The final fluid used for the platelet adhesion experiments consisted of platelets suspended in Tyrodes buffer containing albumin (0.35% wt/vol) and apyrase (1 μL/mL) at a concentration of 250,000 /μL, with washed red cells added at 40% hematocrit. The red cell suspension was centrifuged immediately prior to adding to the platelet suspension. The final platelet concentration was adjusted to 250,000 /μL by addition of Tyrodes buffer with 0.35% wt/vol albumin. The final suspension was then stored at 37°C in a water bath until use in adhesion experiments.

## 3.5 Adhesion Experiments

The experiments performed to determine platelet adhesion to test surfaces and polymer films utilized the cone and plate apparatus described previously (Section 3.3).

### 3.5.1 Apparatus and Material Preparation

Prior to an experiment, the plexiglass cones of the apparatus were cleaned by placing them in a detergent solution (4 vol% Liquinox in distilled water). The cones were then rotated at approximately 180 rpm for 2 hours in this solution. This was followed by two rinsing procedures using double distilled water. The four-well plates were washed thoroughly with detergent and allowed to air dry overnight.

The polyurethane films were placed in a vacuum oven at 60°C for 48 h to remove any residual solvent. Several hours prior to the adhesion experiments, the films were removed from the oven, punched out into discs 40 mm in diameter, and rinsed with

methanol to remove any organic surface contamination. The polyurethane discs were then immersed in plain Tyrodes buffer (containing no albumin) and allowed to equilibrate for at least 5 h. These polymer samples were removed from the buffer solution immediately prior to the adhesion experiment and placed directly into the modified four-well plate.

In the case of the collagen-coated surfaces, the substrate polymer (a PVC-PMMA copolymer, Spectrodata, Mississauga, ON) was cut into sheets, 45mm x 85 mm, to accommodate placement under the four-well plates. The sheets were then washed with detergent (Liquinox) and placed in double distilled water. The polymer sheets were coated with collagen by immersion in a solution of acid soluble collagen (bovine achilles tendon, type I) for 3 minutes. The acid soluble collagen solution contains 0.25% wt/vol collagen dissolved in a 0.52 M solution of acetic acid (pH 2.8) and is stored at 4°C until use. The sheets were then transferred to plain Tyrodes buffer (pH 7.3) and allowed to incubate for 30 s. At this point the rapid rise in pH causes the soluble collagen monomer, which adsorbs to the surface, to polymerize rapidly forming a continuous fibrous meshwork on the polymer surface. The coated sheets were then allowed to dry for approximately 15 min prior to use in adhesion experiments.

As shown in Figure 3.15, scanning EM indicates that a uniform collagen meshwork forms on the surface of the base polymer.

### 3.5.2 Platelet Adhesion Experiments

All adhesion experiments were performed the same day the blood was received from the donor to avoid any deterioration in platelet function during prolonged storage.

The test material film, which remained wet from the equilibration step, was placed between the base and four-well plates, thereby forming the base of each well (see Figure 3.11). The plates were screwed together tightly to prevent any leakage from the wells during the experiment. The four-well plate was then placed into the positioning bracket on the base of the cone and plate apparatus.

The final platelet/red cell suspension was then added to each well via syringe (1.2

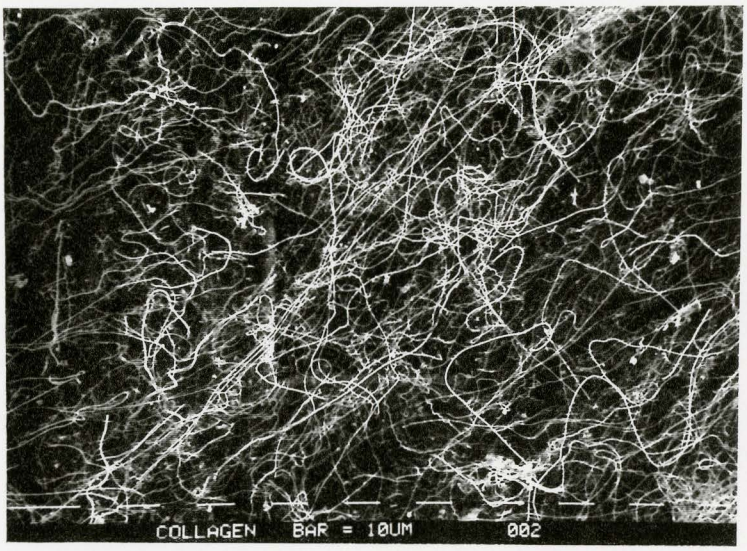


**Figure 3.15** - SEM micrograph of collagen-coated polymer surface.

mL in each well). The cones were lowered until the cone tip touched the base test material. The point of contact was determined by observing the displacement of the test fluid from the center of each well. This is readily noticed since the cone is transparent and the fluid is red. Therefore, a clear white dot is observed in the center of each well when contact is made. It is recognized that this method of determining cone height, while practical, is not precise.

The cones were rotated at a speed previously set on the rpm speed controller After a desired length of time, the cone rotation was stopped and the cones were raised. The four-well plate was removed from the positioning bracket and the suspension was aspirated from the wells with a pipet. The wells were then rinsed out 4 times by pipetting 2 mL of a rinsing solution consisting of Tyrodes buffer with 0.01 M EDTA (ethylenediamine tetraacetic acid) into each well and shaking out. The EDTA was present to disrupt any aggregates due to platelet-platelet interactions. Only platelet-surface interactions are of interest.

The four-well plates were then disassembled and the polymer discs or collagen-coated sheets were removed. A sample disc, 26 mm in diameter, was then punched out from each test surface. The size was deliberately smaller than the well diameter due to the likelihood of significant deviations of the flow pattern near the walls [Hou, 1981]. Therefore the test film sample was taken from the region of the "plate" where steady, laminar flow was expected to occur.

The film samples were then placed into 20 mL scintillation vials (Beckman). As well, 100 μL aliquots of the final platelet/red cell suspension were placed in three scintillation vials to obtain solution counts. One of the four replicates (wells) for each experiment was prepared for SEM evaluation. This involved adding enough glutaraldehyde/sodium cacodylate fixative solution into the scintillation vial to completely immerse the sample. After gamma counting (Minaxi, Canberra Packard Canada) the samples were discarded or sent to Electron Microscopy for SEM preparation. The counts per minute (CPM) determined by the gamma counter were then converted to platelet surface concentration by comparison to the CPM of the suspension of known platelet concentration.

## 3.6 Microscopic Evaluation of Platelet Adhesion

### 3.6.1 Scanning Electron Microscopy

To evaluate the morphological properties of the test surfaces and adherent platelets, scanning electron microscopy was employed. The test surfaces punched out after exposure to the platelet suspension in the cone and plate apparatus were immediately immersed in a 2% glutaraldehyde in 0.1 M sodium cacodylate solution for fixation. A small (7 x 9 mm) sample was cut from the 26 mm diameter disc, fixed and prepared for mounting. These samples were then dehydrated through graded ethanol and dried in a $CO_2$ critical point dryer (Bomar SPC-900). The samples were then mounted on aluminum specimen stubs, coated with gold, and examined in a Philips 501-B scanning electron

microscope.

### 3.6.2 Light Microscopy

To observe the surface distribution of platelets on the test materials, conventional light microscopy was employed. The samples were fixed as described above immediately following the adhesion experiment. They were then immersed in 0.05 M glycine in Tyrodes buffer solution for 30 min and allowed to dry. A solution of rhodamine phalloidin (2.5μL/200 mL Tyrodes) was then applied to the sample surface for 10 min. The samples were then dip rinsed in Tyrodes buffer and mounted on microscope slides. Rhodamine phalloidin is a fluorescent stain which stains the actin filaments of adherent platelets. The slides were then viewed using a Leitz Laborlux S microscope.

# 4.0 RESULTS AND DISCUSSION

## 4.1 Polyurethane Synthesis

A series of six polyurethanes were synthesized. All of the polymers were composed of a PTMO soft segment of either 650 or 980 g/mol, MDI and a chain extender molecule. Three different chain extenders were utilized to synthesize both sulphonated and non-sulphonated polyurethanes. Each polymer was synthesized twice to check repeatability. The nomenclature employed to describe the polymers is as follows: the polymer is first identified by the molecular weight of the PTMO soft segment employed followed by the type of chain extender. For example PTMO 980/MDA refers to the polyurethane synthesized using a 980 molecular weight PTMO and chain extended using MDA. The diisocyanate employed was MDI in all cases.

### 4.1.1 Reaction Yield

The reaction yield for the polyurethane synthesis was determined from the weight of the polymer after precipitation and extensive drying. Yield is expressed as weight percent of the total reagents. The data are presented in Table 4.1.

The sulphonated polyurethane syntheses resulted in yields near 80% while the non-sulphonated polymers exhibited slightly higher values of approximately 90%. The lower yield for the sulphonated polyurethane syntheses is most likely due to the difficulty in precipitating these polymers quantitatively from the reaction medium. The non-sulphonated polyurethanes, on the other hand, are easily precipitated in distilled water. The presence of ionic groups in the sulphonated polyurethanes may result in the formation of a stable emulsion when the polymer solution is poured into water. The emulsion can be broken by the addition of an electrolyte to the precipitation medium. Nonetheless, it is likely that a portion of the polyurethane may resist precipitation and remain in solution.

| Polymer | Reaction Yields (%) | Avg. |
|---|---|---|
| PTMO 980/BDDS | 77.0, 73.0, 84.0 | 78 |
| PTMO 980/BES | 81.8, 80.0 | 80.9 |
| PTMO 650/BDDS | 80.9, 77.0, 68.0 | 75.3 |
| PTMO 650/BES | 81.3, 85.0, 76.0 | 80.8 |
| PTMO 980/MDA | 97.0, 91.4 | 94.2 |
| PTMO 650/MDA | 91.6, 87.3 | 89.5 |

**Table 4.1** - Reaction yields for polyurethanes synthesized.

The reaction yields listed in Table 4.1 for both the BDDS and BES chain extended polyurethanes are similar. This is somewhat surprising since the BES reaction required the use of stannous octoate to catalyze the hydroxyl-isocyanate reaction. Apparently the rates of chain extension for the uncatalyzed BDDS system and the catalyzed BES system were similar.

### 4.1.2 Polyurethane Solubility and Film Casting

The non-sulphonated, MDA-based polyurethanes are soluble in DMF up to a weight/volume concentration of 10%. The sulphonated polyurethanes are only partly soluble in DMF at 6% weight/volume but completely soluble at this concentration in the more polar DMSO. However, the use of DMSO as a casting solvent requires longer casting times since DMSO is far less volatile than DMF.

Upon casting, the films exhibited distinctive qualitative characteristics related to both the type of chain extender employed and the level of sulphonate incorporation. The release of the sulphonated films from the glass casting dishes was significantly more difficult for the higher sulphur content polyurethanes (PTMO 650/BES and PTMO

650/BDDS). This is probably due to the relatively high interfacial energy of the higher sulphonate content polyurethanes, particularly at the polymer-glass interface. As well, the polyurethanes based on the aromatic chain extenders, MDA and BDDS, gave films having a particular type of texture at the air-polymer surface. This roughness is a result of a phenomenon termed Marangoni instability [Woods, 1990]. As the casting solvent evaporates during casting, concentration and temperature gradients develop within the film. This in turn results in the formation of a surface tension gradient. Simply put, this condition produces surface tension-induced convective motion of the fluid within the film as it forms resulting in an uneven surface texture of the cast film referred to as "roll cells" [Woods, 1990]. The presence of roll cells in both the MDA and BDDS, but not BES chain extended polymers suggests that the aromatic chain extenders impart a relatively high surface energy to the respective polyurethanes thereby initiating the Marangoni effect since the casting conditions were identical in all casting procedures.

### 4.1.3 Qualitative Observations

All of the polyurethanes synthesized were more or less flexible. Also, the polymers displayed reasonable mechanical strength. Increasing levels of sulphonate incorporation resulted in decreased flexibility and increased brittleness.

The incorporation of sulphonate ions in the polyurethanes produces a brown, translucent polymer, and increasing sulphonate content results in a deepening of colour. The non-sulphonated (MDA-based) polyurethanes were translucent and slightly yellow in colour.

All of the polyurethanes retained their physical integrity upon prolonged exposure to aqueous environments (water and buffer). This observation is important since any blood-contacting material must remain stable over long periods of exposure to the essentially aqueous blood environment.

## 4.2 Physical Characterization of Polyurethanes

### 4.2.1 Molecular Weight Determination

Molecular weight determination was performed by gel permeation chromatography (GPC). A typical GPC chromatogram is shown in Figure 4.1 for the PTMO 650/MDA polymer. The elution peak attributed to the polymer is somewhat broad indicating a significant polydispersity. The sharp up and down peaks following the polymer peak are due to the LiBr/DMF carrier solvent that the polymer is dissolved in and are present on all chromatograms. Similar observations were made for all six polyurethanes synthesized in this work.

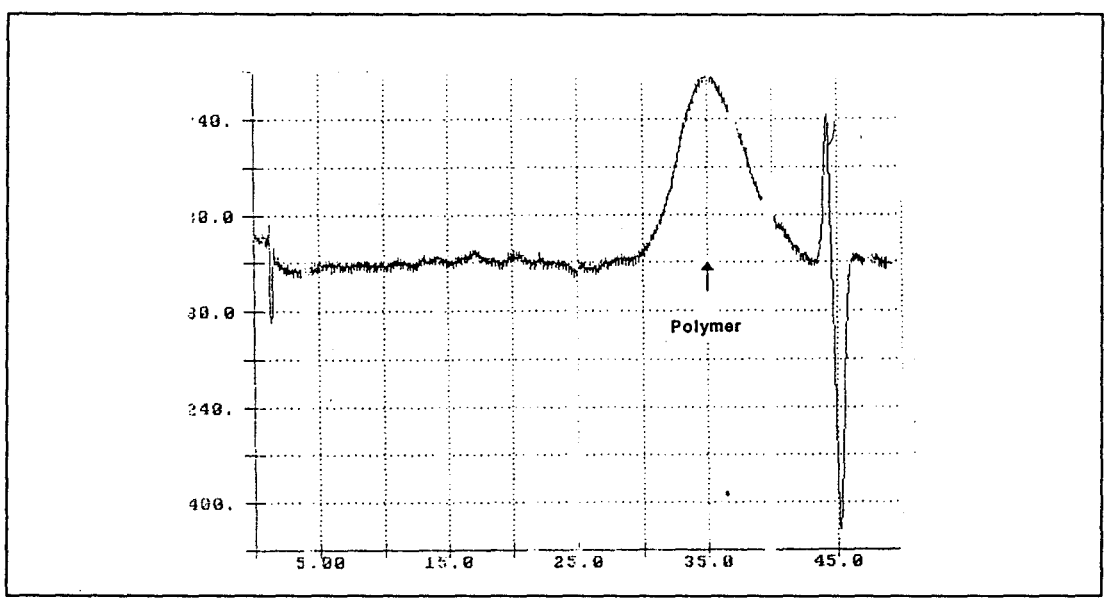


**Figure 4.1** - GPC chromatogram of PTMO 650/MDA polyurethane. X-axis represents the retention time in min and the y-axis relative intensity.

The polyurethane retention times were converted to number average molecular weights by use of a polystyrene calibration curve. The molecular weights thus determined are listed in Table 4.2.

Both BDDS and MDA chain-extended polyurethanes exhibited molecular weights similar to those reported by Santerre for the equivalent PPO based polyurethanes

| Polymer | Polystyrene Equivalent Molecular Weight (No. Avg.) | Avg. |
|---|---|---|
| PTMO 980/BDDS | 49,000, 35,000, 42,800 | 42,267 |
| PTMO 980/BES | 55,000, 53,500 | 54,250 |
| PTMO 650/BDDS | 52,000, 30,000, 41,700 | 41,233 |
| PTMO 650/BES | 34,900, 45,300 | 40,100 |
| PTMO 980/MDA | 59,800, 56,600 | 58,200 |
| PTMO 650/MDA | 59,800, 60,000 | 59,900 |

**Table 4.2** - Number average molecular weights determined by GPC.

[Santerre, 1990]. The BES chain-extended polymers yielded molecular weights comparable to the BDDS chain-extended polyurethanes. Similar Polymers were synthesized by Okkema but molecular weights were not reported [Okkema et al, 1991].

The sulphonated polyurethanes, in general, exhibited molecular weights in the range of 40,000 to 55,000 g/mol, i.e. large enough to impart satisfactory mechanical behaviour to the polymers [Lelah and Cooper, 1986]. The MDA chain-extended polyurethanes exhibited higher molecular weights than all four sulphonated polyurethanes as expected from the higher reaction yields (higher conversions) achieved for the MDA-based polymers. The decreased molecular weight exhibited by the BDDS chain-extended polyurethanes compared to the nonsulphonated analogs (the MDA chain-extended polyurethanes) is likely due to decreased reactivity of the BDDS amine groups resulting from the presence of the electron-withdrawing sulphonate groups. The fact that the molecular weights of the BES chain-extended polymers are comparable to the BDDS polymers demonstrates the effectiveness of the stannous octoate catalyst in promoting the hydroxyl-isocyanate chain extension reaction. In general, the molecular weights listed in Table 4.2 run parallel to the yields (Table 4.1) which, to a first approximation, reflect

reaction conversions.

No significant trend in molecular weight is observed with differing polyol chain length for either the BDDS or MDA chain-extended polyurethanes. However, the BES chain-extended polyurethanes exhibit increasing molecular weight with increasing polyol length at least for the two polymers investigated. A greater variety of PTMO lengths would be necessary to make any definitive statements on the effect of polyol length on overall molecular weight. Polyol length affects prepolymer size and therefore may also affect prepolymer mobility and availability of the end groups for reaction. Therefore, a large prepolymer may be expected to hinder the chain extension process and result in decreased polymer molecular weight. The apparent absence of this effect in the polyurethanes synthesized may be due to the relatively small difference in the PTMO lengths employed.

### 4.2.2 Elemental Analysis

Elemental analysis was performed on all polyurethanes synthesized to determine sulphur content. The data are listed in Table 4.3. Table 4.3 also shows the "theoretical" weight percent sulphur, which would result from a 2 MDI : 1 PTMO: 1 chain extender molar stoichiometry. Comparison of the theoretical and observed sulphur contents allows one to determine the extent of incorporation of the sulphonated chain extender in each case.

The PTMO 980/BDDS polymer displays a sulphur content similar to the PPO analog synthesized by Santerre: 1.3 and 1.4 weight percent respectively [Santerre, 1990]. However, the PTMO 980/BES polymer shows a significantly lower sulphur content than the same polymer synthesized by Okkema et al (1.4 versus 1.8 weight percent, respectively) [Okkema et al, 1991]. As expected, sulphur content increases with decreasing polyol molecular weight for both the BDDS and BES polymers.

Interestingly, the BDDS and BES chain extended polyurethanes yielded very similar sulphur contents in both polyol length forms. However, since each BDDS

| Polymer | Weight % Sulphur | | |
|---|---|---|---|
| | Theoretical | Measured | Measured Avg. |
| PTMO 980/BDDS | 3.43 | 1.32, 1.16, 1.46 | 1.31 |
| PTMO 980/BES | 1.89 | 1.53, 1,23 | 1.38 |
| PTMO 650/BDDS | 4.17 | 1.72, 1.96 | 1.84 |
| PTMO 650/BES | 2.35 | 1.94, 1.50 | 1.72 |

**Table 4.3** - Bulk weight percent sulphur of polyurethanes determined by elemental analysis in comparison to theoretical values.

molecule contains two sulphonate groups, it was expected that the BDDS polymers would exhibit significantly higher levels of sulphonation than the BES polymers. It can be seen that the BES polymers exhibit sulphur contents much closer to the expected or stoichiometric values. While the low level of sulphur in the BDDS polymers is unexpected, it is advantageous from a practical viewpoint as sulphur content above 3 weight percent has been found to give materials having poor physical properties [Santerre, 1990].

The low values of sulphur content as compared to stoichiometry could result from the production of a prepolymer of higher molecular weight than the expected 2 MDI and 1 PTMO form. Branching reactions involving isocyanate groups could also give materials of lower than expected sulphur content. These branching reactions can take place at either the sulphonate groups of the chain extender or the urea or urethane nitrogens yielding biurets and allophanates respectively (Section 2.5.1). Branching during chain extension is the most likely explanation for the low sulphur content, since the prepolymer reaction conditions and reagents are identical for both the BES and BDDS polyurethane

syntheses yet the BES polymers show higher levels of chain extender incorporation.

The branching of BDDS chain-extended (PPO-based) polyurethanes was hypothesized by Santerre as being due to the reaction of isocyanate groups with the BDDS sulphonate groups. This explanation was supported by titration data which suggested that only about half of the incorporated sulphonate groups were in an unreacted state [Santerre, 1990]. Thus, it seems likely that branching from the sulphonate groups may play a significant role in reducing polymer sulphur content below the expected values in the present work for the BDDS-based polymers.

The formation of allophanates and biurets is less likely to be a major factor in the reduction of sulphur content under the reaction conditions used. These side reactions are not usually significant at temperatures below 100°C, whereas the prepolymer reaction temperature was 90°C and the chain extension was carried out at even lower temperatures. As well, these side reactions often lead to polymers which are significantly cross-linked. A high degree of cross-linking would result in insoluble polymers and this was not observed.

Another side reaction which would reduce sulphonate incorporation is the water-isocyanate reaction. Any water contamination would lead to the depletion of available isocyanate groups available for reaction with the sulphonated chain extender resulting in a decreased polymer sulphur content since the diamine formed by the reaction of water with the diisocyanate can react rapidly with available isocyanate groups, thereby providing a competing chain extension reaction. As BDDS requires more time to completely dissolve than BES and the reaction solvent (DMSO) is hygroscopic, the BDDS solution may contain significantly more water than the BES solution when added to the prepolymer in the reaction vessel. This would cause a greater decrease in sulphur content in the BDDS chain-extended polymers than the BES polymers as observed. However, $CO_2$ gas evolution is evident in the reaction solution when water contamination is significant, and this phenomenon was not observed for the polymer syntheses performed. Therefore, any water-isocyanate reaction which may have occurred would have to have

been very limited to escape detection and would not likely be a significant contributor to the reduced sulphur contents observed.

It seems plausible that the use of a catalyst in the BES chain extension reaction may favour the hydroxyl-isocyanate reaction more than in the case of the uncatalyzed amine-isocyanate reaction of BDDS chain extension over the branching reaction involving sulphonate and isocyanate groups. In effect, the activation energy of the isocyanate-hydroxyl reaction may be reduced due to the catalyst so that the branching reaction is limited as compared to the uncatalyzed BDDS chain extension.

### 4.2.3 Differential Scanning Calorimetry (DSC)

To investigate the nature of polyurethane microphase structure, DSC measurements were made. The effect of ion incorporation was observed as well as the influence of the polyol type. The two principal properties that are observable from this analysis are the glass transition temperature (soft domains) and the crystalline melt temperature (hard

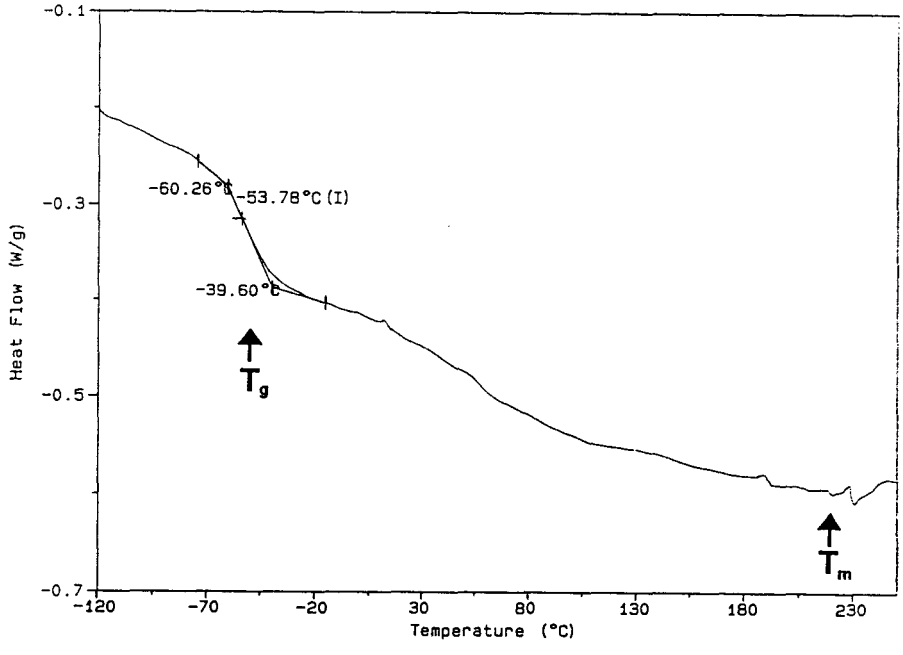


**Figure 4.2** - DSC thermogram for PTMO 980/BDDS

domains). The glass transition temperature ($T_g$) is dependent on the polyol type and is generally located significantly below room temperature. Hard and soft domain phase mixing leads to an increase of the glass transition temperature due to the presence of high melting point hard microdomains in the soft domains. Therefore, the $T_g$ is an indicator of the degree of phase separation. The crystalline melt temperature is an indicator of hard segment microdomain relaxation and disordering and is generally located near 200°C [Lelah and Cooper, 1986]. Therefore a wide temperature range was used to study polyurethane morphology using this technique. Additionally, after the initial heating cycle, the polymers were cooled and reheated to examine the nature of long and short range chain interactions [Lelah and Cooper, 1986]. Typical DSC thermograms are shown in Figures 4.2 and 4.3. These thermograms exhibit a series of transitions for the initial experiment but in the reheat all but two are eliminated, namely the glass transition and the hard segment crystal melt endotherm. Table 4.4 lists the results of the DSC analysis for the six polyurethanes synthesized as well as the two molecular weight forms of PTMO employed. As expected, all of the polymers show an increased $T_g$ with respect to the pure PTMO since some degree of phase mixing is inevitable. As well, the $T_g$ of the 650 molecular weight PTMO is slightly lower than that of the 980.

Cooling and reheating appears to have little effect on the $T_g$ values of the sulphonated polyurethanes. However, the transition appears to be sharper upon reheating indicating an improved degree of phase separation resulting probably from relaxation during the initial heating process. Interestingly, the reheat procedure results in a significant decrease in the $T_g$ values for the non-sulphonated MDA chain-extended polymers as well as an improvement in the sharpness of the transition. As well, all of the polymers display an endotherm in the range of 70 to 100°C on the first heating which is not observed upon reheating. These endotherms are generally attributed to the disordering of domains involving short-range interactions [Lelah and Cooper, 1986]. These short range interactions usually involve either hydrogen bonding involving the urethane or urea nitrogens, or in the case of sulphonated polyurethanes, ionic interactions

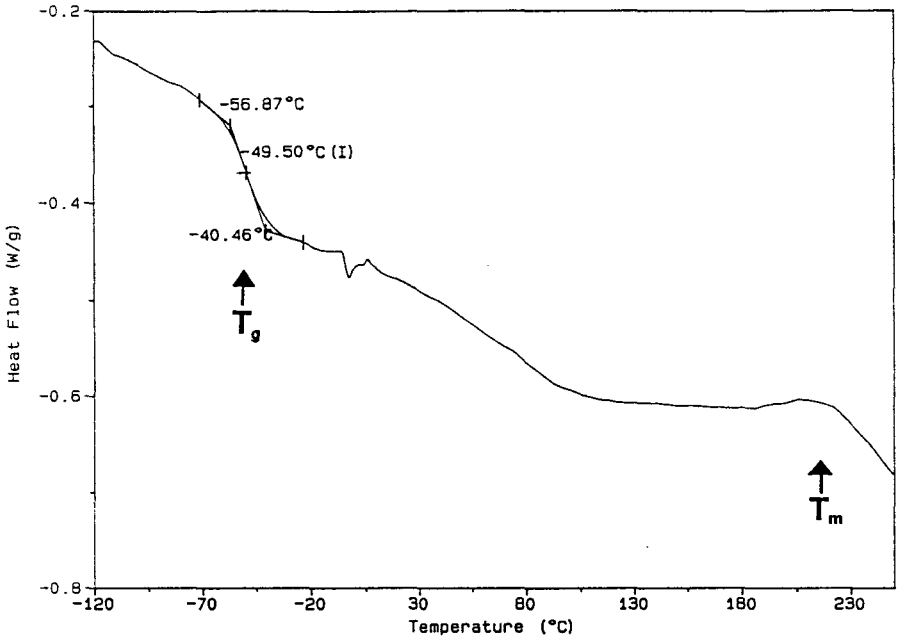


**Figure 4.3** - DSC thermogram for PTMO 980/MDA.

between sulphonate groups. Grasel and Cooper have speculated that ion pair interactions occur in sulphonated polyurethanes and that these interactions result in increased mechanical stability for these polymers in the dry state [Grasel and Cooper, 1989]. The absence of these endotherms upon rapid quenching and reheating suggests that the process of quenching "freezes out" these short range interactions. Rapid cooling after the disruption of the short range interactions does not permit the reestablishment of these domains as the rate of domain formation is slower than the rate of cooling. The crystalline melt endotherms show little change upon quenching and reheating.

The glass transition data listed in Table 4.4 point to a significant dependence of $T_g$ on polyol molecular weight whereas the $T_g$ values appear insensitive to the type of sulphonated chain extender used. However, the MDA-based polymers exhibit lower $T_g$ values as compared to the sulphonated polymers, indicating better phase separation.

| Polymer | Glass Transition Temp. 1st Heat (°C) | Glass Transition Temp. 2nd Heat (°C) | Hard Segment Crystal Melt Temp. (°C) |
|---|---|---|---|
| PTMO 980 | -73.0 | --- | --- |
| PTMO 650 | -78.8 | --- | --- |
| PTMO 980/BDDS | -53.8 | -53.3 | 220 |
| PTMO 980/BES | -51.7 | -50.0 | 205 |
| PTMO 650/BDDS | -31.9 | -33.1 | 200 |
| PTMO 650/BES | -32.2 | -34.5 | 190 |
| PTMO 980/MDA | -49.5 | -55.3 | 225 |
| PTMO 650/MDA | -42.9 | -46.5 | 220 |

**Table 4.4** - Summary of thermal transition temperature data obtained by DSC

The polyurethanes incorporating the 650 molecular weight PTMO exhibit in all cases a significantly higher $T_g$ than the 980 molecular weight PTMO polyurethanes. This indicates a significantly higher degree of phase mixing in these polymers. The cause of this phase mixing may lie in the shorter nature of the 650 PTMO which might serve to restrict chain mobility and reorientation into the typical phase separated morphology. Additionally, a lower interfacial energy may exist between the hard and soft domains in the 650 PTMO polymer serving to reduce the driving force for phase separation. As well, the additional small increase in $T_g$ associated with the incorporation of sulphonated chain-extenders suggest that the sulphonate groups act to a lesser degree to promote phase mixing. Grasel and Cooper have related the loss of order in hard segment domains to the structural interference resulting from ion pair interactions [Grasel and Cooper, 1989]. This hard segment domain disruption is likely to enhance phase mixing to some degree,

a supposition which is supported by the greater increase in $T_g$ values for the PTMO 650 compared to the PTMO 980 sulphonated polyurethanes. The higher sulphonate ion content exhibited by the PTMO 650 polyurethanes can be expected to have a greater disruptive effect on hard segment domain formation and, therefore, to enhance phase mixing. The consistent trend of increasing $T_g$ with decreasing PTMO chain length is thus probably a result of increased phase mixing resulting from both decreased chain mobility and the disruptive nature of the sulphonate groups on domain integrity.

The hard segment melt temperatures listed in Table 4.4 give some insight into the nature of hard segment domain structure. Increasing crystalline melt temperatures result from increasing hard segment cohesion which is generally related to the efficiency of hard segment packing. Therefore any factor that disrupts hard segment packing will result in a decreased crystalline melt temperature.

In a similar manner to the $T_g$ values, the PTMO 650 polyurethanes exhibit lower crystalline melt temperatures ($T_m$) than the PTMO 980 polyurethanes which employ the same chain extender, indicating an increased degree of phase mixing in the former polymers.

The disruptive behaviour of sulphonate ion groups on hard segment packing is again evident from the decreased melt temperature exhibited by the sulphonated polyurethanes as compared to the nonsulphonated polymers. This disruptive behaviour appears to increase with increasing ion content as the PTMO 650 polyurethanes generally exhibit a greater decrease in $T_m$ than the PTMO 980 polyurethanes.

Of the three chain extenders used, the BES-based polymers show the lowest values of $T_m$. The decreased hard segment cohesion exhibited by the BES polyurethanes is most likely due to the pendant side chain group of the BES molecule which acts to physically disrupt chain packing [Okkema et al, 1991]. Therefore, the chemical nature of the chain extender may drastically affect hard segment packing. The disruption of hard segment domain formation is expected to reduce the mechanical strength of the polyurethane as the hard segment domains serve to strengthen the polymer by acting as physical cross-

linking sites.

In summary, polyol chain length appears to affect both the polymer glass transition temperature and the crystalline melt temperature. As well, the degree of sulphonation alters both $T_g$ and $T_m$ values as a result of hard segment disruption probably related to ion pair interactions [Grasel and Cooper, 1989]. Ion-pair interactions may disrupt hard segment packing by interfering with the efficient packing of the hard segments. Hard segment packing may also be influenced by the structure of the chain extender molecule. Specifically, side chain groups will inhibit efficient hard segment chain packing. The morphology of these polyurethanes as revealed by DSC data is expected to influence their mechanical properties as well as their surface characteristics. The latter point will be taken up in section 4.3.

### 4.2.4 Nuclear Magnetic Resonance Spectroscopy (NMR)

Proton NMR spectroscopy was utilized to characterize all six polyurethanes synthesized as well as the individual reagent molecules. The spectra obtained are relatively simple. Peak assignment is based on the spectra of the unreacted constituent molecules utilized in polyurethane synthesis (PTMO, MDI, MDA, BES & BDDS).

The spectrum obtained for PTMO 650 shows two major peaks at approximately 1.6 and 3.4 ppm, corresponding to the methylene protons adjacent to other methylene groups and methylene protons adjacent to an ether oxygen, an electron-withdrawing group (Figure 4.4).

These peaks are large in magnitude allowing for reliable quantitative data regarding polyol incorporation into the polyurethane under study. Smaller peaks are observed at 3.5 and 2.8 ppm. The 3.5 ppm peak results from the methylene protons adjacent to the hydroxyl end groups of the PTMO molecule and the 2.8 ppm peak results from the hydroxyl protons themselves. As both of these peaks depend upon the presence of intact hydroxyl groups, the reaction of the PTMO with MDI during prepolymer synthesis will eliminate these peaks as the hydroxyl groups are reacted with isocyanate

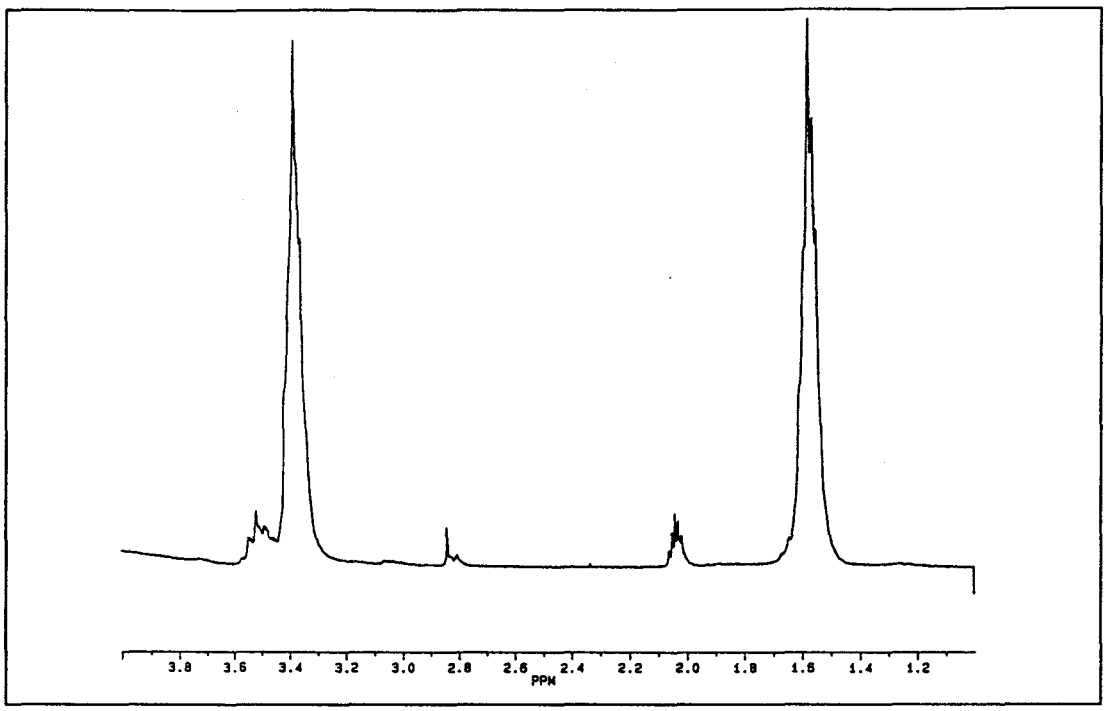


**Figure 4.4** - Proton NMR spectrum of PTMO 650.

groups forming urethane linkages. Therefore, the presence of these peaks in a polyurethane spectrum indicates the presence of unreacted PTMO, and suggests that prepolymer formation was incomplete.

The prominent peaks associated with MDI (Figure 4.5) are the aromatic proton peaks located at 7 to 7.5 ppm. As well, a peak resulting from the methylene protons located between the benzene rings is observed at 3.8 ppm and peaks representing the reacted amine groups are located at 8.5 to 9.5 ppm for MDI incorporated into the polyurethane. However, the methylene and amine proton signals are too weak to allow for reliable quantitation.

The analysis of the BDDS contribution to the polyurethane spectra is difficult since no distinctive protons are present in this molecule. Aromatic protons are also present in MDI as are amine protons. Thus, specific quantitative data regarding the incorporation of the BDDS chain extender into the polyurethanes is difficult to obtain by NMR analysis. The same is true for MDA incorporation.

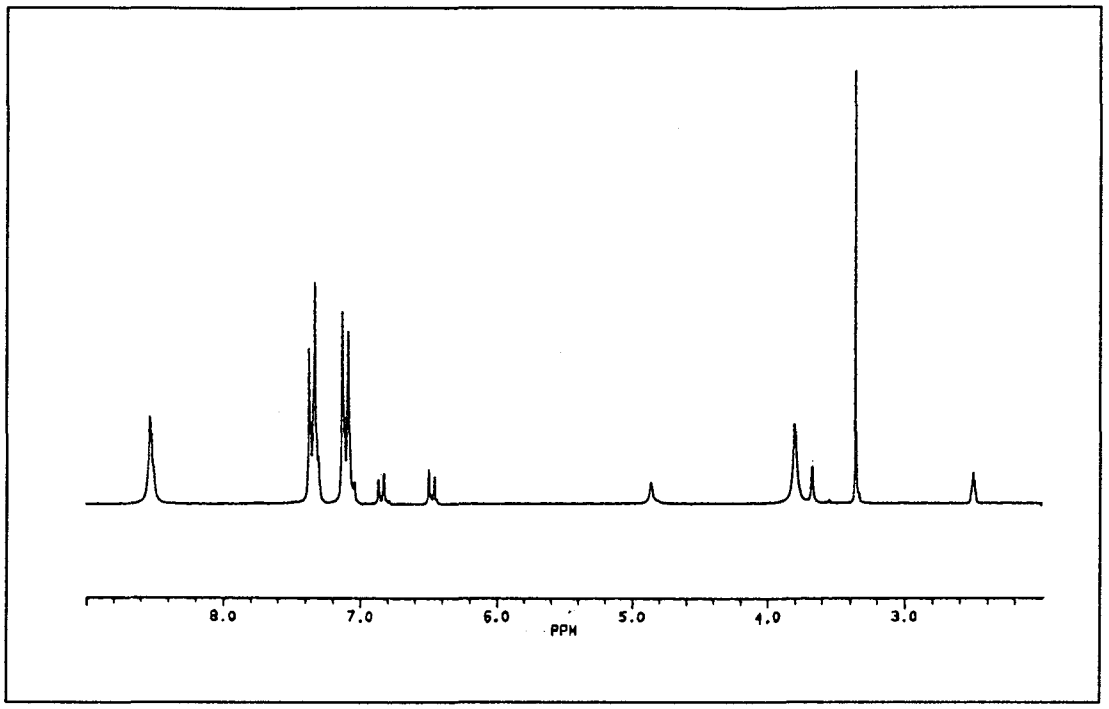


**Figure 4.5** - Proton NMR spectrum of MDI.

Several distinctive peaks are observed for BES at the upfield end of the spectrum. These peaks correspond to the methylene protons adjacent to the sulphonate group at 4.4 ppm and the methylene protons adjacent to the BES nitrogen at 3.6 ppm. However, these peaks are too weak to allow for reliable quantitation.

This point is highlighted by attempts to calculate polymer composition based on the NMR peak integration for the PTMO 980/BES polyurethane (Figure 4.6). Using the aromatic peaks to quantify the number of moles of MDI, the methylene proton peak at 1.5 ppm for PTMO, and the methylene proton peak at 4.4 ppm for BES, the molar stoichiometry obtained is 8 : 5 : 4, MDI : BES : PTMO. As this analysis suggests an excess of chain extender, one would expect the polymer to contain a higher weight percent of sulphur than stoichiometrically predicted. This level of BES incorporation was not observed by elemental analysis or XPS. In fact the elemental analysis and XPS data point to a polyurethane sulphur content less than expected based on stoichiometry.

Thus, it is concluded that this technique could best be utilized as a comparative

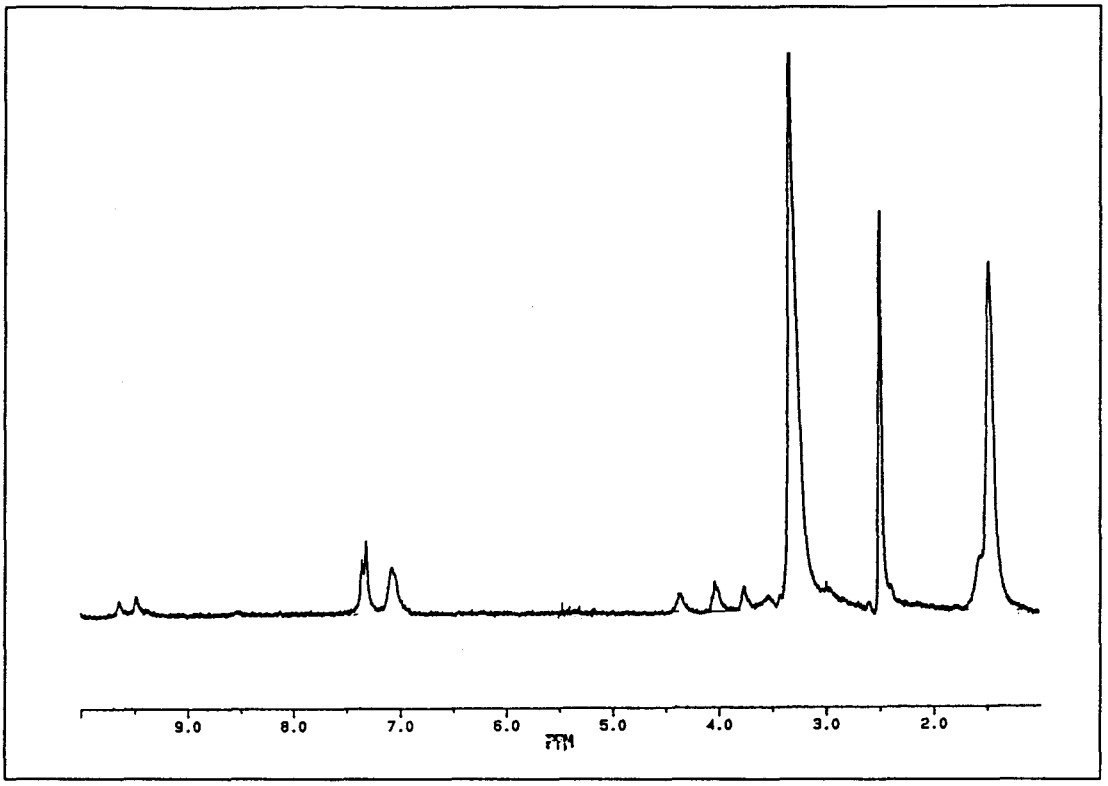


**Figure 4.6** - Proton NMR spectrum for PTMO 980/BES.

or qualitative tool in polyurethane characterization. Therefore, the polyurethane spectra located in Appendix B may be regarded as reference data which may be used to evaluate future syntheses of polymers based on these particular monomers.

### 4.2.5 Water Absorption

Water uptake by polymers intended for blood contact use when placed in contact with aqueous fluids is an important characteristic since the blood environment is largely made up of water. It should be noted that all of the polyurethanes synthesized and tested were found to remain mechanically stable upon prolonged (20 days) exposure to water.

It has been shown previously by Santerre that the incorporation of ionic groups into polyurethanes enhances water absorption [Santerre et al, 1990]. However, no correlation was found, at room temperature, between water uptake and bulk sulphur

content, although increased phase mixing was associated with increased water uptake. It was hypothesized that ion aggregates must be broken up to allow for functional group hydration [Santerre, 1990].

Table 4.5 lists the weight percent increase in polyurethane samples immersed in double distilled water at room temperature for increasing periods of time from 3 to 20 days. For the sulphonated polymers at a given exposure time, a general correlation is immediately apparent between soft segment polyol length and water uptake for the sulphonated polyurethanes. For both the BES and BDDS chain extended polyurethanes, a significant increase in the level of water uptake is observed with decreasing polyol length, probably due to a concomitant increase in sulphur and thus sulphonate ion content.

| Polymer | Sulphur content | Weight % Increase | | |
|---|---|---|---|---|
| | | 3 Day Immersion | 10 Day Immersion | 20 Day Immersion |
| PTMO 980/BDDS | 1.31 | 13.0 ± 1.4 | 13.8 ± 1.7 | 13.3 ± 1.4 |
| PTMO 980/BES | 1.38 | 11.2 ± 0.8 | 14.5 ± 1.1 | 16.2 ± 0.7 |
| PTMO 650/BDDS | 1.84 | 25.9 ± 1.6 | 37.2 ± 1.2 | 44.0 ± 0.8 |
| PTMO 650/BES | 1.72 | 25.1 ± 3.5 | 37.2 ± 2.5 | 36.5 ± 4.3 |
| PTMO 980/MDA | --- | 1.4 ± 0.2 | 0.9 ± 0.6 | 1.1 ± 0.2 |
| PTMO 650/MDA | --- | 1.1 ± 0.1 | 0.9 ± 0.7 | 0.7 ± 0.5 |

**Table 4.5** - Water absorption behaviour of polyurethanes over 20 day immersion period (± standard deviation, n=4)

However, since the PTMO 650 polyurethanes display greater phase mixing (Section 4.2.3), the increase in water absorption can also be correlated with increased

phase mixing, as noted by [Santerre, 1990]. The level of water absorption may, in fact, be an indicator both of bulk polymer sulphonate content and the availability of sulphonate groups for hydration.

The time course of water absorption is shown in Figure 4.6. As already noted the PTMO 650 sulphonated polyurethanes display an enhanced level of water uptake as compared to the PTMO 980 sulphonated polyurethanes over 20 days. As well, the level of absorption continues to increase in the PTMO 650 sulphonated polymers whereas the PTMO 980 sulphonated polymers display an essentially constant level of water absorption over time. The non-sulphonated MDA chain-extended polyurethanes exhibit very little water uptake and no significant difference in uptake between the PTMO 650 and 980 polymers even after 20 days. This result highlights the effect of sulphonate ion incorporation on the water absorption characteristics of polyurethanes.

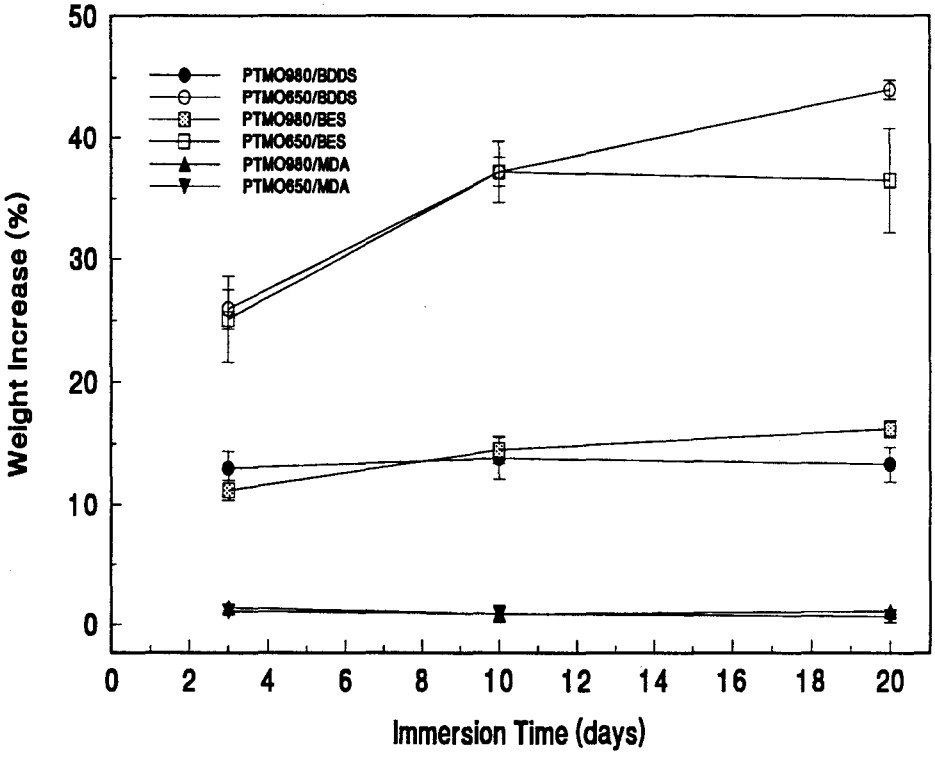


**Figure 4.7** - Water absorption behaviour of polyurethanes over 20 day time period. Error bars represent 1 standard deviation (n=4)

The degree of water absorption displayed by sulphonated polyurethanes appears to be an indicator of bulk polymer sulphonate content. Relatively small increases in polyurethane sulphur content are observed to result in large differences in water uptake responses. This water absorption behaviour appears to be insensitive to the type of sulphonated chain extender employed as BES and BDDS chain extended polyurethanes exhibit very similar water uptake responses for similar levels of bulk sulphonation.

## 4.3 Surface Characterization

When a polymeric material is placed in contact with blood, it is the polymer surface that the blood constituents encounter and interact with. The outermost surface region of the polymer may be very different chemically (and physically) from the bulk, and is generally considered to extend no more than 100 angstroms into the material. Therefore, it is essential to characterize the surface of any blood-contacting biomaterial independently of simple bulk characterization. This is generally accomplished by two approaches: water contact angle, and x-ray photoelectron spectroscopy.

### 4.3.1 Contact Angle

The simplest technique used to characterize the surface of solid polymers is contact angle measurement. This technique has the advantages of being inherently surface-specific as well as non-destructive and capable of being performed in a normal environment. However, the results obtained by this method are considered to be qualitative in nature as no satisfactory relationship has been obtained between measured contact angle and fundamental properties such as solid surface tension. The most commonly used test liquid is water for two main reasons: a) the environment which any blood-contacting biomaterial will be exposed to is largely aqueous, and b) the large surface tension of water allows the measurement of nonzero contact angles of even relatively hydrophilic materials. All contact angles reported were performed using the sessile drop technique with water as the test liquid.

Polymer surfaces have been demonstrated to be mobile [Chen and Ruckenstein,1990], i.e. able to rearrange in response to alterations in environment in order to minimize surface free energy. This being the case, one would expect that the surface region of a segmented polyurethane would contain predominantly polyether soft segment (relatively apolar compared to the sulphonate-containing hard segments) when in contact with air. Conversely, exposure to water would result in a rearrangement favouring polar hard segment domains in the surface region. Incorporation of sulphonate groups is expected to increase the hydrophilicity of the polyurethanes due to the polar nature of this functional group. Thus contact angle analysis may provide an indication of the presence of these functional groups at the polymer-water interface.

Table 4.6 lists the advancing and receding water contact angles obtained for the polyurethanes synthesized. The angles were determined by measuring 10 drops on both sides for each polymer.

| Polymer | Weight % Sulphur | Contact Angle(°) | |
|---|---|---|---|
| | | Advancing | Receding |
| PTMO 980/BDDS | 1.31 | 73.8 ± 1.8 | 33.3 ± 3.0 |
| PTMO 980/BES | 1.38 | 67.7 ± 2.2 | 21.6 ± 2.1 |
| PTMO 650/BDDS | 1.84 | 67.8 ± 1.3 | 30.3 ± 4.8 |
| PTMO 650/BES | 1.72 | 59.0 ± 1.9 | 15.2 ± 2.8 |
| PTMO 980/MDA | --- | 78.9 ± 2.0 | 58.4 ± 2.9 |
| PTMO 650/MDA | --- | 75.2 ± 0.9 | 52.9 ± 2.0 |

**Table 4.6** - Advancing and receding contact angle measurements performed by sessile drop technique (± standard deviation, n=20)

Increasing polyurethane sulphur content is expected to result in a corresponding decrease in advancing and receding water contact angles due to an attendant increase in polymer hydrophilicity with ion incorporation. Table 4.6, however, shows no such simple trends. For example, although PTMO 650/BDDS contains approximately 30% more bulk sulphur than PTMO 980/BES, the advancing water contact angles are almost identical and the receding contact angle is significantly lower for PTMO 980/BES. As well, although elemental analysis showed essentially equivalent bulk sulphur contents for both the BES and BDDS chain-extended polyurethanes, the water contact angles are significantly different for the BES and BDDS chain-extended polymers. However, the contact angle is observed to decrease with increasing sulphur content for a given chain-extender. For example, the advancing and receding contact angles for both the BDDS and BES chain-extended polymers are observed to decrease with increasing sulphur content. The MDA chain-extended polyurethanes exhibit the highest advancing and receding contact angles for both the PTMO 980 and PTMO 650 forms. Therefore it appears that while the level of bulk sulphur incorporation has a significant effect on polymer surface energetics, as reflected in the contact angle, there are also other phenomena at work. Among these phenomena are the chemical nature of the polymer surface based upon factors such as the degree of phase mixing and the difference between surface and bulk composition due to redistribution of the microdomains.

All of the materials exhibit contact angle hysteresis, which is greater for the sulphonated than for the non-sulphonated polymers. The presence of hysteresis has been interpreted as showing that reorientation favouring polar groups at the polymer surface may occur rapidly in response to the introduction of the water droplet [Okkema and Cooper, 1991]. The polar nature of water dictates that the preferential exposure of polar groups of the polymer will serve to reduce the interfacial free energy of the system [Wu, 1982]. Thus as the contact line of the liquid withdraws, the previously wetted surface of the polymer is exposed and the three-phase line resides in this region [Woods, 1990]. If the polymer surface has reoriented to a more polar form, the subsequent contact angle

measured will be substantially decreased. It must be noted, however, that other factors may affect contact angle hysteresis such as surface roughness and the incomplete removal of a liquid from the test surface as the drop recedes, resulting from polymer swelling and film adsorption to the test surface during advancing angle measurement [Wu, 1982]. As the non-sulphonated polymers were shown to swell to a far lesser degree than the sulphonated polymers, the contribution of this phenomenon may be largely responsible for the differences in hysteresis. However, since polyurethanes exhibiting similar swelling behaviour (eg. PTMO 650/BDDS and PTMO 650/BES) show significant differences in hysteresis, it appears that the surface energies of the different polymers may depend on more than simple swelling during contact angle measurement. The greater hysteresis shown by the BES polyurethanes may be indicative of higher conformational mobility at least in the surface region in comparison to the BDDS polymers.

In conclusion, the data indicate that the BES chain-extended polyurethanes show greater wettability than the BDDS chain-extended polyurethanes. As anticipated, the sulphonated polyurethanes exhibit increased hydrophilicity in comparison to the nonsulphonated polyurethanes and this difference is most striking in the receding contact angle measurements. Thus, it appears that while the bulk physical characteristics of the BDDS and BES chain-extended polyurethanes are very similar for a given PTMO length, the surface characteristics detectable by contact angle are significantly different.

### 4.3.2 X-ray Photoelectron Spectroscopy (XPS)

In an attempt to obtain chemical information regarding the composition of the surface regions of the synthesized polyurethanes, XPS was performed. Presently, XPS is the most surface specific analytical technique available, enabling the approximately uppermost 100 Å of a material to be characterized.

Three take-off angles were employed to obtain a depth profile of the elements present in the polymer. Take-off angles of 90°, 30° and 20° (relative to the surface) were employed, with the 90° angle resulting in the greatest (approximately 100 Å) and the 20°

angle giving the smallest surface penetration (approximately 30 Å). Atomic composition data for carbon, nitrogen, oxygen, sulphur and silicon were obtained from a survey spectra (0 to 1000 eV) and are listed in Table 4.7.

| Polymer | Take-Off Angle (°) | Atom Percent | | | | | C-C | C-O | C=O |
|---|---|---|---|---|---|---|---|---|---|
| | | $C_{1s}$ | $N_{1s}$ | $O_{1s}$ | $S_{2p}$ | $Si_{2s}$ | | | |
| PTMO 980/BDDS | 90 | 70.8 | 3.6 | 21.8 | 0.26 | 3.5 | 51.9 | 43.6 | 4.5 |
| | 30 | 69.1 | 2.6 | 21.9 | 0.17 | 6.2 | 58.7 | 37.0 | 4.3 |
| | 20 | 68.1 | 2.3 | 21.0 | 0.14 | 8.6 | 57.6 | 39.9 | 2.5 |
| PTMO 980/BES | 90 | 73.2 | 2.8 | 21.0 | 0.36 | 2.6 | 51.3 | 45.6 | 3.1 |
| | 30 | 73.2 | 1.8 | 20.4 | 0.16 | 4.4 | 54.9 | 43.2 | 1.9 |
| | 20 | 72.5 | 1.4 | 19.9 | 0.15 | 6.0 | 58.5 | 38.5 | 2.9 |
| PTMO 650/BDDS | 90 | 73.3 | 3.4 | 20.3 | 0.57 | 2.4 | 54.3 | 42.5 | 3.2 |
| | 30 | 72.1 | 2.5 | 20.5 | 0.41 | 4.5 | 56.0 | 41.9 | 2.1 |
| | 20 | 72.4 | 1.8 | 20.0 | 0.29 | 5.6 | 51.6 | 46.2 | 2.1 |
| PTMO 650/BES | 90 | 71.8 | 4.4 | 21.4 | 0.77 | 1.6 | 53.3 | 42.7 | 4.0 |
| | 30 | 74.5 | 2.8 | 19.5 | 0.51 | 2.7 | 54.4 | 42.5 | 3.2 |
| | 20 | 73.7 | 2.4 | 20.0 | 0.37 | 3.5 | 55.9 | 41.6 | 2.5 |
| PTMO 980/MDA | 90 | 72.6 | 5.7 | 18.5 | 0.29 | 2.8 | 56.2 | 39.2 | 4.6 |
| | 30 | 70.8 | 4.9 | 19.2 | 0.23 | 4.9 | 55.5 | 41.6 | 3.0 |
| | 20 | 69.9 | 4.2 | 19.9 | 0.28 | 5.8 | 62.2 | 35.1 | 2.8 |
| PTMO 650/MDA | 90 | 73.4 | 5.4 | 18.1 | 0.21 | 2.9 | 60.1 | 37.0 | 2.9 |
| | 30 | 71.4 | 4.4 | 19.0 | 0.22 | 5.0 | 60.3 | 36.7 | 3.0 |
| | 20 | 70.1 | 3.5 | 19.4 | 0.23 | 6.8 | 63.3 | 35.0 | 1.6 |

**Table 4.7** - XPS data for polyurethanes at three take-off angles (data precision is ± 10%).

As well, the carbon signal is broken down to the hydrocarbon (C-C), ether (C-O), and urea/urethane (C=O) contributions by high resolution analysis of the C1s peak.

Analysis of the relative contributions of these different carbon "species" to the overall carbon content of the polyurethanes yields insight into the relative amount of hard and soft segment near the surface. As urethane/urea carbon is present only in the hard segment of the polyurethanes, the relative concentration of this species is indicative of the surface concentration of the hard segment. For all of the polyurethanes synthesized, the urea/urethane carbon contribution is observed to decrease as the sampling depth decreases (Table 4.7), suggesting enrichment of the relatively non-polar soft segment at the polyurethane surface in vacuo. However, an increase in the ether carbon contribution associated with PTMO is not observed as the sampling depth decreases.

The presence of nitrogen and sulphur exclusively in the hard segment of the polyurethanes also enables monitoring of the hard segment surface profile. In agreement with the urea/urethane carbon data, both sulphur and nitrogen show relative depletion close to the polymer surface while the carbon and oxygen contributions remain relatively constant throughout the sampling region. The surface concentrations of sulphur are of prime importance, as the incorporation of the sulphonate ion to modify polyurethane blood-contacting response requires that the sulphonate group be available at the polymer surface. A slightly greater decrease in the surface concentration of sulphur with sampling depth is observed for the BES chain-extended polymers than for the BDDS chain-extended polymers for the same chain length PTMO.

The presence of significant quantities of silicon in the surface region of the polyurethanes is noted in Table 4.7. As none of the polyurethane "monomer" molecules contains silicon, it is likely that the silicon represents surface contamination. The variable take-off angle data shows surface enrichment of silicon, suggesting contamination of the surface with silicon-containing materials at some stage of the polymer preparation and handling. Three possible sources of this contamination are: use of a silicone-based joint grease during polyurethane synthesis; possible leaching of silica from the glass casting dishes during polymer film casting; deposition of silicone-based pump oil vapours during sample drying in the vacuum oven. If the silicon content is regarded purely as surface

contamination, the C, N, O and S atomic percentages may be recalculated by eliminating the Si contribution since this atom is not integral to the actual chemical structure of the polymers. These data are listed in Table 4.8.

| Polymer | Take-Off Angle (°) | $C_{1s}$ | $N_{1s}$ | $O_{1s}$ | $S_{2p}$ |
|---|---|---|---|---|---|
| PTMO 980/BDDS | 90 | 73.4 | 3.7 | 22.6 | 0.27 |
| | 30 | 73.7 | 2.8 | 23.3 | 0.18 |
| | 20 | 74.5 | 2.5 | 23.0 | 0.15 |
| PTMO 980/BES | 90 | 75.2 | 2.9 | 21.6 | 0.37 |
| | 30 | 76.6 | 1.9 | 21.3 | 0.17 |
| | 20 | 77.2 | 1.5 | 21.2 | 0.16 |
| PTMO 650/BDDS | 90 | 75.1 | 3.5 | 20.8 | 0.58 |
| | 30 | 75.5 | 2.6 | 21.5 | 0.43 |
| | 20 | 76.6 | 1.9 | 21.2 | 0.31 |
| PTMO 650/BES | 90 | 73.0 | 4.5 | 21.8 | 0.78 |
| | 30 | 76.6 | 2.9 | 20.0 | 0.52 |
| | 20 | 76.4 | 2.5 | 20.7 | 0.38 |
| PTMO 980/MDA | 90 | 75.5 | 5.9 | 19.2 | 0.30 |
| | 30 | 74.4 | 5.2 | 20.2 | 0.24 |
| | 20 | 74.2 | 4.5 | 21.1 | 0.30 |
| PTMO 650/MDA | 90 | 75.6 | 5.6 | 18.6 | 0.22 |
| | 30 | 75.2 | 4.6 | 20.0 | 0.23 |
| | 20 | 75.2 | 3.8 | 20.8 | 0.25 |

**Table 4.8** - XPS data corrected for silicon surface contamination (data precision is ± 10%).

The elimination of the Si contribution to the total atomic amount alters the data only slightly from those in Table 4.7. The trend of decreasing sulphur and nitrogen with decreasing sample depth remains, as well as the relative elevation of sulphur content for the BES polyurethanes compared to the BDDS polyurethanes.

An unexpected result is the presence of significant levels of sulphur in the nonsulphonated polymers (Table 4.7). Since none of the constituent molecules forming these polymers contains any sulphur atoms and the sulphur content appears to be relatively consistent throughout the sampling depth observed, it may be surmised that the

sulphur is also present in the form of a contaminant. The most likely source of this contamination is residual reaction solvent, DMSO, which is relatively non-volatile and difficult to remove completely. For the sulphonated polymers it should be noted that the sulphur concentration shows depth dependence similar to the nitrogen concentration, indicating hard segment surface depletion as expected. Therefore, it appears that these polymers do not contain the same levels of residual DMSO as the MDA-based polymers. The cause of the residual solvent remaining in the MDA-based polymers is uncertain, but may relate to the physical structure of the solid which may affect the ability of DMSO to diffuse out. The sulphur content measured by 90° take-off angle is of particular interest for comparison to the elemental analysis sulphur data. The 90° sampling depth may be considered to give bulk polymer atomic concentrations. Comparison of the 90° data with the stoichiometric concentrations which would result from a 2 : 1 : 1, MDI : PTMO : chain extender monomer feed, shown in Table 4.9, should yield the same sulphur content as elemental analysis assuming the reaction goes to completion (as discussed in Section 4.2.2).

As conventional elemental analysis showed, the BES polyurethanes yield sulphur contents significantly closer to stoichiometric than the BDDS polyurethanes. It appears that the 90° sampling depth of approximately 100 Å in XPS experiments yields sulphur contents very similar to those determined by elemental analysis for the PTMO 650 polyurethanes, while the PTMO 980 polyurethanes exhibit a sulphur content lower by about 50% than found by elemental analysis (about 1/2 of expected). Table 4.10 gives a comparison of the sulphur content for elemental analysis and the 90° XPS data.

These data may indicate that the PTMO 980 polyurethanes exhibit a surface region of soft segment enrichment considerably thicker than 100 Å, so that the 90° take-off angle data cannot be considered to be representative of the bulk. It may be hypothesized that the enhanced phase-mixed nature of the PTMO 650 compared to the 980 polyurethanes leads to a thinner surface region of soft segment enrichment. While the phase-mixed nature of these polymers apparently does not completely inhibit the surface enrichment

| Polymer | Atomic Concentration (%) | | | |
|---|---|---|---|---|
| | C | N | O | S |
| PTMO 980/BDDS | 74.6 (73.4) | 4.8 (3.7) | 19.0 (22.6) | 1.6 (0.27) |
| PTMO 980/BES | 75.2 (75.2) | 4.3 (2.9) | 19.7 (21.6) | 0.9 (0.37) |
| PTMO 650/BDDS | 73.6 (75.1) | 5.7 (3.5) | 18.9 (20.8) | 1.9 (0.58) |
| PTMO 650/BES | 74.2 (73.0) | 5.2 (4.5) | 19.6 (21.8) | 1.0 (0.78) |
| PTMO 980/MDA | 79.8 (75.5) | 5.0 (5.9) | 15.1 (19.2) | --- (0.30) |
| PTMO 650/MDA | 79.8 (75.6) | 6.1 (5.6) | 14.1 (18.6) | --- (0.22) |

**Table 4.9** - Theoretical atomic concentrations based on a 2:1:1 reaction stoichiometry (90° XPS data in parentheses).

of the soft segment domains it may preclude larger scale domain formation thus limiting the scale of surface reorientation (i.e. to depths greater than 100 Å). However, the more phase segregated PTMO 980 polyurethanes may be capable of larger scale reorganization of the surface corresponding to depths greater than the 90° take-off angle sampling depth.

In summary, the data obtained by XPS appear to agree broadly with the elemental analysis results concerning bulk sulphur content. In the vacuum environment utilized for XPS measurement there appears to be depletion of hard segment atomic species suggesting soft segment surface enrichment for all polyurethanes synthesized. However,

| Polymer | Sulphur Content<br>Percent of Stoichiometric | | |
|---|---|---|---|
| | Elemental Analysis | XPS 90° Take-off | $\frac{\text{XPS}_{90}}{\text{Elemental}}$ (%) |
| PTMO 980/BDDS | 44 | 17 | 39 |
| PTMO 980/BES | 73 | 41 | 56 |
| PTMO 650/BDDS | 44 | 31 | 70 |
| PTMO 650/BES | 73 | 78 | 107 |

**Table 4.10** - Sulphur content measured by XPS and elemental analysis as percent of that expected from stoichiometry and comparison of XPS and elemental analysis data.

the surface composition of these polyurethanes in an aqueous environment such as blood is very likely to be different, probably favouring the polar hard segment groups. The large values of water contact angle hysteresis described in Section 4.3.1 support the idea of surface reordering induced by the aqueous environment favouring the surface enrichment of hydrophilic constituents of the polyurethane (particularly the sulphonate groups).

## 4.4 Platelet Adhesion to Control Surfaces

The novel cone and plate device developed for platelet interaction studies was tested to assess its validity under varying experimental conditions using two control surfaces, namely collagen-coated and albumin-coated polymer films. The highly platelet-reactive collagen surface served as a positive control while the platelet passive albumin surface was employed as a negative control. The reactivity of platelets toward both of these types of material is well documented [Zijenah et al, 1990 ; Amiji et al, 1992]. The control surfaces were employed to observe platelet adhesion responses to the variation of experimental variables such as cone rotational speed, exposure time, and the presence/absence of red cells. Trends in platelet adhesion data obtained by varying these parameters provide insight into the suitability of the device for platelet-surface interaction studies.

It should be noted here that due to the relatively high Reynolds number flow conditions utilized in these studies, that some nonidealities in the shear flow field will occur. However, the analysis performed by Hou [1981] described in Section 2.4.7 suggest that these nonidealities have a relatively small impact on the fluid shear rate and that the use of Equation 2.4 yields reasonably accurate shear rate values. While the data of Hou [1981] show increasing deviation of actual shear rate from that predicted using Equation 2.4 with increasing cone angle and Reynolds number, it appears that the deviation will remain relatively small for the conditions utilized here (7° cone angle and Reynolds numbers from 0 to 3000). Additionally, the greatest deviations in shear rate are noted for the region at the periphery of the cone and the plate material sampled in the following experiments is of lesser diameter than the cone so that the regions most likely to be affected by flow disturbances are not sampled. Nonetheless, it should be noted that the shear rates listed here which were calculated by Equation 2.4 should most accurately be regarded as good approximations where the actual fluid shear rate may vary slightly across the cone radius and from that assumed by as much as 5 to 10%.

### 4.4.1 Collagen Surface

The majority of the platelet adhesion experiments performed to investigate the experimental apparatus employed collagen-coated polymer as the test surface. The strong tendency of platelets to adhere to collagen fibrils makes this surface ideal to study the effect of experimental conditions on the level of platelet adhesion. Platelet adhesion has been shown to be shear rate dependent as well as time dependent [Grabowski et al, 1972]. The effect of shear is believed to result mainly from the unique properties of red cells in flow [Goldsmith and Turitto, 1986]. Thus, trends in platelet surface deposition with shear rate and time were studied, and the role of red cells was evaluated by performing adhesion experiments in the presence and absence of red cells.

#### 4.4.1.1 Time Dependence of Platelet Adhesion

The rate of adhesion of platelets to a surface can be viewed as a result of both the rate of transport of platelets to the surface and the subsequent rate of "reaction" of platelets with the surface. The highly reactive collagen test surfaces would be expected to result in transport-limited platelet adhesion as any platelet which encountered the collagen surface would very likely adhere. It should be noted that a monolayer or "carpet" of adherent platelets occurs in the range of 60,000 to 80,000 platelets/mm$^2$. However, as surface coverage becomes significant, the reactivity of the surface will probably be reduced, resulting in a decreasing platelet adhesion rate. Thus, adhesion-time curves are expected to show an initial rapid increase in adhesion number followed by a declining rate of adhesion, and eventually a plateau level of adherent platelets.

Platelet adhesion experiments were carried out over a series of times ranging from 0 to 15 min. The data are summarized in Table 4.11. The adhesion-time curves obtained for a variety of fluid shear rates are shown in Figure 4.8. Similar curves are observed for the range of fluid shear rates tested. In all cases, a rapid rise in platelet adhesion levels is noted followed by a transition to relatively constant plateau values at approximately 10 min.

| Shear Rate ($sec^{-1}$) | Time (min) | Platelet Surface Density (platelets/$mm^2$) |
|---|---|---|
| 0 | 0 | 1677 ± 231 |
| | 2 | 2030 ± 186 |
| | 5 | 1696 ± 247 |
| | 10 | 1534 ± 77 |
| | 15 | 1795 ± 282 |
| 50 | 0.5 | 1914 ± 308 |
| | 1 | 3909 ± 661 |
| | 2 | 7026 ± 842 |
| | 5 | 9298 ± 1415 |
| | 10 | 20408 ± 2456 |
| | 15 | 14799 ± 1955 |
| 100 | 0.5 | 3089 ± 980 |
| | 1 | 6089 ± 940 |
| | 2 | 10545 ± 2956 |
| | 5 | 14594 ± 2175 |
| | 10 | 35042 ± 2937 |
| | 15 | 27985 ± 4395 |
| 150 | 0.5 | 4030 ± 1453 |
| | 1 | 9474 ± 2565 |
| | 2 | 13214 ± 5424 |
| | 5 | 21898 ± 3145 |
| | 10 | 40910 ± 3096 |
| | 15 | 37438 ± 7322 |
| 300 | 0.5 | 3568 ± 894 |
| | 1 | 10071 ± 1444 |
| | 2 | 22303 ± 3314 |
| | 5 | 36855 ± 5338 |
| | 10 | 73319 ± 10113 |
| | 15 | 72349 ± 6873 |

**Table 4.11** - Platelet adhesion to collagen-coated surfaces obtained using cone and plate device (± 95% confidence interval)

The apparently paradoxical observation of nonzero adhesion levels at zero time results from the fact that a finite time interval (approximately 40 sec) is required to introduce the platelet suspension into the wells of the apparatus, lower the cones prior to rotation, and raise the cones after the experiment. The zero time value of adhesion is the amount of adhesion that occurs in the period the platelet suspension is in contact with the test surface but the fluid is not being sheared due to cone rotation. This level of adhesion, which is the same for every experiment on a given surface, can thus be

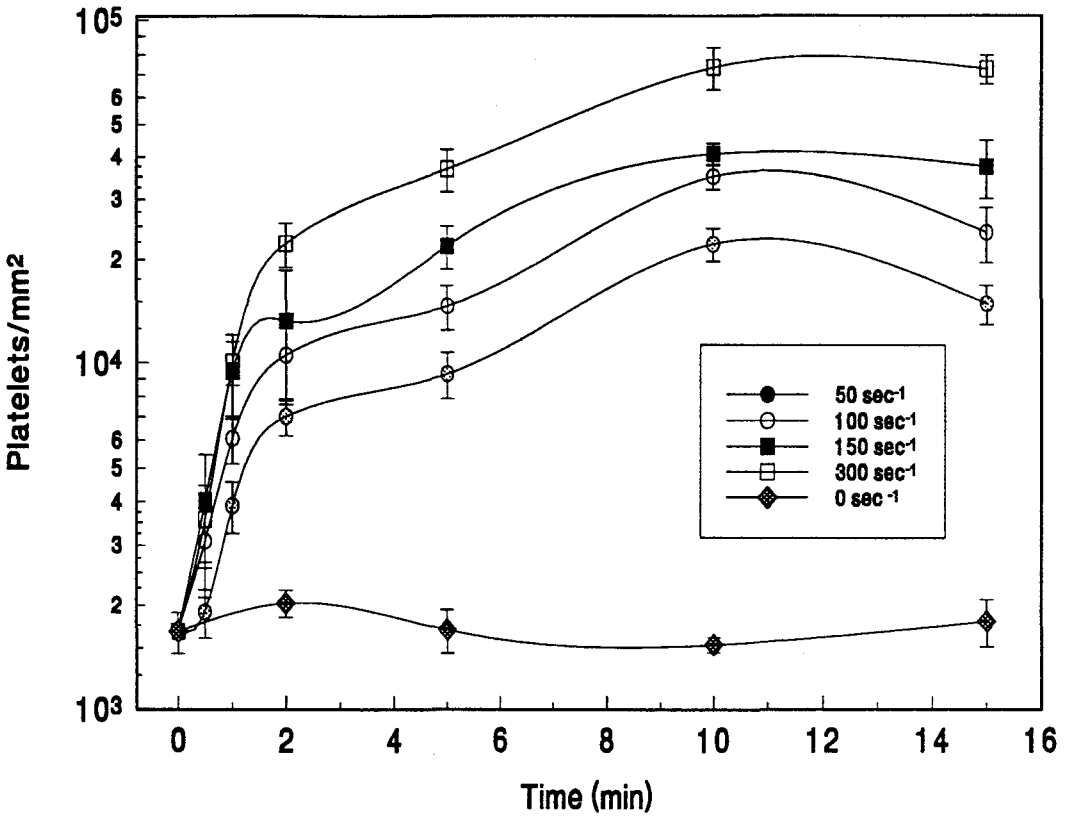


**Figure 4.8** - Platelet adhesion to collagen-coated surfaces (error bars represent 95% confidence interval. Curves fitted by cubic spline method.

regarded as a "background" or "baseline" adhesion response characteristic of the experimental system.

The overall shape of the adhesion-time curves is similar to those obtained by several other researchers using a variety of perfusion devices [Turrito and Baumgartner, 1979 ; Sakariassen et al, 1989 ;Grabowski et al, 1972]. However, the numerical platelet adhesion values obtained here are difficult to compare to those of other researchers since a variety of experimental methods have been employed using a variety of platelet and red cell concentrations, suspension media and fluid shear rates. Alteration of any of these

experimental variables may result in a significant alteration of the platelet adhesion observed.

The rate of platelet adhesion over the time period studied is shown in Figure 4.9.

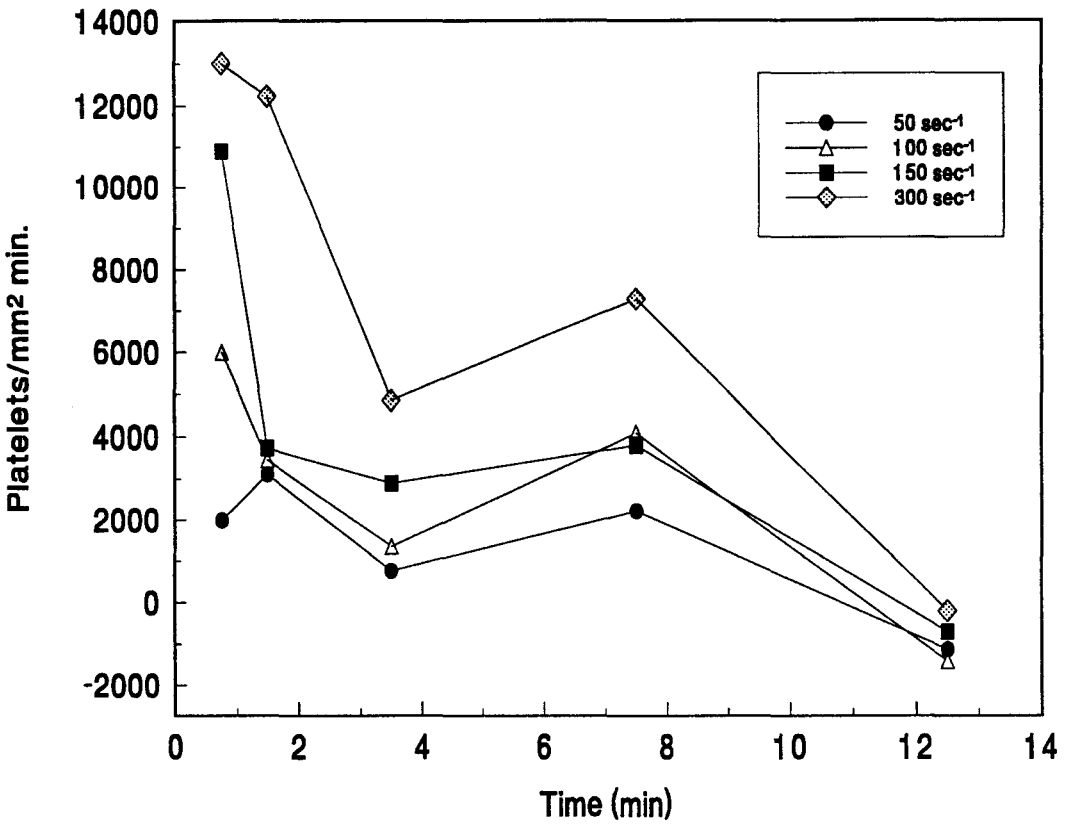


**Figure 4.9** - Rate of platelet adhesion to collagen-coated surface obtained using 4 fluid shear rates.

These data were obtained by approximating the slope of the adhesion-time curves of Figure 4.8 at the midpoints of each time point as a straight line. In this way an approximate rate of adhesion was calculated and plotted against the midpoints of the time points used to evaluate adhesion in Figure 4.8. A more accurate analysis would require more experimental points as well as the use of a more sophisticated technique for evaluating the slope of the adhesion-time curves. However, the analysis performed shows a general trend of decreasing rate of adhesion over time, eventually reaching a zero or

slightly negative value suggesting the arrest of adhesion or perhaps some platelet detachment. A decreasing number of sites for attachment on the reactive collagen surface results in a decreased rate of adhesion over time. The decrease in the rate of platelet adhesion with time suggests that platelet-platelet interactions (i.e. aggregation) are not significant probably because the use of EDTA in the rinse fluid disrupts platelet-platelet interactions mediated by the calcium ion-dependent GP IIb-IIIa receptor. The presence of flow is also expected to limit platelet aggregation. Regions of flow stagnation are believed to promote thrombosis by allowing the local accumulation of platelet-activating substances [Goldsmith and Turitto, 1986].

A decreasing rate of adhesion is noted for decreasing fluid shear rates, most notably at short times, where platelet surface coverage is low. An increased rate of fluid shear is expected to increase platelet transport to the test surface, leading to an increased deposition rate [Grabowski et al, 1972]. This dependence of adhesion rate on shear rate suggests a transport-limited adhesion mechanism as expected for the highly reactive collagen surfaces employed.

An interesting feature of Figure 4.9 is the apparent reversal in platelet adhesion rate between 2 and 5 min. As seen in Figure 4.8, a transient levelling off in adhesion is observed in this interval similar to behaviour observed by Smith and Dangelmaier [1990]. However, these researchers did not extend their observations beyond 5 min. A subsequent increase in adhesion up to 10 minutes may be a result of the recruitment of more platelets by the surface via the release of adherent platelet granule constituents, several of which can act to stimulate platelets [Hawiger, 1989]. Such additional adhesion is analogous to "second wave" phenomena in platelet aggregation experiments [Kinlough-Rathbone and Mustard, 1987] The lack of observation of this behaviour by other experimenters using perfusion devices may indicate that it is linked to the "closed" nature of the present apparatus. No fluid enters and leaves the test region, allowing for the possibility that released granule products may accumulate and act to stimulate a "second wave" of adhesion.

#### 4.4.1.2 Shear Rate Dependence of Platelet Adhesion

The nature of the shear flow imparted to the platelet suspension is expected to affect the level of platelet adhesion. In particular, the transport of platelets to the test material surface is expected to be augmented by increasing levels of fluid shear rate. This phenomenon is a direct result of the physical behaviour of red cells in shear flow [Grabowski et al, 1972]. However, fluid shear may also act to dislodge weakly adherent platelets from the test surface. Therefore, a dynamic balance is created in which the fluid shear may act both to increase and decrease platelet adhesion. The net result on adhesion density will depend on the strength of the adhesive bond between platelet and surface.

The experiments performed employed fluid shear rates varying from 0 to 300 $s^{-1}$. These fluid shear rates were obtained by varying the rotational speed of the cones from 0 to 350 rpm. Figure 4.8 shows the adhesion-time curves obtained employing five fluid shear rates, including zero. As expected, increasing levels of fluid shear rate result in increasing initial rates of platelet deposition. In addition, and unexpectedly, the plateau levels of adhesion at longer times also increase with increasing shear rate. A decrease in shear rate should lead to decreased platelet transport to the test surface resulting in a reduced rate of deposition as observed. However, the plateau levels of adhesion are expected to be independent of shear rate if a monolayer of platelets is deposited (a platelet monolayer should contain 60,000 to 80,000 platelets/$mm^2$). In contrast to this expectation, Figure 4.10 shows an increasing shear rate dependence of platelet deposition with time, even at the longest time where plateau levels are apparently reached. It is clear that full monolayers are not formed at the lower shear rates, although it is possible that such monolayers would be formed at longer times. The apparent partial monolayer limits at low shear rates are otherwise difficult to explain.

It is apparent from Figure 4.8 and Table 4.10 that in the absence of shear, platelet deposition is relatively low up to 15 min. The zero shear adhesion curve shows an essentially constant level of deposition over the period of the experiment. This suggests that the combined rate of settling and diffusion of platelets in the suspension medium is

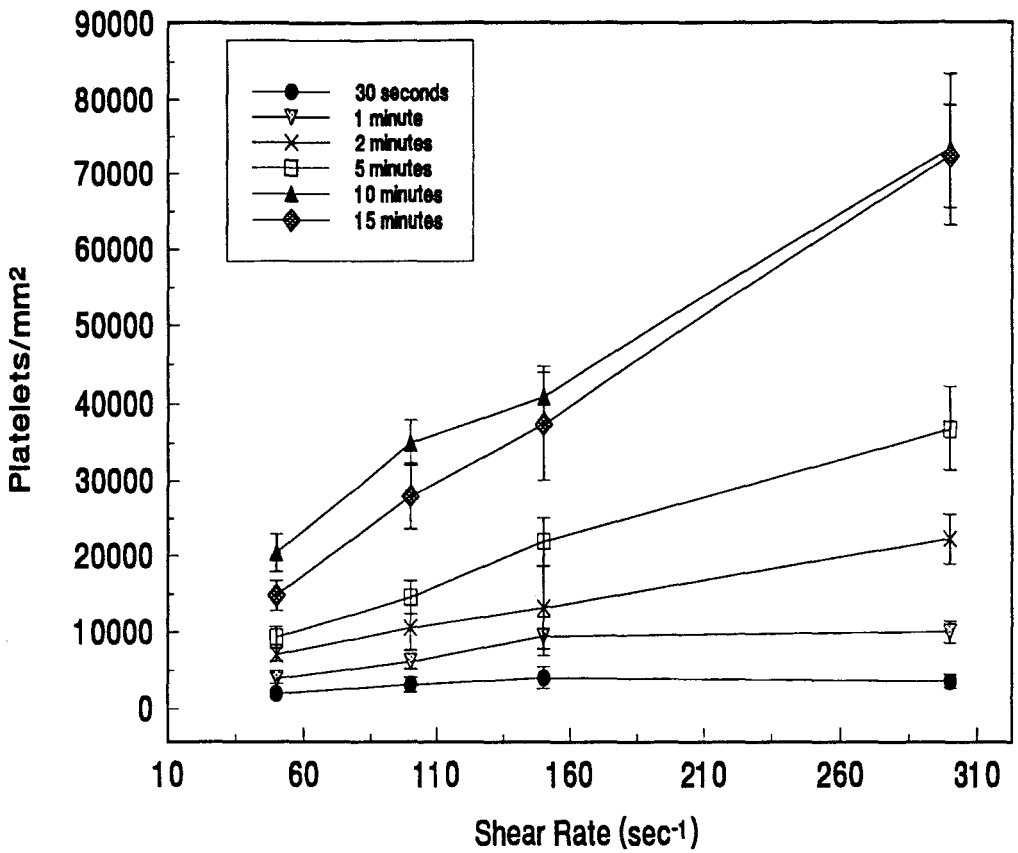


**Figure 4.10** - Shear rate dependence of platelet adhesion to collagen coated surface (error bars represent 95% confidence interval)

too low to result in increasing levels of platelet deposition over a 15 min period. Comparison of platelet deposition values with those predicted by Brownian motion diffusion is given in Figure 4.11. The Brownian motion deposition curve was obtained by use of Equation 2.3 (assuming diffusion-limited adhesion mechanism) and a diffusion coefficient of $10^{-7}$ $cm^2/s$ [Grabowski et al, 1972].

Whereas the adhesion curve predicted by diffusion exhibits a smoothly increasing number of adherent platelets over time, the experimental data show a more rapid increase followed by an essentially constant level of adhesion. This behaviour may result from

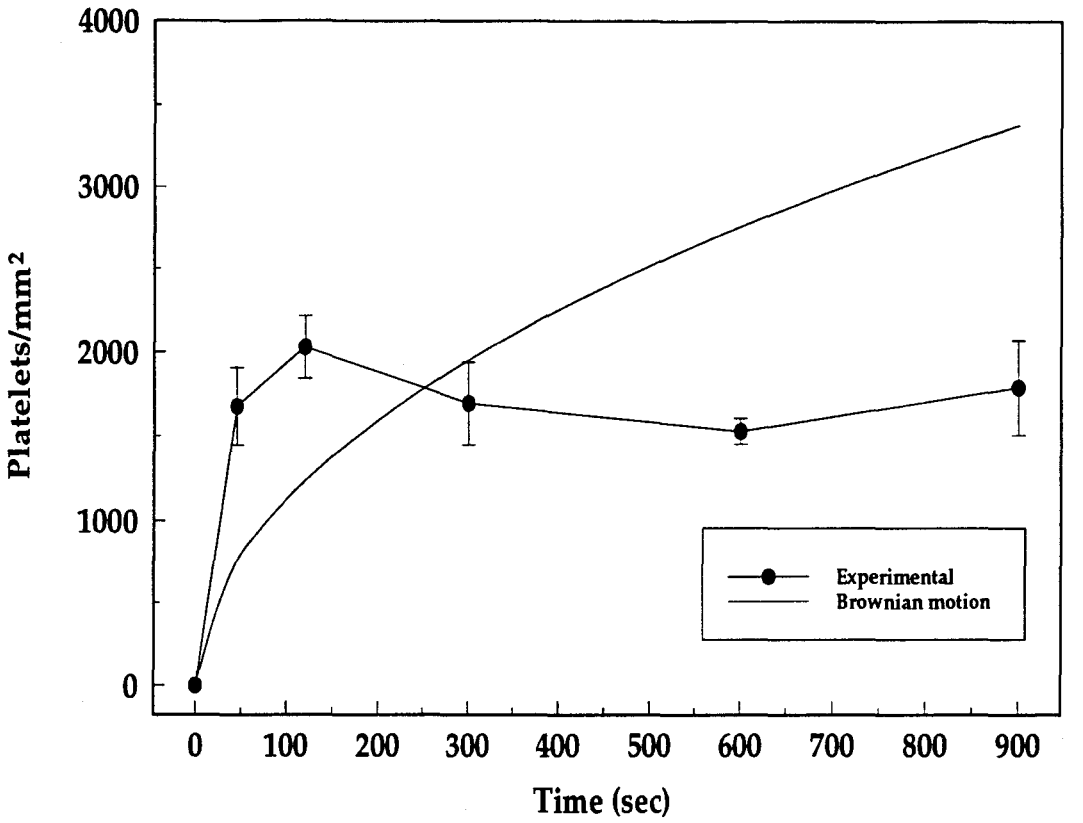


**Figure 4.11** - Comparison of platelet adhesion predicted by Brownian motion transport and experimental observation (error bars represent 95% confidence interval).

the method of introduction of the platelet suspension into the wells and the nature of the platelet suspension itself. The more rapid rate of adhesion compared to that predicted is most likely due to the convective mixing action which takes place as the suspension fluid is introduced to each well via syringe. Secondly, the diffusion equation assumes the medium can be considered as a continuum. The presence of relatively large particles in the suspension (other platelets and red cells) could result in a decrease in platelet diffusivity due to impedance of platelet motion. This decrease in platelet transport would serve to lower the level of platelet adhesion with respect to the prediction over time as

is seen at the longer times in Figure 4.11.

It was of some concern that the deviations from laminar flow at the periphery of the cone and plate device would alter platelet transport and deposition in an unpredictable way. The systematic shear rate dependence of platelet adhesion to the collagen test surfaces observed argues against this, and is consistent with previous reports [Nievelstein et al, 1988 ; Sakariassen et al, 1990]. The general trends in the data indicate that the flow field created in the cone and plate gap is probably laminar as assumed, and that the relative fluid shear rates imparted by the rotating cone can be approximated by Equation 2.4.

#### 4.4.1.3 Effect of Red Cells on Platelet Adhesion

Red cells have the effect of augmenting platelet transport in flowing blood. The rotation and other motions of red cells in flow creates increased local mixing. This physical effect of red cells has been shown to increase the effective diffusion coefficient of platelets by two orders of magnitude [Grabowski et al, 1972].

Figure 4.12 shows the platelet adhesion response observed over 15 min at 150 $s^{-1}$ shear rate at 40% and 0% hematocrit. Platelet deposition is greatly reduced at 0% compared to 40% hematocrit. It is also seen that platelet adhesion using the red cell-free suspension at 150 $s^{-1}$ is comparable to that noted in the zero shear experiment at 40% hematocrit. This suggests that the flow field present in the gap between the cone and plate is essentially laminar and not significantly disturbed. Any secondary flows present in the flow field would be expected to result in increased platelet transport to the test surface leading to an increased level of platelet deposition. Conversely, a laminar flow field would produce no convection in the direction of the test surface. Therefore, in the absence of the physical mixing of circulating platelets by flowing red cells, no increased adhesion should occur with respect to the static case as is observed. The presence of shear may, in fact, serve to reduce the number of adherent platelets by dislodging weakly adherent platelets which may remain adherent in the static experiment (Figure 4.12). Thus, the platelet adhesion data using a red cell-free suspension support the conclusion

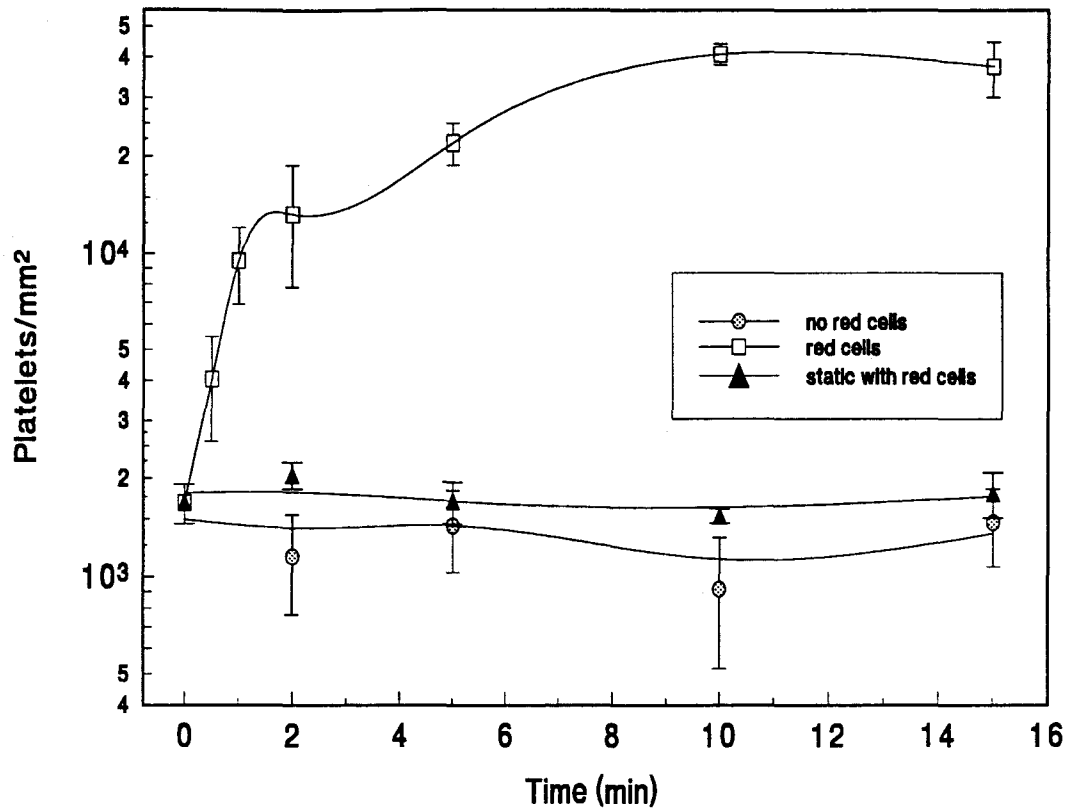


**Figure 4.12** - Effect of the presence of red cells on platelet adhesion to collagen-coated surface at 150 $s^{-1}$ shear rate (error bars represent 95% confidence interval).

that the fluid flow fields are essentially laminar with minimal secondary flows.

#### 4.4.1.4 Microscopic Evaluation

Both scanning electron microscopy and optical microscopy were employed to gain information regarding the physical morphology and surface density of the adherent platelets. The physical morphology of the adherent platelets can provide indications of the degree of activation of the platelets. Additionally, platelet-platelet and platelet-surface interactions may be differentiated by microscopic evaluation.

Figure 4.13 shows platelets adherent to a collagen surface after 2 min of exposure

to 300 $s^{-1}$ fluid shear rate. The distribution of collagen fibers appears to be relatively

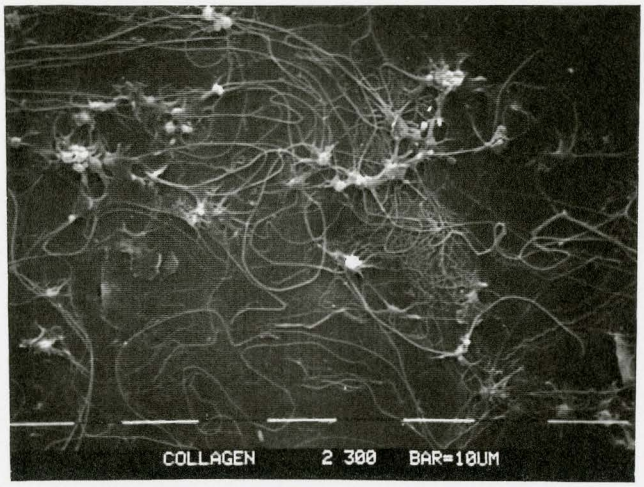


**Figure 4.13** - Scanning electron microphotograph of platelets adherent to collagen surface (fluid shear rate=300 $sec^{-1}$, time=2 minutes).

uniform. However, areas of the base polymer film remain uncovered. Some of these bare regions appear to be larger than platelets (approximately 2μm in diameter), indicating that a fraction of the platelets transported to the surface during the experiment may contact the base polymer surface without interacting with a collagen fibril. This would suggest that the effective surface area of the collagen coating is somewhat less than the area of the support film. Thus, the calculated platelet densities may be somewhat less than the true densities on collagen, since total surface area is used in the calculations. However, the coverage of collagen fibrils over the polymer film surface is extensive and it is possible that smaller fibrils are present which are not resolved at the level of magnification used. Indeed, greater surface coverage by collagen fibrils is evident at

higher magnification (Figure 4.14). No attempt was made to measure the surface density of collagen achieved by the coating procedure. However, the procedure was carried out identically for each experiment to minimize (ideally to eliminate) the possibility of variable extent of collagen surface coating.

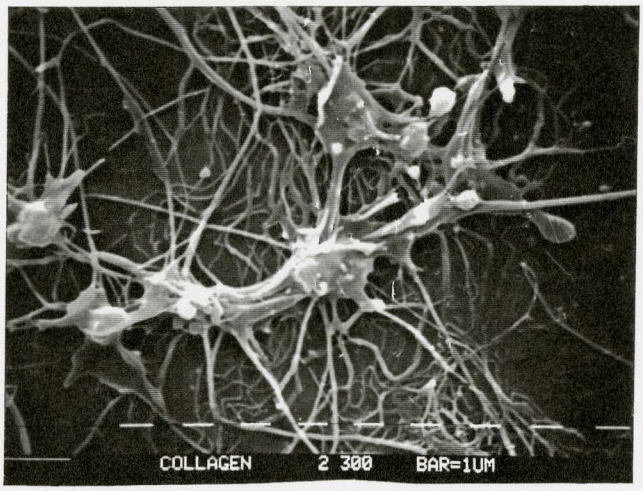


**Figure 4.14** - High magnification photograph of platelets adherent to collagen-coated surface

Platelets adherent to the collagen surface appear to be activated and well-spread, showing pseudopod and granulomere formation at short times of exposure. The adherent platelets observed in Figure 4.13 do not appear to be deposited randomly over the entire surface but rather form local adherent aggregates. The platelets adhere in aggregates on the collagen surface, not piling directly atop one another but exhibiting interconnecting pseudopod formation and membrane fusion as well as interaction with the collagen fibrils. This reaction to collagen fibrils has been previously documented by Barnhart et al [1972] and appears to be a common feature of platelet-collagen adhesive interactions.

The presence of many randomly distributed collagen fibrils makes the observation of platelet fine morphological features difficult. However, Figure 4.14 clearly shows adherent platelets exhibiting activation and pseudopod formation. The degree of platelet

granule secretion is difficult to assess by morphological observation but is likely to occur rapidly in response to collagen stimulation [Sixma, 1987 ; Packham, 1991]. The degree of platelet activation observed is not surprising as fibrillar collagen is considered a strong platelet agonist and is believed to mediate the platelet response to the subendothelial region of the injured vessel [Packham, 1991].

Light microscopic evaluation was performed to assess the overall surface distribution of adherent platelets on the collagen surface. Figure 4.15 shows the observed platelet distribution on a collagen-coated surface exposed to 300 $s^{-1}$ of fluid shear for 2 min. A series of photographs taken over various regions of the surface show an essentially uniform distribution of adherent platelets over the test surface at the level detectable by light microscopy. Since the experimental apparatus developed is expected to produce a uniform rate of shear across the entire test surface, uniformity of platelet coverage is expected. Significant flow disturbances and deviations from laminar flow behaviour would likely lead to significant variations in fluid shear rate over the test surface, which would be expected to create a non-uniform pattern of deposition across the radius of the test surface. In particular, any regions of flow stagnation would be expected to exhibit an enhanced platelet adhesion response. Flow stagnation is believed to be a contributing factor to thrombogenesis in vivo through accumulation of platelet activating and coagulation factors [Goldsmith and Turitto, 1986]. Thus, the uniformity of platelet deposition observed over the collagen test surface can be regarded as an indication of the laminar nature of the flow field in the cone and plate apparatus.

#### 4.4.1.5 Platelet Diffusion Calculations

Equation 2.3 permits the calculation of diffusion coefficients using platelet surface deposition versus time data. Effective platelet diffusion coefficients were thus determined for the five fluid shear rates employed in the adhesion experiments. The estimates of diffusivity in the present work were obtained using a modified form of Equation 2.3 in which the kinetic term was neglected. The transport-limited nature of

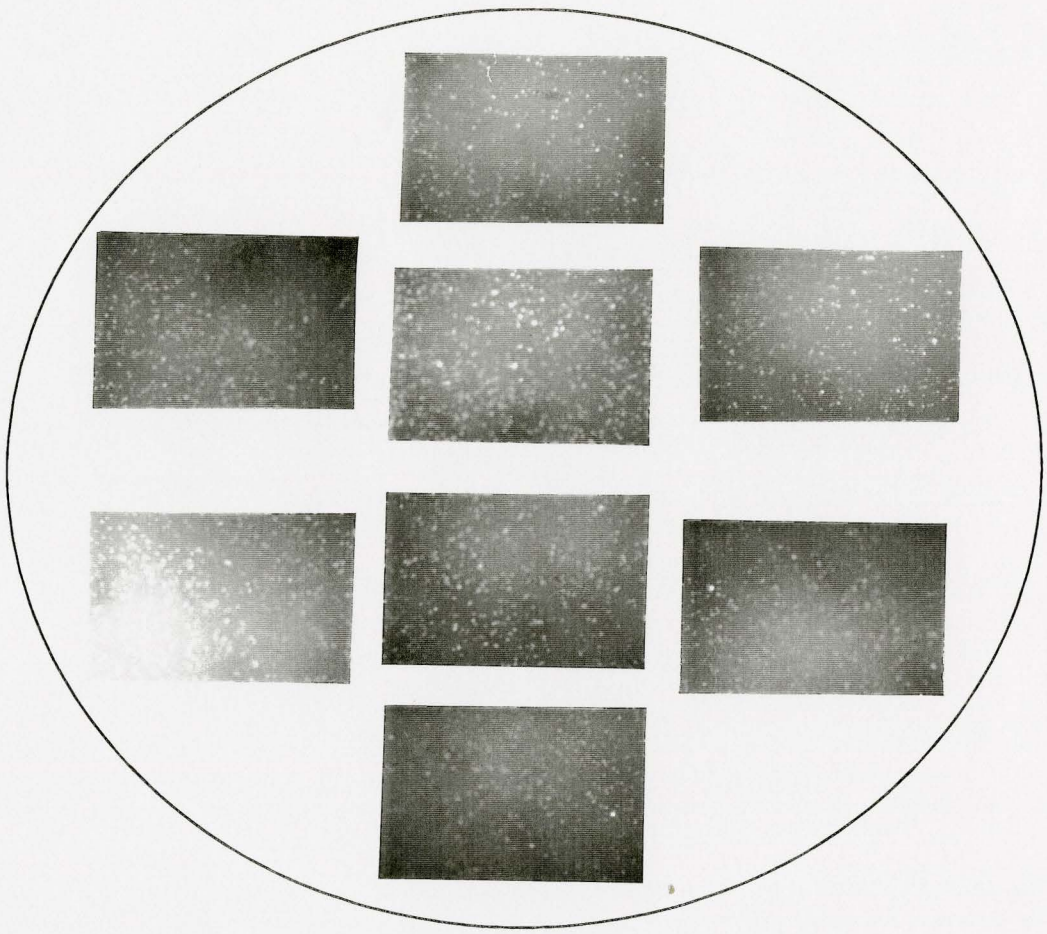

**Figure 4.15** - Optical microscopic photograph of platelet deposition to collagen-coated surface. Rectangular areas arranged to correspond to position on the disk cut from the "plate" of the cone-and-plate device.

initial adhesion resulting from the high reactivity of the collagen surface justifies the omission of the kinetic term. Only initial experimental adhesion results (up to 5 min) were utilized in the diffusion calculations. At longer times, the adhesion-time curves showed plateaus at about 10 min indicating a fundamental change in the adhesion mechanism, most likely due to the increasing coverage of the test surface by adherent

platelets. It appears that the reactivity of fluid phase platelets with adherent platelets is very different from the reactivity of platelets with collagen fibrils since increasing coverage of the test material results in a reduced rate of adhesion, with levelling off in adhesion at longer time.

Rearrangement of Equation 2.3, omitting the kinetic term, yields

$$M = \left[\frac{2C_o}{\pi^{1/2}}\sqrt{D}\right]t^{1/2} \tag{4.1}$$

The adherent platelet surface density was therefore plotted against the square root of time for the five fluid shear rates employed (Figure 4.16).

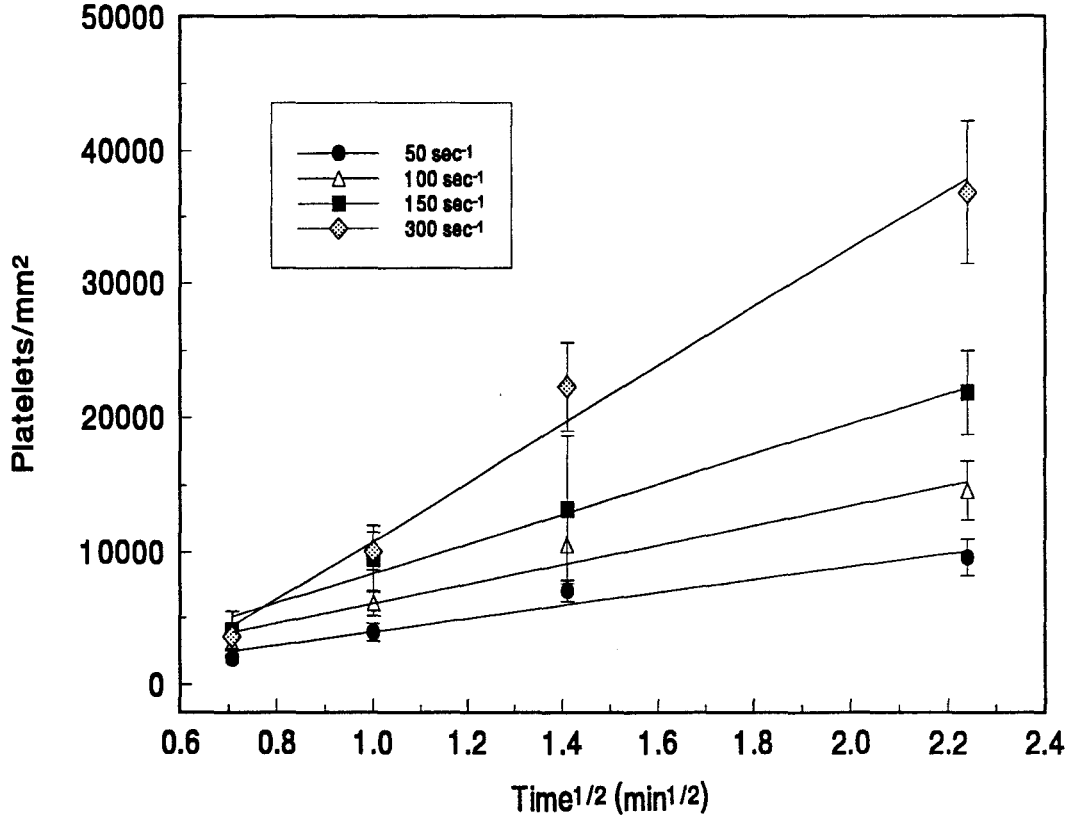


**Figure 4.16** - Regression of early time adhesion results (error bars represent 95% confidence interval).

| Shear Rate ($sec^{-1}$) | Effective Diffusion Coefficient x $10^7$ ($cm^2/sec$) |
|---|---|
| 0 | 0 |
| 50 | 0.44 ± 0.20 |
| 100 | 0.96 ± 0.58 |
| 150 | 2.53 ± 2.37 |
| 300 | 9.65 ± 4.11 |

**Table 4.12** - Effective platelet diffusion coefficients obtained from Equation 4.1 (± 95% confidence interval)

The effective diffusion coefficients calculated in this manner are listed in Table 4.12 for fluid shear rates varying from zero to 300 $s^{-1}$. The experimental points were then linearly regressed and the slope of the least squares fit was determined, thus permitting the determination of the effective platelet diffusion coefficient by Equation 4.1.

The diffusion coefficients thus determined compare reasonably well with results obtained by other researchers [Feuerstein et al, 1975 ; Grabowski et al, 1972]. Figure 4.17 shows the dependence of the platelet diffusion coefficient on fluid shear rate. A polynomial curve fit to the diffusion coefficient points was performed. The relationship determined was

$$D = a+b\gamma+c\gamma^2 \qquad (4.2)$$

$D$ = *diffusion coefficient*
$\gamma$ = *fluid shear rate*
$a,b,c$ = *constants*

where $a=0.0334\times10^{-7}$, $b=0.000301\times10^{-7}$ and $c=0.000106\times10^{-7}$. This equation was found

to give a statistically good fit to the data obtained ($r^2$=0.99926). Increasing levels of shear produce increasing diffusion coefficient values as observed by Grabowski et al [1972].

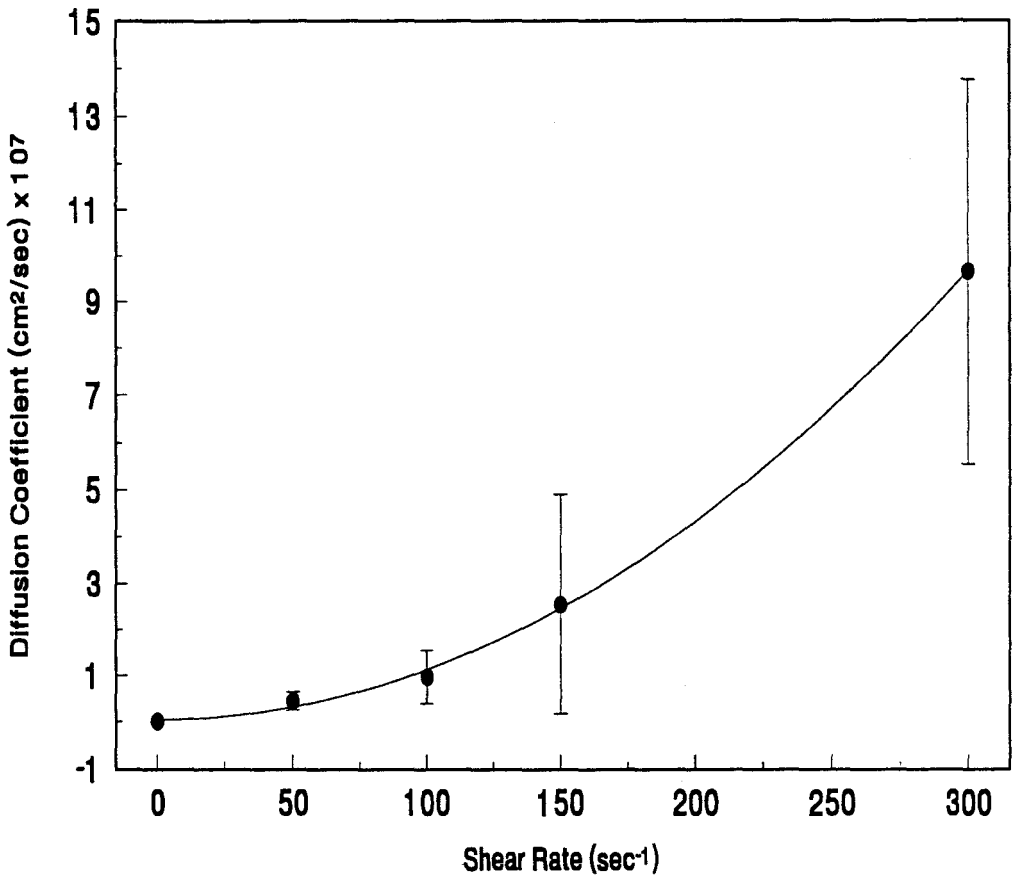


**Figure 4.17** - Shear rate dependence of platelet diffusion coefficient (error bars represent 95% confidence interval).

A lack of fit test was performed on all regressions performed to determine the applicability of Equation 4.1 in fitting the experimental data. The F values obtained were significantly lower than the critical F values indicating no lack of fit in any case. This analysis indicates that the model used is adequate to fit the measured data points. However, as the coefficient of determination, $r^2$, was found to vary from 0.52 to 0.85, the correlation between the model prediction and sample is not very strong. Thus, the large

amount of pure error associated with the experimental data reduces the coefficient of determination while also decreasing the F value calculated for the lack of fit test. This indicates that the model fit is acceptable but not very highly correlated with the measured data points. Therefore, it appears that the variability inherent in the experimental data precludes any precise diffusion coefficient calculations. The values obtained should be regarded as crude approximations. Sophisticated flow visualization techniques are generally employed to determine platelet diffusion coefficients [Goldsmith and Turitto, 1986]. The large variability present in the experimental data obtained is a result of several factors, primarily variability in platelets from donor to donor and thus from experiment to experiment.

Nonetheless, the observed trend of increasing diffusion coefficient with increasing fluid shear rate and the reasonably good agreement of diffusion coefficient values with those obtained by other researchers, indicates that the cone and plate apparatus yields reliable platelet adhesion data over the range of fluid shear rates utilized.

### 4.4.2 Albumin-coated Surface

Platelet adhesion experiments were also performed using albumin-coated test surfaces. It has been well documented that platelets do not adhere readily to surfaces covered with albumin [Packham et al, 1969 ; Park et al, 1986 ; Amiji et al, 1992]. Therefore, the albumin surfaces were employed as a negative control to study the possibility that the apparatus itself causes significant platelet activation thereby resulting in elevated adhesion to any surface, even one which is known to be unreactive. Platelet activation may be expected to result either from platelet interactions with the cone surface during the experiment or from local increases in shear rate as a result of fluid turbulence, for example in the peripheral regions of the cone-plate gap.

Platelet adhesion to the albumin surfaces was measured at a fluid shear rate of 300 $s^{-1}$. This value was chosen because it was observed to elicit the greatest amount of platelet deposition on the collagen surface. Additionally, any flow disturbances which

may affect platelet-surface interactions are likely to be most significant at the highest shear rate. Therefore, this fluid shear rate provides a severe test of the passive nature of the albumin test surface. Lower rates of fluid shear are expected to yield lower values of platelet adhesion.

Table 4.13 lists the measured values of platelet surface density obtained using the albumin surfaces. The values may regarded as essentially zero since the number of counts registered on the gamma counter was not significantly greater than background. This assertion is borne out by the SEM results shown in Figure 4.18, indicating no adherent platelets at all.

| Time (min) | Platelet Density (platelets/mm $^2$) |
|---|---|
| 0 | 53 ± 19 |
| 2 | 90 ± 13 |
| 5 | 104 ± 31 |
| 10 | 110 ± 18 |
| 15 | 96 ± 18 |

**Table 4.13** - Platelet surface deposition on albumin-coated surface ± 95% confidence interval, n=4 (fluid shear rate=300 $sec^{-1}$, time=2 minutes).

The levels of platelet adhesion observed on the albumin surfaces are drastically reduced in comparison to those on the collagen surfaces at fluid shear rates of 300 $s^{-1}$ (Figure 4.19). Thus, it is apparent that the apparatus does not disturb the flow or activate the platelets to any significant extent.

In conclusion, it has been found that positive (collagen) and negative (albumin)

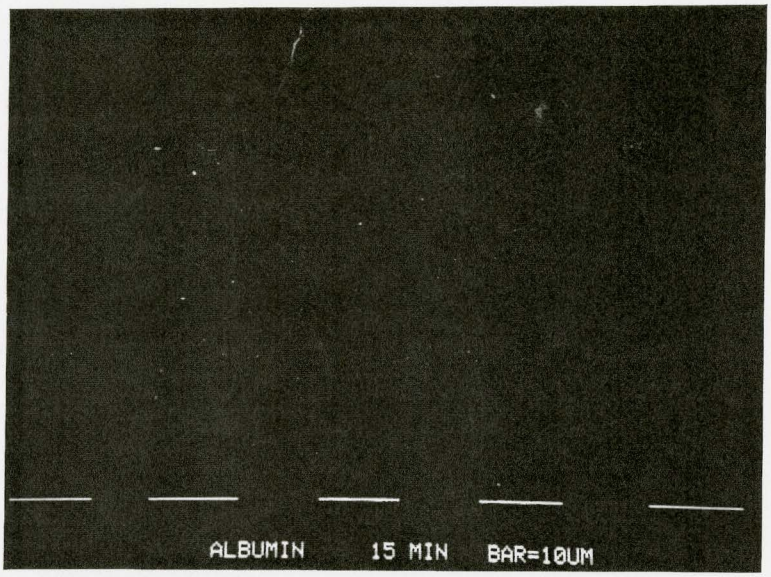


**Figure 4.18** - SEM photomicrograph of albumin surface after exposure to platelet suspension for 15 minutes at 300 $s^{-1}$

control surfaces elicit a predictable platelet adhesion response when employed in the cone and plate flow apparatus developed. The apparatus appears to produce uniform, essentially laminar fluid flow fields between the cone and plate, thus allowing easy control of fluid shear rate. In addition, the nature of the flow produced does not appear to stimulate platelets in a significant manner. Thus the apparatus may be utilized to study platelet-surface interactions for any test surface of interest which can be fabricated in the form of a flat film. As discussed below, the device was used to study platelet adhesion to a series of polyurethanes synthesized and characterized as described previously

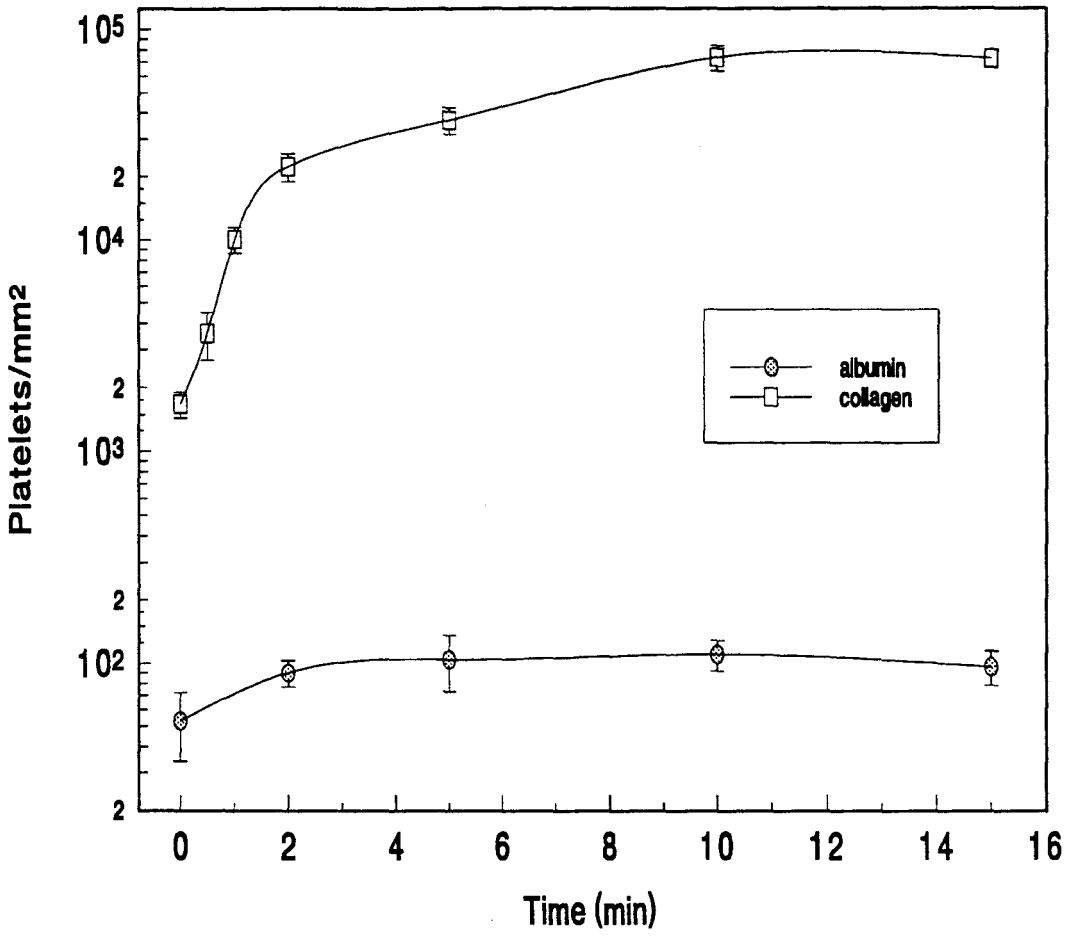


**Figure 4.19** - Comparison of platelet adhesion to collagen and albumin surfaces at 300 $s^{-1}$ fluid shear rate.

## 4.5 Platelet Adhesion to Polyurethanes

The polyurethanes described in sections 4.1 to 4.3 were developed to be tested and characterized as possible blood-contacting biomaterials. The promise shown by sulphonate-containing polyurethanes previously synthesized in this lab in terms of coagulation response [Santerre et al, 1992a] led to the need to examine the platelet response to these materials. The platelet adhesion response to non-sulphonated polyurethanes was also tested. A comparison of the platelet reactivity of the sulphonated and non-sulphonated polyurethane surfaces should help to elucidate the contribution of the sulphonate groups to the platelet response.

The platelet deposition-time curves obtained using the collagen-coated surfaces indicate that a plateau in adhesion occurs by 10 min. Therefore, the polyurethane platelet adhesion studies were performed over a 10 min interval to observe the time-dependence of the adhesion process. Fluid shear rates of 100 and 300 $s^{-1}$ were chosen to examine the effect of fluid shear on platelet deposition to the polyurethane surfaces.

All of the polyurethane experiments were performed using a suspension medium containing albumin as outlined in Section 3.4.3. The lack of plasma proteins (except albumin) in the suspension medium is likely to modify the nature of the platelet-surface interaction relative to blood since adhesion is generally believed to be mediated by adhesive proteins adsorbed to the polymer surface [Brash, 1985 ; Lelah and Cooper, 1986 ; Packham, 1991 ; Tamada and Ikada, 1993] . However, the absence of plasma proteins simplifies the experimental system and permits the examination of the platelet interaction with the polymer surface itself. In addition, the absence of the coagulation system makes it possible to maintain normal calcium ion concentrations, which are important for platelet function.

### 4.5.1 Non-Sulphonated Polyurethanes

The MDA chain-extended polyurethanes were employed as "classical" polyurethanes analogous to the BDDS polyurethanes but without the sulphonate groups.

The platelet adhesion response to surfaces of this nature has been extensively studied by others [Lelah et al, 1986]. Such polymers are regarded as relatively biocompatible in comparison to other materials. Nonetheless, they are still thrombogenic and presumably reactive to platelets.

The platelet adhesion response to these surfaces was measured for comparison to the sulphonated polyurethanes. As will be seen, the levels of platelet adhesion to the non-sulphonated polyurethanes are markedly different from those observed for the sulphonate-containing polymers, as one might expect. However, unexpectedly, platelet adhesion to these polyurethanes was observed to be much lower than to the sulphonate-containing polymers, suggesting, in turn, lower thrombogenicity.

#### 4.5.1.1 Time and Shear Rate Dependence of Adhesion

The platelet adhesion-time curves measured from 0 to 10 min are shown in Figure 4.21. As can be seen, the level of platelet deposition observed on the MDA-based polyurethanes is very low in comparison to the collagen surfaces (Section 4.4).

In contrast to the collagen surfaces there does not appear to be any strong dependence of adhesion on time: the deposition values shown in Figure 4.21 are relatively constant although an increase in deposition is observed at 10 min and 100 $s^{-1}$ shear rate. It must be noted, however, that the levels of adhesion are much lower than for collagen, and accurate measurement of such small numbers of adherent platelets is difficult since the radioactivity levels are often no more than twice the background values. Therefore, the levels of deposition shown in Figure 4.21 may be regarded as very low. This conclusion is supported by SEM observations.

Figure 4.21 also shows no obvious effect of fluid shear rate on the level of platelet deposition to the non-sulphonated polyurethanes. The absence of a shear-dependent adhesion response suggests that adhesion is reaction-rate limited. An increase in shear rate must result in an elevation of the rate of platelets transported to the test surface. Conversely, increased rates of shear can also be expected to exert increased shearing

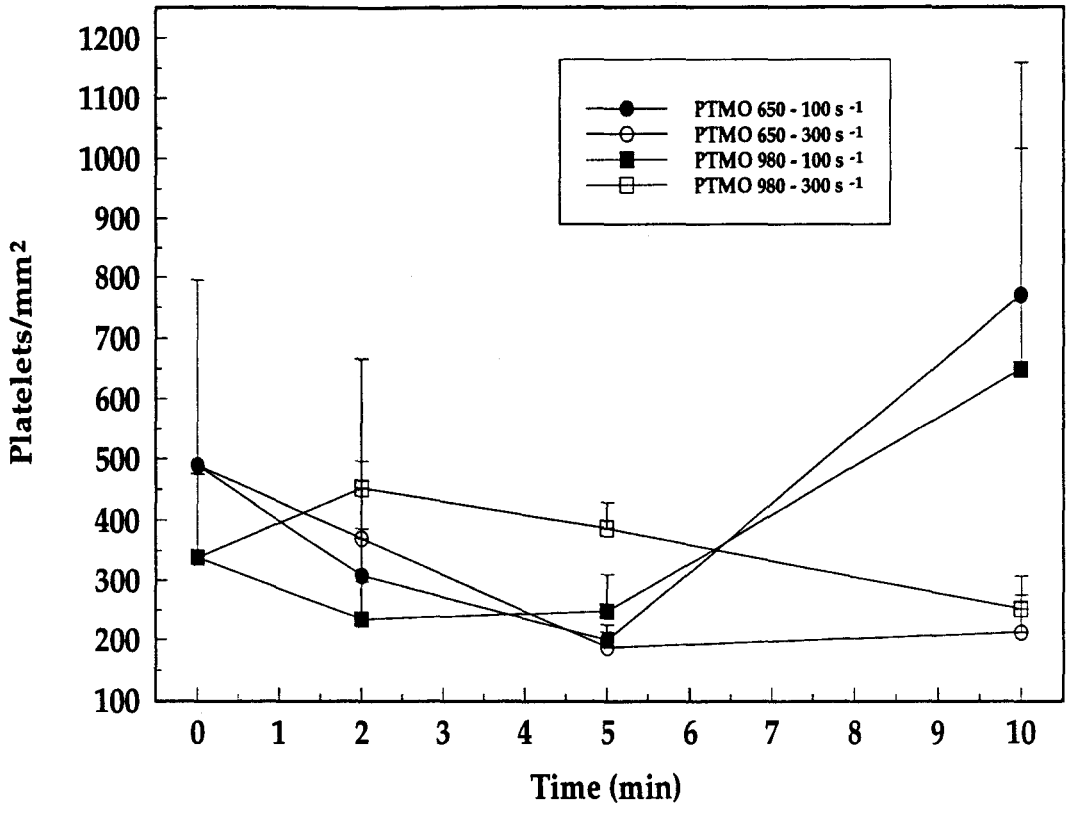


**Figure 4.21** - Platelet adhesion kinetics on MDA chain-extended polyurethanes at both 100 and 300 $s^{-1}$ (error bars represent 95% confidence intervals).

forces capable of dislodging adherent platelets. The low values of platelet deposition to the non-sulphonated polyurethane surfaces indicate that either the platelets do not readily adhere to the surface or adhere weakly and are dislodged. The level of platelet adhesion does appear to be slightly lower at 100 $s^{-1}$ shear rate for both the PTMO 650/MDA and PTMO 980/MDA polymers up to approximately 5 min. Beyond this point, however, the level of adhesion at 100 $s^{-1}$ is greater than at 300 $s^{-1}$ for both polymers, possibly indicating that the platelet-surface adhesive interaction is relatively weak for these polymers. Higher levels of fluid shear may result in increased removal of weakly adherent platelets. Indeed, a gradual reduction in the number of adherent platelets over time is noted at 300

$s^{-1}$, while a slight increase is observed at 100 $s^{-1}$. This result would suggest that, in the absence of the plasma proteins (other than albumin), platelets are not able to form strong adhesive interactions with the non-sulphonated polyurethane surfaces. Since the adhesive interaction is strengthened by the spreading of the platelet after contact, it is possible that, in the absence of adhesive proteins, the platelet is not readily able to directly interact with the surface in such a way to facilitate spreading. The platelet spreading mechanism is believed to be mediated by the interaction of the GPIIb-IIIa receptor with plasma proteins such as fibrinogen and fibronectin [deGroot, 1990]. Therefore, in the absence of adhesive plasma proteins in the test system, spreading and strong platelet-surface interactions may not be possible.

#### 4.5.1.2 Effect of PTMO Molecular Weight on Platelet Adhesion

The ratio of hard to soft segment in the surface of polyurethane solids has been implicated as an important physical parameter which may affect platelet deposition [Hanson et al, 1980 ; Costa et al, 1981]. Generally, the hard segment components are believed to elicit a greater thrombogenic response than the soft segment, although no consensus has been reached on this point. Variation of the molecular weight of PTMO used in polyurethane syntheses without changing the reaction stoichiometry results in variation of the relative contributions of the hard and soft segment. Decreasing the polyol molecular weight results in an increased hard segment concentration. Thus, it was anticipated that polyol chain length would influence platelet deposition.

The contact angle data listed in Table 4.6 indicate that the PTMO 650 polymer is slightly more hydrophilic than the PTMO 980 version. The presence of hydrophilic hard segments at the surface is expected to increase wettability. However, the XPS data listed in Table 4.7 show a greater surface concentration of nitrogen (indicative of hard segment components) in the PTMO 980 than in the PTMO 650 polyurethane. Therefore, it does not appear that the hard segment contributions to these two polymer surfaces are greatly different.

The platelet deposition profiles for the PTMO 650 and PTMO 980 polymers shown in Figure 4.21 do not appear to exhibit any dependence on polyol chain length. This result can be rationalized by two considerations. First, the variation in PTMO molecular weights employed in the polyurethane syntheses was relatively small (650 versus 980). Therefore, the variation in soft segment concentration resulting from the different polyols is not dramatically different, possibly making any changes in platelet response imperceptible. Secondly, Lelah et al have shown that blood response to polyurethanes cannot be predicted solely by hard and soft segment surface concentrations, but also depends on hard segment conformation [Lelah et al, 1986]. This conformation will obviously be a function of the type of hard segment molecules employed. On this basis, the similarity in the platelet deposition characteristics of the two polyurethanes employing PTMO 650 and PTMO 980 is not surprising since the hard segment constituent molecules are the same.

The nature of the hard segment appears to be of greater importance than its surface concentration at least over the range studied here. Since the diisocyanate portion of the hard segment is identical in all of the polyurethanes synthesized, the platelet deposition response may be expected to be influenced mainly by the nature of the chain extender. This possibility is examined via the platelet response data for the sulphonated polyurethanes based on the BDDS and BES chain extenders.

#### 4.5.1.3 Scanning Electron Microscopy

SEM observation of the non-sulphonated polyurethanes after exposure to the platelet suspension reveals few attached platelets. The adherent platelets observed appear either to have adhered to the surface singly or in small aggregates (Figures 4.22 and 4.23). The lack of significant platelet aggregation in the present experiments in which fibrinogen is absent is not surprising since platelet-platelet interactions are believed to be facilitated by fibrinogen bridging between adjacent platelets. Additionally, surface aggregation has been demonstrated to increase with time up to 60 minutes, beyond the

experimental times investigated here [Lelah et al, 1986].

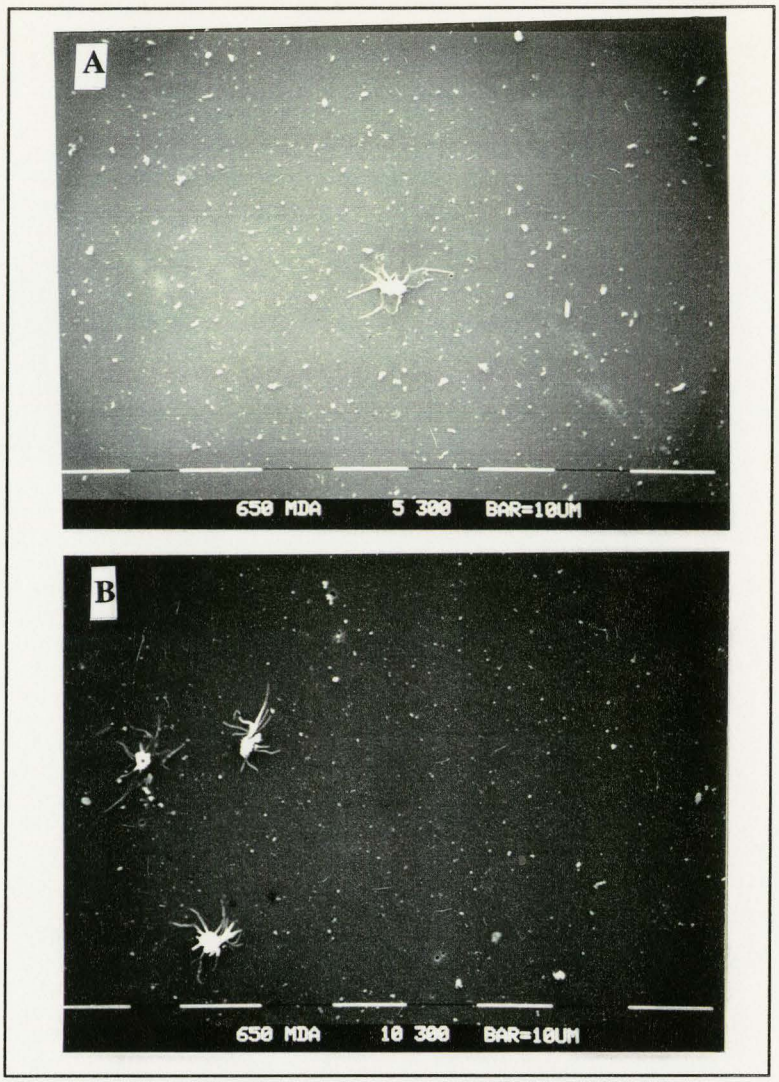


**Figure 4.22** - Platelets adherent to PTMO 650/MDA polyurethane A) 5 min B) 10 min (300 $s^{-1}$ shear rate).

In general, the adherent platelets exhibit features associated with the early stages of platelet activation. They appear to be dendritic in form, extending a number of spiny pseudopods. Several of the extended pseudopods appear to be in the early stages of flattening, possibly indicating a gradual transformation to the well-spread morphology typical of longer observation times [Goodman et al, 1989].

Therefore, it appears that the platelets which remain adherent throughout the period of observation and preparation for SEM exhibit a typical morphological response. However, the number of adherent platelets observed is very low perhaps indicating that a significant number of adherent platelets became detached during preparation for SEM.

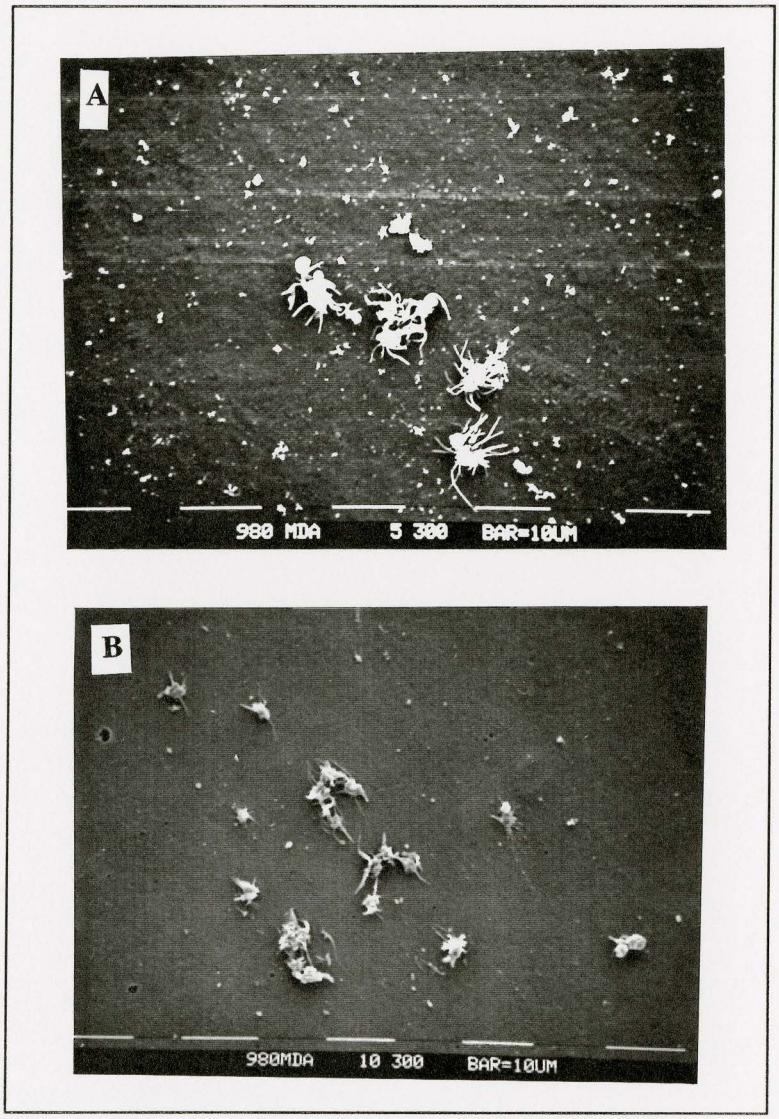


**Figure 4.23** - Platelets adherent to PTMO 980/MDA polyurethane A) 5 min B) 10 min (300 $s^{-1}$ shear rate).

#### 4.5.1.4 Final Remarks on Adhesion to Non-Sulphonated Polyurethanes

Several researchers have demonstrated high levels of platelet deposition to PTMO-based non-sulphonated polyurethanes [Lelah et al, 1986 ; Okkema and Cooper, 1991 ; Park et al, 1992] in comparison to the levels observed in this work. Comparison of platelet adhesion results between different laboratories is complicated by the different experimental systems employed. However, in the other works cited, more or less normal quantities of the plasma proteins were present in the platelet suspension medium. Since adsorbed plasma proteins are believed to influence platelet adhesion, the lack of plasma proteins, other than albumin, in this work may be responsible for the relatively mild platelet response observed.

Albumin is the only plasma protein present in the platelet suspension medium in this work, and the passivation of surfaces by adsorption of albumin is well documented as discussed previously. Therefore, it is possible that the albumin present in the platelet suspension medium may rapidly adsorb to the polyurethane surface rendering it passive towards platelet adhesion. The diffusion coefficient of albumin is greater than that of platelets [Slack et al, 1993] allowing the albumin to reach the surface prior to the majority of platelets in the fluid. Indeed, comparison of the platelet adhesion kinetics at 300 $s^{-1}$ shear rate for the non-sulphonated polyurethanes and the albumin-coated surface shows similar behaviour (Figure 4.24).

The concentration of albumin in the platelet suspension medium is 3.5 mg/mL, i.e. about 10% of that in plasma. This concentration is however high enough that a monolayer of adsorbed albumin would be deposited rapidly [Silver et al, 1993c]. Therefore, it may be that significant surface coverage of albumin occurs during the platelet adhesion experiments, resulting in suppression of the platelet adhesion response. It thus seems likely that the low values of platelet deposition to the non-sulphonated polyurethane surfaces may be largely due to the nature of the test fluid employed. The lack of adhesive plasma proteins and the presence of albumin, a non-adhesive protein with respect to platelets, probably inhibits platelet-surface interactions to a large degree. Thus,

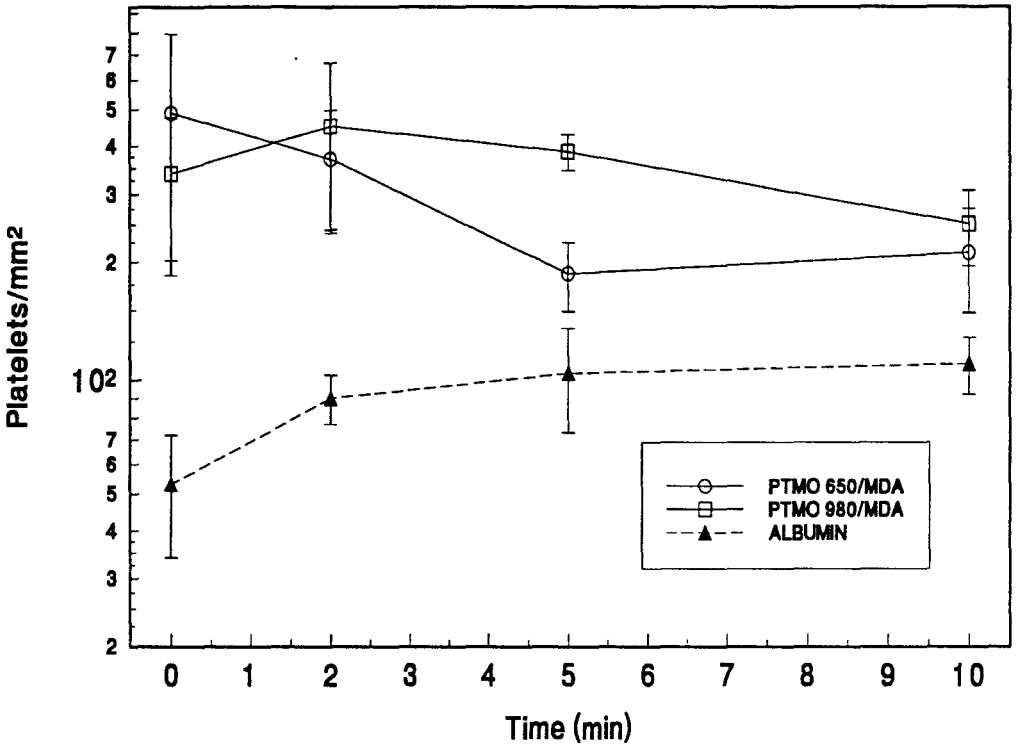


**Figure 4.24** - Comparison of platelet deposition kinetics on MDA-based polyurethanes and albumin-coated surface (shear rate 300 $s^{-1}$, ± 95% confidence intervals are shown).

studies employing a more physiological platelet suspension medium should be carried out to further characterize the platelet-surface interactions of these polymers.

### 4.5.2 Sulphonated Polyurethanes

It has been shown that sulphonate ion-containing polyurethanes exhibit an improved blood-contacting response in comparison to conventional, non-sulphonated polyurethanes [Grasel and Cooper, 1986 ; Santerre, 1990]. This improved blood compatibility has been demonstrated both by decreased platelet deposition and prolonged

plasma coagulation times on these surfaces. However, increased fibrinogen adsorption has also been observed suggesting the possibility that the adsorbed fibrinogen is in an altered condition which renders it relatively non-reactive towards platelets [Silver et al, 1992]. The use of a fibrinogen-free platelet suspension medium in this work enables one to observe directly (albeit through the probable intermediary of an albumin layer) the interaction of platelets with the sulphonate ion-containing polyurethane surface. From the adhesion data in Figure 4.25, it is immediately evident that the level of platelet deposition which occurs on the sulphonated polyurethanes is much greater than was observed on the non-sulphonated polyurethanes. Thus, the incorporation of sulphonate functional groups into the polyurethane appears to promote platelet adhesion in the absence of fibrinogen and other adhesive proteins, and sulphonate groups are inherently platelet-reactive independent of the role of fibrinogen.

#### 4.5.2.1 Time Dependence of Adhesion

The platelet adhesion-time curves shown in Figures 4.26 and 4.27 show a common trend of increasing levels of deposition over time in contrast to the non-sulphonated polyurethane deposition data. Moreover, the time-dependent nature of the adhesion was not universal. For example, the BES chain-extended polyurethanes exhibit a rapid increase in deposition followed by an essentially constant plateau value for both fluid shear rates tested, as was also noted for the collagen-coated surfaces. However, the BDDS chain-extended polymers appear to exhibit a relatively slow, continuous increase in platelet deposition over time at 100 $s^{-1}$ and a more rapid increase in adhesion to a plateau value at 300 $s^{-1}$.

The rate of platelet adhesion to the polymer surfaces is primarily dependent on the chain extender. For both shear rates, the BES chain-extended polyurethanes show high initial rates of adhesion which decrease sharply beyond 5 minutes. In contrast, the BDDS chain-extended polymers display a lower initial rate of adhesion, which does not fall off at longer times. The kinetics of platelet adhesion to the BDDS and BES-based

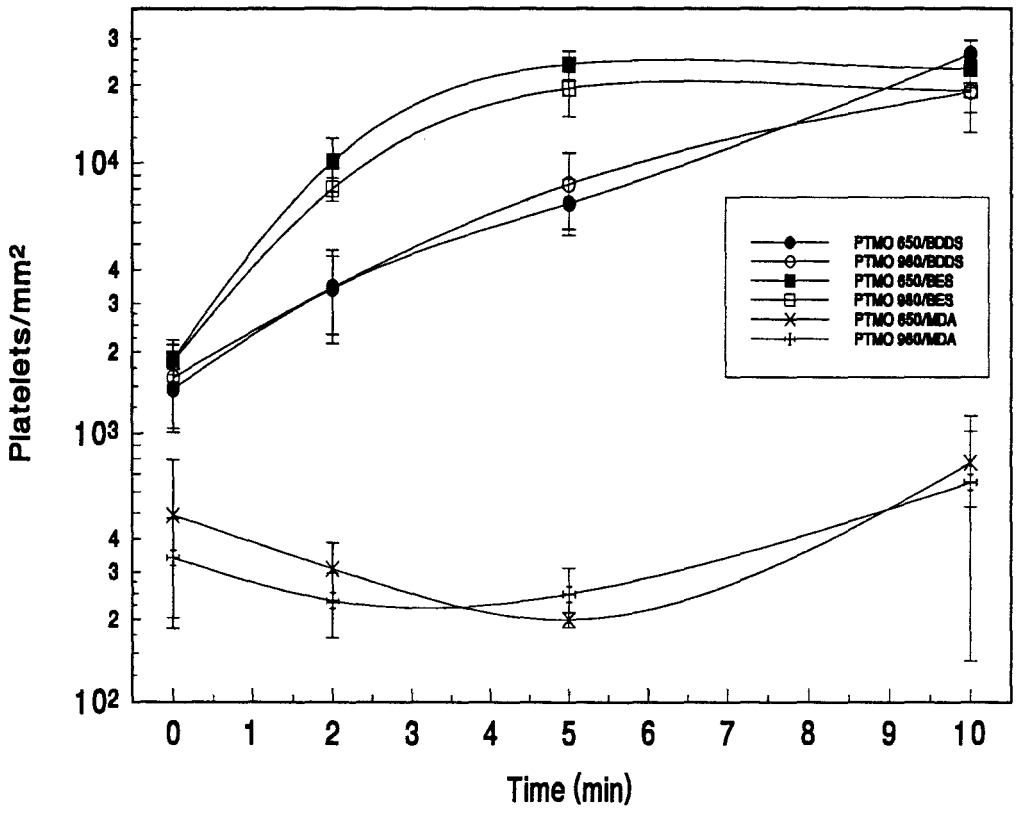


**Figure 4.25** - Comparison of platelet adhesion kinetics on sulphonated and non-sulphonated polyurethanes at 100 $s^{-1}$ fluid shear rate (±95% confidence intervals)

polyurethanes thus appear to be very different, suggesting that the interactions between the circulating platelets and these two types of polymer surface are significantly different.

The level of platelet deposition observed on the sulphonated polyurethanes is much greater than exhibited by the non-sulphonated polyurethanes, suggesting that platelets interact with the sulphonate groups in some specific manner. In fact, the level of platelet deposition noted for the sulphonated polyurethanes is similar to that observed for the collagen surfaces (Figures 4.26 and 4.27). This is somewhat surprising since it has been

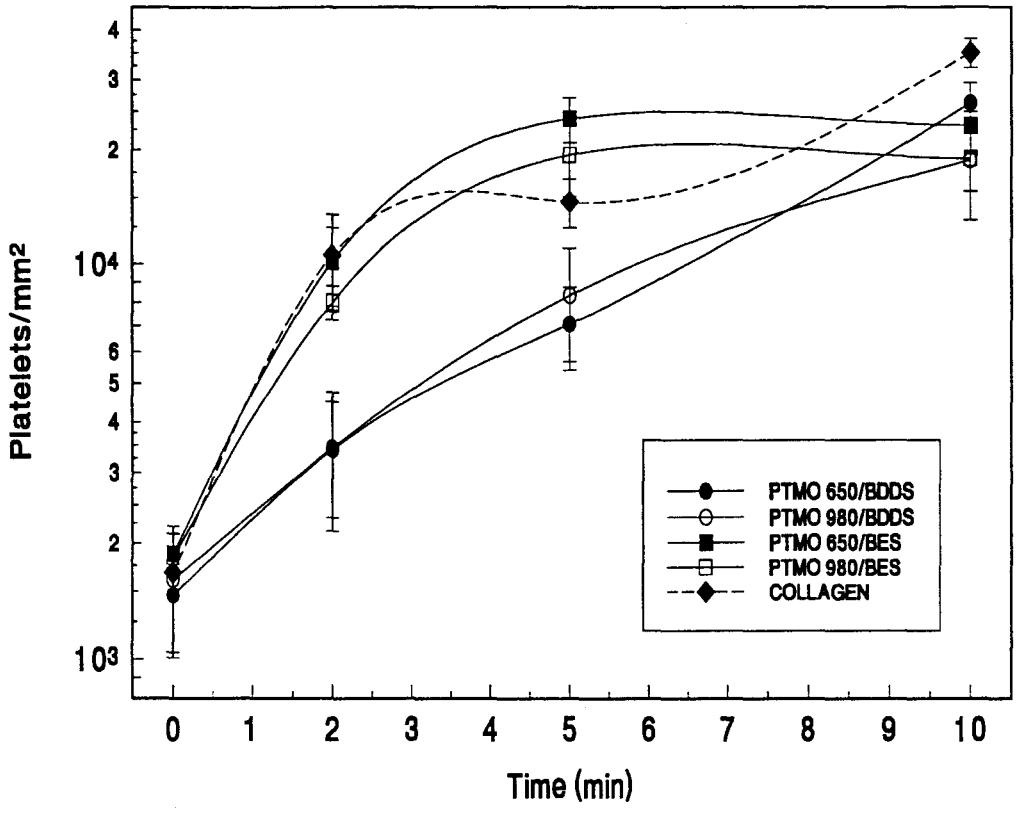


**Figure 4.26** - Platelet adhesion kinetics on sulphonated polyurethanes at 100 $s^{-1}$ fluid shear rate (±95% confidence intervals)

reported by others that platelet deposition on sulphonated polyurethanes is less than on non-sulphonated polyurethanes [Okkema et al, 1991 ; Ito et al, 1991]. However, it should again be stressed that the studies of Okkema et al [1991] and Ito et al [1991] were performed in the presence of the adhesive plasma proteins.

It is evident that, at both fluid shear rates employed, the level of platelet deposition is strongly dependent on the type of sulphonated chain extender employed. Since the level of sulphonation is mainly dependent on the molecular weight of the polyol and was found to be similar for the BES and BDDS chain extended polyurethanes, it

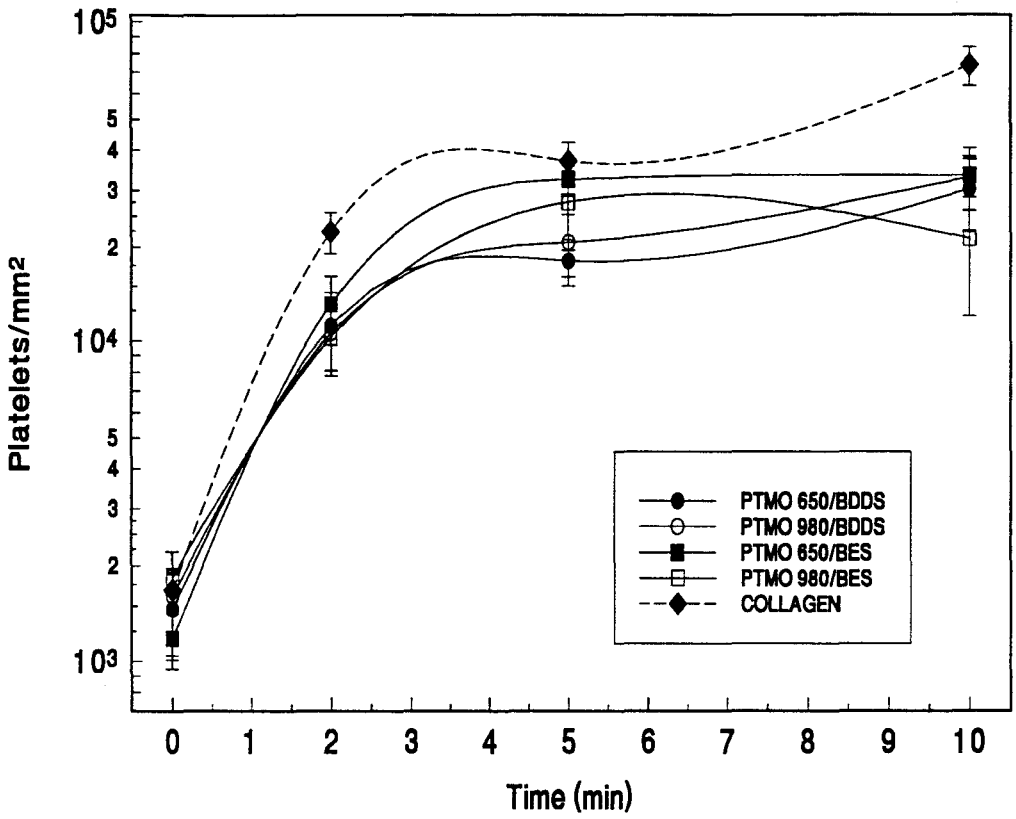


**Figure 4.27** - Platelet adhesion kinetics on sulphonated polyurethanes at 300 $s^{-1}$ fluid shear rate (±95% confidence intervals)

appears that the platelet adhesion response may also depend on the chemical environment of the sulphonate groups at the polymer surface. Additionally, since each BES molecule contains one sulphonate group, while each BDDS molecule contains two, the surface distribution of sulphonate groups may be distinctly different, and this may also play a role in the platelet-surface interactions. The chemical structure of the chain extender may also affect platelet interactions. The sulphonate group of the BES molecule is attached to the end of a short aliphatic side chain while the BDDS sulphonate groups are attached directly to the aromatic benzene rings of the molecule. It is possible that the BES

sulphonate groups may have greater mobility, permitting them to interact more readily with sites (receptors) on the platelet membrane. The effect would be similar to the spacer molecule concept used in grafting heparin and other "ligands" to surfaces in an attempt to enhance activity while bound [Ebert and Kim, 1982 ; Han et al, 1989 ; Park et al, 1992].

Another possible explanation for the effect of the chain extender on platelet adhesion may lie in the degree of flexibility or conformational mobility that the chain extender imparts to the polymer molecules. The BES chain-extended polymers are expected to be more flexible than the BDDS polymers since the BES molecule has more conformational mobility than BDDS. As well, the decreased hard segment crystallization noted in the BES polymers may indicate enhanced hard segment mobility within the hard domains. Increased conformational mobility may allow for more rapid surface reorientation of the polar hard segment components when the polymer is exposed to the aqueous environment of the platelet suspension. This reorientation could serve to increase the sulphonate content at the polymer surface. The low values of receding water contact angle for the BES polyurethanes (Table 4.6) suggest that the surface region reorients on exposure to the water drop, and since the BES polymers showed significantly lower receding contact angles than the BDDS polymers, it is possible that the BES polymer chains are more mobile in the film surface. Increased conformational mobility may also lead to greater hard segment enrichment at the aqueous polymer interface and, thus, greater sulphonate ion content at the interface available to interact with the circulating platelets. It must be noted that the XPS data (Table 4.7) do not show significantly elevated sulphur concentrations for the BES in comparison to the BDDS polymers. However, the in vacuo environment of the XPS analysis may inhibit any surface reorientation favouring the polar sulphonate groups.

#### 4.5.2.2 Shear Rate Dependence of Adhesion

The adhesion data are regrouped to show the shear rate dependence of adhesion to the sulphonated polyurethanes in Figures 4.28 and 4.29. The BDDS chain-extended polyurethanes (Figure 4.28) exhibit a significant shear rate dependence, with a marked increase in adhesion at

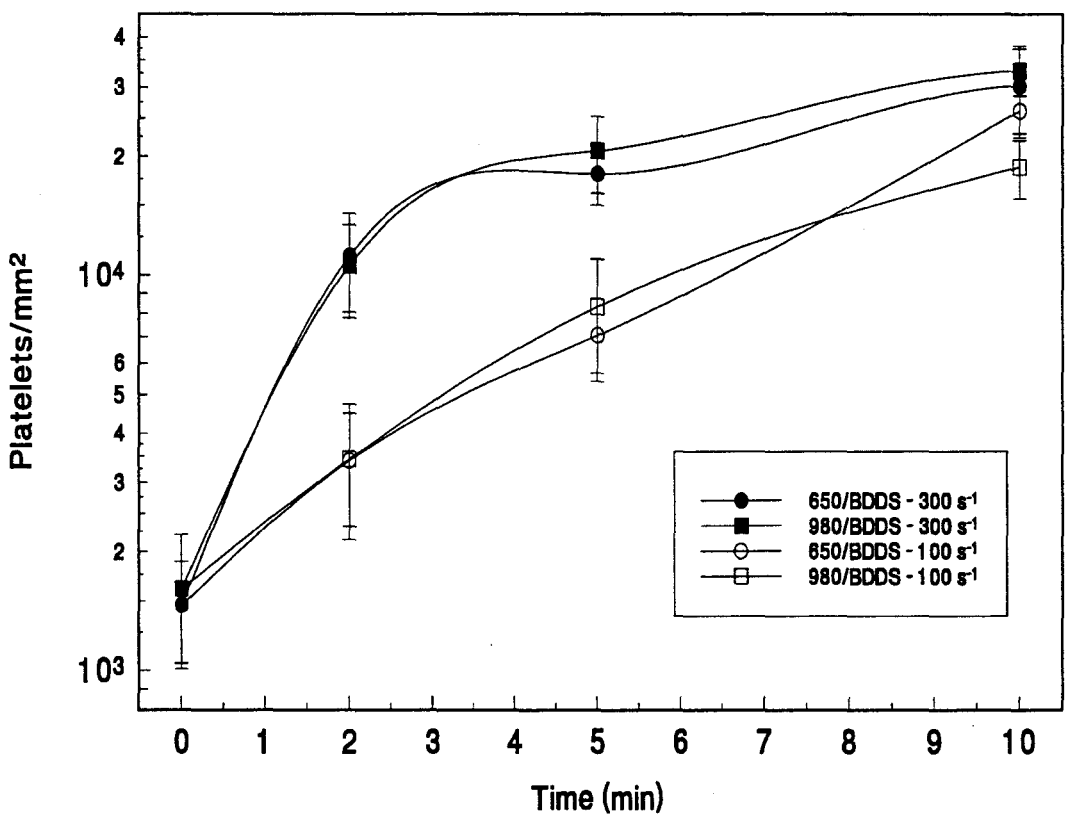


**Figure 4.28** - Platelet adhesion kinetics on BDDS chain-extended polyurethanes at 100 and 300 $s^{-1}$ shear rates (±95% confidence intervals).

at 300 $s^{-1}$ compared to 100 $s^{-1}$ up to 10 min where the adhesion becomes similar. The data thus suggest a strong shear rate dependence of adhesion at short times. However, since the level of deposition obtained at 100 $s^{-1}$ is significantly lower than observed on

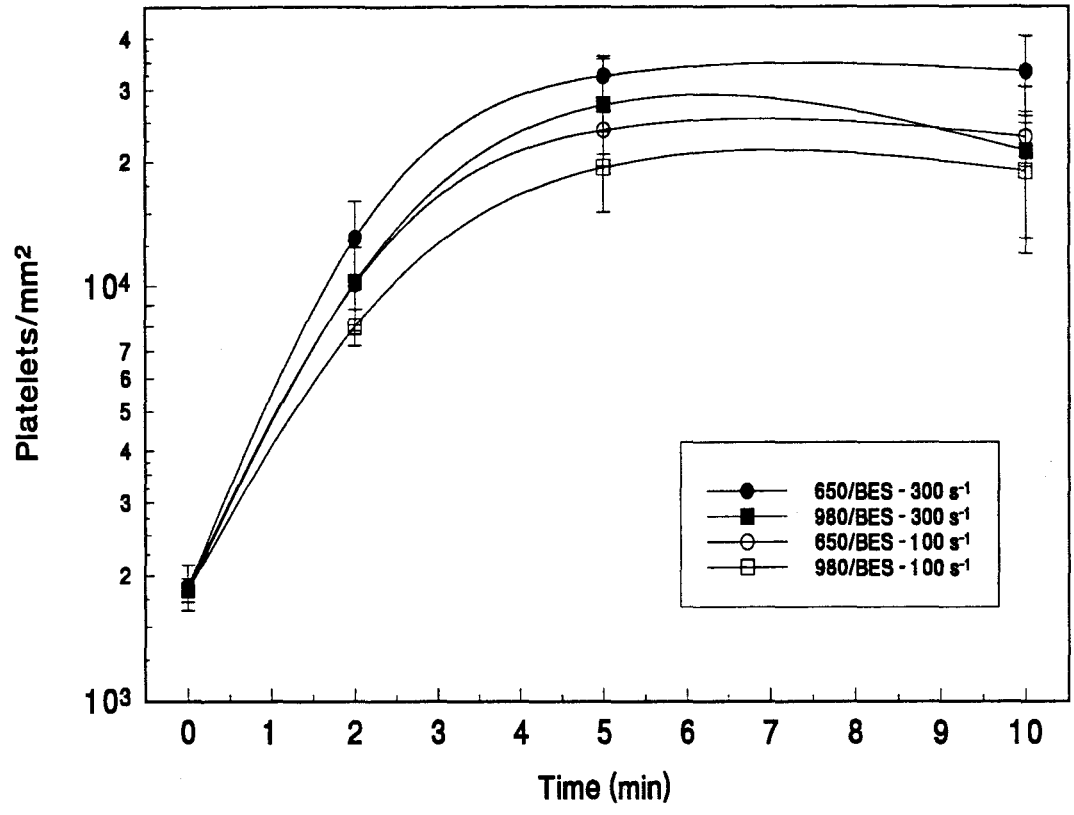


**Figure 4.29** - Platelet adhesion kinetics on BES chain-extended polyurethanes at 100 and 300 $s^{-1}$ fluid shear rate (±95% confidence intervals)

the collagen surfaces (assumed to be transport-limited), it is very likely that the adhesion mechanism is also reaction rate dependent and that not every platelet that is transported to the surface adheres.

Interestingly, a strong dependence of platelet deposition on shear rate is not observed for the BES polyurethanes (Figure 4.29). A slight increase in deposition is evident with increasing shear rate, but the effect is very small compared to that observed for both the BDDS polymers and the collagen surfaces. This observation would suggest that platelets are more reactive to the BES than to the BDDS polymer. The similarity of

platelet adhesion kinetics on the BES polymer and the collagen surface at 100 $s^{-1}$ suggest that the adhesion reaction is transport-limited under these conditions. However, as the shear rate increases and more platelets are transported to the surface in a given time, the interaction will become reaction rate limited and there does not appear to be a great dependence on fluid shear rate. This explanation implies that the reactivity of the BES polymer is such that at short times any platelet that is transported to the surface immediately reacts. At the higher rate of shear, the rate of transport of platelets to the surface presumably exceeds the rate of reactivity of the platelets with the surface. Thus, a transition from transport to reaction rate-limited adhesion occurs. It would be possible to test this hypothesis by measuring the platelet deposition to the BES polymers at lower fluid shear rates such as 50 $s^{-1}$. In this case, the shear rate dependence may become evident as a reduced rate of platelet transport to the surface which will presumably lead to reduced levels of platelet adhesion.

#### 4.5.2.3 Effect of Polyol Chain Length

Variation of the polyol chain length employed in the polyurethane synthesis gave significantly different levels of sulphonation. Increasing polyol chain length was observed to result in decreasing sulphur content (Table 4.3). It was therefore expected that a dependence of platelet adhesion on polyol chain length would be observed. In general, however, such a dependence was not readily apparent. A small increase in platelet deposition is seen for the PTMO 650/BES compared to the PTMO 980/BES polymer at both 100 and 300 $s^{-1}$ shear rate (Figure 4.29). However, no dependence of platelet deposition on polyol chain length is observed for the BDDS chain-extended polymers at either shear rate (Figure 4.28). Work by Okkema et al [1991] (using an ex vivo dog experiment) showed no difference in platelet deposition for two BES chain-extended polyurethanes of differing sulphur content.

Therefore, it appears that the polyol chain length employed has little effect on the levels of platelet adhesion on sulphonated polyurethanes. The absence of any polyol

chain length dependence was also noted for the non-sulphonated polyurethanes (Section 4.5.1.2). The dramatic dependence of platelet adhesion levels on the type of chain extender suggests that above a certain threshold the concentration of the sulphonate groups is less important for platelet adhesion than the other properties imparted to the polyurethane by the chain extender such as conformational mobility and hard segment domain structure.

#### 4.5.2.4 Scanning Electron Microscopy

The morphology of adherent platelets is indicative of the reactivity of the surface in contact. For example, differences in platelet spreading may be indicative of differences in thrombogenicity of these surfaces [Goodman et al, 1989 ; Park et al, 1990]. Scanning electron microscopy performed on the sulphonated polyurethanes revealed adherent platelets which were generally in the early stages of activation and spreading (Figures 4.30 - 4.33). The adherent platelets exhibit pseudopod formation and some spreading, and appear to adhere singly to the polyurethane surfaces, generally displaying an absence of platelet-platelet interactions.

The zero time adherent platelets on all four sulphonated polyurethane surfaces appear to be in the very early stages of spreading, exhibiting long, thin pseudopods and essentially spherical granulomere (Figures 4.30 - 4.33). As the exposure times are extended to 5 and 10 minutes the adherent platelets display pseudopods which have flattened and spread somewhat, in some cases merging to give a characteristic "fried egg" appearance [White and Gerrard, 1978]. As well, the central granulomere is easily distinguishable and relatively spherical in shape (Figures 4.30 - 4.33). This central clustering of the platelet granules is generally believed to be a precursor to granule release [White and Gerrard, 1978].

Therefore SEM appears to show adherent platelets which are in the early stages of the spreading reaction. The degree of spreading noted is consistent with the observations of Goodman et al [1989] who observed fully spread platelets on a PTMO-

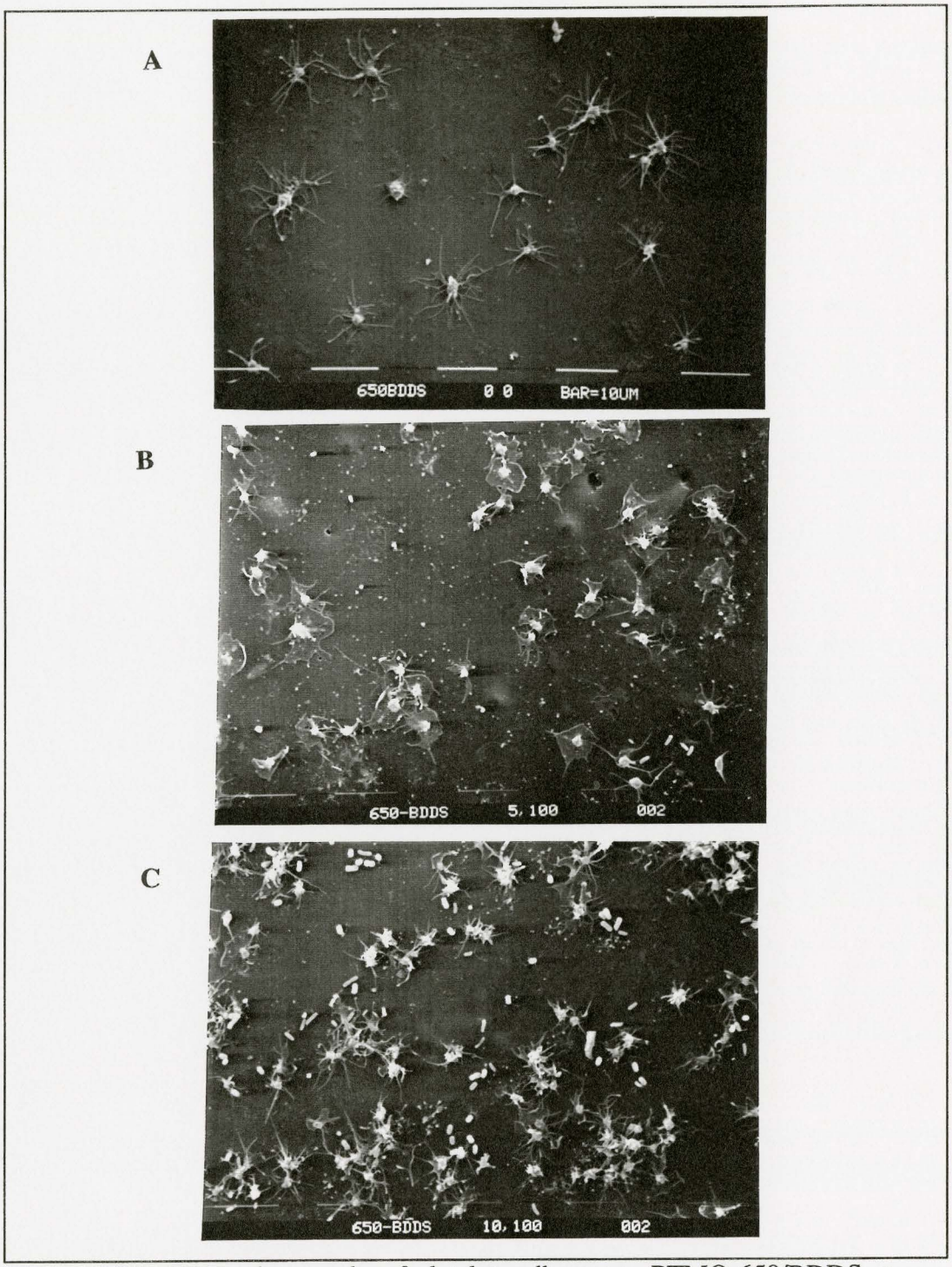


**Figure 4.30** - SEM micrographs of platelets adherent to PTMO 650/BDDS at A) 0 min B) 5 min C) 10 min (100 $s^{-1}$ shear rate)

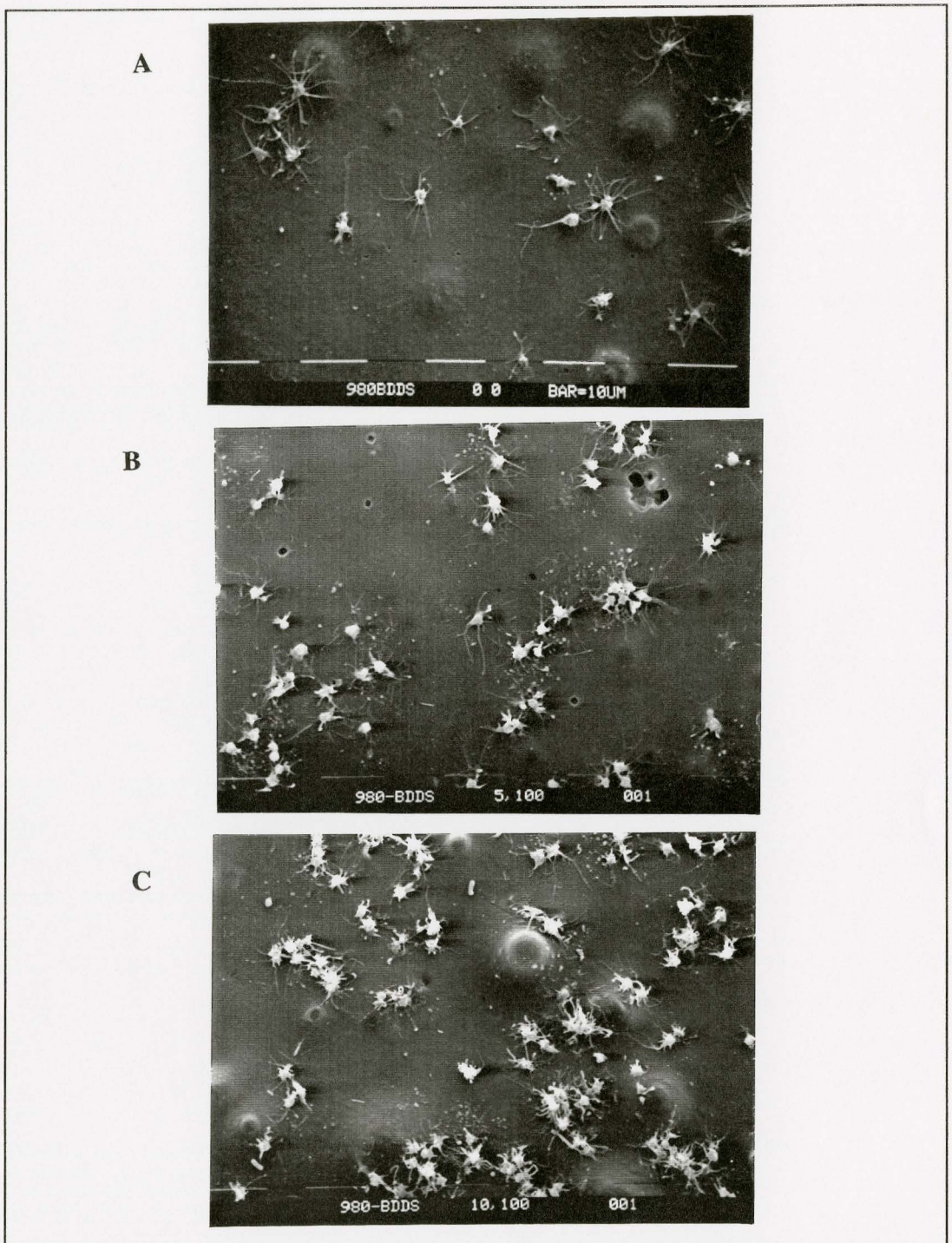


**Figure 4.31** - SEM micrographs of platelets adherent to PTMO 980/BDDS at A) 0 min B) 5 min C) 10 min (100 $s^{-1}$ shear rate)

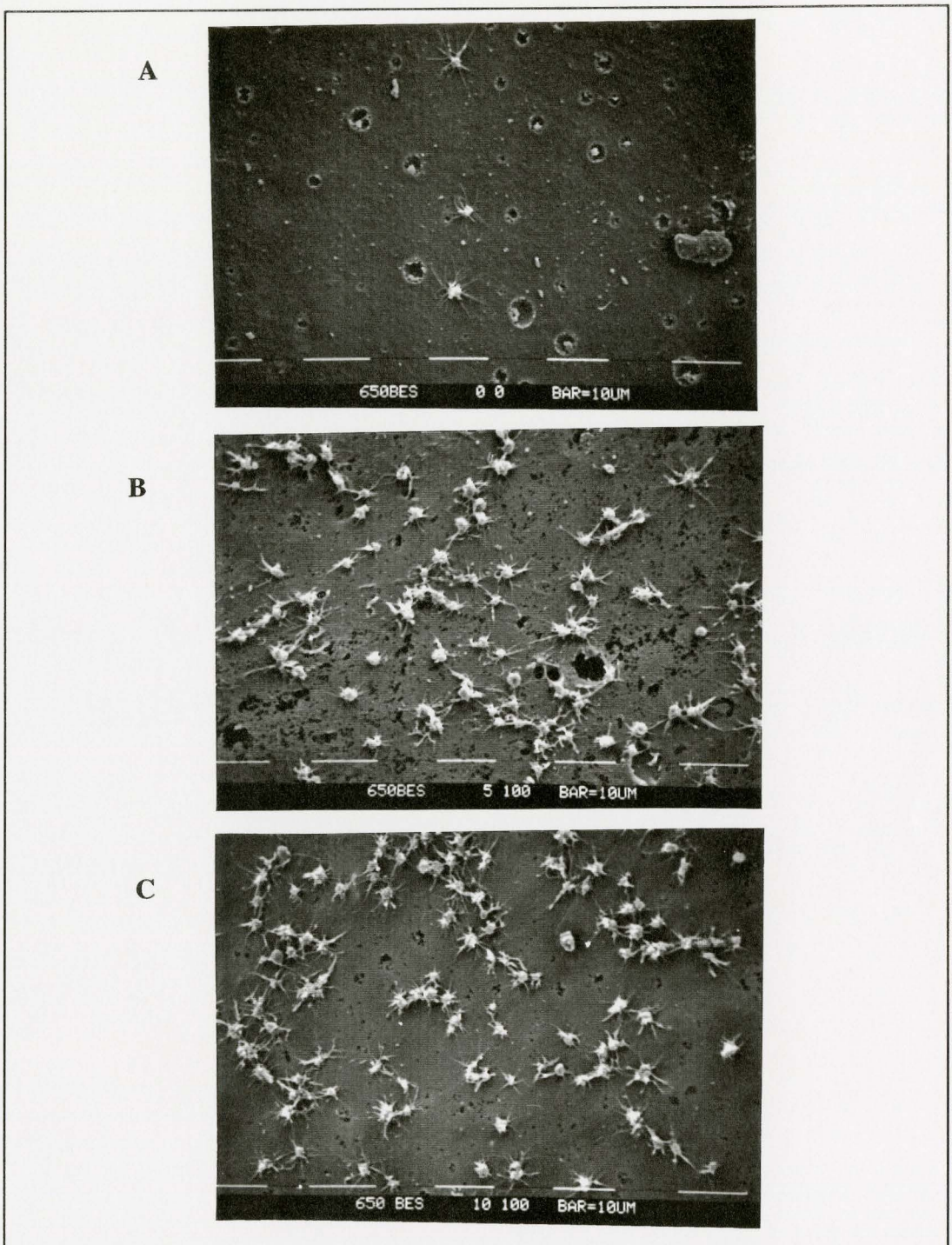


**Figure 4.32** - SEM micrographs of platelets adherent to PTMO 650/BES at A) 0 min B) 5 min C) 10 min (100 $s^{-1}$ shear rate)

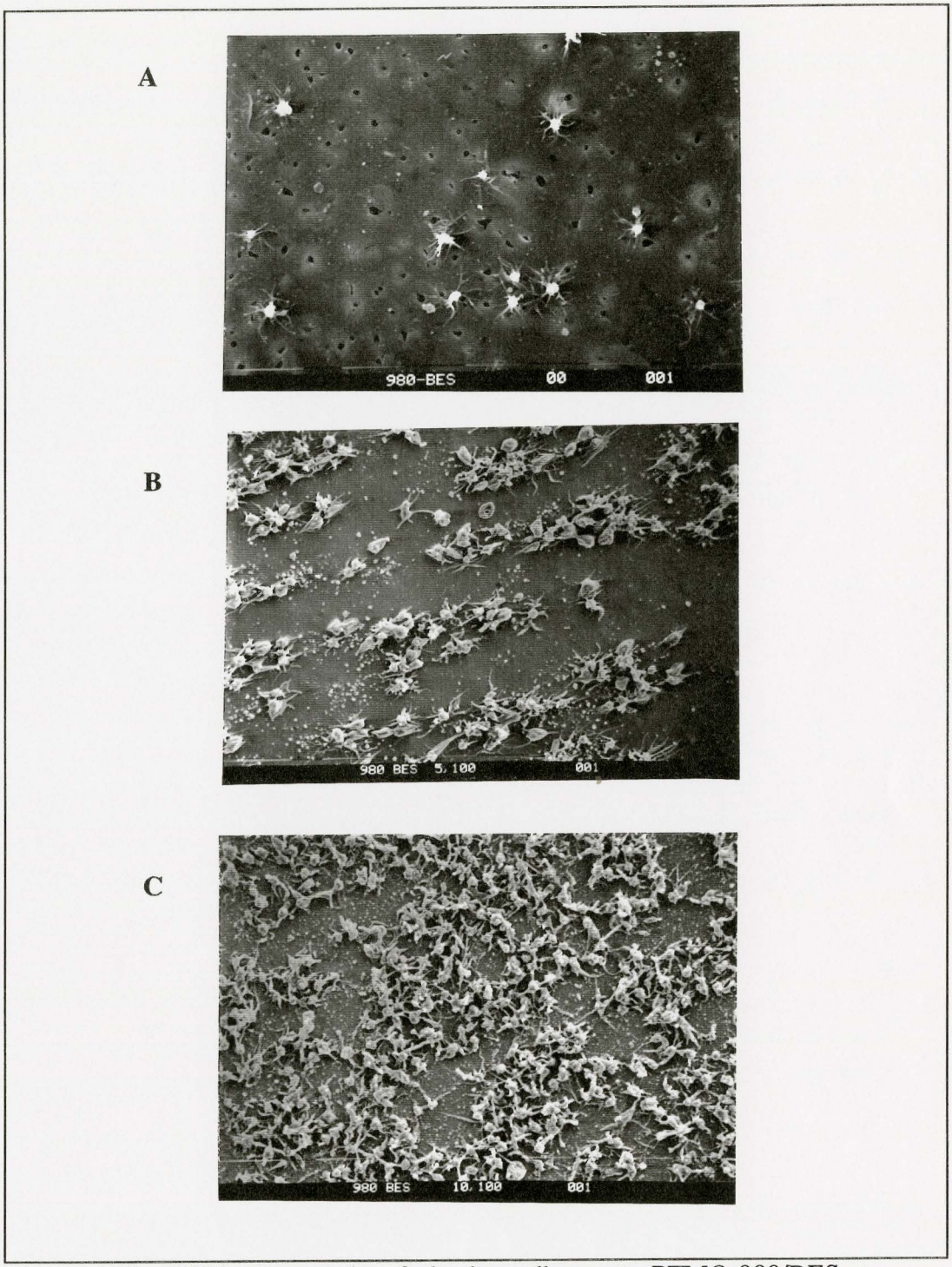


**Figure 4.33** - SEM micrographs of platelets adherent to PTMO 980/BES at A) 0 min B) 5 min C) 10 min (100 $s^{-1}$ shear rate)

based polyurethane after 20 to 30 minutes of incubation in a Tyrodes buffer platelet suspension. It is quite possible that the platelets are interacting with the polyurethane surfaces in this system via an intermediary albumin layer. Park et al [1990] noted platelets obtained a fully spread morphology on albumin precoated glass within approximately 1 hour using a phosphate buffered saline platelet suspension. Thus, it seems reasonable to conclude that if the experimental times were extended in this system, a gradual progression to fully spread platelets would be observed.

In addition, it is apparent from the SEM micrographs of Figures 4.30 - 4.33 that some significant surface irregularities are present on the polymer surfaces. For example, the PTMO 980/BDDS polymer surfaces exhibit "humps" in the surface which are about 10 μm in diameter. These "humps" are believed to be bubbles in the film that originated during the film casting procedure. Why the PTMO 980/BDDS films were the only ones to exhibit these structures is uncertain. The surfaces of the BES polymers appear to be "pitted" showing relatively large "craters". These features are believed to result from the existence of small air bubbles in the film casting solution as well as the some polymer degradation, due to the slight solubility of the polymers in ethanol, which is used in the SEM preparation.

#### 4.5.2.5 Concluding Remarks on Platelet Adhesion to Sulphonated Polyurethanes

The relatively high level of platelet deposition on the sulphonated polyurethanes is not in agreement with previously reported data [Grasel and Cooper, 1989]. Sulphonation of polyurethanes has generally been found to reduce the number of adherent platelets observed [Okkema et al, 1991 ; Ito et al, 1991]. In contrast, it is apparent from the work reported here that sulphonation results in greatly enhanced platelet deposition.

Interest in incorporating sulphonate functional groups is potentially to impart heparin-like properties to the polyurethane surface rather than to influence directly platelet interaction properties [Grasel and Cooper, 1989]. Nonetheless, it is pertinent to consider knowledge of the interaction of heparin with platelets. Heparin is believed to bind to

platelets by an ionic interaction between the negatively charged sulphate groups of heparin and positively charged amino acids on the platelet membrane [Sobel and Adelman, 1988]. This mechanism is believed to play a role in heparin-associated thrombocytopenia [Sobel and Adelman, 1988 ; Greinacher et al, 1993]. Therefore, it appears that the ability of platelets to interact directly with sulphonate functional groups may be significant and is likely the mechanism responsible for the relatively high levels of platelet deposition observed on the sulphonated polyurethanes.

The non-thrombogenic response previously noted for sulphonated polyurethanes [Grasel and Cooper, 1989 ; Ito et al, 1991] may be due to the nature of fibrinogen and thrombin binding to the sulphonated polymer surface. This binding is believed to interfere with fibrin formation and act in a heparin-like way to catalyze the inhibition of thrombin by ATIII [Silver et al, 1992]. As well, fibrinogen may bind to the sulphonated surface in such a way as to inhibit the ability of the molecule to interact with platelet membrane receptors, resulting in a surface which is somewhat passive towards platelet adhesion [Lindon et al, 1986]. The experimental system used by Okkema was an ex vivo dog shunt, i.e. non-anticoagulated whole blood. Ito et al used an in vitro experiment with a plasma medium. Therefore, the proposed non-thrombogenic action of the sulphonate groups via interactions with the plasma proteins presumably occurred before platelet arrival at the surface. The lack of significant quantities of plasma proteins other than albumin in the experimental system employed in this work could thus serve to alter significantly the platelet response observed. It appears that in the absence of these plasma proteins, platelets are able to interact strongly with sulphonate groups on the polyurethane surface. The presence of significant quantities of albumin in the platelet suspension medium does not appear to inhibit platelet adhesion to the sulphonated polymers. This suggests (a) that albumin does not readily adsorb to the sulphonated surfaces, or (b) that adsorption alters the conformation of albumin to render it platelet-reactive, or (c) that albumin does adsorb to the surfaces but is easily displaced allowing direct platelet-surface interaction to occur, or (d) that despite considerable albumin adsorption there is a strong

"see-through" effect of the sulphonate groups for platelet binding sites. Detailed studies of albumin adsorption to these surfaces would be required to decide among these possibilities, although it seems that options (c) and (d) are the most plausible. In general it has been found in this laboratory that sulphonated surfaces exhibit extensive protein binding [Santerre, 1990 ; Woodhouse, 1993]. Also, albumin binding on surfaces generally leads to profound passivation towards platelets adhesion (for example, in the present work as reported in Section 4.4.2), although Silver et al [1993c] have shown significant levels of platelet deposition on sulphonated polyurethanes precoated with albumin in a canine ex vivo shunt system. Thus, options (a) and (b) appear to be less likely than (c) and (d) to provide explanations for the high platelet reactivity of these materials in the present experimental system.

In conclusion, it appears that the presence of sulphonate groups greatly increases the adhesive interactions between platelets in a flowing suspension and polyurethanes. This interaction is most likely a direct ionic interaction between the platelet membrane and sulphonate groups. Additionally, the level of adhesion on the sulphonated polyurethanes is dependent on the exact identity of the sulphonated chain extender employed, suggesting that the physical characteristics of the polymer imparted by the chain extender may also significantly influence the tendency of platelets to adhere to the polymer surface. The physical characteristics likely to be affected by the chain extender are the conformational mobility of the polymer, the hard segment domain structure and the hydrophilicity of the polymer. These physical properties have been implicated previously as determinants of polyurethane thrombogenicity [Merrill, 1987].

The interaction of platelets and polymer surfaces thus appears to be dependent on a number of physical and chemical properties of the polymer. It is evident that in the absence of plasma proteins (other than albumin), platelets adhere extensively to sulphonate-containing polyurethanes. This supports the hypothesis that the reduced platelet adhesion noted in plasma or blood-based systems is a result of the interaction of plasma proteins with the sulphonated polymer surface.

# 5.0 SUMMARY, CONCLUSIONS AND RECOMMENDATIONS

## 5.1 Summary of Research

1) A novel cone-and-plate experimental flow system was developed to study the interactions of platelets with any type of surface which can be fabricated in the form of a flat film. The device was designed to allow extensive experimental data to be gathered using relatively small volumes of blood since the availability of human blood is limited and donor to donor variation is significant due to diet, lifestyle and other differences.

2) A series of polyurethane elastomers which were believed to have potentially good blood-contacting properties were synthesized and characterized. Four sulphonated and two non-sulphonated polyurethanes were synthesized. These polymers were extensively characterized both physically and chemically. In addition, the platelet adhesion response to these surfaces was investigated using the cone-and-plate apparatus. Sulphonate ion incorporation was found to have a profound effect on many of the physical characteristics of the polymers as well as to increase the level of platelet adhesion dramatically compared to analogous non-sulphonated polyurethanes.

3) The experimental reproducibility and reliability of the cone-and-plate device was investigated by measuring the platelet adhesion response to control surfaces for which the platelet response has been documented. The control surfaces employed were collagen-coated PVC/PMMA copolymer as a highly adhesive surface and an albumin-coated polymer as a minimally adhesive surface. A reproducible and predictable dependence of platelet adhesion on such parameters as fluid shear rate, time and hematocrit was demonstrated using these control surfaces, suggesting that the device may be employed as a reliable tool for the study of platelet-surface interactions.

4) Effective platelet diffusion coefficients were calculated using the adhesion data for the collagen test surfaces. These calculations were made assuming a diffusion-limited

adhesion mechanism to the highly reactive collagen test surfaces. The subsequent regression analysis yielded diffusion coefficients which were shear rate dependent as expected and of the same order of magnitude as those calculated previously by other researchers. This provides additional evidence that the experimental device is able to generate reliable platelet adhesion data.

5) Microscopic techniques were employed to examine the degree of activation of the adherent platelets. This type of experimental observation enables one to determine better the platelet reactivity of the various surfaces by observing the morphology of the adherent platelets. In general, the adherent platelets showed similar morphological responses on all of the polymer surfaces studied with respect to pseudopod formation and spreading which is typical of the early stages of platelet activation.

## 5.2 Conclusions

1) A series of sulphonated polyurethanes were synthesized and characterized. The molecular weights of the polymers were analyzed by GPC and ranged from 35,000 to 50,000, large enough to impart satisfactory mechanical properties to the polymers. Elemental and XPS analyses showed an increasing sulphonate content with decreasing PTMO molecular weight as expected due to an increasing contribution of the sulphonate-containing hard segment to the polymer chain.

2) Differential scanning calorimetry provided some insight into the structural morphology of the polymers. Polyol chain length affected both the glass transition temperature ($T_g$) and the hard domain crystalline melt temperature ($T_m$). An increase in phase-mixing of the PTMO 650 polyurethanes was evident from the elevated $T_g$ values observed for these polymers. As well, the crystalline melt temperature was observed to decrease with decreasing PTMO molecular weight indicating less efficient hard segment packing. In addition, the BES chain-extended polymers showed decreased values of $T_m$ in comparison to the analogous BDDS polymers. This is likely to be due to the disruption of hard segment packing as a result of the pendant side chain group of BES.

3) All of the sulphonated polyurethanes displayed significant water absorption when measured over a 20 day period. The degree of water absorption displayed by the sulphonated polymers appears to be an indicator of bulk sulphonate content with relatively small increases in sulphur content resulting in large differences in the water uptake responses.

4) X-ray photoelectron spectroscopy and water contact angle measurements were carried out to investigate the surface properties of the polyurethanes. Contact angle analysis showed an increased hydrophilicity for the BES in comparison to the BDDS polymers despite the fact that the bulk sulphur contents measured by elemental analysis were very similar. No simple correlation between bulk sulphur content and water contact angle was evident. The data obtained by XPS agreed broadly with the elemental analysis concerning bulk sulphur content. A trend of decreasing nitrogen and sulphur content at the surface was evident and indicative of soft segment enrichment at the polymer surface as expected for the vacuum environment of the XPS experiment.

5) The experimental cone-and-plate apparatus developed to study platelet-surface interactions was tested under varying experimental conditions using collagen and albumin coated polymers as test surfaces. Using the collagen-coated surfaces, a dependence of adhesion on time and shear rate, which was predictable from previous research reported in the literature, was observed. Increasing time led to increasing levels of adhesion to a plateau value and increasing shear rate resulted in increasing adhesion as well. In the absence of shear, very little platelet adhesion was observed over the range of times observed.

6) The presence of red cells in the platelet suspension was also investigated. In the absence of red cells, very little adhesion was observed over the time of study. In fact, the level of adhesion in the absence of red cells was similar to that observed for the static experiment, thus highlighting the ability of red cells to increase effective platelet diffusion in shear flow.

7) The adhesion data obtained using the collagen-coated materials was used to

calculate effective platelet diffusion coefficients. A trend of increasing diffusion coefficient with increasing fluid shear rate and a reasonably good agreement of the diffusion coefficient values with those obtained by other researchers was apparent indicating that the apparatus yields reliable platelet adhesion data.

8) The use of an albumin coated test surface resulted in essentially no adherent platelets at even a high rate of shear (300 $s^{-1}$). This indicates that the device does not serve to activate platelets to the extent that they will bind to normally non-adhesive surfaces.

9) Microscopic techniques were employed to characterize the adherent platelets. SEM showed platelets in the early stages of activation with pseudopod formation and spreading apparent. Light microscopic analysis showed an essentially uniform layer of adherent platelets over the sample disk surface as expected since the fluid shear rate is expected to be constant across the sample.

10) Very high levels of platelet adhesion were observed for the sulphonate-containing polyurethanes. The non-sulphonated analogs exhibited very little adhesion at any time or shear rate tested while the sulphonated polymers showed a characteristic increase with time and shear rate.

11) Platelet adhesion to the sulphonated polyurethanes was dependent on shear rate and type of chain extender. The BES chain-extended polymers displayed greater levels of adhesion than the BDDS polymers even though the bulk sulphur contents were similar. Increasing levels of adhesion were observed with increasing shear rate; however, this trend was less dramatic for the BES polymers.

12) Scanning electron microscopy showed adherent platelets in the early stages of activation. Pseudopod formation, some initial spreading and granulomere formation were observed on all of the polyurethane surfaces.

## 5.3 Recommendations for Future Study

1) The use of a more physiological platelet suspension medium to perform the platelet adhesion experiments would be desirable. A platelet suspension containing some or all of the plasma proteins would yield more immediately relevant results since protein adsorption is believed to precede platelet-surface interactions. If possible, it would be most desirable to use a whole blood system with the use of an anticoagulant such as PPACK or heparin, which is compatible with normal calcium ion concentrations to more closely mimic the in vivo system.

2) An in-depth study of the flow field in the cone-and-plate device using flow visualization techniques would be of benefit in assessing the range of cone rotational speeds and cone angles which are practical for use. Study of the possible onset of vortex formation at high rotational speeds would enable the experimenter to define better the actual flow field and the areas of turbulent and laminar flow.

3) An investigation of red blood cell damage (lysis) caused by the apparatus would also be useful in determining the safe operating range of the device. For example, red cell damage would be more likely to occur at higher rotational rates, thus limiting the use of the device to slower rotational speed studies. Additionally, the level of platelet adhesion to the cone and well surfaces should be studied and the most platelet passive materials should be utilized for cone and well fabrication.

4) In addition, other experimental responses could be studied in relation to platelet-surface interactions using the experimental apparatus. These include platelet release reactions, platelet microparticle formation, and specific platelet receptor-ligand binding. As well, the addition of an inverted microscope to the apparatus would allow for real-time adhesion observation.

5) With regard to polyurethane development, a wider range of sulphonate ion incorporation would be useful to ascertain better the effect of this functionality on the platelet adhesion response to these surfaces. Although the range of sulphonate incorporation is limited by materials considerations such as water solubility and material

flexibility, it is possible to achieve a wider range of sulphonate concentrations than was synthesized here while still retaining the desirable mechanical properties associated with polyurethanes in general.

6) It would be of interest to examine the adsorption profiles of several plasma proteins (fibrinogen, albumin, antithrombin III, etc.) to the polyurethanes synthesized. In particular, the adsorption characteristics of albumin would be of interest since albumin is the only plasma protein present in the platelet suspension medium and albumin-coated surfaces have been shown to be anti-adhesive towards platelets. Indeed it is possible that some of the differences in adhesion observed among the surfaces are due to differences in albumin adsorption.

7) Finally, it would be of interest to investigate the surface chemistry of the polyurethanes developed in the hydrated state using cold stage XPS [Silver et al, 1993]. It is widely held that the hydrated surface chemistry of polyurethanes is significantly different from the non-hydrated form, with the presence of the high energy hard domains being favoured at the surface. Since, the sulphonate groups in the polymers produced here are present in the hard segment, it is possible that a significant increase in the surface concentration of these groups would occur in the hydrated state. As well, since the platelet suspension medium is an aqueous solution, it would be more relevant to study the surface chemistry of the polymers in the hydrated form.

## 6.0 REFERENCES


Adams, G.A., **The Platelets: Physiology and Pharmacology**, ed. Longrecker, G., Academic Press, Chapt. 2, 1985

Adams, N. and Lodge, A.S., *Philosophical Transactions of the Royal Society of London*, **256**: 149, 1964

Aitken, R.R. and Jeffs, G.M.F., *Polymer*, **18**: 197, 1977

Amiji, M., et al, *Journal of Biomaterials Science Polymer Edition*, **3**: 375-388, 1992

Andrade, J.D., **Surface and Interfacial Aspects of Biomedical Polymers**, Plenum Press, 1985

Back, L.H., et al, *Journal of Biomechanics*, **10**: 339-353, 1977

Bale, M.D., et al, *Blood*, **74**: 2698-2706, 1989

Barnhart, M.I. et al, *Annals of the New York Academy of Science*, **201**: 360-390, 1972

Baumgartner, H.R., *Microvascular Research*, **5**: 167-179, 1973

Belval, T., et al, *Microvascular Research*, **28**: 279-288, 1984

Bentfield-Barker, M.E. and Bainton, D.F., *Blood*, **59**: 472-481, 1982

Bordenave, L., et al, *Journal of Biomedical Materials Research*, **27**: 1367-1381, 1993

Brash, J.L., *Annals of the New York Academy of Science*, **283**: 356-371, 1977

Brash, J.L., *Macromolecular Chemistry Suppl.*, **9**: 69, 1985

Brash, J.L., *Annals of the New York Academy of Science*, **516**: 206-222, 1987

Bruil, A., et al, *Biomaterials*, **13**: 915-923, 1992

Brunstedt, M.R., et al, *Journal of Biomedical Materials Research*, **27**: 255-267, 1993

Buist, J.M., **Developments in Polyurethanes**, Applied Science Publishers, Chapt. 3, 1978

Casu, B.J., *Annals of the New York Academy of Science*, **550**: 1-17, 1989

Cazenave, J.P., et al, *Journal of Laboratory Clinical Medicine*, **95**: 60-70, 1979

Chen, J.H. and Ruckenstein, E., *Journal of Colloid and Interface Science*, **135**: 496-507, 1990

Chien, S., **The Red Blood Cell**, ed. Surgenor, D.M., Academic Press, 1975

Chien, S., *Blood Cells*, **3**: 283-303, 1977

Chinn, J.A., et al, *Thrombosis and Haemostasis*, **65**: 608-617, 1991

Cho, C.S., et al, *Journal of Biomedical Materials Research*, **27**: 199-206, 1993

Coleman, D.L., et al, *Journal of Biomedical Materials Research*, **16**: 381-398, 1982

Colman, R.W., *Proceedings of the Society for Experimental Biology and Medicine*, **197**: 242-248, 1991

Coughlin, S.R., *Thrombosis and Haemostasis*, **66**: 184-187, 1993

Day, H.J., et al, *Thrombosis et Diathesis Haemorrhagica*, **33**: 648, 1975

deGroot, P.G. and Sixma, J.J., *British Journal of Haematology*, **75**: 308-312, 1990

Dieterick, D., et al, *Angew Chem.*, **9**: 40, 1970

Doery, J.C.G., et al, *British Journal of Haematology*, **25**: 657-669, 1973

Dosne, A.M., et al, *Microvascular Research*, **11**: 111-114, 1976

Ebert, C.D. and Kim, S.W., *Thrombosis Research*, **26**: 43-57, 1982

Eckstein, E.C., et al, *Microvascular Research*, **36**: 31-39, 1988

Eisenberg, A. and King, M., **Ion Containing Polymers: Physical Properties and Structure**, Academic Press, 1977

Feuerstein, I.A., et al, *Transactions of the American Society of Artificial Internal Organs*, **21**: 427-435, 1975

Foidart, J.M., et al, *Laboratory Investigation*, **42**: 336-342, 1980

Fujimura, A., et al, *Life Sciences*, **50**: 1043-1047, 1992

Fukuyama, M., et al, *Thrombosis Research*, **54**: 253-260, 1989

Furie, B. and Furie, B.C., *Cell*, **53**: 505-518, 1988

Goldsmith, H.L. and Turitto, V.T., *Thrombosis and Haemostasis*, **55**: 415-435, 1986

Goodman, S.L. et al, *Journal of Biomedical Materials Research*, **23**: 105-123, 1989

Goodman, S.L., et al, *Journal of Colloid and Interface Science*, **139**: 561-570, 1990

Grabowski, E.F., et al, *Industrial Engineering Chemistry Fundamentals*, **11**: 224-232, 1972

Grasel, T.G. and Cooper, S.L., *Journal of Biomedical Materials Research*, **23**: 311-338, 1989

Greinacher, A., et al, *British Journal of Haematology*, **84**: 711-716, 1993

Griffiths, D.F. and Walters K., *Journal of Fluid Mechanics*, **42**: 379, 1970

Han, D.K. et al, *Journal of Biomedical Materials Research*, **23**: 87-104, 1989

Han, D.K., et al, *Journal of Biomedical Materials Research*, **27**: 1063-1073, 1993

Harfenist, E.J., et al, *Blood*, **70**: 827-831, 1987

Harkness, J., *Biorheology*, **8**: 171-193, 1971

Harrison, P. and Cramer, E.M., *Blood Reviews*, **7**: 52-62, 1993

Hawiger, J., *Human Pathology*, **18**: 111-122, 1987

Hawiger, J., *Methods in Enzymology*, **169**: 191-195, 1989

Haycox, C.L. and Ratner, B.D., *Journal of Biomedical Materials Research*, **27**: 1181-1193, 1993

Hellum, A.J., *Scandinavian Journal of Clinical Investigation*, **12**: 1-117, 1960

Hemker, H.C. and Kahn, M.J.P., *Nature*, **215**: 1201, 1967

Hemler, M.E., et al, *Journal of Biological Chemistry*, **263**: 7660-7665, 1988

Heuser, G. and Krause, E., *Rheologica Acta*, **18**: 553-564, 1979

Hirsh, J., **Hemostasis and Thrombosis**, ed. Colman, R.W., et al, J.B. Lippincott Company, Introduction, 1987

Hirsh, J., *The New England Journal of Medicine*, **324**: 1865-1875, 1991

Holme, S., *Blood Cells*, **18**: 421-430, 1992

Holmsen, H., et al, *Biochemical Journal*, **208**: 9-18, 1982

Hoppmann, W.H. and Miller, C.E., *Transactions of the Society of Rheology*, **7**: 181-193, 1963

Hou, T.H., *Rheologica Acta*, **20**: 14-22, 1981

Hovingh, P., et al, *Biochemical Journal*, **237**, 573-581, 1986

Hwang, K.K.S., et al, *Journal of Macromolecular Science-Physics*, **B23**: 153-174, 1984

Ingerman-Wojenski, C., et al, *Journal of Clinical Investigation*, **67**: 1292-1296

Ip, W.F. and Sefton, M.V., *Journal of Biomedical Materials Research*, **25**: 875-887, 1991

Ito, Y., et al, *Journal of Biomedical Materials Research*, **23**: 191-206, 1989

Ito, Y., et al, *Journal of Biomedical Materials Research*, **24**: 227-242, 1990

Ito, Y., et al, *Journal of Biomedical Materials Research*, **25**: 1347-1361, 1991

Jaffe, E.A. and Mosher, D.F., *Journal of Experimental Medicine*, **147**: 1779-1791, 1978

Jozefowicz, M. and Jozefonvicz, J., *Pure Applied Chemistry*, **56**: 1335-1344, 1984

Kambic, H.E. et al, **Biomaterials in Artificial Organs**, C&E.N., 31-49, 1986

Kane, W.H., et al, *Journal of Biological Chemistry*, **255**: 1170, 1980

Kaplan, K.L., et al, *Blood*, **53**: 604-618, 1979

Kefalides, N.A., **Hemostasis and Thrombosis**, ed. Colamn, R.W., et al, J.B. Lippincott Company, Chapt. 37, 1987

Keller, S.R. and Skalak, R., *Journal of Fluid Mechanics*, **120**: 27-47, 1982

Kieffer, N. and Phillips, D.R., *Annual Review of Cell Biology*, **6**: 329-357, 1990

Kieffer, N., et al, *American Journal of Pathology*, **140**, 57-73, 1992

King, M.J. and Waters, N.D., *Rheologica Acta*, **9**: 164-170, 1970

Kinlough-Rathbone, R.L., et al, *Thrombosis and Haemostasis*, **37**: 291-308, 1977

Kinlough-Rathbone, R.L. and Mustard, J.F., **Platelets in Biology and Pathology III**, Elsevier Science Publishers, Chapt. 8, 1987

Kunicki, T.J., et al, *Journal of Biological Chemistry*, **263**: 4516-4519, 1988

Legrand, C., et al, *Blood*, **73**: 1226-1234, 1989

Lelah, M.D. and Cooper, S.L., **Polyurethanes in Medicine**, CRC Press, 1986

Lelah, M.D. et al, *Journal of Biomedical Materials Research*, **20**: 433-468, 1986

Letcher, R.L., et al, *American Journal of Medicine*, **70**: 1195-1202, 1981

Lin, H.B., et al, *Biomaterials*, **13**: 905-914, 1992

Lindon, J.N. et al, *Blood*, **68**: 355-362, 1986

Loftus, J.C., et al, *Journal of Cell Biology*, **98**: 2019-2025, 1984

Mann, K.G., et al, *Journal of the American Society of Hematology*, **76**: 1-16, 1990

Marcum, J.A., et al, *Journal of Clinical Investigation*, **74**: 341-350, 1984

Maynard, J.R., et al, *Blood*, **50**: 387-396, 1977

McManama, G.P., et al, **Platelet Responses and Metabolism**, ed. Holmsen, H., CRC Press, 63-79, 1986

Merrill, E.W., *Annals of the New York Academy of Sciences*, **516**: 196-203, 1987

Moncada, S., et al, *Nature*, **263**: 663-665, 1976

Morton, L.F., et al, *Biochemistry Journal*, **258**: 157-163, 1989

Mulvihill, J.N., et al, *Journal of Biomedical Materials Research*, **24**: 155-163, 1990

Murphy, S., *Seminars in Hematolgy*, **22**: 3, 1985

Murphy, S., et al, *Transfusion*, **31**: 16-20, 1991

Mustard, J.F., et al, *British Journal of Haematology*, **22**: 193-204, 1972

Mustard, J.F. , et al, *Blood*, **52**: 453-466, 1978

Nesheim, M.E., et al, *Methods in Enzymology*, **215**: 316-328, 1992

Nievelstein, P., et al, *Arteriosclerosis*, **8**: 200-206, 1988

Niewiarowski, S. and Varma, K.G., **Hemostasis and Thrombosis**, ed. Colman, R.W., et al, J.B. Lippincott Company, Chapt. 26, 1987

Nishizuka, Y., *Journal of the American Medical Association*, **262**: 1826-1832, 1989

Nojiri, C., et al, *Transactions of the American Society of Artificial Internal Organs*, **34**: 386-398, 1988

Noshay, A. and McGrath, J.E., **Block Copolymers**, Academic Press, 365-368, 1977

Okkema, A.Z. and Cooper, S.L., *Biomaterials*, **12**: 668-676, 1991

Okkema, A.Z., et al, *Journal of Biomedical Materials Research*, **25**: 1371-1395, 1991

Okoshi, T., et al, *Journal of Thoracic and Cardiovascular Surgery*, **105**: 791-795, 1993

Packham, M.A., et al, *Journal of Laboratory Clinical Medicine*, **73**: 686-697, 1969

Packham, M.A., **Atherosclerosis**, ed. Gotleib, A.I., et al, Plenum Press, 209-225, 1991

Park, K., et al, *Journal of Biomedical Materials Research*, **20**: 589-612, 1986

Park, K. et al, *Biomaterials*, **11**: 24-31, 1990

Park, K.D., et al, *Journal of Biomedical Materials Research*, **26**: 739-756, 1992

Peerschke, E.I., et al, *Blood*, **55**: 841-847, 1980

Phillips, D.R., et al, *Blood*, **71**: 831-843, 1988

Ratner, B.D., *Journal of Biomedical Materials Research*, **27**: 283-287, 1993

Roth, G.J., *Blood*, **77**: 5-19, 1991

Roth, G.J., *Immunology Today*, **13**: 100-105, 1992

Ruggeri, Z.M., *Thrombosis and Haemostasis*, **70**: 119-123, 1993

Sakariassen, K.S., et al, *Journal of Laboratory Clinical Medicine*, **102**: 522-535, 1983

Sakariassen, K.S., et al, *Blood*, **63**: 993-1003, 1984

Sakariassen, K.S., et al, *Thrombosis and Haemostasis*, **60**: 392-398, 1988

Sakariassen, K.S., et al, *Methods in Enzymology*, **169**: 37-70, 1989

Sakariassen, K.S., et al, *Arteriosclerosis*, **10**: 276-284 1990

Salzman, E.W., *Journal of Laboratory Clinical Medicine*, **62**: 724-735, 1963

Santerre, J.P., **PhD Thesis**, McMaster University, 1990

Santerre, J.P., et al, *Journal of Biomedical Materials Research*, **26**: 1003-1018, 1992a

Santerre, J.P. et al, *Journal of Biomedical Materials Research*, **26**: 39-57, 1992b

Saunders, J.H. and Frisch, K.C., **Polyurethanes: Chemistry and Technology**, Interscience Publishers, Part I, 1967

Schmid-Schoenbein, H., et al, *Journal of Applied Physiology*, **26**: 674-678, 1969

Schmid-Scoenbein, H., et al, *Microvascular Research*, **6**: 366-376, 1973

Seymour, R.W. and Cooper, S.L., *Macromolecules*, **6**: 48, 1973

Shibuta, R., et al, *Journal of Biomedical Materials Research*, **20**: 971-987, 1986

Shulman, N.R. and Jordan, J.V., **Hemostasis and Thrombosis**, ed. Colman, R.W., et al, J.B. Lippincott Company, Chapt. 18, 1987

Silver, J.H., et al, *Biomaterials*, **13**: 339-344, 1992

Silver, J.H., et al, *Journal of Biomedical Materials Research*, **27**: 735-745, 1993a

Silver, J.H., et al, *Journal of Biomedical Materials Research*, **27**: 1443-1457, 1993b

Silver, J.H.,et al, *Biomaterials*, **14**: 834-844, 1993c

Slack, S.M., et al, *Thrombosis and Haemostasis*, **70**: 129-134, 1993

Slattery, J.C., *Journal of Applied Polymer Science*, **8**: 2631, 1964

Smith, J.B. and Dangelmaier, C., *Analytical Biochemistry*, **187**: 173-178, 1990

Sobel, M. and Adelman, B., *Thrombosis Research*, **50**: 815-826, 1988

Spathis, G., et al, *Journal of Macromolecular Science-Physics*, **B29**: 31-48, 1990

Stemerman, M.B., **Hemostasis and Thrombosis**, ed. Colman, R.W., et al, J.B. Lippincott Company, Chapt. 35, 1987

Suzuki, H., et al, *Blood*, **71**: 850-860, 1988

Takahara, A., et al, *Journal of Biomedical Materials Research*, **25**: 1095-1118, 1991

Tamada, Y. and Ikada, Y., *Journal of Colloid and Interface Science*, **155**: 334-339, 1993

Tanner, R.I., *Transactions of the Society of Rheology*, **14**: 483, 1970

Thakur, M.L. et al, *Thrombosis Research*, **9**: 345-357, 1976

Turian, R.M., *Industrial Engineering Chemical Fundamentals*, **11**: 361-368, 1972

Turitto, V.T., et al, *Industrial Engineering Chemical Fundamentals*, **11**: 216-223, 1972

Turitto, V.T. and Baumgartner, H.R., *Microvascular Research*, **17**: 38-54, 1979

Turitto, V.T., *Progress in Thrombosis and Hemostasis*, **6**:, 139-177, 1982

van Breugel, H., et al, *Arteriosclerosis*, **8**: 332-335, 1988

Vroman, L. and Leonard, E.F., *Annals of New York Academy of Science*, **283**: 65-76, 1977

Walters, K., **Rheometry**, Chapman and Hall, 1975

Weiss, H.J., *New England Journal of Medicine*, **293**: 531-541, 1975

White, J.G., *Scanning Microscopy*, **1**: 1677-1700, 1987

White, J.G. and Gerrard, J.M., **The Blood Platelets in Transfusion Therapy**, Alan R. Liss Inc., New York, 1978

White, J.G. and Gerrard, J.M., **Hemostasis and Thrombosis**, ed. Colman, R.W., et al, J.B. Lippincott Company, Chapt. 21, 1987

White, J.G. and Krumwiede, M., *Blood*, **69**: 1196-1203, 1987

White, J.G., *Laboratory Investigation*, **68**: 497-498, 1993

Woodhouse, K.A., **PhD Thesis**, McMaster University, 1992

Woods, D.R., **Surfaces, Colloids and Unit Operations, Part II**, 7th ed., McMaster University, 1990

Wu, S., **Polymer Interface and Adhesion**, Marcel Dekker Inc., New York, 1982

Yau, W., Kirkland, J., and Bly, D., **Modern Size Exclusion Chromatography**, Wiley Interscience, 1979

Young, B.R., et al, *Transactions of the American Society of Artificial Internal Organs*, **28**: 498-503, 1982

Yung, W. and Frojmovic, M.M., *Thrombosis Research*, **28**: 361-377, 1982

Zhu, L. et al, *Transactions of the American Society of Artificial Internal Organs*, **36**: 811-816, 1990

Zijenah, L.S., et al, *Biochemical Journal*, **268**: 481-486, 1990

Zucker, M.B. and Vroman, L., *Proceedings of the Society of Experimental Biology and Medicine*, **131**: 318-320, 1969

## APPENDIX A

* The following preparations were obtained from D.W. Perry.

### TYRODES BUFFER PREPARATION

*Stock Solution I*

| | | |
|---|---|---|
| NaCl | 160 g | |
| KCl | 4 g | |
| $NaHCO_3$ | 20 g | |
| $NaH_2PO_4$ | 1 g | (1.16 g $NaH_2PO_4 \cdot H_2O$) |

* Make up to 1.0 Litre with deionized, distilled water.

*Stock Solution II*

0.1 M $MgCl_2 \cdot 6H_2O$ Mol. Wt.=203.31

* Dissolve 20.33 g in 900 mL of deionized, distilled water. Bring to a total volume of 1.0 L.

*Stock Solution III*

0.1 M $CaCl_2 \cdot 6H_2O$ Mol. Wt.=219.09

* Dissolve 21.91 g in 900 mL of deionized, distilled water. Bring to a total volume of 1.0 L.

## PLAIN TYRODES

To 50 mL of Stock Solution I, add deionized water to make 1.0 L. Adjust pH to 7.35.

## TYRODES ALBUMIN

To 50 mL of Stock Solution I, add 750 mL of deionized water, 10 mL of Stock Solution II, and 20 mL of Stock Solution III. Dissolve 3.5 g of Bovine albumin (obtained from Boehringer Mannheim - fatty acid free) and 1.0 g of dextrose. Dilute to 1.0 L, adjust pH to 7.35, mOs 290.

## ACID CITRATE DEXTROSE PREPARATION

| | | |
|---|---|---|
| Trisodium Citrate | 25 g | |
| Citric acid | 14 g | (or citric acid monohydrate 15 g) |
| Dextrose | 20 g | |

* Dissolve in 1.0 L of deionized water, adjust pH to 4.5, mOs 450. Use 1 part ACD solution plus 6 parts whole blood.

## ACETIC ACID SOLUBLE COLLAGEN PREPARATION

1) Add 12 mL of glacial acetic acid to 388 mL of distilled water.

2) Add 1 g of Sigma bovine tendon collagen and allow to hydrate overnight at 4°C.

3) Homogenize collagen solution at full speed for 30 min in ice using 1 quart container of Sorvall omninex homogenizer.

4) Centrifuge homogenate at 2500g for 15 min at room temperature. Pellets formed should be very small, if any.

5) Pool all collagen (buttons and supernatent) and mix by stirring. Suspension should appear silky. If suspension looks granular, rather than silky, repeat steps 3,4 and 5.

6) Store collagen in aliquots at 4°C. Do not freeze.

* Dilutions should be made in cold, unbuffered media, preferably 0.9% NaCl.

| | |
|---|---|
| Collagen | 0.25% |
| pH | 2.8 |
| mOs | 540 |
| Acetic acid | 0.522 M |

# APPENDIX B: NMR Spectra of Polyurethanes

**PTMO 650/MDA**

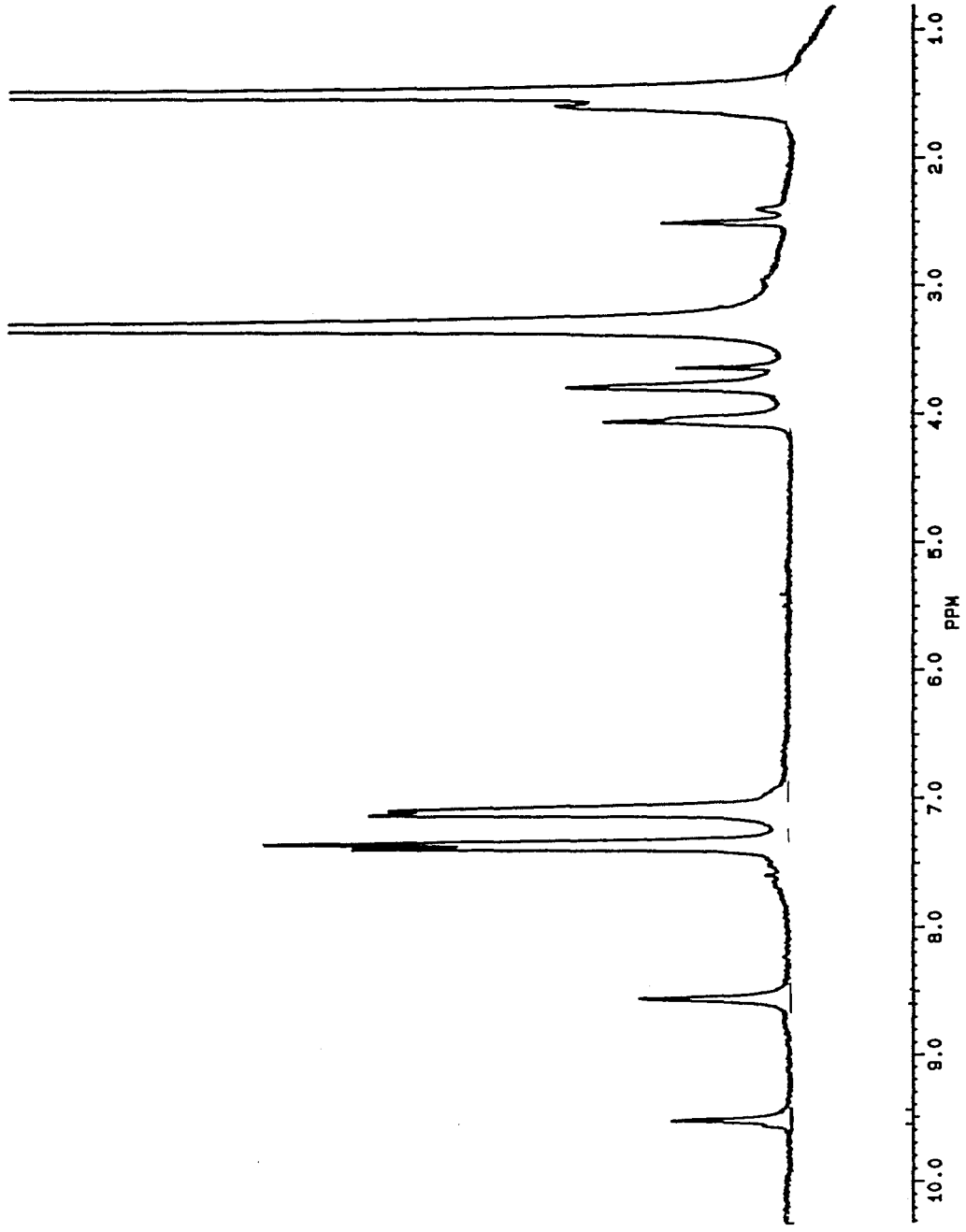

**PTMO 980/MDA**

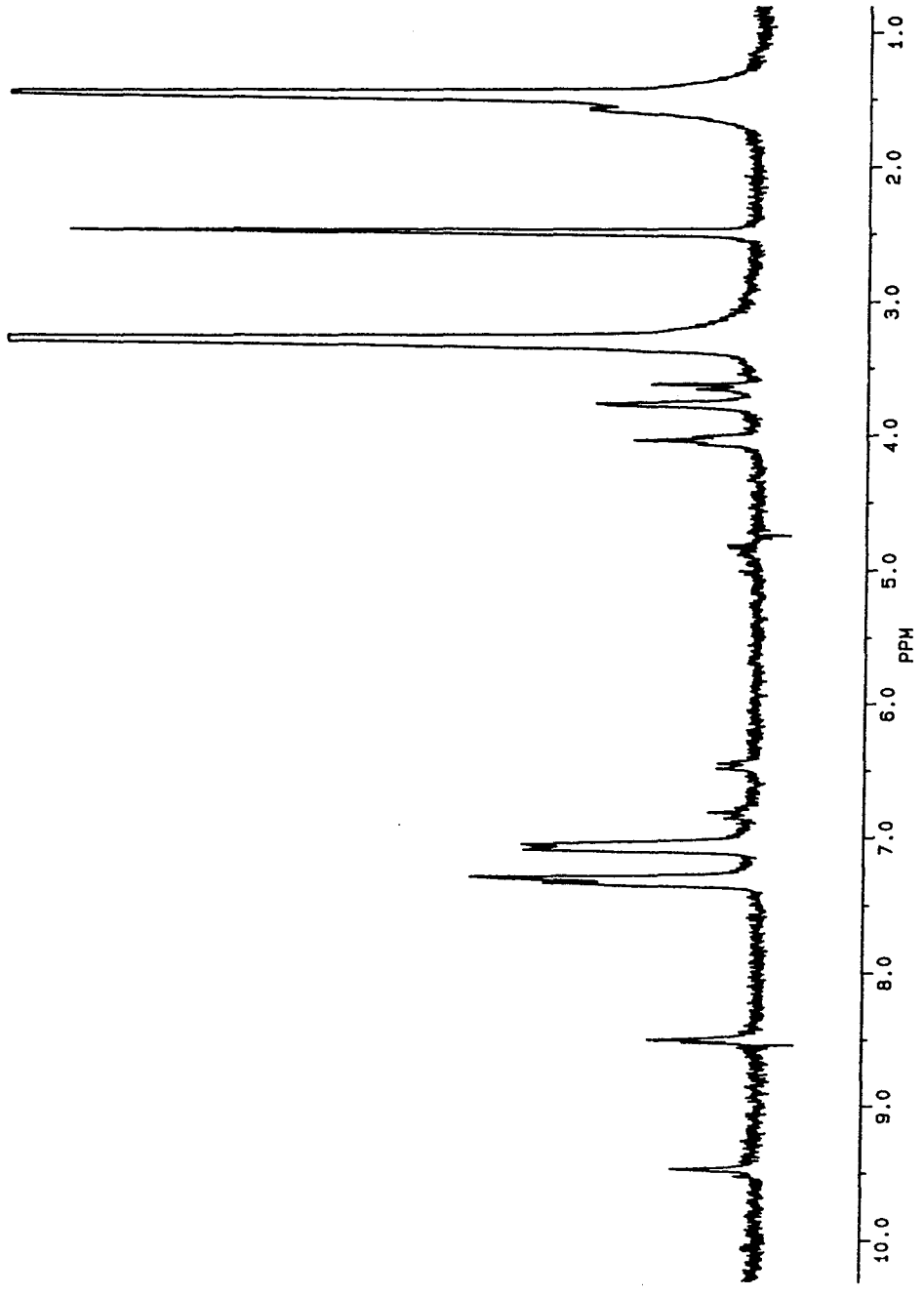

**PTMO 650/BES**

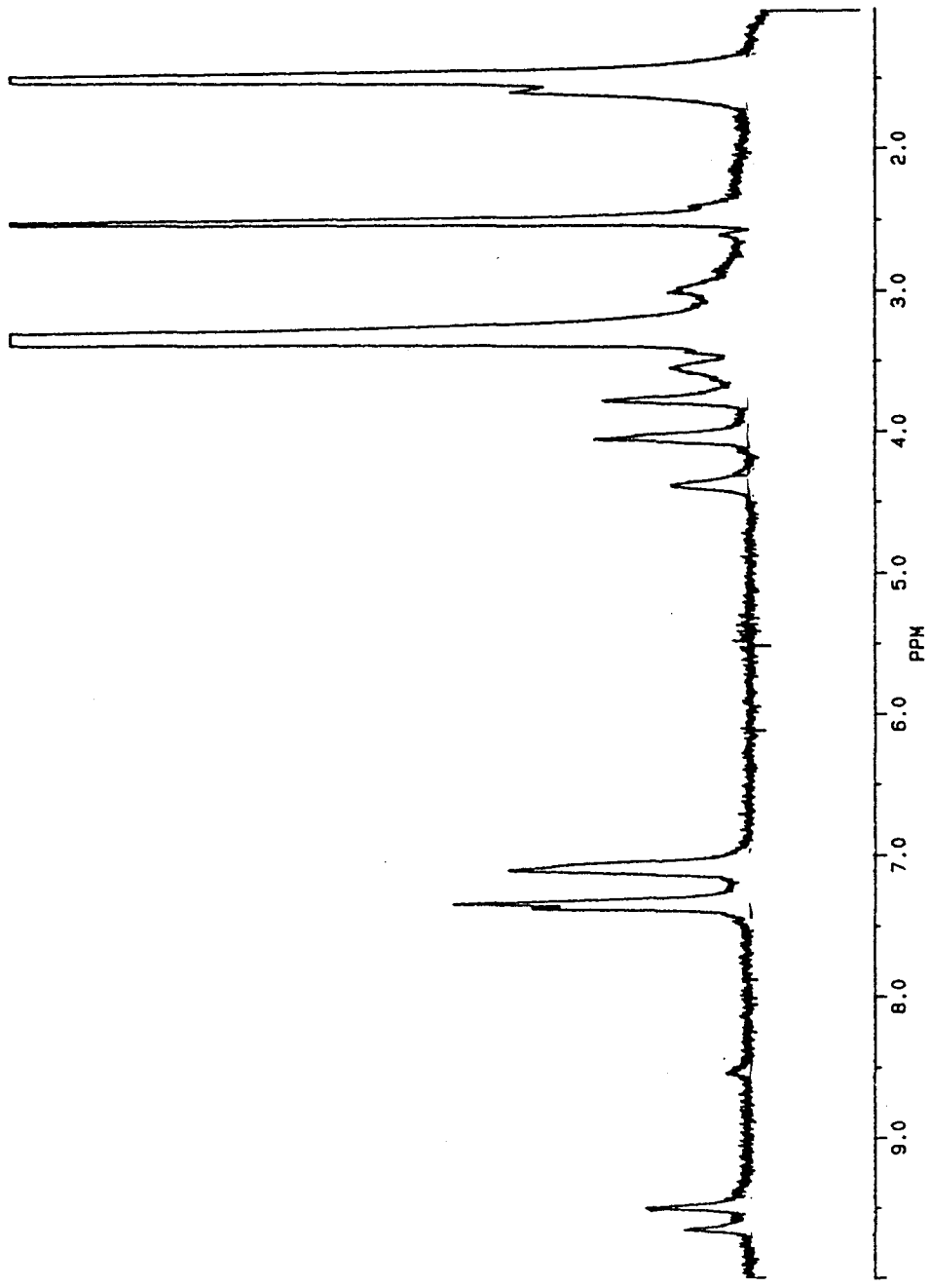

**PTMO 980/BES**

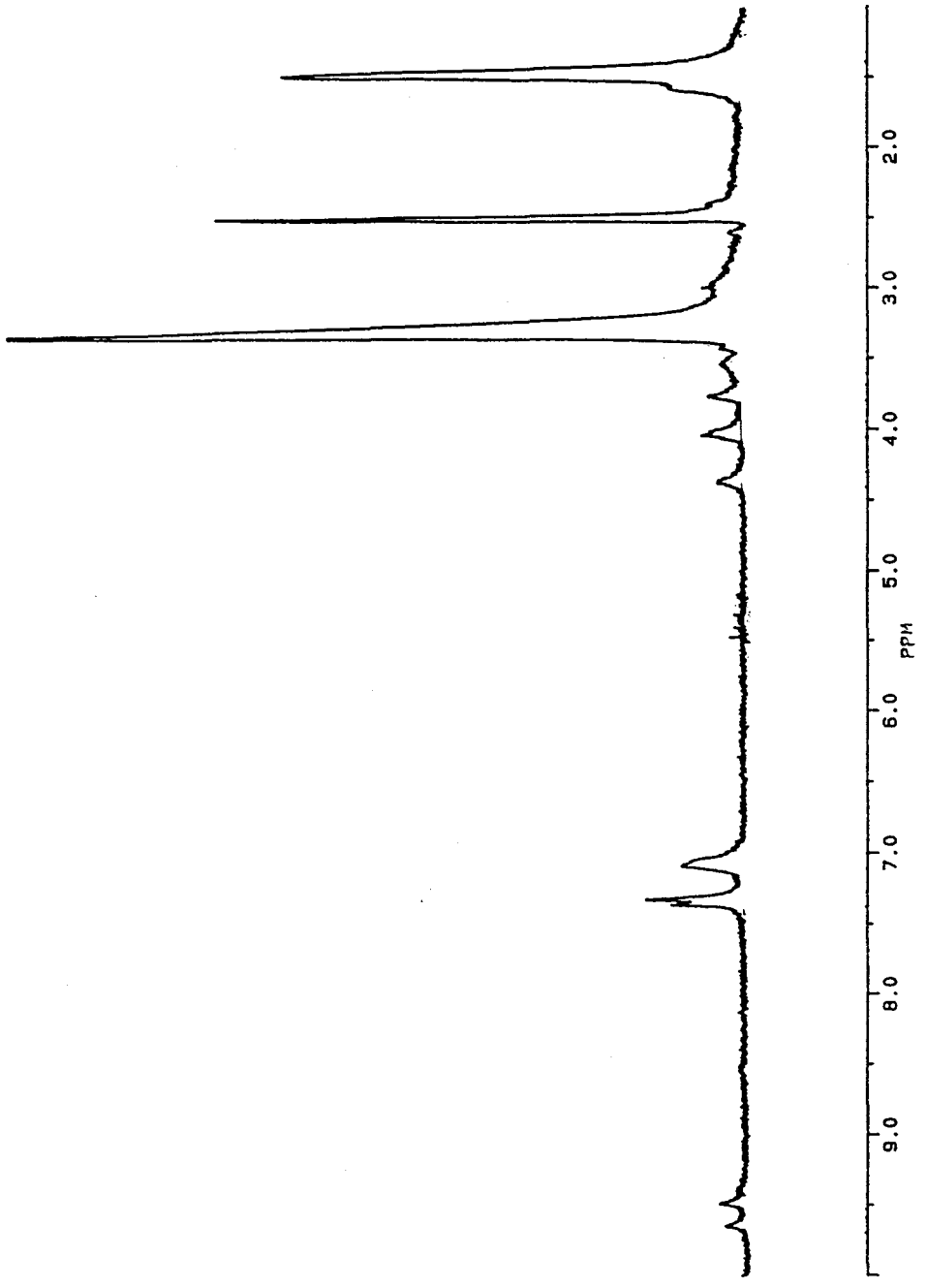

**PTMO 650/BDDS**

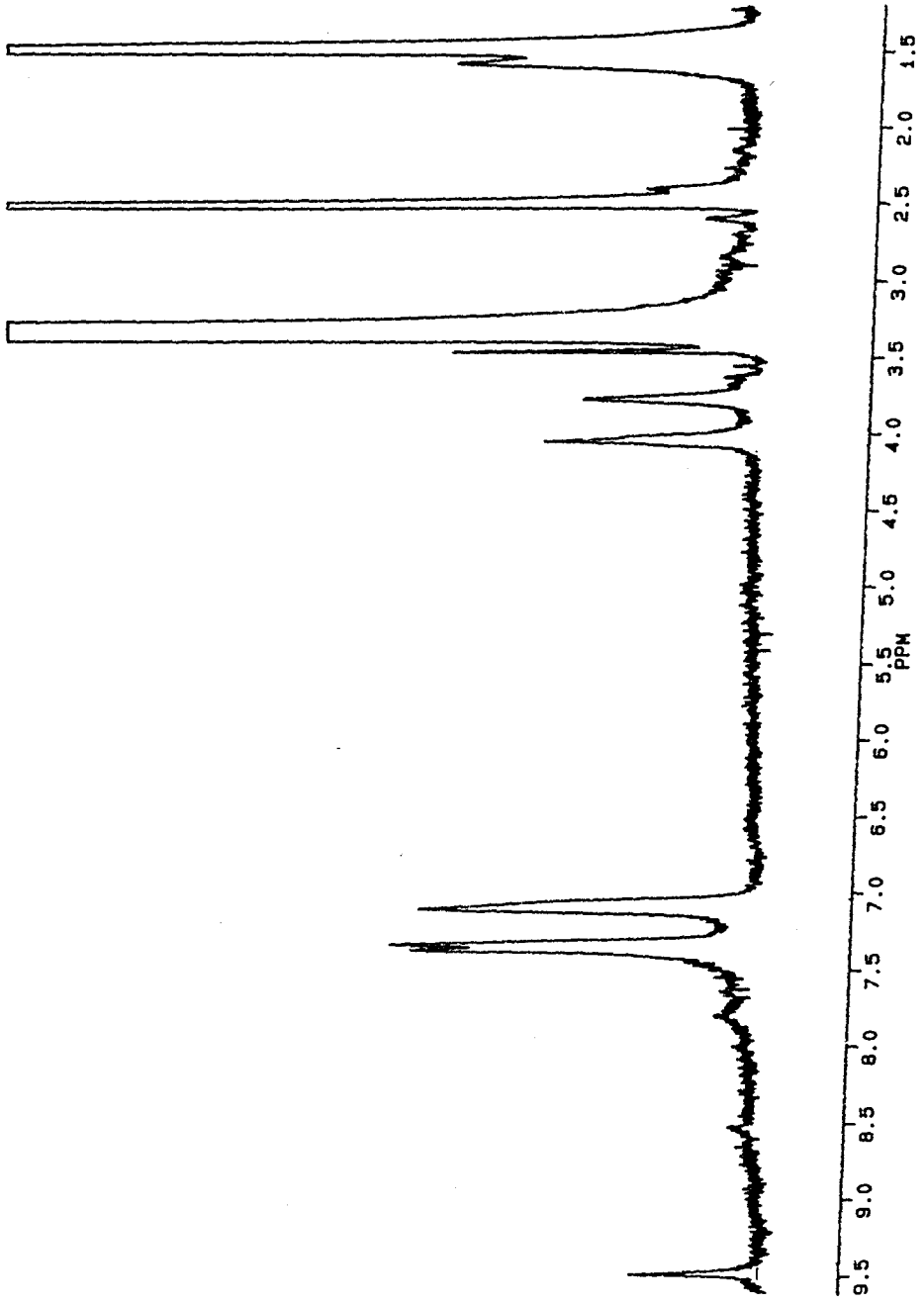

**PTMO 980/BDDS**